



Studies toward the Synthesis and Biological Activity of *Illicium* Sesquiterpenoids *via* C–H Functionalization

Johannes Martin Richers



Vollständiger Abdruck der von der Fakultät für Chemie der Technischen Universität München
zur Erlangung des akademischen Grades eines

Doktor der Naturwissenschaften (Dr. rer. nat.)

genehmigten

D I S S E R T A T I O N

Vorsitzender: apl. Prof. Dr. Wolfgang Eisenreich

Prüfer der Dissertation: 1. Prof. Dr. Konrad Tiefenbacher

2. Prof. Dr. Tobias Gulder

Die Dissertation wurde am 19.05.2017 bei der Technischen Universität München eingereicht
und durch die Fakultät für Chemie am 21.07.2017 angenommen.



To my parents,
who taught me to learn
from success and failure.

*«The commonality between science and art
is in trying to see profoundly—to develop strategies
of seeing and showing» —Edward R. Tufte*

Acknowledgment

My thanks are due, first and foremost, to my doctoral advisor, *Prof. Dr. Konrad Tiefenbacher*. His excellent guidance, as well as his profound knowledge and chemical intuition have allowed me to grow, personally and professionally. I am particularly grateful for his appreciation of art and design in science which has enabled me to pursue my artistic ambitions. By allowing a high degree of freedom paired with constant availability, the atmosphere throughout my doctoral studies has been characterized by encouragement and trust.

I am also indebted to *Prof. Dr. Thorsten Bach*. As the Chair for Organic Chemistry, he is an impressive researcher and I owe him a debt of gratitude for teaching me the importance of perfectly drawn six-membered rings. Furthermore, I would like to thank *Prof. Dr. Tobias Gulder* and *apl. Prof. Dr. Wolfgang Eisenreich*, the members of the committee, as well as *Ms. Voigt* for all the organizational efforts. My gratitude extends to the collaboration partners from the Max-Planck-Institute for Psychiatry, *Claudia Sippel* and *Prof. Dr. Felix Hausch* for their help in the measurements of neuronal growth. In addition, I would like to acknowledge my colleagues and co-workers in the Tiefenbacher group as well as the Bach group. In particular, I would like to express my gratitude to *Michael Heilmann* for his determination, his passion and his sense of humor which fostered a great working environment. Furthermore, I am thankful for the help of *Dr. Alexander Pöthig*, who introduced me to the art of crystallography and always supported and encouraged me to pursue ambitious goals.

Over the course of my dissertation, I have had the chance to work with a series of very talented students. From the practical organic courses to the research internships, working with students has taught me the responsibility that comes with heading a laboratory. It was a particularly rewarding experience to pass on knowledge to my research students: *Camilla Meyer*, *Lorenzo Catti*, *Maximilian Ackermann*, *Michael Heilmann*, *Tobias Gmelch*, *Manuel Rondelli*, *Severin Merget*, *Joachim Preinl*, *Marc Kloberg*, *Michael Röhr*, *Manuel Einsiedler*, *Eva Esslinger*, and *Tobias Schirmer*. Thank you for your motivation and your curiosity.

The unconditional trust and support of my parents and my family is greatly appreciated. Last but not least, I owe a debt of gratitude to my partner Julia—the source of strength and joy in life.

Zusammenfassung

Neurodegenerative Krankheiten stellen unsere alternde Gesellschaft vor ernsthafte Herausforderungen. Mit jährlich Millionen neuen Fällen ist hier insbesondere die ALZHEIMER-Krankheit weltweit für den Großteil der bekannten Fälle von Demenz verantwortlich. Die Forschung in diesem Gebiet ist jedoch limitiert durch die unbekannt genauen Mechanismen der Krankheit, einem Mangel an potentiellen Zielstrukturen für die Entdeckung von Wirkstoffen sowie einem Defizit an synthetischen Wegen und Methoden für die Synthese derartiger Moleküle auf effiziente und skalierbare Weise.

Allerdings bergen neurotrophe Naturstoffe als privilegierte pharmakologische Strukturen ein signifikantes Potential für die Entwicklung von therapeutischen Wirkstoffen gegen Neurodegeneration. Jedoch wurden bisher nur wenige Studien durchgeführt, die ein gemeinsames Pharmakophormotiv und die Struktur-Aktivität Beziehung untersuchen. Deshalb stellt diese Arbeit Studien zu strukturell vereinfachter Analoga der neurotrophen Sesquiterpene der *Illicium* Familie vor. Eine präzise synthetische Route erlaubt die Herstellung des Kohlenstoffgerüsts von (\pm)-Merrilactone A (**1**) und (\pm)-Anislactone A/B (**2**) im Grammaßstab. Durch Modifikation der Kernstruktur, insbesondere der Variation des Oxidationsniveaus und der Veränderung der funktionellen Gruppen, wird damit der Zugang zu einer Serie von Strukturanaloga geschaffen. Insgesamt wurden 15 Gerüstderivate der Naturstoffe hergestellt und hinsichtlich ihrer Aktivität zur Steigerung des Neuritenwachstums untersucht. Die Studien weisen darauf hin, dass strukturell vereinfachte Naturstoffanaloga die vielversprechende biologische Aktivität beibehalten und durch eine direkte synthetische Route zugänglich sind.

Da γ -Lactone ein essentieller Teil der *Illicium* Sesquiterpene darstellen, wurde besonders diesem Strukturmerkmal besondere Aufmerksamkeit gewidmet. Deshalb wird hier die erste allgemeine Methode vorgestellt, die die Einführung von Lactonringen durch eine Amid-dirigierte C-H Funktionalisierung mit guten bis exzellenten Ausbeuten und großer Substratbreite erlaubt. Hierfür wird ein elektronarmes Amid als dirigierende Gruppe eingesetzt um nichtaktivierte C(sp³)-H Bindungen durch radikalische 1,5-Wasserstoffabstrahierung zu funktionalisieren. Die gebildeten γ -Bromoamide werden anschließend unter milden Bedingungen zu γ -Lactonen umgesetzt. Die Methode ist nicht auf tertiäre oder sekundäre Positionen beschränkt, sondern gestattet außerdem die Funktionalisierung von primären nichtaktivierten sp³-hybridisierten Positionen in einer Eintopfreaktion. Die breite Toleranz gegenüber funktionelle Gruppen macht die Methode geeignet für die späte Einführung von Lactonen in komplexe Kohlenstoffgerüste.

Abstract

Neurodegenerative diseases pose serious challenges for our aging society. With millions of new cases each year, ALZHEIMER's disease in particular is responsible for the majority of reported cases of dementia worldwide. Research in this field is limited by the disease's unknown precise mechanisms and the lack of potential target structures for drug development, as well as a deficiency of synthetic routes and methods which allow the synthesis of such molecules in an efficient and scalable manner.

Neurotrophic natural products hold potential as privileged structures for the development of therapeutic agents against neurodegeneration. However, only a few studies have been conducted to investigate a common pharmacophoric motif and the structure–activity relationships (SARs). Therefore, this work presents studies of structurally more simple analogs of neurotrophic sesquiterpenes of the *illicium* family. A concise synthetic route enables preparation of the carbon framework of (±)-Merrilactone A (**1**) and (±)-Anislactone A/B (**2**) on a gram scale. This has allowed access to a series of structural analogs by modification of the core structure, including variation of oxidation levels and alteration of functional groups. In total, 15 framework derivatives of the natural products have been synthesized and tested for their neurite outgrowth activities. The studies indicate that the promising biological activity can be retained by structurally simplified natural product analogs, which are accessible by a straightforward synthetic route.

Since γ -lactone rings are an essential part of the *illicium* sesquiterpenes, this structural feature has received particular attention. Therefore, a general method is presented that allows for the introduction of lactone rings by amide directed C–H functionalization with good to excellent yields and unprecedented substrate scope. Here, an electron-deficient amide is utilized as a directing group to functionalize nonactivated C(sp³)-H bonds through radical 1,5-hydrogen abstraction. The γ -bromoamides formed are subsequently converted to γ -lactones under mild conditions. The method described is not limited to tertiary and secondary positions but also allows the functionalization of primary nonactivated sp³-hybridized positions in a one-pot sequence. The broad functional group tolerance renders this method suitable for the late-stage introduction of γ -lactones into complex carbon frameworks.

Table of Contents

ACKNOWLEDGMENT	VIII
ZUSAMMENFASSUNG	VIII
ABSTRACT	IX
TABLE OF CONTENTS	X
1 INTRODUCTION	1
2 PHARMACOPHORES: TARGETS, STRUCTURES, AND DISEASES.....	2
2.1 Neurodegenerative Diseases	3
3 SYNTHESIS: NATURAL PRODUCTS AND TOTAL SYNTHESIS	5
3.1 Natural Products, Terpenes, and Sesquiterpene Lactones	5
3.2 <i>Illicium</i> Sesquiterpenes.....	6
3.3 Biosynthesis.....	8
3.4 Biological Activity	9
3.5 Previous Synthetic Studies	10
3.6 Historic Perspective and Modern Total Synthesis.....	16
4 METHODOLOGY: C–H FUNCTIONALIZATION	17
4.1 Reactivity of Carbon-Hydrogen bonds	17
4.2 Historic Perspective of C–H Functionalization.....	18
4.3 Overview of C–H Functionalization Methods	24
4.4 Terminology and Impact.....	31
5 MOTIVATION AND OBJECTIVE	33
5.1 Retrosynthetic Analysis.....	33
5.2 Synthesis of Lactones	34
6 RESULTS AND DISCUSSION	35
6.1 Synthesis of Lactones <i>via</i> C–H Functionalization of Non-Activated C(sp ³)–H Bonds.....	35
6.2 A Six-Step Total Synthesis of α -Thujone and D ₆ - α -Thujone, enabling facile Access to Isotopically Labelled Metabolites	40
6.3 Synthesis and Neurotrophic Activity Studies of <i>Illicium Sesquiterpene</i> Natural Product Analogs.41	
7 SUMMARY AND OUTLOOK	49

8 EXPERIMENTAL SECTION	50
8.1 General Information.....	50
8.2 Synthetic Procedures and Analytical Data	52
8.3 Neurite Outgrowth Assay	123
8.4 X-Ray Crystallographic Data	124
8.5 DFT-Calculations and Computational Details	131
9 BIBLIOGRAPHIC DATA OF COMPLETE PUBLICATIONS	153
10 PUBLICATION SUMMARIES	154
11 REPRINT PERMISSIONS	157
10.1 American Chemical Society	157
10.2 Royal Society of Chemistry	157
10.3 John Wiley & Sons, Inc.	158
12 INDEX OF ABBREVIATIONS	159
13 REFERENCES	161

1 Introduction

Nature's ability to create functional matter has at all times inspired researchers to study structural complexity. The art of describing, understanding, and predicting molecular processes has led to various essential discoveries. In particular, a great number of substances found in nature are today widely used as medication against illness and disease, such as the first antibiotic *Penicillin*, the analgesic *morphine*, or the anti-malarial *Artemisinin*. Accordingly, synthetic organic chemists have developed ways to replicate in the laboratory some of the most intriguing molecules and construct variations of them. Such molecules facilitate biology and medicine, as they often find uses as biological tools and drug candidates for clinical development.^[1] In addition, the ability to produce such substrates synthetically enables the investigation of underlying mechanism and—by derivatization—potentially improves corresponding properties. Here, the development of synthetic methods plays a fundamental role. Efficient reactions that enable the selective transformation, modification, and functionalization of target structures are the essential tools for synthetic organic chemists and define the way they approach the synthesis of organic molecules.

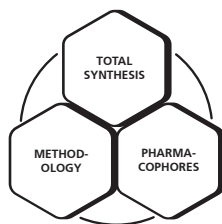


Figure 1.1. The intersection of three research sectors: total synthesis, pharmacophores, and methodology.

The investigation of molecular complexity has acquired a significant importance in three research sectors: (i) pharmacophores—the description of potential drug candidates, (ii) total synthesis—the construction of complex molecules, and (iii) methodology—the development of new synthetic methods (see figure 1.1). Interestingly, these fields are often united in setting the elegance of nature as the foundation and motivation for scientific endeavor. Although these individual areas themselves leave plenty of room for innovation, in modern sciences it is specifically the interconnection of research that facilitates new discoveries. Hence, after establishing the scaffold of these three segments this work aims to present results from a multidisciplinary standpoint by combining synthesis, methodology, and pharmacophores.

2 Pharmacophores: Targets, Structures, and Diseases

The utilization of molecular substances in order to treat, cure, or prevent diseases is an essential part of modern medicine and a great example of the importance of chemical sciences. Various plants, herbs, and spices have been identified and used since prehistoric times to alleviate pain and infirmities. Likewise, elements and extracts from plants and organisms have been employed in traditional medicine. A closer analysis of the active ingredients often reveals specific organic molecules that are associated with the corresponding therapeutic effect. The identification of such molecules facilitates and furnishes pharmacology and drug discovery, and can lead to the development of pharmaceutical drugs. Here, new candidate medications are identified, tested, and optimized in order to maximize their positive effects. One excellent example of this development is *antibacterial compounds*. The serendipitous discovery and isolation of the substance benzyl penicillin (**3**, Penicillin G) from the mold *Penicillium notatum* in 1928 by A. FLEMING marked the start of modern antibiotics.

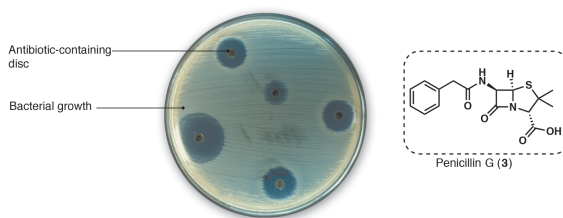


Figure 2.1. Structure of Penicillin G (**3**) and susceptibility test of staphylococcus bacteria to antibiotics by the KIRBY-BAUER disc diffusion method resulting in a zone of inhibition.

The antibacterial property of this compound (see figure 2.1) revolutionized medicine in the twentieth century. Penicillin antibiotics are still widely used today as one of the most effective and safe medicines, though following their extensive use many types of bacteria have developed resistance. Consequently, the increasing demand for new antibiotics aligns with the modifications of existing compounds and, more importantly, the search for new target structures. Although the precise mode of action of such medicine candidates are often not fully understood, scientists try to deduce activity relationships from the corresponding structure. In general, the desired physiological effect is a result of the binding to a specific biological target and therefore defined by the molecular geometry. However, in many cases it is not the whole molecule, but a key structural feature that is responsible for the relevant pharmacological interaction. Thus, in the context of molecular entities used as pharmaceuticals, the concept of *pharmacophores* has emerged. A Pharmacophore is the essential part of a molecular structure that

undergoes a particular biological or pharmacological interaction. Generally, it refers to the abstract descriptions of molecular features that are responsible for pharmacological effects and molecular recognition. Pharmacophores are defined by the International Union of Pure and Applied Chemistry (IUPAC) to be “an ensemble of steric and electronic features that is necessary to ensure the optimal supramolecular interactions with a specific biological target and to trigger (or block) its biological response”.^[2] As recently summarized by GADEMANN and co-workers, in some cases the structural complexity of a drug can be reduced while retaining or even improving key biological parameters such as potency or selectivity. Such simplified natural product analogs often display significantly reduced molecular weights and condensed structural complexity, and therefore are accessible with a reduced number of synthetic steps. The importance of such concepts are notably revealed in light of the drastic effects some diseases still have today.^[3]

2.1 Neurodegenerative Diseases

Diseases associated with the impairment of brain functions such as PARKINSON'S disease and ALZHEIMER'S disease are a serious challenge for aging societies.^[4] ALZHEIMER'S disease is responsible for 60% of the 47 million reported cases of dementia worldwide, with more than 7 million new cases every year.^[5] Dementia is a description of a set of symptoms—usually of a chronic or progressive nature—that is characterized by a difficulty in processing thoughts, an inability in learning new information, and poor memory. Further, dementia results in the deterioration of cognitive functions and is one of the major causes of dependency and disability among elderly populations worldwide. The consequence of neurodegenerative diseases such as ALZHEIMER'S is damage to brain cells, particularly in the cortex. Although, the disorder's underlying mechanism is not fully understood, two major factors are often cited in its progression: *plaques* and *tangles*.

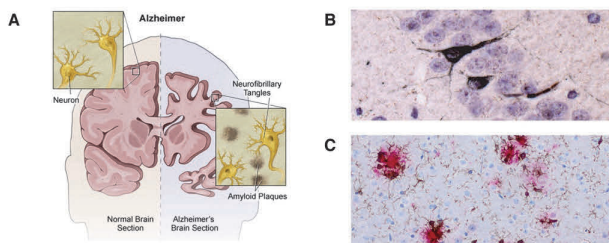


Figure 2.2. The effect of Alzheimer's disease on the brain. **A:** Schematic comparison of a normal brain section and an Alzheimer's brain section with illustrations of neuron cells, neurofibrillary tangles and amyloid plaques.^[6] **B:** Brain section with tau protein tangles that closely resemble neurofibrillary tangles (stained with Gallyas–Braak method)^[7] **C:** Immune cells of the brain with microglia (brown) and cluster around the beta-amyloid deposits (red) in a mouse model for Alzheimer's disease.^[8]

Embedded in the membrane, amyloid precursor proteins (APP) facilitate neuron growth and activate repair mechanisms. Dysfunctional APPs are converted by the enzymes α - and γ -secretases to soluble truncated protein residues. However, if this enzymatic interconversion follows the amyloidogenic pathway, the activity of β -secretase is responsible for cutting the protein into fragments that exhibit decreased solubility. This leads to the formation of beta-amyloid monomers. Because of the monomers' strong affinity, they have a tendency to clump together and form beta-amyloid plaques. By disrupting neuron–neuron signaling, these plaques impair brain functions. The initiation of immune responses causes inflammation and damages surrounding cells. Furthermore, amyloid plaque can also deposit itself around blood vessels and form amyloid angiopathy, which weakens the walls of the blood vessels and increases the risk of hemorrhage.

As opposed to beta-amyloid plaques, another substantial part of ALZHEIMER's disease occurs inside the cells: tangles (see Figure 2.2). Neurons are held together by their cytoskeleton, which mainly consists of tubular polymers: the microtubules. The stability and flexibility of these microtubules is provided by tau proteins which are primarily active in the axon's distal portions. The transfer of phosphate groups to the tau proteins by activation of kinase leads to deformation and results in destabilization of the cytoskeleton. The accumulation and tangling of tau proteins results in neurofibrillary tangles. The blocked signal pathway of neurons and the non-functional microtubules can lead to apoptosis. The decay of neurons is followed by the narrowing of the gyri—the characteristic ridges of brain—as well as widening of the sulci—the grooves between the gyri. With atrophy, the ventricles—fluid filled cavities in the brain—get larger. Such physiological changes are ultimately linked to cognitive impairment and mental decline.

Currently, there is no cure for ALZHEIMER's. The approved drugs, such as donepezil^[9] or memantin^[10], do not treat the underlying disease or delay its progression, but help mask the symptoms. The precise mechanisms of these drugs, however is not fully understood. Nevertheless, it is generally accepted that many symptoms are, on the one hand, related to substantial loss of elements of the cholinergic system. In this case, donepezil inhibits hydrolysis of acetylcholine by reversibly inactivating the cholinesterases. The increased acetylcholine concentrations counteracts the cholinergic deficit particularly in the cerebral cortex.^[11] Memantin on the other hand, targets the glutamatergic system and acts as uncompetitive antagonist at NMDA receptors.^[12] By blocking harmful effects of glutamate, the release of ion channels connected to the receptors is re-enabled for physiological signals: learning and memory processes can continue. However, the positive effects of the drugs on attended symptoms are relatively low. Meanwhile, the global cost of dementia is estimated to be \$605 billion, which is equivalent to 1% of the entire world's

corresponding prefix, for example, *hemi-* (C₅), *mono-* (C₁₀), *sesqui-* (C₁₅), *di-* (C₂₀), *sester-* (C₂₅), and *triterpenes* (C₃₀). Whereas structurally the most decisive factor is attributed to the carbon framework, additional functional groups, such as hydroxyls, carbonyls and lactones play a critical role in defining the molecule's chemical properties and subsequently the pharmacologically relevant interactions. Thus, the natural product class of terpenes can further be divided into specific sub-classes in respect to the presence of specific functional groups, such as lactones.

Sesquiterpene lactones are a class of chemical compounds mostly consisting of natural sesquiterpene derivatives containing a lactone ring. More than 4000 representatives of the substance class are known and many of them can be found as secondary metabolites in plants. The majority of these compounds possess a broad variety of auspicious biological activities directed toward different predated organisms.^[14]



Figure 3.2. Molecular structures of the sesquiterpene lactones Artemisinin (4), Lactucin (5), and Picrotoxinin (6).

Many of the natural-product-containing herbs are used in traditional medicine such as Artemisinin (4)—isolated from sweet wormwood, a highly-effective anti-malarial agent,^[15] Lactucin (5)—found in lettuce, a bitter solid with analgesic and sedative properties,^[16] and Picrotoxinin (6)—isolated from the Indian Berry, a non-competitive GABAA ion channel blocker (figure 3.2).^[17] Since plants are an important source of natural products, the examination of specific genera often reveals whole families of structures that share certain structural elements or functional properties.

3.2 *Illicium* Sesquiterpenes

Illicium, from the Latin *illicere*, “to allure”, is a genus of flowering plants, with most species native to eastern Asia, several parts of North America and the Caribbean. A variety of natural products were isolated from members of the *illicium* genus, such as Chinese star anise.^[18]

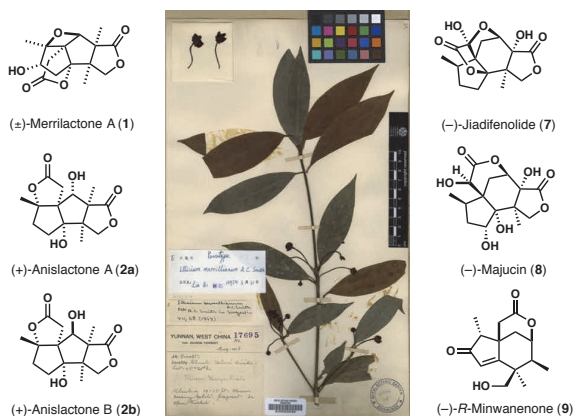


Figure 3.3. Selection of natural products of the *illicium* sesquiterpene family and image of *illicium merrillianum* as part of the herbarium of the Royal Botanic Garden Edinburgh.^[19]

In the year 2000, FUKUYAMA and co-workers reported the isolation and characterization of a series of natural products that were isolated from the wooden pericarps of *illicium merrillianum*.^[20] Structures such as Merrilactone A (1), Anisactone A/B^[21] (2a/2b) and Jiadifenolide (7) form part of a family of *illicium* sesquiterpenes (see figure 3.3).^[22] They have received significant attention from the scientific community not least because of their interesting structural features, as well as their promising biological activity.^[20-21] In line with closely related natural products, these compounds show a high degree of similarity in light of their core structure and functional features.

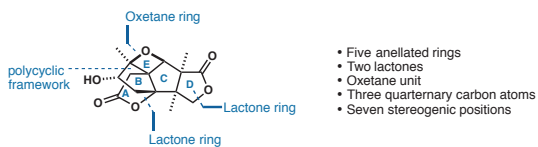


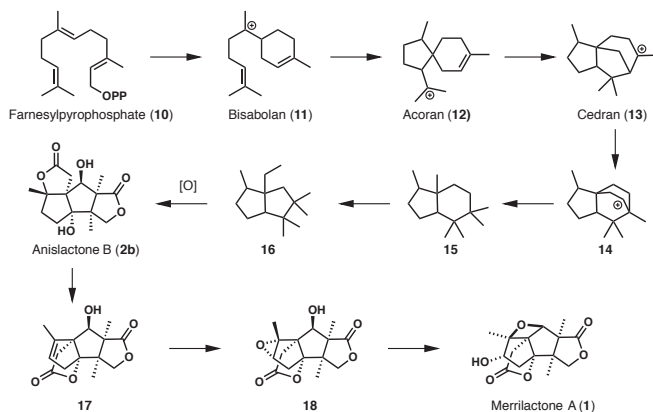
Figure 3.4. Structural features of Merrilactone A, e.g. oxetane ring, polycyclic framework, lactone rings.

Central to the cage-like structures lies a highly substituted carbon ring, which is connected to a number of further carbon rings and oxygen heterocycles. In case of Merrilactone A (figure 3.4), the structure is defined by four contiguous quaternary carbon atoms and exhibits a high degree of oxy-functionalization, that is, two lactone moieties, a hydroxyl group, and an oxetane ring.

3.3 Biosynthesis

In nature, the introduction of chemical complexity—for example, the biosynthesis of terpene natural products—generally proceeds in multiple phases. In the first step—the cyclase phase—the carbon framework is constructed with the aid of enzymes catalyzing a series of reactions including cyclizations, and rearrangements, as well as hydrogen- and alkyl-shifts. In the second step—the oxidation phase—the corresponding carbon frameworks are decorated. Oxidative adjustments such as hydroxylations of activated and non-activated C–H bonds are performed by highly specialized enzymes, that is, powerful oxidases of the heme and non-heme iron enzyme families. Ultimately, this finely tuned process chain is able to generate a myriad of molecular structures, including examples of highly entangled polycyclic structures such as Merrilactone A.

The biosynthesis of Merrilactone A (**1**) starts from dimethylallylpyrophosphate (DMAPP) and isopentenyl pyrophosphate (IPP), which are formed from acetyl-CoA *via* the intermediacy of mevalonic acid in the HMG-CoA reductase pathway. In the first step, the enzyme farnesyl pyrophosphate synthase catalyzes the sequential reaction between DMAPP and two units of IPP, yielding farnesyl pyrophosphate (**10**)—the biosynthetic parent compound of the *illicium* sesquiterpenes.



Scheme 3.1. Proposed biosynthesis pathway of the *illicium* sesquiterpenes Merrilactone A (**1**) and Anisactone B (**2b**) from Farnesyl pyrophosphate (**10**).

As depicted in scheme 3.1, Bisabolane (**11**), generated by the cleavage of pyrophosphate and subsequent cyclization, is enzymatically transformed to Acorane (**12**) and Cedrane (**13**) to form the tricyclic intermediate **14**. According to the mechanism proposed by FUKUYAMA and co-workers, all characteristic sesquiterpenes found in *illicium* star anise can be traced back to this intermediate.^[20b] Carbon–carbon bond

cleavage results in the formation of compound **15**, from which after repeated bond cleavage and rearrangement the carbon framework of the natural product is formed. Introduction of the oxygen functionalities gives rise to Anislactone B (**2b**), which allows the semi-synthetic access to **1** by chemical conversion over compound **17** and **18**.^[23] In cases of the biosynthetic transformation, a similar process can be assumed.

3.4 Biological Activity

Based on biological studies on the cortical neurons of fetal rats, many *illicium* sesquiterpenes, for example, Merrilactone A- or Jiadifenine-type structures, are attributed with significant neurotrophic activities.^[24]

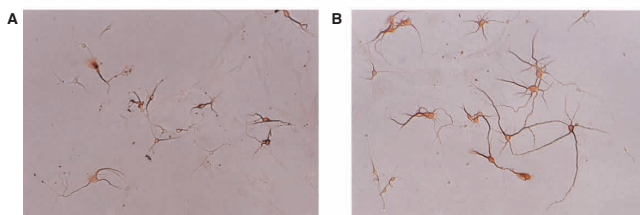
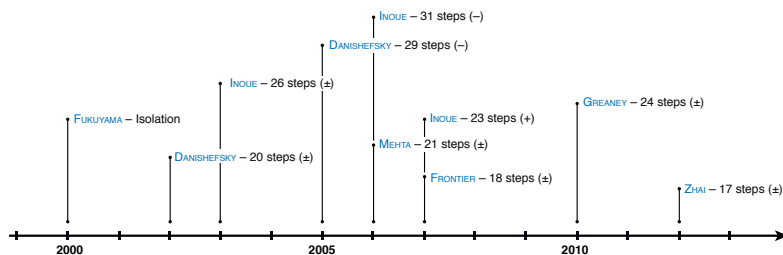


Figure 3.5. Neurotrophic effect of **1** in a six-day-old culture of rat cortical neurons; (A) control culture treated with 0.5% EtOH; and (B) culture treated with (\pm)-**1** (0.1 mmol/L).^[20a]

The enhancement of neurite outgrowth, that is, axons and dendrites, can be observed already at concentration levels of natural product (\pm)-**1** as low as 0.1 $\mu\text{mol/L}$ (see Figure 3.5).^[20a] As a small, non-peptidic molecule, compound (\pm)-**1** provides an alternative to neurotrophic factors which ensure preservation of the neurological system, that is, the outgrowth of neurites and synaptic connectivity. Although, neurotrophic factors are classified as potential therapeutics against neurodegenerative disease such as PARKINSON'S or ALZHEIMER'S^[25], their clinical application is, however, limited by their poor bioavailability, high molecular weight, and the unfavorable pharmacokinetic, as well as the problems associated with the blood–brain-barrier permeability.

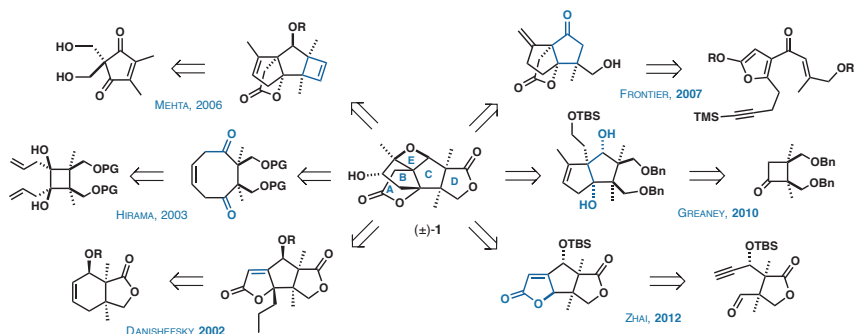
3.5 Previous Synthetic Studies

Because of their challenging structures and attractive biological activity, the *illicium* sesquiterpenes, and particularly Merrilactone A, have been the target of a series of synthetic studies that have resulted in a number of successful total syntheses.



Scheme 3.2. Timeline of total synthesis toward the natural product Merrilactone A.

As depicted in scheme 3.2, the research published toward Merrilactone A can be summarized in a timeline starting with the year 2000 in which the isolation and the structure of the natural product was described. In the following years, a series of strategies and synthetic routes were established.^[26] Besides the six total syntheses of racemic (\pm)-1, three syntheses of optically active material were presented including the synthesis of unnatural (+)-1. The different strategic disconnections led to various sequences in which the polycyclic framework is constructed.



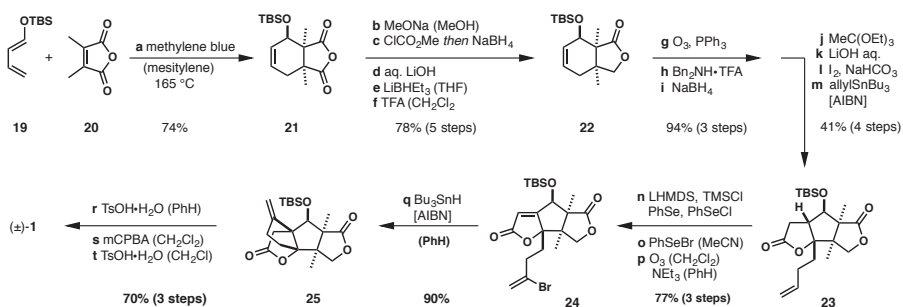
Scheme 3.3. Retrosynthetic analysis of published synthetic approaches to Merrilactone A.

The retrosynthetic routes of previous total syntheses and the corresponding key intermediates are summarized in scheme 3.3. A variety of remarkable reactions have been implemented, including pericyclic

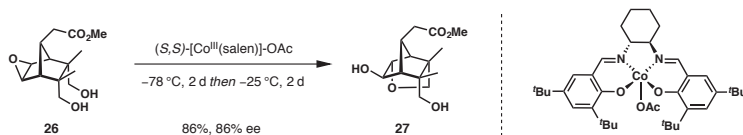
reactions, cycloadditions, ring contraction, and ring expansion reactions. Interestingly, almost all routes utilize synthons and intermediates where most of the oxygen functionalities are already implemented. Additionally, they all share the same final sequence, which is the introduction of the strained oxetane ring. Given these points, the molecular complexity of the *illicium* sesquiterpenes has inspired organic synthetic chemists to conceive a collection of elegant strategies with remarkable inventiveness.

Danishefsky's Synthesis

In 2002, only two years after the characterization of the natural product, the racemic total synthesis of (\pm)-Merrillactone A was presented by V. B. BIRMAN and S. J. DANISHEFSKY.^[27]



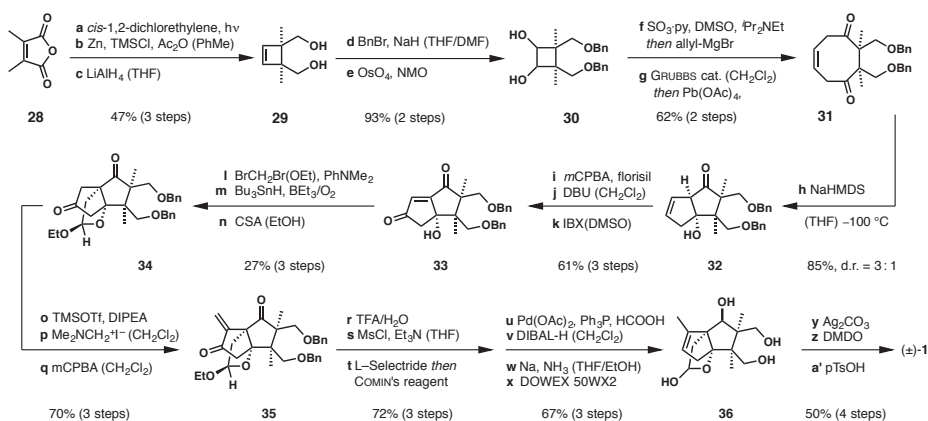
The construction of the five rings follows the sequence [D→C→A→B→E]. As a key step, DANISHEFSKY and co-workers utilized a DIELS–ALDER reaction in order to construct **21** with the C/D ring motif in the desired diastereomeric configuration (see scheme 3.4). Further modifications allow for the construction of **23**. With the two quaternary centers in place, compound **24** is then transformed to **25** *via* a free radical cyclisation in order to close ring **B**. Hence, the route developed allows the construction of racemic Merrillactone A in 20 steps.



DANISHEFSKY and co-workers were later able to develop a strategy for the asymmetric synthesis of the natural product, where a chiral cobalt salen catalyst was employed to open the symmetrical *meso*-epoxide **26** enantioselectively (scheme 3.5). This led in 2005 to the first total synthesis of enantiomerically pure (–)-Merrilactone A in 29 steps.^[28]

INOUE and HIRAMA's Synthesis

In 2003, M. INOUE, M. HIRAMA, and co-workers presented their synthetic route toward (±)-Merrilactone A with a synthetic strategy for the cyclic structure that follows the sequence [B/C→D→A→E].^[29]



Scheme 3.6. INOUE–HIRAMA's route to (±)-Merrilactone A. TMSCl = chlorotrimethylsilane; Grubbs cat. = (PCy₃)₂Cl₂Ru=CHPh; DBU = Diazabicycloundecene; mCPBA = *meta*-chloroperbenzoic acid; L-Selectride = LiBH(s-Bu)₃; COMIN's reagent = 2-Tf₂N-5-chloropyridine.

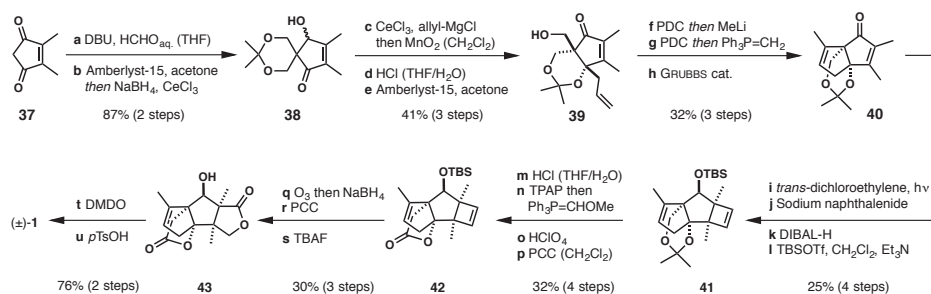
The key step of the synthesis is a transannular aldol reaction (**h**). Desymmetrization of cyclooctadienone **31** by selective deprotonation allows for the diastereoselective C–C bond formation, giving rise to bicyclic keto alcohol **32**. Further modifications include the introduction of the A-ring and installation of the missing carbon in order to complete the natural product framework **34**. After adjusting the redox state on various positions, the deprotected tetraol **36** is oxidized to the desired bislactone with remarkable chemo- and stereoselectivity.

This approach was later refined and the asymmetric total synthesis of (–)-**1** was published in 2006.^[30] The utilization of a chemo- and enantioselective dihydroxylation under SHARPLESS conditions with the catalyst

(DHQ)₂PHAL yields an enantiomerically pure lactone, which led to the establishment of the absolute configuration in the natural products. Furthermore, a flexible asymmetric route to the unnatural enantiomer (+)-1 was presented in 2007.^[31] Here, a chiral lithium amide promoted the enantioselective transannular aldol reaction, establishing the absolute stereochemistry of four chiral centers of the bicyclo[3.3.0]octane moiety.

MEHTA's Synthesis

In 2006, G. MEHTA and co-workers delineated the total synthesis of (±)-1 in a stereo- and regioselective diversity orientated approach. The natural product was formed in 21 linear steps from commercially available starting material.^[32]

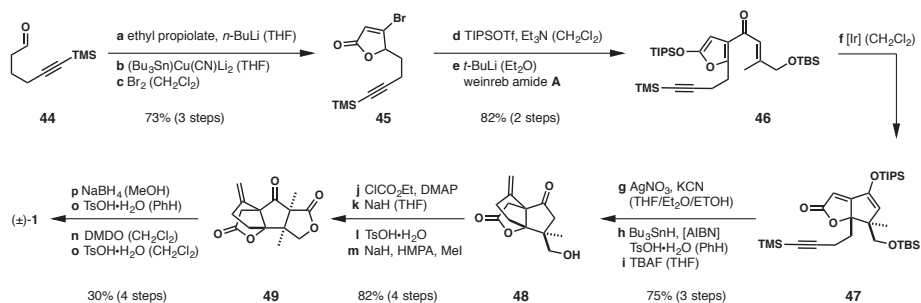


Scheme 3.7. MEHTA's route to (±)-Merrilactone A. DBU = 1,8-diazabicyclo[5.4.0]undec-7-ene; PDC = pyridinium dichromate; GRUBBS cat. = (PCy₃)₂Cl₂Ru=CHPh; DIBAL-H = diisobutylaluminum hydride; TBS = *tert*-butyldimethylsilyl; Tf = trifluoromethanesulfonyl; TPAP = tetra-*n*-propylammonium perruthenate; PCC = pyridinium chlorochromate; TBAF = tetra-*n*-butylammonium fluoride; DMDO = dimethyl dioxirane; *p*TsOH = *para*-toluenesulfonic acid.

As depicted in scheme 3.7, MEHTA's route involves a ring-closing metathesis and a [2+2] photocycloaddition as key steps and follows the sequence [C→B→A→D→E]. Further modification of the photocycloaddition product **41** then sets the stage for ozonolysis of the cyclobutene ring and subsequent reductive work-up. Only the desired regioisomer is formed, presumably because of the steric shielding of the bulky TBS group. Finally, subsequent oxidation to the lactone, and the already established sequence of epoxidation and oxetane formation, gives rise to the natural product (±)-1.^[32]

FRONTIER'S Synthesis

In 2007, A. FRONTIER and co-workers presented the total synthesis of racemic Merrilactone A. The 18-step synthetic route, which is based on a [A/C→B→D→E] strategy, uses a 4 π -electrocyclization as the key step.^[33]

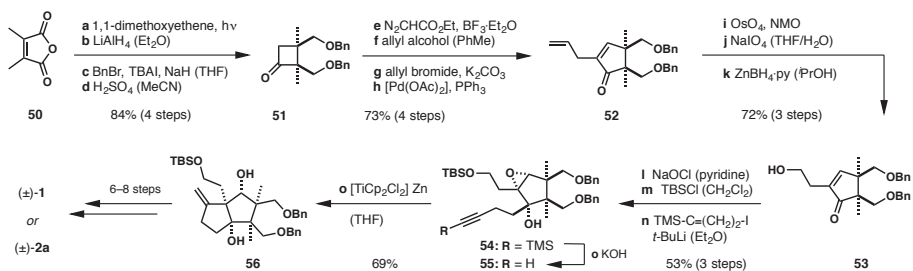


Scheme 3.8. FRONTIER'S route to (±)-Merrilactone A. The reduction of **49** with sodium borohydride yields a mixture of diastereomers from which the undesired product could be separated and recycled by reoxidation. WEINREB amide **A** = (*E*)-4-((*tert*-butyldimethylsilyloxy)-*N*-methoxy-3-methylbut-2-enamide). TIPSOTf = triisopropylsilyl triflate; [Ir] = Ir[(dppp)(CO)(DIB)CH₃]²⁺ 2 Br⁻; DMP = Dess–Martin periodinane; DMDO = 3,3-dimethyldioxirane.

As depicted in scheme 3.8, the synthesis of ketone **46** was achieved by the conversion of a higher order stannyl cuprate to the alkynyl ester accompanied by *in situ* lactonization to **45** and subsequent protection and reaction with a WEINREB amide. The following silyloxyfuran NAZAROV cyclization, which is catalyzed by a dicationic iridium complex, yields the single diastereomeric product **47**. Necessary adjustments to the carbon center, as well as a lactonization sequence, starting from the carbonate, leads to the formation of tetracycle **49**, which after reduction is isomerized and converted to natural product **1** following the known procedures.^[33-34]

GREANEY'S Synthesis

In 2010, M. F. GREANEY and co-workers published the formal synthesis of (±)-Merrilactone A in 24 steps along the first total synthesis of (±)-Anislactone A in 22 steps. The synthesis is characterized by a direct approach to the B-cyclopentane ring using a sequence of photocycloaddition, ring expansion, and stereoselective 1,2 addition as the key C–C bond-forming steps.

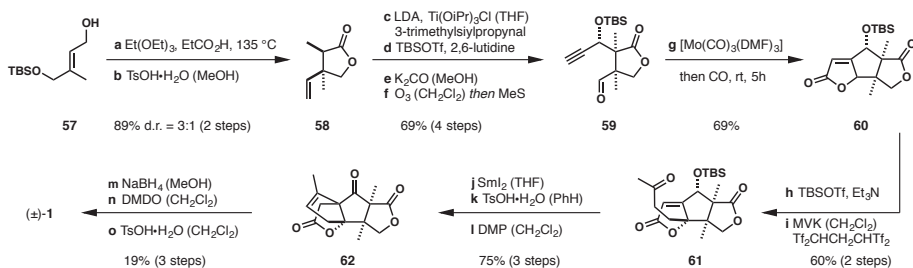


Scheme 3.9. GREANEY's route to (±)-Merrillactone A and (±)-Anisactone A. TBAI = tetrabutylammonium iodide, NMO = *N*-methyl-morpholine *N*-oxide.

As depicted in scheme 3.9, the route starts with a [2+2] photocycloaddition from which, after reduction, protection, and hydrolysis, product **51** is formed. A TIFFENEAU–DEMJANOV rearrangement and further transformation yields the ring-expanded enone **52**, which is converted to **53**. After epoxidation, protection, and alkylation, the defining reductive epoxide cleavage-cyclization of **55** sets the quaternary carbon center at the heart of the sesquiterpene framework structure **56**. Further transformations then give rise to (±)-**1** and (±)-**2a** in 6–8 steps, respectively.

ZHAI's Synthesis

The shortest synthesis of Merrillactone A to date was presented by H. ZHAI and co-workers in 2012. With the ring construction strategy [D→C→A→B→E] this concise route is defined by a series of efficient reactions for the construction of the framework as well as a cycloaddition reaction for the formation of a lactone ring.^[35]



Scheme 3.10. ZHAI's route to (±)-Merrillactone A. The reduction of **62** with sodium borohydride yields a mixture of diastereomers from which the undesired product could be separated and recycled by re-oxidation to **62**. LDA = lithium diisopropylamide, TBSOTf = *tert*-butyldimethylsilyl trifluoromethanesulfonate, MVK = methyl vinyl ketone; DMP = DESS–MARTIN periodinane, DMDO = 3,3-dimethyldioxirane.

Construction of the D-ring by a sigmatropic rearrangement of **57** and further transformation to lactone **59** sets the stage for the key step of ZHAI's route: a molybdenum catalyzed hetero PAUSON–KHAND reaction (scheme 3.10). Then, a vinylogous MUKAIYAMA–MICHAEL reaction and a free radical reaction to structure **62** allows for completion of the synthesis in 17 steps from commercially available starting material.

3.6 Historic Perspective and Modern Total Synthesis

Since the pioneering work of F. WÖHLER and his discovery in 1828 that organic substances, such as urea, can be generated from inorganic material, the research towards the synthesis of natural products has developed into a well-established research field.^[36] R. B. WOODWARD's work of the 1960s, in particular, has influenced the field dramatically.^[37] He showed that not only relatively simple organic compounds could be synthesized, but also that highly complex structures like strychnine^[38] and even vitamin B12^[39] are accessible by total synthesis. With the development of the retrosynthetic analysis, E. J. COREY introduced a systematic approach for solving and planning organic syntheses.^[40] Equipped with a toolbox of organic reactions, highly specialized catalysts, and a variety of available starting materials, researchers have started to tackle ever-increasing challenges. The field of total synthesis has certainly made significant progress in the past decades. However, there are many voices who claim that the synthesis of complex molecules *per se* no longer presents an insurmountable challenge. This claim is typically underlined by referring to successful syntheses of extremely complex natural products such as Erythropoietin^[41] or fragments of Maitotoxin.^[42] With examples of structures with such high degrees of complexity, it today seems clear that in principle any given structure is synthesizable, given enough man-power and funding resources. However, this general criticism demands a closer inspection. Clearly, the synthesis of natural products often requires a huge investment of resources and a substantial amount of working hours. However, upon completion, sometimes only scarce amounts of material are delivered. A good example is the terpene Taxol, which is used in cancer treatment on ton-scale.^[43] Although leading scientists have established a variety of routes, the synthetic approaches are not yet capable of providing enough material for therapy, because of the length (38–51 linear steps) and the low yield (max 0.4%) of the synthetic routes presented.^[44] Therefore, the necessary amounts have to be isolated from natural sources or produced by biotechnological processes. This might seem a reasonable solution on first sight, but a practical synthetic path would provide many advantages, not least because of the potential discoveries of more potent derivatives. Clearly, today's challenges associated with total synthesis have changed. Thus, the field's progress towards efficiency and scalability as the fundamental principle is one of the more essential developments.^[45] A modern synthesis has to be efficient, scalable and short. Consequently, in order to

approach the “ideal synthesis”,^[46] new concepts and retrosynthetic approaches have to be investigated, including the development of efficient methods for late-stage modifications. For this, one of the most promising concepts can be found in the rise of Carbon–Hydrogen bond functionalization as a research field.

4 Methodology: C–H Functionalization

4.1 Reactivity of Carbon-Hydrogen bonds

Carbon–hydrogen bond functionalization (C–H functionalization) in general refers to the replacement of a C–H bond by any other bond in the form of C–X, whereby for X the restriction $X \neq H$ applies. Particularly, it refers to a process in which a carbon–hydrogen bond is cleaved and hydrogen is exchanged with a different functional group (FG), for example, oxygen, nitrogen, or carbon. The strong C–H bond is therefore replaced with a weaker, easier to functionalize one.



Scheme 4.1. General reaction scheme for the replacement of a C–H bond with a C–FG bond.

The general reaction in scheme XX depicts the replacement of an aliphatic C(sp³)–H bond with a functional group. It represents the contrasting concept of the classical approach in which the functionalization of organic compounds relies on pre-established functionalities, for example, carbon electrophiles, nucleophiles, or carbon multiple bonds. C–H bond functionalization has the potential to change the strategies for how organic molecules are prepared. Since carbon hydrogen bonds are traditionally considered to be unreactive due to high chemical stability, a number of obstacles remain before this potential can be harnessed.

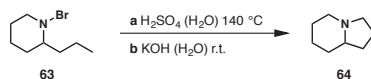
Table 4.1. Physical properties of carbon–hydrogen bond of methane (CH₄).

C(sp ³)–H bond (H ₃ C–H)	value
Bond length	1.09 Å
Dissociation energy ΔH (at 298 K)	439 kJ/mol
Bond energy E	413 kJ/mol
Electronegativity difference $\Delta\chi$	0.35
pK _A value (water)	~48
pK _A value (DMSO)	~56

The physical properties of a typical covalent carbon–hydrogen bond, for example, the C–H bond of methane, are summarized in table 4.1. From this, the chemical properties can be deduced: (i) the inertness of the saturated hydrocarbon compound is a consequence of the high bond energy $E = 413$ kJ/mol, and (ii) C–H bonds are considered to be non-polar because of the small electronegativity difference between carbon and hydrogen ($\Delta\chi(\text{C–H}) = 0.35$, calculated from C(2.55) and H(2.20) using PAULING’s scale). As a result, the acidic strength of C–H bonds is very low ($\text{pK}_\text{A}(\text{CH}_4) = \sim 56$). From the perspective of molecular orbitals, all valence electrons are involved in the formation of bonds. The absence of non-bonded lone pairs and the relative low energies of the occupied orbitals, as well as the high energy of the lowest unoccupied orbitals result in the general low reactivity of aliphatic carbon–hydrogen bonds.

4.2 Historic Perspective of C–H Functionalization

Despite the obvious challenges associated with the functionalization of carbon–hydrogen bonds, the first examples of such transformations can be traced back to over a century ago. One of the oldest strategies for the directed functionalization of non-activated C–H bonds is the HOFMANN–LÖFFLER–FREYTAG reaction. Starting from *N*-halogenated amines, this reaction facilitates intramolecular halogenation and ultimately leads to heterocyclic reaction products. In 1879, little was known about the molecule piperidine except the formula $\text{C}_5\text{H}_{11}\text{N}$. Particularly, there was no knowledge of the structural identity of the C_5H_{10} -fragment. On the assumption that this fragment was merely an “associate” of known unsaturated components, A. W. HOFMANN began to treat piperidine with concentrated hydrochloric acid and elementary bromine in the hope that it would provide evidence for the suspected addition products.^[47] Although it turned out that this hypothesis was untrue, his subsequent experiments in alkaline media revealed that (i) *N*-halogenated derivatives are accessible from piperidine and 2-propylpiperidin by treatment with bromine, and that (ii) these derivatives disintegrate easily to re-form the starting material.^[48] Regarding 2-propylpiperidine Hofmann noted: “*Es ist gerade [diese] Verbindung gewesen, welche in jüngster Zeit mit Vorliebe studirt [sic] worden ist und es hat sich gezeigt, dass dieselbe in mannichfache [sic] und zum Teil ganz bemerkenswerthe Umbildungen erleidet, dass sie sich namentlich mit Leichtigkeit durch Abspaltung von Bromwasserstoffsäure in analoge wasserstoffärmere Basen verwandeln lässt.*”^[49]



Scheme 4.2. The first synthesis of (±)- δ -coniceine by directed C–H functionalization.

Upon treatment of *N*-bromo-2-propylpiperidine (**63**) with hot sulfuric acid and subsequent alkaline work-up, HOFMANN succeeded in synthesizing the bicyclic tertiary amine (\pm)- δ -coniceine (**64**).^[47a, 49] It was only ten years later that E. LELLMANN from the University of Tübingen commented on the constitution and the structure of the amine product with the assumption that the outcome of this reaction consists of the bicyclic amine **64**: “Berücksichtigt man ferner, daß besonders leicht fünfgliedrige Ringe, bestehend aus vier Kohlenstoffatomen und einem anderen (O, S, N) sich bilden, so wird man als vorläufig wahrscheinlichsten Ausdruck für die Constitution des δ -Coniceins schreiben müssen.”^[50]

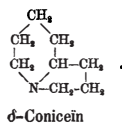
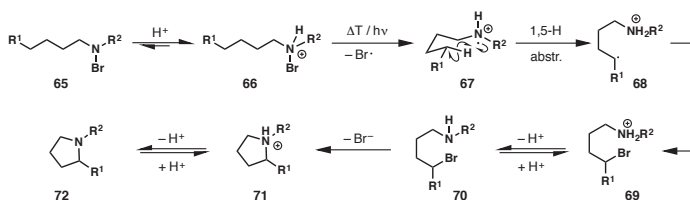


Figure 4.1. Structural formula of δ -Coniceine from the publication “Über die Coniceine” by E. LELLMANN.^[50]

The proposed structure in figure 4.1 was later confirmed by K. LÖFFLER and H. KAIM. In the following years LÖFFLER and his colleague C. FREYTAG began to apply the “Hofmann method” to non-cyclic, secondary amines, resulting in the successful conversion of a series of substrates. In their corresponding publication, an elegant synthesis of nicotine was reported and the researchers conclude: “Demnach scheint diese Methode allgemeiner Natur zu sein und eine einfache Bildung *N*-alkylierter Pyrrolidine darzustellen.”^[51]

A detailed mechanistic description as a radical chain reaction was postulated by WAWZONEK and co-workers^[52] which was later confirmed by E. J. COREY and W. R. HERTLER as part of an experimental study.^[47a, 53]



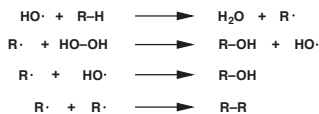
Scheme 4.3. WAWZONEK mechanism of the acid-catalyzed HOFMANN–LÖFFLER–FREYTAG reaction (R^1 = Alkyl, aryl, H; R^2 = Alkyl, acyl, H; Cl / I possible instead of Br).

The classic HOFMANN–LÖFFLER–FREYTAG reaction usually takes place under acidic reaction conditions (scheme 4.3). First, the *N*-halogenated amine **65** is converted to the corresponding ammonium salt **66** by protonation. Initiation by heat, chemicals, or light leads to a formation of the *N*-centered radical **67** by

homolytic cleavage of the N–X bond. The resulting ammonium radical cation can undergo a 1,5-hydrogen abstraction *via* a six-membered transition state. Recombination with the halogen radical yields the δ -functionalized ammonium **69**, which after deprotonation can undergo an intermolecular substitution. Upon treatment with base, the cyclization product **71** then reveals the cyclic amine **72** as the reaction product.

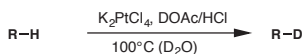
As stated above, the initiation step of the HOFMANN–LÖFFLER–FREYTAG reaction can be achieved by various methods, for example, initiation by heat (thermal), by radical starters (chemical), or irradiation with light. In the case of thermal initiation, the literature contains varying temperature details, typically in the range of 60°C to 140°C.^[47a] An experimental determination of the optimal reaction temperature is in most cases necessary, since it highly depends on the substrate and already small deviations (~5°C) can result in lower yields. The initiation step can also be performed with the aid of catalytic amounts of chemical substances, for example, hydrogen peroxide (H₂O₂), potassium peroxodisulfate (K₂S₂O₈), or ammonium iron(II) sulfate (NH₄)₂Fe(SO₄)₂—known as MOHR’s salt. However, the most practical initiation method was found in the exposure to light in the UV-range. Usually, this process proceeds at room temperature or alternatively at 0 °C for minimization or avoidance of premature and undesired decay of the *N*-halogen compounds. Interestingly, when the photochemical conversion takes place under the influence of oxygen, COREY and HERTLER suggest an induction period of several minutes. Generally, oxygen as a diradical molecule has a restraining effect on the reaction process, which substantiates the mechanistic description of the free radical process.^[47a, 53] In contrast to the thermal and chemical initiations, for the radical initiation with light the generation of **XX** (scheme XX) does not proceed by a cleavage of the ammonium ion **XX**, but directly from the *N*-halogenated amines **XX**. They are—as opposed to their corresponding conjugated acids—able to absorb UV-light allowing for the homolytic cleavage of the N–C bond. Since, for instance, the equilibrium of *N*-chloro dialkylamine and its corresponding conjugated acid in a sulfuric acid solution of c(H₂SO₄) = 1 mol/L lies almost completely on the side of the unprotonated amine, the initiation of the reaction solely relies on the small amounts of *N*-chloro amine molecules ($\lambda_{max} = 263 \text{ nm}$, $\epsilon_{max} = 300 \text{ L mol}^{-1}\text{cm}^{-1}$).^[47a, 53] Subsequently, the resulting neutral nitrogen radicals are protonated to the corresponding ammonium radical cations, which then continue to react according to the reaction path in scheme XX. Thus, the *process of initiation* decelerates with decreasing pH levels. The *total reaction*, however, is still acid catalyzed, which can be deduced from the experimental comparison of the reaction yields of *N*-chloro dibutylamine depending on the concentration of sulfuric acid.^[47a]

The HOFMANN–LÖFFLER–FREYTAG reaction is highly selective and the transfer of the hydrogen to the internal radical fragment usually proceeds *via* the favored six-membered transition state (1,5-H abstraction and migration). According to COREY and HERTLER, this circumstance is merely defined by two factors: (i) the linearity of the hydrogen transfer and (ii) the minimization of angle tensions and steric repulsion during the transition state. The closer the atoms are arranged in a linear configuration (N–H–C angle = 180°), the lower the activation barrier of the process. The same dependency holds true for the loss of angle tension and steric interaction, which is why 1,3- and 1,4-H migrations are not observed. Conversely, for transition states with eight or more atoms (1,7-H abstractions and higher) the influence of these factors vanishes. Here, formation of the cyclic transition state is hampered due to loss of entropy associated with larger sizes of organized transition geometries. Hence, abstractions in δ - and ϵ -position (1,5-H and 1,6-H migration) are favored for these types of C–H functionalization. Although the HOFMANN–LÖFFLER–FREYTAG reaction is a unique example of ingenuity that has undoubtedly changed the field dramatically, there are more discoveries that have had a similar impact and still influence organic chemistry today.



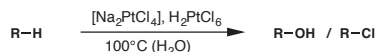
Scheme 4.4. Mechanistic description and formation of radical species of the FENTON chemistry.

In 1894, H.J.H FENTON published an article about the oxidation of tartaric acid in the presence of iron ions.^[54] According to a mechanistic description postulated by MERZ and WATERS (scheme 4.4), the conversion of Fe^{2+} ions with hydrogen peroxide – “FENTON’s reagent” – allows for the formation of highly reactive hydroxyl radicals that can undergo free radical reactions.^[55] This was followed by further discoveries, such as the *electrophilic auration* in non-aqueous media described by KHARASCH and ISBELL in 1931^[56] or the discovery of the first *cyclometallation* by CHATT and DAVIDSON in 1965.^[57] Here, it was shown that for $\text{Ru}(\text{dmpe})_2$ -complexes an intramolecular activation of $\text{C}(\text{sp}^3)\text{-H}$ bonds is feasible. Four years later—GARNETT and HODGES had just discovered the first catalytic H/D-exchange for aromatic carbon centers with K_2PtCl_4 —SHILOV and co-workers achieved the corresponding exchange reaction for sp^3 -hybridized atoms.^[58]



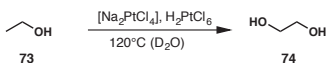
Scheme 4.5. General description of a platinum mediated hydrogen-deuterium exchange.

Whereas the appreciation of this discovery at that time was relatively low, today the reaction is highly regarded and rated among the first examples of C–H activations with metal complexes (scheme 4.5).^[58–59] Shortly thereafter, SHILOV in 1973 published further results from his studies on the reaction with Pt²⁺ ions. It was shown that the addition of stoichiometric amounts of PtCl₆²⁻ ions as an oxidation agent resulted in the conversion of aliphatic substrates to hydroxylated or chlorinated reaction products.



Scheme 4.6. General description of a SHILOV-type platinum catalyzed functionalization.

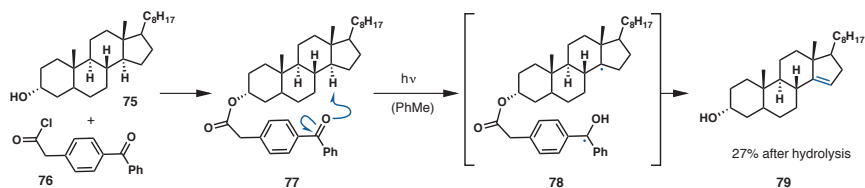
At the beginning of the 1990s, LABINGER and BERCAW submitted the so-called “SHILOV chemistry” to a closer mechanistic inspection with the focus on alcoholic substrates and described the SHILOV reaction in respect to the conversion of ethanol to the corresponding reaction products (see scheme 4.6).^[60]



Scheme 4.7. Platinum catalyzed terminal C–H functionalization of ethanol to ethyleneglycol.

The decisive factor here is less the detailed mechanistic process than the general insights that can be drawn from the reaction. For all hydrogen/deuterium exchange reactions, the formation of several multi-deuterated products was observed. This circumstance was evidence enough for GARNETT and HODGES to postulate that the H/D exchange proceeds *via* an intermediate metal-carbon complex, which subsequently results in the cleavage of the C–H bond. Today, this intermediate is known as the σ -complex and its existence has been experimentally proven.^[60] Even though GARNETT and HODGES were not fully aware of the implications, this finding is inevitably connected to a common characteristic shared by the reactions above: *regioselectivity*. Surprisingly, the analysis of the reaction products always revealed the same tendency for the selective cleavage of the fundamentally more stable, *primary* C–H bond (see scheme 4.7). This type of reactivity contradicts what was known from electrophilic or radical oxidation. Although, usually, the substantially more reactive tertiary, allylic, or benzylic positions are favored, here an opposed reactivity sequence is observed (aromatic C–H > Cycloalkane > primary C–H > secondary, tertiary C–H).^[59–61] This circumstance becomes particularly apparent when looking at the reaction of ethanol (**73**) to ethyleneglycol (**74**) in scheme 4.7. Treatment of alcohols with oxidation agents—such as Cr(VI) compounds—usually leads to the oxidation of highly activated C–H bonds geminal to the hydroxy group and formation of aldehydes. Conversely, utilization of the SHILOV system shows a significant selectivity for terminal positions.

Despite the importance of these early examples of extraordinary reactivity, the impact on organic synthesis at that time was rather moderate and the methods were perceived as curiosities. Especially with respect to the possibilities of natural products, the results of simple chemical processes seemed inferior to the results of the biochemical tools. Most enzyme-catalyzed reactions are stereoselective: selective in the choice of substrate, selective in the type of chemical reaction performed, and selective in the region of the molecule attacked when there are several possibilities. “Enzymatic processes frequently achieve levels of selectivity which are not yet attainable by simple chemical means.”^[62] This, however, changed drastically, particularly in the 1960s and 1970s with the pioneering work of BARTON and BRESLOW.



Scheme 4.8. “Remote functionalization” of 3 α -cholestanol (75) with a benzophenone based directing group 76.

Demonstrating the feasibility of directed C–H oxidation in highly complex steroidal substrates such as cholesterol 75 (see scheme 4.8) has allowed hydrocarbon oxidations to move into the spotlight of organic chemistry. Terms such as “remote functionalization”^[62] and “biomimetic chemistry”^[63] were defined in that context. Just as these terms have passed into scientific parlance and are still used very frequently today, C–H functionalization methodology has developed a unique diversity and widespread implementation.

4.3 Overview of C–H Functionalization Methods

Due to the variety of mechanisms exploited in achieving C–H functionalization, a complete representation of the methods available is neither practical nor expedient. Instead, the existing methodology can be summarized and categorized in order to delineate the range of reactions and demonstrate the tangibility of the concept. Accordingly, here the focus is set on non-activated aliphatic carbon–hydrogen bonds. In particular, such reactions are emphasized that allow the introduction of oxygen functionality to sp^3 -hybridized carbon centers.

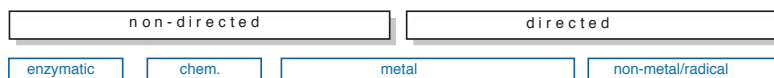
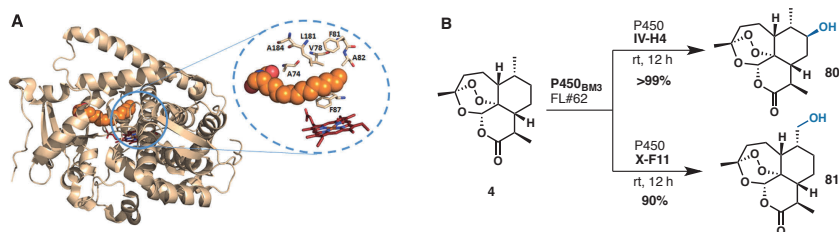


Figure 4.2. General categorization of C–H functionalization methods.

In general the C–H functionalization reactions can be divided into two classes: those occurring without coordination prior to the cleavage of the C–H bond (non-directed/innate) and those directed by coordination to an existing functional group within the target prior to the cleavage of the C–H bond (directed).^[64] As such, the methods can be further divided into subcategories: enzymatic, chemical, metal-based, and non-metal/radical methods (see figure 4.2).

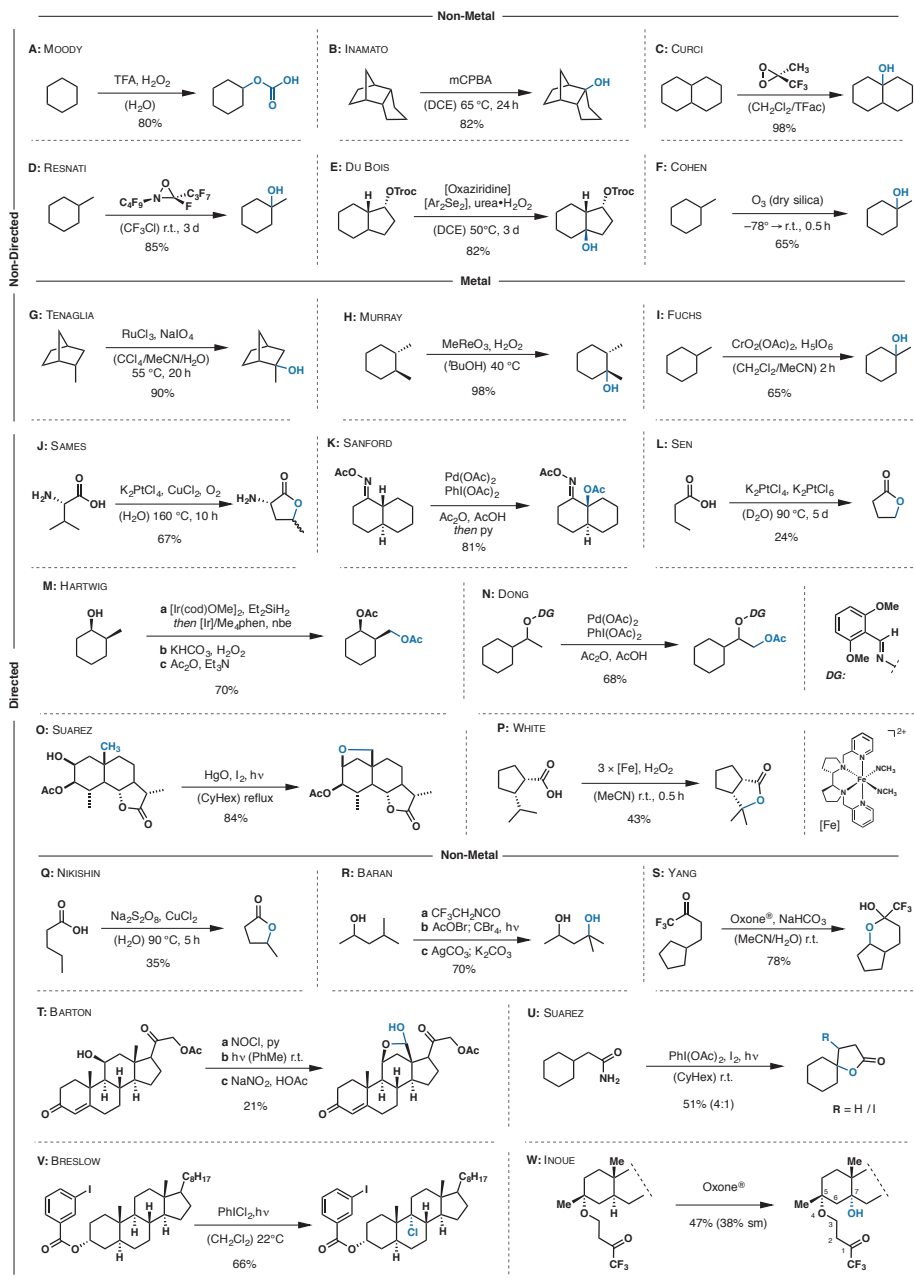
The *biochemical* approach toward C–H functionalization harnesses the potential of powerful enzymatic systems such as cytochrome P450.^[65] These enzymes can be modified by directed evolution in order to provide an optimal conversion for specific targets, as well as high regio- and chemoselectivity.^[66] Because of the chiral nature of protein structures, it is furthermore possible to render the catalysts suitable for diastereo- and enantioselective transformations.^[66b]



Scheme 4.9. **A:** Crystal structure of P450_{BM3} (heme domain) in complex with *N*-palmitoylglycine (PDB code: 1JPZ).^[65] The bound substrate is displayed as sphere models (orange), and the heme is displayed as stick model (red). The dotted circle highlights the first-sphere active site.^[67] **B:** Functionalization of Artemisinin (**4**) with a P450 biocatalyst.

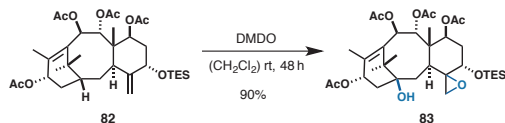
As illustrated in scheme 4.9, FASAN and co-workers developed a strategy to hydroxylate isolated sp^3 C–H bonds selectively. Using Artemisinin (**4**) as a model substrate, they described a P450 oxidation biocatalyst capable of hydroxylating remote, unactivated aliphatic sites in a complex scaffold.^[67] Both the secondary and the primary positions are accessible (**80** and **81**), after extensive optimization of the enzyme. Notably, a major disadvantage of such “tailor-made” enzymes is that the outstanding activity and selectivity of these systems is at the cost of the substrate scope. The inherent limitation is the result of adjustments and the structural tuning of the catalytically active pocket, which is optimized for the specific substrate and the geometry of the enzyme-substrate complex. Consequently, this allows only limited structural variability. Thus, one important strategic objective for chemical methods should lie in the general applicability to complement biochemical approaches.^[66a]

As illustrated in scheme 4.10, the *chemical methods* for the innate conversion of non-activated C–H bonds include strong oxidants such as hydrogen peroxide^[68] or *meta*-chloroperoxybenzoic acid (**B**, scheme 4.10).^[69] In addition, the oxidation can be performed with hydrogen peroxide and trifluoroacetic acid (**A**, scheme 4.10).^[68, 70] Often, such methods depend on relatively harsh reaction conditions, that is, high temperatures, acidic media, and an excess of oxidants. Therefore, the selective functionalization with a good conversion and without over-oxidation often presents a challenge.^[71] Nevertheless, C–H oxidation methods are available that can allow functionalizations under controlled conditions. Such systems exploit the reactivity of strained ring systems such as dioxiranes or oxaziridines,^[72] as well as the highly reactive ozone^[73]. Dioxiranes are known as the smallest cyclic organic peroxides, with the most prominent examples being dimethyldioxirane (DMDO) and methyl(trifluoromethyl)dioxirane (TFDO).^[74] While TFDO is known to be ~100 times more reactive than DMDO,^[75] these heterocyclic compounds are both used for a variety of oxidations.^[76] Dioxirane compounds are highly unstable but can be isolated and stored at -20 °C in solutions with typical concentrations of 0.07–0.1 M for DMDO and ~0.8 M for TFDO.^[77] Although the most practical methods have been described for the generation *in situ*,^[78] ketone-free solutions can also be obtained. However, in certain cases the reagent is more potent in a less polar solvent, for example, dichloromethane. Dioxiranes are commonly used for epoxidations of alkenes and when generated from chiral ketones they can also be utilized for enantioselective transformations, that is, SHI epoxidation.^[79] Most importantly, the chemical properties of dioxiranes enable their use as a highly reactive O-transfer reagent.^[80] Hence, the direct oxidation of aliphatic carbon centers is possible under relatively mild reaction conditions, as well as with control over the regio- and chemoselectivity.



Scheme 4.10. C–H functionalizations: directed and non-directed methods, and metal and non-metal methods.

Whereas electron withdrawing groups decrease the reactivity towards the electrophilic attack of dioxiranes, donor substituents enhance the reactivity and sometimes even alter the site-selectivity.^[81] In the literature, there are numerous examples for the functionalization of non-activated C–H bonds by DMDO or TFDO, including the transformation of relatively simple compounds,^[82] as well as application of the method to highly complex systems.^[81, 83]



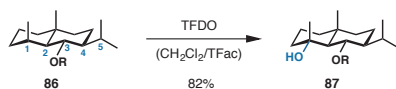
Scheme 4.11. Epoxidation and hydroxylation of the Taxane framework with DMDO.^[84]

In 2000, ORITANI reported on the functionalization of Taxane derivative **82** by treatment with DMDO (scheme 4.11). The reaction conditions allowed the transformation of the disubstituted olefin to the epoxide, as well as the introduction of the hydroxy group by selective functionalization of the bridgehead carbon–hydrogen bond. In this case, the tetra-substituted olefin remains untouched, presumably due to sterical hindrance of the quaternary carbon center.^[84]



Scheme 4.12. Epoxidation and hydroxylation of the cholestane framework with TFDO.

In the case of compound **84** (scheme 4.12), not only are the four double bonds of the cholestane framework epoxidized, but, most importantly, the selective hydroxylation of the isopropyl side chain at C²⁵ is observed.^[85] Another good example for the control over the selectivity, which can be achieved with dioxirane oxidation in complex polycyclic carbon structures, was disclosed by the BARAN group.



Scheme 4.13. Selective innate Hydroxylation of the equatorial C–H bond of the dihydrojunenol derivative with (trifluoromethyl)methyl dioxirane. R = –C(O)NHCH₂CF₃.

As part of the synthetic studies of Eudesmane terpenes, the successfully cyclized dihydrojunenol framework **86** was treated with a freshly-prepared solution of TFDO (see 4.13).^[86] One of the questions when applying the “C–H oxidation logic” to synthesis is whether the crucial transformations can take place in a predictable or at least comprehensible manner. In order to provide an answer to this question, the reactivity tendencies discussed above have to be considered. Since tertiary positions preferably react with TFDO, there are theoretically five sites available for oxidation of compound **86** (see scheme 4.13, C¹–C⁵). Using ¹³C-NMR chemical shifts (δ), the relative electronegativity trends were established as follows: $\delta(\text{C}^3) = 73.6 \text{ ppm} > \delta(\text{C}^2) = 55.2 \text{ ppm} \approx \delta(\text{C}^4) = 50.2 > \delta(\text{C}^1) = 27.5 \approx \delta(\text{C}^5) = 26.6$. This implies that the introduction of the electron withdrawing carbamate group has significantly depleted the electron density of the surrounding tertiary centers, so that three of the five positions are deactivated against an electrophilic attack. The most likely tertiary C–H bonds to be oxidized therefore are C¹ and C⁵. The C⁵–H bond shows not only a higher electron density but also should be sterically more accessible. However, the C¹–H bond is oxidized selectively. The origin of this selectivity can be explained by (i) the inherent tendency of dioxiranes to selectively oxidize equatorially orientated C–H bonds in preference to those adopting an axial configuration, and (ii) the strain-release effects in the transition state during oxidation.

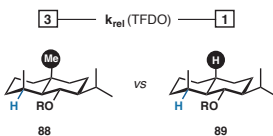
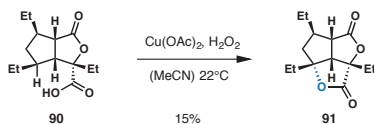


Figure 4.2. Comparison of the reaction rates of two substrates with different substituent in the axial position (Me vs H) for the oxidation with TFDO. **R** = $-\text{C}(\text{O})\text{NHCH}_2\text{CF}_3$.

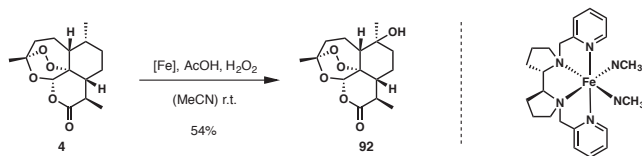
The relative enhancement of the reaction rate due to strain release was already discussed in 1955 by A. ESCHENMOSEER.^[87] An investigation of the oxidation of secondary steroid alcohols with equatorial positions, in comparison to the axially orientated counterpart with chromic acid, resulted in the hypothesis that “the faster the rate-limiting step, the bigger the reduction of non-classical strain in the molecule”.^[87] This subject was investigated experimentally with two bicyclic terpenoid frameworks with different axial substituents (see figure 4.2, marked in black). Oxidation of a 1:1 mixture of both structures revealed the significantly faster reaction to the product of axially methylated **88** (a 3:1 mixture is obtained with TFDO; a control experiment with dry ozone gave a 4:1 mixture).^[88] The relative rate constant $k_{\text{rel}} = 3$ confirms the energy minimization which most likely stems from reduction of the 1,3-diaxial interaction. These results highlight that “in order to plan complex-molecule total syntheses that utilize one or multiple C–H activation steps, a profound understanding of even the subtlest reactivity trends is needed.”^[88]

The properties of *transition-metal systems* such as the FENTON chemistry^[54] have not only laid the foundation for many discoveries,^[59, 89] but also broadened the spectrum of potent oxidants for C–H functionalization with metal-oxo species on high oxidation states, such as methyltrioxorhenium^[90] or chromium(IV) oxides.^[91] In particular, the Gif-chemistry^[92] was developed specifically for the selective functionalization of saturated hydrocarbons. Here the typical system consists of Fe(II) salts, picolinic acid as ligand, and oxidant (*t*-BuOOH, H₂O₂) in Pyr/AcOH as solvents.^[93] As presented by DJERASSI in 1953, catalytic amounts of ruthenium tetroxide can be used for C–H functionalization by *in situ* oxidation with sodium periodate.^[94] Inspired by natural systems, metal porphyrins are powerful oxidants and are used in a variety of applications including C–H oxygenation and can be employed for asymmetric catalysis.^[95] Whereas non-directed methods rely solely on the innate differentiation of possible functionalization sites, directed methods occur by pre-coordination to functional groups within the target. There are many example for directing groups, with the most prominent for metal-based methods being polar coordinating functionalities.^[61a, 96]



Scheme 4.14. Directed C–H oxidation as the final step for the total synthesis of Gracilioether F (**90**).

A good example for the application of such directed methods is the total synthesis of Gracilioether F (**90**) by M. K. BROWN and co-workers which is based on a crucial metal-catalyzed C–H oxidation as the key step (see scheme 4.14).^[97] Although, in a relatively low yield, the last step of the synthesis (**90**→**91**) was achieved by the utilization of a copper catalyst with a reactivity that is most likely related to the FENTON radical chemistry. As one of the first examples for a transition metal based method capable of achieving selective oxidation of unactivated alkanes, the SHILOV system shows selectivity for terminal C–H bonds (*vide supra*). This quality can be further enhanced and adjusted by using functional groups serving as coordinating directing groups. SHILOV-type chemistry under harsh reaction conditions provides access to C–H functionalized products from carboxylic acids. Here, the primary non-activated methyl group is hydroxylated to give rise to the γ -lactone (**J**, scheme 4.10). In addition, a variety of platinum- and palladium-based systems^[98] have been developed and successfully used for directed C–H functionalization.^[60, 99] By employing palladium acetate and periodinanes as oxidants, SANFORD and co-workers described an elegant method for the oxime-directed acetoxylation of non-activated C–H bonds (**K**, scheme 4.10).^[100]



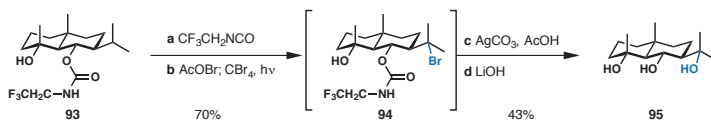
Scheme 4.15. Iron catalyzed C–H functionalization of Artemisinin with the WHITE–CHEN catalyst.^[101]

The WHITE–CHEN catalyst can be used to hydroxylate C–H bonds (**P**, scheme 4.10) in a regio- and chemoselective fashion. The reaction is suitable for application to complex systems, such as the synthesis of the Artemisinin (**4**) in scheme 4.15. Here, the iron-based coordination complex is used along hydrogen peroxide and an acetic acid additive to oxidize aliphatic sp^3 C–H.^[101] The regioselectivity of the system can be explained by steric and electronic effects, but the use of carboxylic acids as directing groups can override the innate reactivity and allow for selective and effective conversions.^[102]

Most *directed methods* often have the requirement that specific substituents are installed and subsequently removed in order to render a functional group more capable of binding the catalyst or reagent. However, by exploiting the high reactivity of free radical species, such a cumbersome transformation can often be avoided.

Methods for C–H oxidation by *radical mechanisms*^[103] go back over a century ago, and over the decades a variety of new methods have been presented.^[104] In particular, remote intramolecular free radical reactions were developed that utilize the reactivity of oxygen and nitrogen radicals.^[105] Although the mechanism is not fully understood, the method presented by NIKISHIN and co-workers is based presumably on a single electron transfer and the high reactivity of the corresponding acyloxy radical. Despite possible decarboxylations as side reactions, they were able to isolate the respective lactone (**O**, scheme 4.10).^[104, 106] Discovered in 1960, the BARTON reaction involves a homolytic oxygen nitrogen bond cleavage, followed by remote hydrogen abstraction, radical recombination, and tautomerization to form an oxime (**T**, scheme 4.10). Because of the possibility to functionalize otherwise inert substrates, this reaction was developed expansively and used to create a number of steroid analogs. Similarly, the “hypiodite” reaction can be used for the synthesis of compounds that contain a five- or six-membered ether ring with remarkable precision and efficiency.^[107] This type of reaction was later investigated in detail, for example, as the key steps for the synthesis of natural products (**M**, scheme 4.10).^[108] As published by YANG and co-workers, trifluoro ketones can be employed as directing groups for the synthesis of acetals. Here, by reaction with Oxone[®] the dioxirane formed *in situ* allows for the site-specific functionalization (**S**, scheme 4.10).^[78, 109] In addition, the trifluoromethyl ketone can be employed for remote oxidations of

complex steroid structures (**W**, scheme 4.10).^[110] As discussed above in detail, one of the most important examples for remote intramolecular free radical C–H functionalization is the HOFMANN–LÖFFLER–FREYTAG reaction. Originally, this method was carried out under acidic conditions, but it has been shown that weakly basic and neutral conditions might also be employed. Consequently, modifications of this reaction were developed, such as the reaction conditions presented by SUÁREZ and co-workers. Here, hypervalent iodine reagents^[111] in the presence of iodine are used to generate the nitrogen-centered radical.^[108, 112] Interestingly, the reaction conditions can also be applied to the synthesis of lactones by amidyl radicals (**U**, scheme 4.10).^[113] By employing a carbamate directing group, BARAN and co-workers re-visited this reactivity and devised a method to synthesize 1,3-diols by the oxidation of non-activated tertiary and benzylic positions (**R**, scheme 4.10).^[114] This radical mediated hydroxylation method was then used as the key step in the synthesis of eudesmane terpenes.^[86]



Scheme 4.16. Selective C–H functionalization of the isopropyl sidechain of the Epiajanol derivate **XX** with the use of trifluoroethylcarbamate as directing group.

As depicted in scheme 4.16, the electron-deficient carbamate acts as a directing group for the remote oxidation of the terpene framework **93**. The sequence of *N*-bromination, homolytic bond cleavage induced by irradiation and 1,6-hydrogen abstraction yields the tertiary bromide **94**. Subsequent cyclization and hydrolysis then gives rise to the corresponding triol **95**. The work represents another step towards the generation of a set of rules and logic for the use of C–H oxidation in terpene synthesis.^[86]

4.4 Terminology and Impact

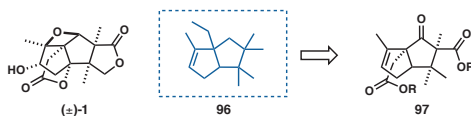
Since the reactivity associated with C–H functionalization has a history of its own and is characterized by a great number of groundbreaking discoveries, the term under which the process was described has exhibited a certain dynamic: The conversion and the replacement of the carbon–hydrogen bond often involves a transition metal and then the reaction usually proceeds *via* an intermediate metalorganic species.^[89] This specific interaction between the metal and the C–H bond under formation of an R–M species is known as “C–H activation”.^[59] Since the discussed transformations in general do not imperatively involve such intermediates, the whole process of replacing a C–H bond with a different bond has to be distinguished from C–H activation. Therefore, the term C–H functionalization summarizes a variety of

transformations, for example, halogenations, oxygenation, and coupling reactions. Accordingly, the term C–H oxidation explicitly emphasizes a change of the oxidation state. In recent years, however, the more general term “functionalization” has been predominantly used since it highlights the versatility and refers to a variety of synthetic transformation including cyclizations, bi-aryl couplings, and the introduction of versatile functional groups (C, N, O, B and halogen) at both sp^2 - and sp^3 -centers.^[115]

C–H functionalization chemistry has the potential to change the way researchers approach organic synthesis.^[116] It could enable the conversion of abundant and inexpensive hydrocarbons into more valuable complex organic compounds.^[117] Furthermore, innovative strategic disconnections in the planning stage and potential late-stage modifications^[118] of established structures can reveal new routes and synthetic accesses.^[119] In addition, new methods that exploit the concept of “H as a leaving group”^[120] and are characterized with high chemo-, regio-, and stereoselectivities, as well as a broad functional group tolerance, enable a variety of new applications.^[61b] Despite the challenges to be met, C–H functionalization chemistry often reveals its full potential when applied to fields such as the total synthesis of natural products or as the underlying concepts for the investigation of pharmacophores.^[121]

5 Motivation and Objective

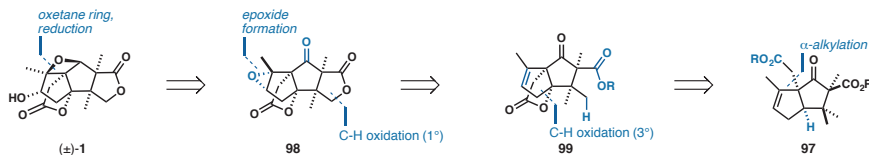
The natural products of the *illicium* sesquiterpene family hold significant potential as pharmacophoric motifs in the development of therapeutic agents for the treatment of neurodegenerative diseases. Despite the high oxygen functionality of the natural products, previous studies toward Merrilactone A or Anislactone A/B have focused on synthetic routes that rely on pre-functionalized synthons and sequences with pre-established oxygen functionalities. A new approach that relies on the a late-stage modification of the carbon framework by C–H functionalization seems, therefore, highly desirable especially in light of the focus on efficiency, scalability, and diversity.



Scheme 5.1. Natural product (±)-1, carbon skeleton and simplified terpenoid structure.

As depicted in scheme 5.1, application of the C–H oxidation logic results in a dramatic simplification of the terpenoid structure. These simplified core structures are opted for as they allow the identification of a scalable synthetic access to *illicium* terpenoids, as well as to investigation into the potential retention of biological activity. For this purpose, the goal is to establish an efficient synthesis of the natural product's framework and to use the carbon skeleton as a platform for C–H functionalization reactions. Hence, the aim is to establish a library of natural product analogs and investigate the activity potential. In order to examine the structure–activity profile, a suitable neuro assay has to be used to reveal those structural derivatives that exhibit neurotrophic properties and capabilities of initiating neuronal outgrowth.

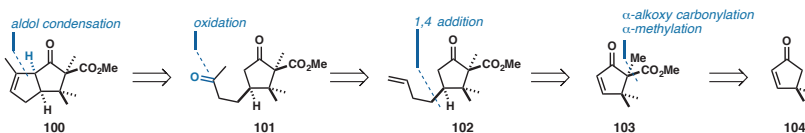
5.1 Retrosynthetic Analysis



Scheme 5.2. Retrosynthetic analysis of Merrilactone A (1).

The retrosynthetic analysis of (±)-Merrilactone A (1) begins with the strategic disconnection of the oxetane ring and reduction (see scheme 5.2). As has been shown by previous studies, this transformation can be achieved *via* a PAYNE-like rearrangement. Consequently, the required epoxide ring can be derived from

the corresponding olefin. The key steps are the disconnections of the lactone rings. Here, a C–H functionalization of a primary C(sp³)–H bond of **98** is required, as well as the C–H functionalization of the tertiary position in **99**. This results in the simplified core structure of the *illicium* sesquiterpene carbon framework **97**. An α -alkylation of the β,γ -unsaturated ketone then allows for the modification of the cis-bicyclo-[3.3.0]-octane moiety.

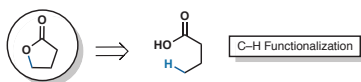


Scheme 5.3. Retrosynthetic analysis of the framework of (\pm)-**1**.

Synthesis of the bicyclic structure is achieved by a sequence of reactions, that is, aldol condensation, oxidation, and a 1,4-addition to enone **103** (scheme 5.3). Finally, α -methylation of the 1,3-dicarbonyl compound, as well as an α -alkoxycarbonylation, reveals the commercially available dimethylcyclopentenone (**104**)^[122] as a starting point of the synthetic route.^[123]

5.2 Synthesis of Lactones

Since one of the major structural challenges associated with a C–H oxidation approach to the *illicium* sesquiterpenes lies in the synthesis of their oxygen-containing heterocycles, methods for the synthesis of lactones by C–H functionalization are to be specifically investigated. Although there are a few methods available for the introduction of lactone rings to complex carbon frameworks, the direct functionalization of non-activated primary C(sp³)–H bonds poses an especially significant challenge.



Scheme 5.4. General retrosynthetic analysis of lactones by C–H functionalization.

Consequently, the development of a general method for the synthesis of lactones which is based on C–H functionalization (see scheme 5.4) might allow the application to complex polycyclic substrates. Accordingly, the feasibility, scope, and limitations of such C–H functionalization methods have to be examined and established.

6 Results and Discussion

6.1 Synthesis of Lactones via C–H Functionalization of Non-Activated C(sp³)–H Bonds

Reproduced from *Org. Lett.* 2016, 18, 6472–6475 with permission from the American Chemical Society (ACS). © ACS 2017

Lactone rings occur as a common and widespread structural motif in natural and synthetic compounds. In particular, many fine chemicals, natural products, and pharmaceuticals comprise saturated γ -lactones. Naturally occurring lactones, such as γ -decalactone, often contribute to the aroma of various foods and fruits or exhibit interesting biological activities such as the neurotrophic sesquiterpene jiadifenolide or the antibacterial peptidoglycan biosynthesis inhibitor avenaciolide (Figure 6.1).^[124] Most methods for synthesizing saturated γ -lactones, such as halolactonization or intramolecular substitutions, depend on prefunctionalized γ -positions, with either electrophilic or nucleophilic properties (Figure 6.1).^[125] In nature, however, in many cases such oxygen heterocycles are introduced by selective oxidation of scarcely functionalized carbon frameworks by powerful oxidases such as the heme and non-heme iron enzyme families.^[66a]

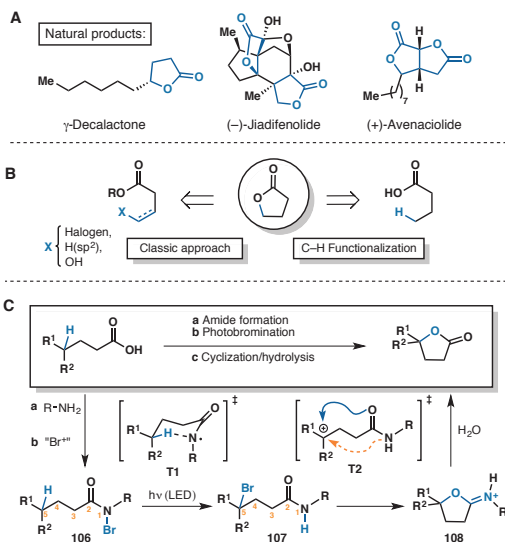
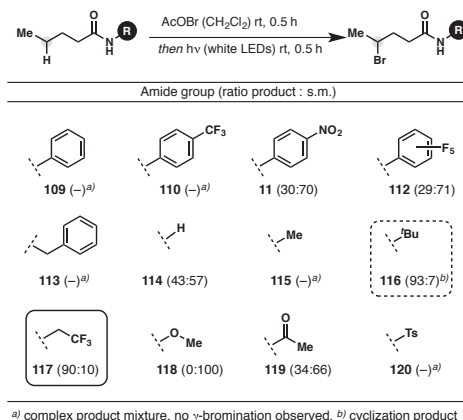


Figure 6.1. A: Selection of natural products containing γ -lactones. B: Retrosynthetic approaches towards γ -lactones. C: Mechanistic description for the lactone formation.

Since the pioneering observations of HOFMANN, LÖFFLER and FREYTAG,^[47, 51, 107a] a variety of methods have been established to directly transform C–H bonds. New concepts enabling innate and directed C–H

functionalizations with control over regio- and stereoselectivity are emerging, including transition metal-catalyzed reactions.^[64, 121c, 126] Nevertheless, the extraordinary properties of nitrogen-centered radicals and the high selectivity of radical hydrogen abstractions still inspire scientists to develop novel methods for controlled oxidation in a variety of applications.^[105d, 114, 127] Since the 1960s, there have been reports that amidyl radicals can in principle be used to form γ -lactones *via* hydrogen abstraction.^[113, 128] Nevertheless, such a lactonization has not found application in synthesis. As SUÁREZ stated in 2005,^[105b] this is due to the narrow scope, the low chemical yields and poor reproducibility of the procedures published. A method that allows for the functionalization of non-activated tertiary, secondary and also primary C–H bonds is highly desirable but not available so far. Ideally, it would operate under mild conditions and tolerate a wide variety of functional groups. In order to find solutions for this challenge, we conducted a systematic investigation of the radical-mediated synthesis of lactones utilizing amidyl directed C–H functionalization. This strategy would follow the mechanism depicted in Figure 6.1. Here, the carboxylic acid is converted to the amide, followed by *N*-bromination to the labile *N*-bromo species **106**. Upon irradiation, this compound forms a nitrogen-centered radical, which can undergo 1,5-H abstraction *via* the six-membered transition state **T1**. Radical recombination gives rise to the γ -bromoamide **107**, which then should allow for cyclization to form the iminium lactone **108** over the amide.^[129] Hydrolysis then yields the lactone.

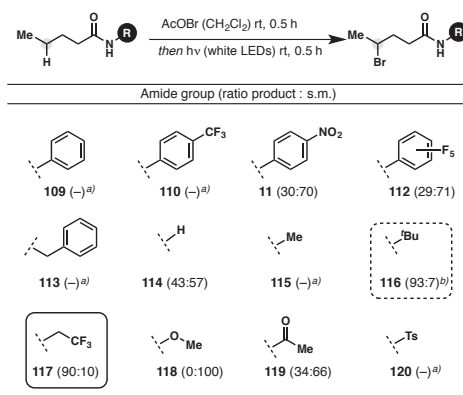
Table 6.1. Screening of *N*-Substituents.



First, different substituents were screened for their aptitude to achieve the desired C–H functionalization on the test substrate pentanoic amide (Table 6.1). Acetyl hypobromite and white LED light were used to generate the *N*-bromo species and initiate the radical reaction, respectively. It became evident that many

substituents show either no γ -bromination (**109**, **110**, **113** and **120**) or moderate ratios of product to starting material (**111**, **112**, **114** and **119**). Very good results were obtained with *t*-butyl amide **116** (93:7, Table 1). However, the *t*-butyl amide underwent spontaneous cyclization to the iminium lactone which proved to be unreactive under a variety of hydrolysis methods, presumably due to the steric bulk of the *t*-butyl group. Calculations and experiments have indicated that especially electron-deficient amidyl radicals tend to readily undergo hydrogen abstractions.^[127a, 130] Since the trifluoroethyl group has proven to be suitable for the carbamate directed synthesis of 1,3-diols as demonstrated by the BARAN group,^[114] we investigated the reaction with trifluoroethyl substituted amide **117**. We were pleased to observe that in this case the hydrogen abstraction led to formation of the C–H functionalized product in an excellent ratio (90:10) without formation of any side products. With a simple route to the γ -bromoamide established, we turned our attention to different cyclization methods and found that formation of the iminium lactone could be easily induced with the addition of silver(I) tetrafluoroborate under mild conditions.^[131] Attempts to isolate and purify the iminolactone after deprotonation with base, however, were unsuccessful.^[132] Instead, facile hydrolysis was achieved at room temperature by directly adding water to the reaction mixture. This finding was unexpected in that *t*-butyl iminolactones (Figure 6.1, **108**, R = *t*-butyl), formed from *t*-butyl amides could only be hydrolyzed under harsh conditions, such as refluxing sulfuric acid.^[105a, 128b] In contrast, we were able to isolate the lactones under very mild conditions. This underscores the advantageous properties of the trifluoroethyl amide as directing group, as it displays an optimal balance of electron deficiency, *O*-nucleophilicity and hydrolyzability.

Table 6.2. Synthesis of tertiary, secondary and primary γ -Lactones.



^{a)} complex product mixture, no γ -bromination observed. ^{b)} cyclization product

Next, we looked at a series of simple substrates to evaluate whether different aliphatic sp^3 -positions can be functionalized. Starting from commercially available carboxylic acids, Table 6.2 shows a series of γ -lactones, which were synthesized by conversion of the respective amides in a one-pot lactonization protocol (for screening details, see Supporting Table S1). Notably, not only tertiary (**121**, **122**, **123**) and secondary (**124**, **125**, **126**), but also primary $C(sp^3)$ -H bonds (**127**, **128**, **129**) were found to be readily functionalized this way, giving rise to the respective γ -lactones in good to excellent yields. Besides compounds with various alkyl lengths, also spirocyclic structures (**123**) as well as α -substituted lactones (**125**, **127**, **128**) are accessible.

In order to investigate the scope and the limitations of the reaction, a series of more complex structures were synthesized and converted to the respective lactones. Here, the fully optimized protocol was utilized (Supporting Table S1). As depicted in Table 6.3, the lactone moiety could be introduced to a variety of structures with different functional groups such as ketones (**130**), protected amines (**131**), aryl units (**132**), and electron deficient olefins (**133**). Also complex polycyclic γ -lactones (**134**, **135**) and bislactones (**136**) were synthesized. In several cases (**132b**, **133b**, **135b**, **136b**, **137b**), yields could be improved by utilizing AgOAc instead of $AgBF_4$ to promote cyclization.

As for most C-H oxidation methods, electron-rich alkenes and enones do not tolerate the radical reaction step; in case of an epoxide-containing substrate we investigated, γ -bromination was successful, but the cyclization conditions required were not compatible (see Supporting Table S2). Moreover, a limitation was found in case of sterically hindered substrates: α -quaternary amides failed to undergo N -halogenation, while one substrate with a sterically very demanding γ -substituent failed to undergo H-abstraction. DFT calculations indicated that in this case the transition state energy was considerably higher than in case of regular substrates (further discussion and mechanistic details based on DFT calculations can be found in the Supporting Information). After having investigated the scope of the reaction, we were interested to see if it is possible to alter the regio- and chemoselectivity by incorporating specific structural features. Substrate **137a** with benzylic C-H bonds in the δ -position diverged from the usually favored transition state and gave rise to the six-membered lactone **137b**. This trend was also observed in case of compound **138a**, where the γ -position was blocked by a quaternary center. Here, also a seven-membered transition state initially led to formation of the δ -bromoamide. However, upon cyclization the system yielded γ -lactone **138b**, presumably *via* 1,2-methyl shift. It is important to note that spatially suitably arranged nucleophilic groups, such as an ester, can outcompete the amide in the cyclization, as shown in the conversion of ester **139a** to γ -lactone amide **139b**.

Table 6.3. Scope and Limitations.

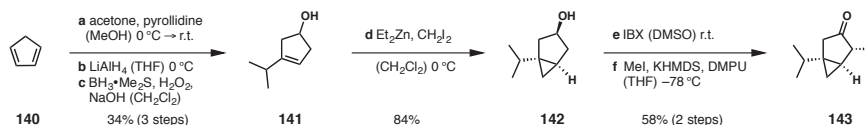
Entry	Substrate	Product	Yield (% ^{a)})
1			49% (85% brsm)
2			48% (90% brsm)
3			75%
4			93%
5			61% ^{c)}
6			20% (29% brsm)
7			37%
8			63%
9			54% (76% brsm)
10			26% (67% brsm)

R = CH₂CF₃; TCP = Tetrachloro phthalimide. ^{a)} isolated yield. ^{b)} AgOAc then AcOH, H₂O
^{c)} determined with CH₂Br₂ as internal standard.

6.2 A Six-Step Total Synthesis of α -Thujone and D₆- α -Thujone, enabling facile Access to Isotopically Labelled Metabolites

Reproduced from *Chem. Commun.* **2016**, 52, 11701–11703 with permission from the Royal Society of Chemistry © RSC 2016

The monoterpene α -Thujone (**143**) is found in a variety of plants and therefore are present in diverse herbal products.^[133] The most famous product containing Thujone is certainly *Absinth*, produced from wormwood. It had been a popular spirit drink in the 19th century but later was prohibited due to concerns about its toxicity.^[134] Absinth was connected to severe health problems, including hallucinations, depressions, convulsions, blindness and mental deterioration. However, more recent studies propose that most of these effects were caused by alcohol intoxication.^[134] Nevertheless, thujone is neurotoxic and was shown to inhibit the gamma-aminobutyric acid A (GABAA) receptor, which leads to excitations and convulsions at higher concentrations in animal studies.^[135] The metabolism of Thujone was investigated both *in vitro* and *in vivo*. Whereas, the major metabolite in *in vitro* studies is clearly the 7-OH- α -thujone (**143**)^[135], *in vivo* studies, point to 2-OH- α -thujone and 4-OH- α -thujone as the main metabolites.



Scheme 6.1. Synthetic route to thujone. KHMDS = Potassium hexamethyldisilazide; DMPU = 1,3 Dimethyl-tetrahydropyrimidin-2(1*H*)-one; IBX = 2-Iodoxybenzoic acid.

After having developed a concise route to Thujone (see scheme 6.1) and its isotopically labelled derivative, we turned to the preparation of the most important metabolites. The oxidation of **143** to 7-OH- α -Thujone (**144**) was described in the literature utilizing ozone as the oxidant.



Scheme 6.2. Hydroxylation of Thujone with TFDO.

However, these conditions lead to considerable over-oxidation and a reduced yield of **144** (47%). After screening several oxidants, we found that methyl-(trifluoromethyl)dioxirane (TFDO) led to a clean conversion to **144** (Scheme 6.2).

6.3 Synthesis and Neurotrophic Activity Studies of *Illicium* Sesquiterpene Natural Product Analogs

Reproduced from *Chem. Eur. J.* **2017**, *23*, 3178–3183 with permission from John Wiley & Sons, Inc. © Wiley 2017

The awe-inspiring structural diversity of natural products has always motivated organic chemists to investigate and develop new synthetic routes, methods and applications. Significant discoveries have been made by studying the chemical structure of these compound and their properties. In particular, the investigation of promising biological activities has resulted in an array of applications of natural products and their analogs as pharmaceuticals. Therefore, natural products are often used as a starting point for drug discovery, in which lead compounds undergo extensive optimization and structural variation.

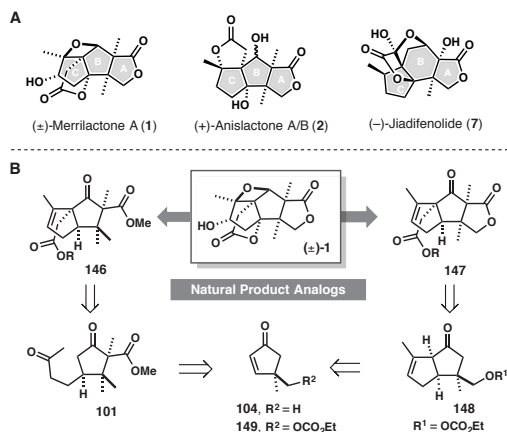
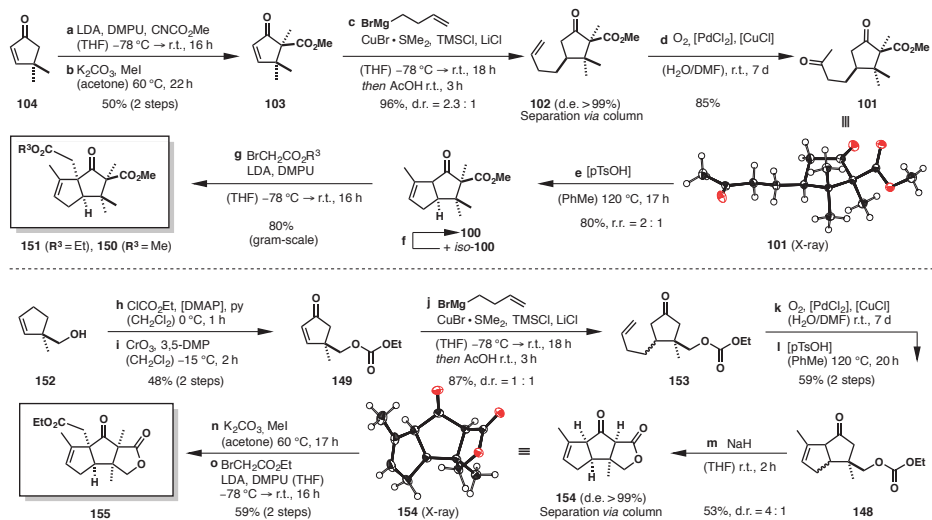


Figure 6.2. A: Neurotrophic sesquiterpene natural products with their core structure (marked in grey). B: Natural product analogs and retrosynthesis.

However, the complexity of natural products can often only be constructed *via* lengthy synthetic routes which may hamper drug discovery. One approach to circumvent this issue is to reduce the complexity of the natural products, while retaining the desired biological activity. Such strategies have been recently summarized by GADEMANN and co-workers who described the promising role of natural product based fragments in drug discovery. They highlighted examples where the structural complexity of natural products was reduced successfully.^[136] Structurally more simple analogs, accessible *via* shorter synthetic routes, can greatly improve chemical tractability and can therefore overcome the limitations of lengthy chemical syntheses.

Since the discovery of several neurotrophic natural products which form part of the *illicium* family, for example, Merrilactone A (**1**),^[137] Anislactone A/B (**2**),^[21] and Jiadifenolide (**7**)^[124] (Figure 6.2A), these compounds have received remarkable attention from the synthetic community,^[26-35, 138] not least because of their challenging chemical structure and their promising biological activity.^[22, 124, 137, 139] The polycyclic small molecules are capable of promoting outgrowth in neuronal cultures.^[140] Therefore, these privileged structures are considered to hold potential for the development of pharmaceuticals for the treatment of neurodegenerative diseases such as PARKINSON'S or ALZHEIMER'S.^[25] In contrast to protein neurotrophins,^[141] for example nerve growth factor (NGF) or brain-derived neurotrophic factor (BDNF), small-molecule neurotrophin-like compounds have been investigated because of their desirable pharmacokinetic properties and pharmacological advantages, that is, low molecular weight, high serum stability and most importantly blood-brain-barrier permeability.^[142] In the case of majucin-type sesquiterpenes, such as Jiadifenolide (**7**), several studies were conducted in order to determine a common pharmacophoric motif.^[139] These investigations led to the identification of several potent analogs and therefore have shown that certain synthetic derivatives can have activities comparable to the natural product. Although a great number of synthetic studies on Merrilactone A (**1**) and Anislactone A/B (**2**) have been performed, no systematic investigation on their structure-activity relationship is available. This might be due to the length of the syntheses reported. As a consequence, variations of the carbon frameworks of the natural products are not readily accessible. We realized that in order to overcome this limitation a synthetic route, which provides simple access to the core structure, was required. An efficient synthesis of the carbon framework would then allow for versatile modification and preparation of natural product derivatives.

We focused our studies on the structural core motif (see figure 6.2A, marked in grey), which consists of a highly substituted central ring structure surrounded by additional rings including a cyclopentane and a γ -lactone. Specifically, our aim was to synthesize structural simplified analogs, investigate their neurite outgrowth activity and ultimately learn about the structure-activity relationship. Importantly, we have placed the emphasis on synthesizing simplified analogs, that is, carbon framework derivatives of (\pm)-**1** and (\pm)-**2**. Two rationally simplified structural derivatives **146** and **147** (Figure 6.2B) were designed by altering the oxidation state and by targeted disconnection of hydroxy functionalities, for example, oxetane and lactone moieties. The synthetic strategy towards these two derivatives is based on the rapid construction of the polycyclic structure from readily available enones. Retrosynthetically, structure **146** (Figure 6.2B) can be traced back to cyclopentenone **104** *via* ring disconnection to diketone **101**. Analogously, lactone **147** is constructed from bicyclic ketone **148**. Here, the γ -lactone ring is attached by employing the pre-functionalized enone **149**.

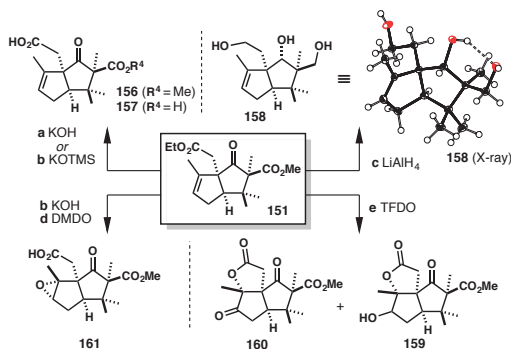


Scheme 6.3. Synthesis of the carbon frameworks **150**, **151** and **155**. **f** [pTsOH] (PhMe) 120 °C, 17 h, quant., r.r. = 2:1. LDA = lithium diisopropylamide, DMPU = 4-dimethyl-aminopyridine, THF = tetrahydrofuran, TMSCl = trimethylsilylchloride, DMF = N,N-dimethylformamide, DMP = 3,5-dimethyl pyrazole.

Synthesis of the core structure (depicted in scheme 6.3) starts with commercially available dimethylcyclopentenone (**104**) which was subjected to an α -methoxycarbonylation using MANDER's reagent,^[143] followed by methylation of the 1,3-dicarbonyl with methyl iodide. A 1,4-addition of the *in situ* formed cuprate gave rise to **102** in excellent yield (96%) and with a diastereoselectivity of 2.3:1. The two diastereomers could be separated *via* column chromatography. After WACKER-oxidation, the desired *syn*-configuration of diketone **101** was confirmed by X-ray crystal structure analysis. Attempts to close the cyclopentene ring failed under a variety of basic conditions. However, treatment with *p*-toluene sulfonic acid^[144] provided bicyclic ketone **100**, along with conjugated *iso*-**100** (r.r. = 2:1), which could be recycled *via* acidic equilibration. Finally, α -alkylation with bromo alkyl acetate yielded structures **150** and **151** (R = Et or Me). The route described allows for the gram-scale access to diastereomerically pure carbon framework derivatives of the natural products.

Furthermore, we were interested in structure derivatives carrying the intact eastern lactone ring. Thus, alcohol **152** was found to be a suitable starting point.^[145] Functionalization with chloroformate and allylic oxidation with chromium(VI) oxide^[146] gave enone **149** in 48% yield over two steps. 1,4-Addition, Wacker-oxidation and acidic cyclization provided deconjugated **148** exclusively. Notably, the carbonate group

survived these transformations, serving not only as a protecting group for the primary alcohol, but also as building block and precursor for the lactone moiety, which was introduced by treatment with sodium hydride. At this point, the diastereomers could be separated *via* column chromatography and the desired *syn*-configuration of bowl-shaped **154** was confirmed by X-ray crystal structure analysis. The 1,3-dicarbonyl compound allowed for two selective α -alkylations, first with potassium carbonate and methyl iodide and then using LDA and bromo ethyl acetate. The concise route provided access to the complete carbon framework structure **155**, which resembles the (\pm)-Merrillactone A core structure including the eastern lactone ring.



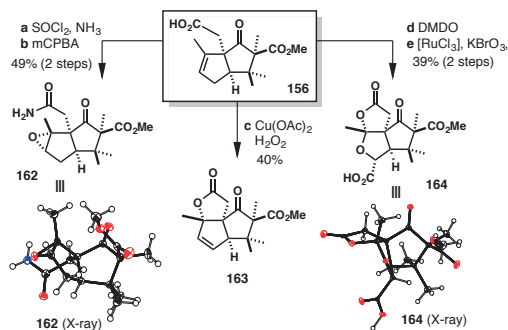
Scheme 6.4. Synthetic pathways starting from diester **16** to different derivatives of the natural product framework. **a** KOTMS (THF) r.t., 4–6 d, 85–95%; **b** KOH, H₂O (MeOH) 70 °C, 2 h, 90%; **c** LAH, (THF) –78 °C → r.t., 18 h, 73%; **d** DMDO, (ac) r.t., 2 h, quant.; **e** TFDO (TFac) –20 °C, 17 h, 64% (1:1). KOTMS = potassium trimethylsilylanolate, DMDO = dimethyldioxirane, TFDO = trifluoromethyl(methyl)dioxirane; TFac = 1,1,1-trifluoroacetone.

With the carbon framework in hand, we turned our attention to further modifications of the core structure (see Scheme 6.4). Saponification of diester **151** under standard conditions (KOH in aqueous media) allowed for selective hydrolysis of the sterically more accessible ester to yield monoacid **156**. However, the second ester group proved to be unreactive even under forcing conditions, presumably because of the steric bulk of the quaternary carbon center in α -position. Furthermore, in case of successful formation of the β -keto acid, isolation of the product was thwarted by spontaneous decarboxylation. Ultimately, diacid **157** was accessible by employing potassium trimethylsilylanolate and subsequent facile hydrolysis of the silyl ester.^[147]

For the investigation of the core structure at different oxidation levels, we turned our attention to reductive modifications of the framework. Unfortunately, a selective reduction of the carbonyl functionalities proved to be challenging. Only mixtures of different oxidation states or decomposed material were obtained with a variety of reagents—including borohydrides, aluminum hydrides or BOUVEAULT–BLANC

conditions.^[148] However, triol **158** was accessible by employing lithium aluminum hydride reduction with careful choice of the work-up method. The configuration of the secondary alcohol, pointing outside of the bowl shape structure, was unambiguously confirmed by X-ray crystal structure analysis.

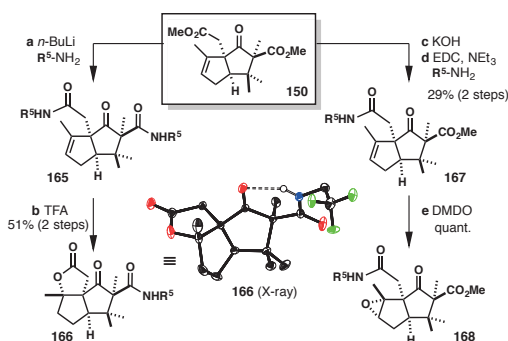
Apparently, direction of the hydride by the primary β -alcohol group or preorganization by the hydrogen bonding (visible in the product's solid state structure) must have allowed for the hydride attack from the sterically more hindered concave side. In order to further vary the functionality of the olefin containing ring, we examined the epoxidation of ester **151** with TFDO. Surprisingly, the reaction yielded not the epoxide, but a mixture of lactones **159** and **160**. These Anisactone-type cyclic structures were presumably formed by opening of the epoxide intermediate. The alcohol group formed was then further oxidized to the ketone under the reaction conditions. Notably, the use of milder DMDO yielded the desired epoxide **161**, after saponification.



Scheme 6.5. Synthesis of epoxy amide **162**, and unexpected oxidation products **163** and **164**. **a** SOCl₂, NH₃ (CH₂Cl₂) 50 °C, 2 h, 74%; **b** *m*CPBA (CH₂Cl₂) r.t., 18 h, 83%; **c** Cu(OAc)₂, H₂O₂ (MeCN/H₂O) r.t. 1.4 h, 40%; **d** DMDO (ac) r.t., 2 h, quant.; **e** [RuCl₃], KBrO₃, [py] (MeCN/H₂O) 60 °C, 17 h, 39% (2 steps). *m*CPBA = *meta*-chloroperbenzoic acid, DMDO = dimethyldioxirane.

As depicted in Scheme 6.5, conversion of monoacid **156** with thionyl chloride, followed by reaction with aqueous ammonia and subsequent epoxidation with *m*-CPBA yielded amide **162** in 49% yield over two steps. X-ray structure analysis confirmed the structure and unequivocally proved the convex orientation of the epoxide. Carboxylic acid **156** was also exposed to oxidative conditions in order to increase the oxidation level of the carbon framework. Treatment with copper(II) acetate and hydrogen peroxide^[97] yielded allylic lactone **163**—an unprecedented product for these reaction conditions. Even more surprising was the formation of oxidation product **164** in the reaction of the epoxidized acid with ruthenium(II) chloride and potassium bromate.^[149] The product was apparently formed by carbon–carbon bond scission

of the epoxide, subsequent oxidations and acetalization. Fortunately, a single crystal suitable for X-ray crystallography was obtained, which allowed structure elucidation of the unexpected product.



Scheme 6.6. Synthesis of amide derivatives. $R^5 = \text{CH}_2\text{CF}_3$. **a** $n\text{-BuLi}$, $R^4\text{-NH}_2$ (THF) -78°C , 2 h; **b** TFA (CH_2Cl_2) r.t., 40 h, 51% (2 steps); **c** KOH, H_2O (MeOH) 70°C , 2 h; **d** EDC, $R^4\text{-NH}_2$, [DMAP], NEt_3 (CH_2Cl_2) r.t., 16 h, 29% (2 steps); **e** DMDO, (ac) r.t., 14 h, quant.. TFA = trifluoroacetic acid, EDC = 3-(ethyl-iminomethyleneamino)-*N,N*-dimethylpropan-1-amine, DMDO = dimethyl dioxirane.

Additionally, amide derivatives of ester **150** were investigated (Scheme 6.6). After saponification, the amide group^[150] was introduced by coupling with EDC. Also in this case, the alkene could be epoxidized under mild conditions using DMDO. As it turned out, synthesis of diamide **165** was surprisingly challenging, presumably because of the steric hindrance of the α -quaternary carbon center. All attempts to convert diacid **167** to the diamide failed to give difunctionalized product. However, after having tested a variety of conditions, it was found that direct treatment of the ester **150** with deprotonated amine allowed for conversion of both ester groups. By employing trifluoroacetic acid, diamide **32** could be further transformed to Anisilactone-type structure **166**, which was confirmed by X-ray structure analysis.

In order to investigate the activity profile, we analyzed the effect of the prepared compounds on neuronal cells. Previous studies have shown that natural products of the *illicium* family and their structural analogs were capable of promoting NGF-mediated neurite outgrowth in neuronal cells (rat PC12 cells and primary cell cultures).^[139b, 151] To explore the scope and species-independence of the neurotrophic activity of *illicium* sesquiterpenes, we here used mouse N2a cells—an established model for neurite outgrowth.^[152]

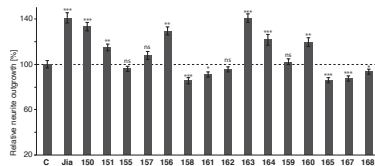


Figure 6.3. Relative neurite outgrowth of N2a-cells with selected compounds (at 1000 nM concentration) in comparison to control (C, DMSO). Jia = 7, (-)-Jiadifenolide, concentration: 1000 nM. Data represent averages of three independent runs (analysis of >25 cells for each run). Error bars indicate \pm s.e.m. *** $P \leq 0.001$, ** $P \leq 0.01$, * $P < 0.05$, ns = not significant.

We first validated the biological activity of a natural *illicium* sesquiterpene (synthetic Jiadifenolide 7^{[138][153]}) in this model and found that it potently enhanced serum deprivation-induced neurite outgrowth (140% compared to DMSO) with the strongest effect at a concentration of 1000 nM (Figure 6.3 and data not shown). Since our synthetic approach has provided access to a variety of framework analogs, we next explored the biological profile of the synthetic derivatives. Figure 6.3 shows a graphical representation of the results of the biological activity study with the relative neurite outgrowth of the N2a cells in comparison to the control run (DMSO). An overview of the selected compounds and their activities is given in Table 6.4.

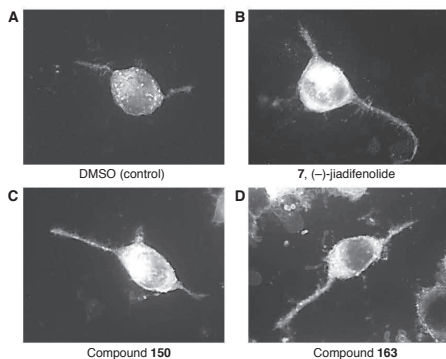
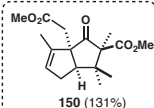
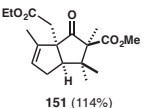
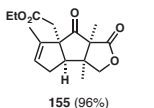
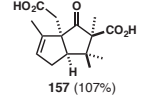
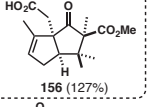
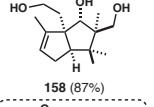
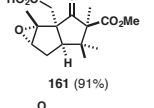
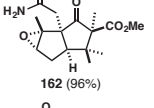
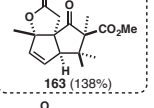
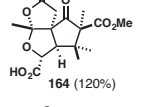
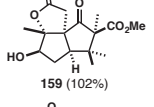
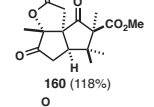
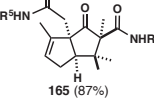
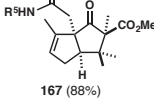
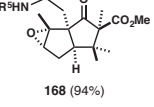


Figure 6.4. Representative images of N2a-cells after cell differentiation and neurite outgrowth. **A:** DMSO (control); **B:** (-)-Jiadifenolide (reference); **C:** compound 150; **D:** compound 163 (all at 1000 nM concentration).

Figure 6.4 depicts representative images of selected N2a cells after neurite outgrowth in the presence of selected compounds. The prolonged dendrites are visible in case of neurotrophically active compounds (Figure 6.4B,C,D) relative to the control (Figure 6.4A, DMSO). Several compounds such as 150, 23 and 163

were identified that were almost as potent as (-)-Jiadifenolide (**7**), while being structurally highly simplified. A SAR analysis suggests that structural variations at the northern carboxy group are tolerated (methyl ester **150** or acid **156**), while modifications of the western olefin reduce (compounds **160** and **164**) or abolish activity (compounds **159** and **161**). Likewise, derivatization of the eastern ester moiety abrogated activity (compare **151**→**155**). The inactivity of **155** was surprising since this eastern lactone motif (ring A in figure 6.2) is present in Merrilactone A and bioactive Jiadifenolide analogs.^[139b] Furthermore, the distinct neurite outgrowth by lactone **30** (138%) is remarkable, considering that the structure shows a high degree of similarity to the Anislactone structure, especially in light of the position of the γ -lactone moiety. Although it has been shown that Merrilactone A can be readily converted to the related natural product,^[20b] to the best of our knowledge the biological activity of Anislactone A/B has not yet been validated. The results presented confirm that the natural product Merrilactone A can be structurally simplified while retaining biological activity. The most active derivatives (**150**, **156**, **163**) are accessible in 6–8 synthetic steps with high yields from commercial starting materials.

Table 6.4. Overview of carbon framework derivatives and neurite outgrowth.

Compound (neurite outgrowth) ^a		
C, DMSO (100%)	3, (-)-Jiadifenolide (140%)	
 150 (131%)	 151 (114%)	 155 (96%)
 157 (107%)	 156 (127%)	 158 (87%)
 161 (91%)	 162 (96%)	 163 (138%)
 164 (120%)	 159 (102%)	 160 (118%)
 165 (87%)	 167 (88%)	 168 (94%)

R⁵ = CH₂CF₃, a) Relative neurite outgrowth [%] in comparison to control (DMSO)

7 Summary and Outlook

In summary, the first general method that allows for the introduction of lactone rings by amide directed C–H functionalization with good to excellent yields and unprecedented scope has been successfully developed. Although nitrogen radical chemistry has been known since the age-old HLF reaction, this work features two major advances by employing the trifluoroethyl amide as the directing group: (i) The highly efficient hydrogen abstraction, which is not limited to tertiary and secondary sp^3 -positions, but is also suitable for the conversion of primary non-activated methyl groups, and (ii) the efficient cyclization and mild hydrolysis, which allows for the direct and simple synthesis of γ -lactones in a one-pot fashion in the presence of a variety of functional groups. In total, nineteen different substrates were converted successfully, showcasing a highly predictable selectivity, a good functional group tolerance and a broad scope for the functionalization of aliphatic C–H bonds. Since lactones are prominent structural features of many synthetic compounds and natural products, application of this C–H lactonization method will open novel routes including biomimetic late-stage C–H oxidations.

Furthermore, the late-stage C–H oxidation strategy was investigated for the monoterpene natural product α -Thujone. Here, a short synthetic route which relies on the functionalization of dimethylfulvene has allowed the preparation of the main metabolites of α -Thujone including 7-OH- α -Thujone which is accessible by C–H hydroxylation using TFDO.

In addition, a series of structural analogs derived from the neurotrophic *illicium* sesquiterpene natural products (\pm)-Merrilactone A and (\pm)-Anislactone A/B has been synthesized. The concise synthetic route relies on the rapid construction of the carbon skeleton and enables the gram-scale preparation of the diastereomerically pure framework structure. Therefore, access is provided to further modified and functionalized analogs. In total, a library of 15 framework derivatives has been prepared, enabling the analysis of the structure-activity relationship. Our study identifies promising structural derivatives, that is, simplified natural product analogs, which are accessible in only 6–8 synthetic steps and still promote neurite outgrowth (138% compared to control). These results will aid biochemical studies aimed towards elucidating the molecular mechanism and relevant targets underlying the neurotrophic activity of the *illicium* sesquiterpenes and analogs thereof. The simplified compounds could also facilitate the development of new pharmaceuticals for the treatment of neurodegenerative diseases.

8 Experimental Section

8.1 General Information

Experimental: All reactions with air- or moisture-sensitive substances were carried out using standard SCHLENK techniques with Argon (Ar 4.6) as inert gas. Unless indicated otherwise, glass equipment was dried under high vacuum (10^{-3} mbar) at 500–600 °C using a heat gun. Reactions at low temperatures were either performed using cooling baths (–78 °C with dry ice in acetone or isopropanol, 0 °C with ice and water) or with a HUBER cryostat (–80 °C to –5 °C).

Solvents and reagents: Anhydrous Et₂O and THF were taken from a solvent drying system MBRAUN SPS-800. THF was further dried by distillation from sodium/benzophenone under argon atmosphere prior to use. Diisopropylamine was distilled from CaH₂ and stored over 4Å molecular sieve. Solutions of metalorganic reagents (e.g. *n*-BuLi) were titrated with menthol/1,10-phenanthroline prior to using.

Analytical methods and instruments: Analytical thin-layer chromatography (TLC) was performed on MERCK silica gel 60 F₂₅₄ glass-baked plates, which were analyzed by fluorescence detection with UV-light ($\lambda = 254$ nm, 366 nm, [UV]), as well as exposure to standard staining reagents and subsequent heat treatment. The following staining solutions were used: Basic potassium permanganate solution [KMnO₄] (9 g KMnO₄, 60 g K₂CO₃, 15 mL aqueous NaOH-solution (5%) in 900 mL H₂O), acidic cerium ammonium molybdate solution [CAM] (40 g ammonium heptamolybdate, 1.6 g cerium sulfate in 900 mL H₂O with 100 mL conc. H₂SO₄) iodine chamber [I₂] or acidic vanilline solution [Vanilline] (25 g vanilline in 900 mL Ethanol with 10 mL conc. H₂SO₄). Column Chromatographic separations were performed as flash chromatography with MERCK silica 60 (230–240 mesh ASTM, pore size 40–63 μ m).

¹H NMR spectra were recorded at 300 MHz, 360 MHz, 400 MHz or 500 MHz, using a BRUKER AVHD-300, AVHD-400 and AVHD-500 spectrometer respectively. ¹³C NMR spectra were recorded at 75 MHz, 90.6 MHz, 101 MHz or 126 MHz on a BRUKER AVHD-300, AVHD-400 and AVHD-500 spectrometer respectively. Chemical shifts of ¹H NMR and ¹³C NMR spectra (measured at 298 K) are given in ppm by using CHCl₃ and CDCl₃ (7.26 ppm and 77.16 ppm, respectively) or DMSO and DMSO-*d*₆ (2.50 ppm and 39.52 ppm, respectively) as references. Coupling constants (*J*) are reported in Hertz (Hz). Standard abbreviations indicating multiplicity were used as follows: s (singlet), d (doublet), t (triplet), q (quartet), p (pentet), s (sextet), h (septet), m (multiplet), b (broad). For diastereotopic methylene groups, the protons above the molecule plane are marked with α and protons below the molecule plane with β . Infrared spectra were recorded on a JACSO FT/IR-4100 spectrometer. Standard abbreviations indicating signal intensity were used as follows: br (broad), s (strong), m (medium), w (weak). High-resolution mass spectra

were obtained using the electron impact ionization (EI) technique on a THERMO Finnigan MAT 8200 mass spectrometer or the electron spray ionization (ESI) technique on a THERMO Finnigan LTQ FT mass spectrometer. Melting points are not corrected and were measured on a REICHERT AUSTRIA microscope.

Sources of chemicals: Celite[®], copper(II) acetate, copper(I) bromide dimethylsulfide complex, copper(I) chloride, *m*-CPBA, diisopropylethylamine (DIPEA, anhydrous), 4-dimethylaminopyridine (DMAP), 1,3-dimethyl-3,4,5,6-tetrahydro-2(1*H*)-pyrimidinone (DMPU), 3,5-dimethylpyrazol, ethanol (anhydrous), methyl iodide, methyl cyanofornate (MANDER's reagent), palladium chloride, potassium *t*-butoxide, potassium trimethylsilanolate, thionyl chloride, *p*-toluenesulfonamide, trimethylamine (anhydrous), Oxone[®], 1,1,1-trifluoroacetone, 2,2,2-trifluoroethylamine, were purchased from SIGMA-ALDRICH. CDCl₃ (99.8%) was purchased from DEUTERO GmbH. Lithium chloride (anhydrous) was purchased from TCI. Silica gel (0.040–0.063 mm, 230–400 mesh ASTM) and sodium hydride (60% suspension in paraffin oil) were purchased from MERCK. Magnesium sulfate and iodine were purchased from APPLICHEM. Potassium carbonate, sodium sulfate, magnesium, sodium iodide, sodium chloride, monosodium phosphate and ammonium chloride were purchased from GRÜSSING. Acetic acid, acetic anhydride, acetone (anhydrous), acetonitrile (HPLC grade), ammonium hydroxide (25% aq), and sodium hydroxide were purchased from FISHER SCIENTIFIC. Potassium carbonate (anhydrous) was purchased from FLUKA. Trifluoroacetic acid, 2,2,2-trifluoroethylamine hydrochloride and triphenylphosphine were purchased from ALFA AESAR. Acetone (anhydrous), 4Å molecular sieve, bromo ethylacetate, bromo methylacetate, chromium(III) oxide, copper(I) chloride, *n*-hexane (HPLC grade), lithium aluminium hydride, lithium chloride, methanol (HPLC grade), palladium(II) chloride, pyridine, sodium hydride (60% on paraffin wax) and sodium bicarbonate were purchased from VWR. Anhydrous acetonitrile, anhydrous dichloromethane (extra dry, stored over 4 Å MS), *N,N*-dimethylformamide (anhydrous), dimethyl sulfoxide (anhydrous), *n*-butyllithium solution in hexane, diisopropylamine, and methyl iodide were purchased from ACROS ORGANICS. 4-Bromo-1-butene, EDC hydrochloride and HBTU were purchased from CARBOLUTION. Pentane, Et₂O and EtOAc were purchased from BRENNTAG and distilled prior to use. Chemicals were used without further purification, unless stated otherwise.

8.2 Synthetic Procedures and Analytical Data

Preparation of Dimethyldioxirane (DMDO)

Caution! Reactions and subsequent operations involving peroxy compounds should be run behind a safety shield.

According to a modified procedure,^[154] a 1-L round-bottom flask was charged with H₂O (20 mL, MILIPORE water), acetone (30 mL) and NaHCO₃ (24 g, 285 mmol, 3.5 equiv). The white suspension was cooled to 0 °C and stirred for 20 min. Oxone® (25 g, 81.3 mmol, 1.0 equiv) was added in a single portion under gas evolution and the slurry was stirred vigorously for 15 min. After removing the stir bar, the flask containing the slurry was attached to a rotary evaporator with the water bath at room temperature. The bump bulb (250 mL, see figure 8.1) was cooled in a dry ice/isopropanol bath and a reduced pressure of 200 mbar was applied under rotation. After 15 min, the bath temperature was raised to 40 °C and held at that temperature for 15 min.

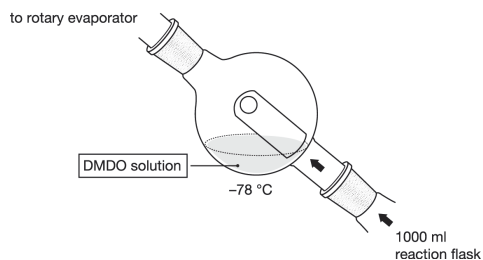


Figure 8.1. Bump bulb set-up for the collection of DMDO solution using a rotary evaporator.

The pale yellow acetone solution which was collected in the bump bulb was decanted into a graduated cylinder to measure the total volume and dried by addition of Na₂SO₄. After filtration, the concentration of the obtained DMDO solution was determined iodometrically by addition of 1 mL of the DMDO solution to a mixture of 0.25 mL saturated KI-solution and 1.0 mL glacial acetic acid. The resulting dark-red solution was titrated with a freshly prepared aqueous Na₂S₂O₃ solution (0.05 M), indicating a typical concentration of 50–100 mM.

Preparation of (Trifluoromethyl)methyldioxirane (TFDO)

According to a modified literature procedure,^[155] a 1-L three-necked round-bottom flask was equipped with over-head stirrer, a septum and a condenser which was attached to a 25 mL receiving flask by a distillation receiver with an argon balloon (see Figure S2). Prior to use, all glassware was rinsed with EDTA-solution (0.1 M) three times, H₂O and acetone. The condenser and the receiving flask were cooled

at $-78\text{ }^{\circ}\text{C}$ by an isopropanol bath with dry ice. The setup was then purged with argon, charged with a slurry of NaHCO_3 (26.0 g) in MILLIPORE water (26 mL) and cooled to $0\text{ }^{\circ}\text{C}$ with an ice bath. Under vigorous stirring, freshly ground Oxone (48.0 g) was added in one portion under strong evolution of CO_2 gas. After 2 min, 1,1,1-trifluoroacetone (24.0 mL) was added to the reaction mixture within 20 sec using a pre-cooled dropping funnel. After few seconds, the pale yellow solution of the methyl(trifluoromethyl)dioxirane in trifluoroacetone started to condense and within 20 min, 8–10 mL of a yellow liquid was collected in the cooled receiving flask.

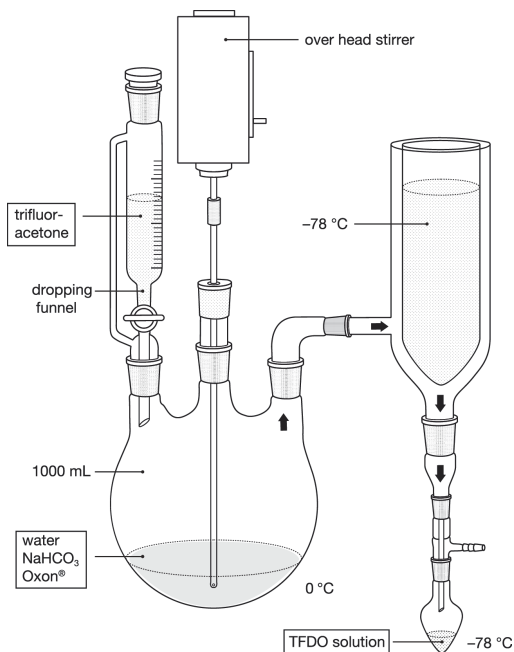


Figure 8.2. Set-up for the synthesis of TFDO.

The receiving flask was tightly closed with a septum, covered with aluminum foil and stored at $-80\text{ }^{\circ}\text{C}$ (low temperature freezer). The concentration of the TFDO solution was determined iodometrically by fast addition of 0.1 mL of the TFDO solution to a mixture of 0.25 mL saturated KI-solution and 1.0 mL glacial acetic acid. The resulting dark-red solution was titrated with a freshly prepared aqueous $\text{Na}_2\text{S}_2\text{O}_3$ solution (0.05 M), indicating a concentration of 0.70 M.

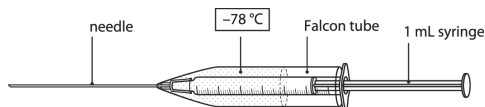


Figure 8.3. Mantle-cooled syringe for handling of volatile or reactive liquids and solutions.

Handling of the volatile liquid was performed at $-78\text{ }^{\circ}\text{C}$ with a mantle-cooled syringe, which was made from of a falcon tube, a syringe filter and a 1 mL syringe. A hole was cut into the tip of the falcon tube. The filter pad was removed from the syringe filter and then connected to the falcon tube with the help of a heat gun. The length of the falcon tube was adjusted to fit the 1 mL syringe (see Figure 8.3). Freshly crushed dry ice was added into the cooling mantle and mixed with isopropanol. The needle was pre-cooled at $-78\text{ }^{\circ}\text{C}$ prior to use. The syringe was then used as usual to pull up and measure the volume of the TFDO-solution.

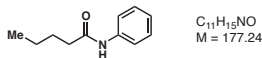
Caution! Reactions and subsequent operations involving peroxy compounds should be run behind a safety shield.

General Procedure for Amidation of Carboxylic Acids

The carboxylic acid (1.00 equiv) was dissolved in CH_2Cl_2 (0.1 M) and the reaction mixture was cooled to $0\text{ }^{\circ}\text{C}$, before EDC•HCl (1.35 equiv) was added, followed by DMAP (0.10 equiv), amine (1.00 equiv) and NEt₃ (1.50 equiv). The reaction mixture was allowed to warm to room temperature and stirred for 14 h, after which saturated NH_4Cl was added to the reaction mixture was extracted with CH_2Cl_2 (3 ×). The combined organic layers were washed with brine, dried (Na_2SO_4), and the solvent was removed *in vacuo*. The crude reaction mixture was subsequently purified by flash column chromatography.

In an alternate procedure, EDC•HCl (1.50 equiv), DMAP (0.10 equiv), amine hydrochloride (1.20 equiv) and NEt₃ (2.50 equiv) was used.

N-Phenylpentanamide (109)



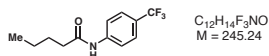
Prepared according to the standard procedure from pentanoic acid (150 mg, 1.47 mmol, 1.00 equiv) and aniline (137 mg, 1.47 mmol, 1.00 equiv). Purification *via* flash column chromatography (8 g silica gel, P/Et₂O = 2/1) provided amide **109** (212 mg, 1.20 mmol, 81%) as a yellow solid.

TLC: $R_f = 0.22$ (P/Et₂O = 2/1) [UV, KMnO_4].

¹H NMR (500 MHz, CDCl₃): δ [ppm] = 7.51 (d, *J* = 8.0 Hz, 2H), 7.31 (t, *J* = 7.8 Hz, 2H), 7.25 (bs, 1H), 7.09 (t, *J* = 7.4 Hz, 1H), 2.35 (t, *J* = 7.6 Hz, 2H), 1.71 (p, *J* = 7.6 Hz, 2H), 1.41 (h, *J* = 7.4 Hz, 2H), 0.94 (t, *J* = 7.4 Hz, 3H).
¹³C NMR (75 MHz, CDCl₃) δ [ppm] = 171.6 (s), 138.1 (s), 129.1 (s), 124.3 (s), 119.9 (s), 37.7 (s), 27.8 (s), 22.5 (s), 14.0 (s).

The spectroscopic data matched those reported in the literature.^[156]

***N*-(4-(Trifluoromethyl)phenyl)pentanamide (110)**



Prepared according to the standard procedure from pentanoic acid (150 mg, 1.47 mmol, 1.00 equiv) and 4-trifluoromethylaniline (237 mg, 1.47 mmol, 1.00 equiv). Purification *via* flash column chromatography (15 g silica gel, P/EtOAc = 9/1) provided amide **110** (308 mg, 1.26 mmol, 87%) as a white solid.

TLC: *R*_f = 0.19 (P/EtOAc = 9/1) [UV, KMnO₄].

M.p.: Δ_m = 110–111 °C.

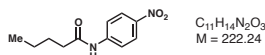
IR (ATR): ν (cm⁻¹) = 3319 (m), 2920 (m), 2851 (w), 1668 (s), 1526 (s), 1405 (s), 1325 (s), 1158 (vs), 1115 (vs), 1066 (vs), 832 (s), 677 (m).

¹H NMR (400 MHz, CDCl₃): δ [ppm] = 7.64 (d, *J* = 8.5 Hz, 2H), 7.63–7.60 (m, 1H), 7.58–7.50 (m, 2H), 2.46–2.28 (m, 2H), 1.80–1.63 (m, 2H), 1.47–1.33 (m, 2H), 0.93 (t, *J* = 7.4 Hz, 3H).

¹³C NMR (101 MHz, CDCl₃): δ [ppm] = 172.0 (s), 141.2 (s), 126.3 (q, *J* = 3.8 Hz), 126.1 (q, *J* = 32.9 Hz), 124.2 (q, *J* = 271.5 Hz), 119.5 (s), 37.7 (s), 27.7 (s), 22.5 (s), 13.9 (s).

HR-MS (EI, 70 eV): calculated for C₁₂H₁₄F₃NO [M⁺]: 245.1027; measured: 245.1022.

***N*-(4-Nitrophenyl)pentanamide (111)**



Prepared according to the standard procedure from pentanoic acid (100 mg, 979 μmol, 1.00 equiv) and 4-nitroaniline (135 mg, 979 μmol, 1.00 equiv). The crude product was washed with HCl (1 M, 3 × 15 mL) and, after being dried, purified *via* flash column chromatography (15 g silica gel, P/Et₂O = 1/1) to yield amide **111** (151 mg, 679 μmol, 69%) as a yellow solid.

TLC: *R*_f = 0.15 (P/Et₂O = 1/1) [UV, KMnO₄].

M.p.: Δ_m = 117–118 °C.

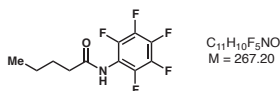
IR (ATR): ν (cm^{-1}) = 3353 (m), 2958 (m), 2924 (m), 2853 (w), 1707 (s), 1596 (m), 1541 (s), 1493 (s), 1320 (s), 1296 (s), 1254 (s), 1161 (s), 1104 (s), 857 (s), 754 (s), 694 (s).

$^1\text{H NMR}$ (400 MHz, CDCl_3): δ [ppm] = 8.39–8.13 (m, 2H), 7.77–7.67 (m, 2H), 7.64 (bs, 1H), 2.50–2.37 (m, 2H), 1.77–1.68 (m, 2H), 1.53–1.34 (m, 2H), 0.95 (t, J = 7.3 Hz, 3H).

$^{13}\text{C NMR}$ (101 MHz, CDCl_3): δ [ppm] = 172.0 (s), 144.0 (s), 143.5 (s), 125.2 (s), 119.1 (s), 37.7 (s), 27.5 (s), 22.5 (s), 13.9 (s).

HR-MS (EI, 70 eV): calculated for $\text{C}_{11}\text{H}_{14}\text{N}_2\text{O}_3$ [M^+]: 222.1004; measured: 222.0999.

***N*-(Perfluorophenyl)pentanamide (112)**



A solution of pentanoic acid (200 mg, 1.96 mmol, 1.00 equiv) in CH_2Cl_2 (10 mL, 0.2 M) was cooled to 0 °C. Pentafluoroaniline (359 mg, 1.96 mmol, 1.00 equiv) was added, followed by NEt_3 (198 mg, 1.96 mmol, 1.00 equiv). Afterwards, phosphoryl chloride (600 mg, 3.92 mmol, 2.00 equiv) was added dropwise, after which NEt_3 (396 mg, 3.92 mmol, 2.00 equiv) was added slowly. The reaction mixture was stirred for three hours, then H_2O (10 mL, cooled to 0 °C) was added slowly and the mixture was stirred for 30 min at room temperature. After extraction of the reaction mixture with CH_2Cl_2 (3×10 mL), the combined organic layers were washed with saturated NaHCO_3 (2×20 mL), HCl (1 M, 2×20 mL) and brine (20 mL), dried (Na_2SO_4) and the solvent was removed *in vacuo*. The crude product was purified by flash column chromatography (15 g silica gel, $\text{P/Et}_2\text{O}$ = 10/1) to provide amide **112** (140 mg, 558 μmol , 28%) as a white solid.

TLC: R_f = 0.18 ($\text{P/Et}_2\text{O}$ = 5/1) [UV, CAM].

M.p.: Δ_m = 74–75 °C.

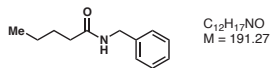
IR (ATR): ν (cm^{-1}) = 3249 (w), 2931 (w), 1679 (s), 1523 (vs), 1490 (vs), 1198 (m), 1004 (s), 993 (s), 956 (vs), 671 (bm).

$^1\text{H NMR}$ (400 MHz, CDCl_3): δ [ppm] = 7.51 (bs, 1H), 2.41 (t, J = 7.6 Hz, 2H), 1.67 (p, J = 8.0 Hz, 2H), 1.38 (h, J = 7.6 Hz, 2H), 0.92 (t, J = 7.2 Hz, 3H).

$^{13}\text{C NMR}$ (101 MHz, CDCl_3): δ [ppm] = 172.4 (s), 143.2 (ddd, J = 250.6, 11.5, 4.7 Hz), 140.2 (dddd, J = 253.3, 17.8, 13.4, 4.1 Hz), 137.8 (dtdd, J = 251.3, 15.8, 5.5, 2.9 Hz), 112.0 (td, J = 14.7, 3.7 Hz), 36.0 (s), 27.6 (s), 22.3 (s), 13.8 (s).

$^{19}\text{F NMR}$ (376 MHz, CDCl_3) δ [ppm] = -145.4 (dt, J = 24.5, 4.1 Hz), -155.9 (t, J = 21.7 Hz), -162.6 (t, J = 21.5 Hz).

HR-MS (EI, 70 eV): calculated for $\text{C}_{11}\text{H}_{10}\text{F}_5\text{NO}$ [M^+]: 267.0683; measured: 267.0676.

N-Benzylpentanamide (113)

Prepared according to the standard procedure from pentanoic acid (150 mg, 1.47 mmol, 1.00 equiv) and benzylamine (157 mg, 1.47 mmol, 1.00 equiv). Purification *via* flash column chromatography (6 g silica gel, P/Et₂O = 5/1) provided amide **113** (241 mg, 1.26 mmol, 86%) as a white solid.

TLC: R_f = 0.19 (P/Et₂O = 1/1) [UV, CAM].

¹H NMR (400 MHz, CDCl₃): δ [ppm] = 7.23 (d, J = 6.8 Hz, 2H), 7.18 (dd, J = 7.5, 4.2 Hz, 3H), 5.65 (bs, 1H), 4.34 (d, J = 5.6 Hz, 2H), 2.12 (t, J = 7.7 Hz, 2H), 1.55 (p, J = 7.5 Hz, 2H), 1.27 (h, J = 7.4 Hz, 2H), 0.82 (t, J = 7.3 Hz, 3H).

¹³C NMR (101 MHz, CDCl₃): δ [ppm] = 173.1 (s), 138.6 (s), 128.8 (s), 128.0 (s), 127.6 (s), 43.7 (s), 36.7 (s), 28.0 (s), 22.6 (s), 13.9 (s).

The spectroscopic data matched those reported in the literature.^[157]

Pentanamide (114)

Pentanoic acid (1.00 g, 9.79 mmol, 1.00 equiv) was dissolved in CH₂Cl₂ (100 mL, 0.1 M), two drops of DMF were added and the reaction mixture was cooled to 0 °C before thionyl chloride (3.49 g, 29.37 mmol, 3.00 equiv) was added dropwise. The reaction mixture was stirred for one hour at 0 °C and then for one hour at room temperature, after which the mixture was cooled to 0 °C and ammonium hydroxide (25% aq., 3.7 mL, 49.0 mmol, 5.00 equiv) was added. After stirring at 0 °C for 30 min and then at room temperature for 30 min HCl (1 M, 50 mL) was added to the reaction mixture, followed by NaCl until the aqueous layer was saturated. The reaction mixture was extracted with CH₂Cl₂ (3 × 50 mL), washed with brine (50 mL), dried (Na₂SO₄) and the solvent was removed *in vacuo*. Purification *via* flash column chromatography (10 g silica gel, P/EtOAc = 1/4) provided amide **114** (432 mg, 4.27 mmol, 44%) as an off-white solid.

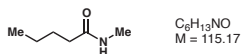
TLC: R_f = 0.17 (P/EtOAc = 1/4) [KMnO₄].

¹H NMR (400 MHz, CDCl₃): δ [ppm] = 5.77 (bs, 1H), 5.53 (bs, 1H), 2.21 (t, J = 7.4 Hz, 2H), 1.61 (p, J = 7.0 Hz, 2H), 1.36 (h, J = 7.0 Hz, 2H), 0.92 (t, J = 7.1 Hz, 3H).

¹³C NMR (101 MHz, CDCl₃): δ [ppm] = 176.0 (s), 35.8 (s), 27.7 (s), 22.5 (s), 13.9 (s).

The spectroscopic data matched those reported in the literature.^[158]

N-Methylpentanamide (115)



Prepared according to the standard procedure from pentanoic acid (300 mg, 2.94 mmol, 1.00 equiv) and methylamine (33% in ethanol, 370 μ L, 2.94 mmol, 1.00 equiv). Purification *via* flash column chromatography (12 g silica gel, P/EtOAc = 1/1) provided amide **115** (276 mg, 2.40 mmol, 86%) as a colorless oil.

TLC: $R_f = 0.18$ (P/EtOAc = 1/1) [$KMnO_4$].

IR (ATR): ν (cm^{-1}) = 3292 (w), 2956 (m), 2931 (w), 2872 (w), 1644 (vs), 1555 (s), 1410 (m), 1159 (m), 693 (bm).

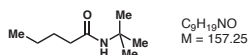
1H NMR (400 MHz, $CDCl_3$): δ [ppm] = 5.62 (bs, 1H), 2.78 (dd, $J = 4.8, 2.4$ Hz, 3H), 2.16 (t, $J = 7.5$ Hz, 2H), 1.60 (p, $J = 7.1$ Hz, 2H), 1.33 (h, $J = 8.4$ Hz, 2H), 0.90 (t, $J = 7.3$ Hz, 3H).

^{13}C NMR (101 MHz, $CDCl_3$): δ [ppm] = 174.0 (s), 36.6 (s), 28.0 (s), 26.4 (s), 22.6 (s), 13.9 (s).

HR-MS (EI, 70 eV): calculated for $C_6H_{13}NO$ [M^+]: 115.0997; measured: 115.0989.

The 1H NMR data matched those reported in the literature.^[159]

N-(*Tert*-butyl) pentanamide (116)



Prepared according to the standard procedure from pentanoic acid (300 mg, 2.94 mmol, 1.00 equiv) and *t*-butylamine (215 mg, 2.94 mmol, 1.00 equiv). Purification *via* flash column chromatography (15 g silica gel, P/Et₂O = 5/1) provided amide **116** (419 mg, 2.66 mmol, 91%) as a white solid.

TLC: $R_f = 0.33$ (P/Et₂O = 2/1) [$KMnO_4$].

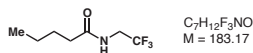
M.p.: $\Theta_m = 47\text{--}48$ °C.

IR (ATR): ν (cm^{-1}) = 3292 (w), 2958 (m), 2928 (m), 2871 (w), 1638 (vs), 1550 (vs), 1455 (m), 1361 (m), 1226 (m), 1099 (w).

1H NMR (300 MHz, $CDCl_3$): δ [ppm] = 5.25 (bs, 1H), 2.11–2.01 (m, 2H), 1.57 (dtd, $J = 8.7, 7.2, 5.7$ Hz, 2H), 1.33 (s, 9H), 1.40–1.25 (m, 2H), 0.90 (t, $J = 7.3$ Hz, 3H).

^{13}C NMR (75 MHz, $CDCl_3$): δ [ppm] = 172.6 (s), 51.1 (s), 37.6 (s), 29.0 (s), 28.0 (s), 22.5 (s), 14.0 (s).

HR-MS (EI, 70 eV): calculated for $C_9H_{19}NO$ [M^+]: 157.1467; measured: 157.1461.

N-(Trifluoroethyl)pentanamide (117)

Prepared according to the standard procedure from pentanoic acid (300 mg, 2.94 mmol, 1.00 equiv) and 2,2,2-trifluoroethylamine (291 mg, 2.94 mmol, 1.00 equiv). Purification *via* flash column chromatography (10 g silica gel, P/Et₂O = 2/1) provided amide **117** (528 mg, 2.94 mmol, 98%) as a white solid.

TLC: R_f = 0.18 (P/Et₂O = 2/1) [KMnO₄].

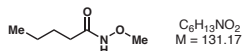
M.p.: Δ_m = 38–39 °C.

IR (ATR): ν (cm⁻¹) = 3298 (m), 2960 (w), 2929 (w), 2859 (w), 1649 (s), 1551 (s), 1398 (m), 1147 (vs), 666 (s).

¹H NMR (300 MHz, CDCl₃): δ [ppm] = 5.86 (bs, 1H), 3.91 (qd, J = 9.1, 6.5 Hz, 2H), 2.29–2.22 (m, 2H), 1.70–1.58 (m, 2H), 1.43–1.28 (m, 2H), 0.92 (t, J = 7.3 Hz, 3H).

¹³C NMR (75 MHz, CDCl₃): δ [ppm] = 173.4 (s), 124.3 (q, J = 278.4 Hz), 40.7 (q, J = 34.6 Hz), 36.3 (s), 27.6 (s), 22.4 (s), 13.8 (s).

HR-MS (EI, 70 eV): calculated for C₇H₁₂F₃NO [M⁺]: 183.0871; measured: 183.0866.

N-Methoxypentanamide (118)

Prepared according to the standard procedure from pentanoic acid (150 mg, 1.47 mmol, 1.00 equiv) and *O*-methylhydroxylamine hydrochloride (147 mg, 1.76 mmol, 1.20 equiv). Purification *via* flash column chromatography (6 g silica gel, P/EtOAc = 1/1) provided amide **118** (158 mg, 1.20 mmol, 82%) as a colorless oil.

TLC: R_f = 0.18 (P/EtOAc = 1/1) [KMnO₄].

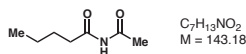
IR (ATR): ν (cm⁻¹) = 3175 (bw), 2958 (m), 2933 (m), 2872 (w), 1654 (vs), 1515 (w), 1464 (w), 1111 (m), 1053 (s), 965 (m), 670 (bm).

¹H NMR (400 MHz, CDCl₃): δ [ppm] = 8.32 (bs, 0.75H), 8.00 (bs, 0.25H), 3.75 (s, 3H), 2.40 (bs, 0.50H), 2.08 (bs, 1.5H), 1.63 (p, J = 7.6 Hz, 2H), 1.36 (h, J = 7.6 Hz, 2H), 0.92 (t, J = 7.3 Hz, 3H).

¹³C NMR (126 MHz, CDCl₃): δ [ppm] = 171.3 (s), 64.6 (s), 33.2 (s), 27.5 (s), 22.5 (s), 13.9 (s).

HR-MS (EI, 70 eV): calculated for C₆H₁₃NO₂ [M⁺]: 131.0946; measured: 131.0941.

The ¹H NMR data indicating (*O*)-*E/Z* isomerism matched those reported in the literature for similar *N*-methoxyamides.^[160]

N-Acetylpentanamide (119)

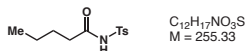
Amide **14** (100 mg, 989 μ mol, 1.00 equiv) was dissolved in acetic anhydride (5 mL, 0.2 M) and H_2SO_4 (98%, 5 μ L, 0.10 equiv) was added. The reaction mixture was stirred at 80 °C for two hours and then cooled to room temperature. After removal of the solvent *in vacuo* the crude product was purified *via* flash column chromatography (3 g silica gel, P/Et₂O = 5/1) to provide imide **119** (127 mg, 887 μ mol, 90%) as a pale yellow solid.

TLC: R_f = 0.50 (P/Et₂O = 2/1) [$KMnO_4$].

¹H NMR (400 MHz, $CDCl_3$): δ [ppm] = 8.68 (bs, 1H), 2.51 (t, J = 7.4 Hz, 2H), 2.36 (s, 3H), 1.63 (p, J = 7.4 Hz, 2H), 1.37 (h, J = 7.1 Hz, 2H), 0.93 (t, J = 7.5 Hz, 3H).

¹³C NMR (101 MHz, $CDCl_3$): δ [ppm] = 173.9 (s), 172.3 (s), 37.2 (s), 26.6 (s), 25.2 (s), 22.3 (s), 13.9 (s).

The spectroscopic data matched those reported in the literature.^[161]

N-Tosylpentanamide (120)

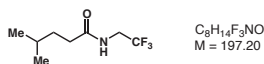
Prepared according to the standard procedure from pentanoic acid (150 mg, 1.47 mmol, 1.00 equiv) and *p*-toluenesulfonamide (251 mg, 1.47 mmol, 1.00 equiv). Purification *via* flash column chromatography (12 g silica gel, P/Et₂O = 2/1) provided imide **120** (230 mg, 901 μ mol, 61%) as a white solid.

TLC: R_f = 0.19 (P/Et₂O = 2/1) [$KMnO_4$].

¹H NMR (300 MHz, $CDCl_3$): δ [ppm] = 8.39 (bs, 1H), 7.94 (dt, J = 8.4, 1.7 Hz, 2H), 7.38–7.31 (m, 2H), 2.44 (s, 3H), 2.24 (t, J = 7.3 Hz, 2H), 1.54 (p, J = 7.4 Hz, 2H), 1.34–1.20 (m, 2H), 0.85 (t, J = 7.3 Hz, 3H).

¹³C NMR (75 MHz, $CDCl_3$): δ [ppm] = 170.9 (s), 145.3 (s), 135.7 (s), 129.8 (s), 128.5 (s), 36.2 (s), 26.5 (s), 22.1 (s), 21.8 (s), 13.8 (s).

The spectroscopic data matched those reported in the literature.^[162]

4-Methyl-N-(2,2,2-trifluoroethyl)pentanamide (S01)

Prepared according to the standard procedure from 4-methylpentanoic acid (400 mg, 3.44 mmol, 1.00 equiv) and 2,2,2-trifluoroethylamine hydrochloride (560 mg, 4.13 mmol, 1.20 equiv). Purification *via*

flash column chromatography (20 g silica gel, P/Et₂O = 2/1) provided amide **S01** (590 mg, 2.99 mmol, 87%) as a colorless oil.

TLC: $R_f = 0.23$ (P/Et₂O = 2/1) [KMnO₄].

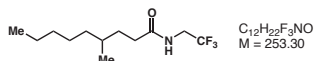
IR (ATR): ν (cm⁻¹) = 3291 (bm), 2959 (m), 2873 (w), 1661 (s), 1549 (s), 1470 (w), 1425 (w), 1396 (w), 1263 (m), 1154 (vs).

¹H NMR (500 MHz, CDCl₃): δ [ppm] = 5.74 (bs, 1H), 3.92 (qd, $J = 9.1, 6.5$ Hz, 2H), 2.28–2.23 (m, 2H), 1.71–1.48 (m, 3H), 0.91 (d, $J = 6.2$ Hz, 6H).

¹³C NMR (126 MHz, CDCl₃): δ [ppm] = 173.5 (s), 124.2 (q, $J = 278.4$ Hz), 40.7 (q, $J = 34.6$ Hz), 34.6 (s), 34.3 (s), 27.9 (s), 22.4 (s).

HR-MS (EI, 70 eV): calculated for C₈H₁₄F₃NO [M⁺]: 197.1027; measured: 197.1031.

4-Methyl-N-(2,2,2-trifluoroethyl)octanamide (S02)



Prepared according to the standard procedure from 4-methylnonanoic acid (500 mg, 2.90 mmol, 1.00 equiv) and 2,2,2-trifluoroethylamine hydrochloride (472 mg, 3.48 mmol, 1.20 equiv). Purification *via* flash column chromatography (20 g silica gel, P/Et₂O = 2/1) provided amide **S02** (520 mg, 2.05 mmol, 71%) as a colorless oil.

TLC: $R_f = 0.25$ (P/Et₂O = 2/1) [KMnO₄].

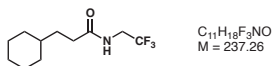
IR (ATR): ν (cm⁻¹) = 3293 (bw), 2957 (w), 2927 (m), 2859 (w), 1661 (s), 1550 (m), 1459 (w), 1424 (w), 1396 (w), 1260 (m), 1156 (vs).

¹H NMR (500 MHz, CDCl₃): δ [ppm] = 5.78 (bs, 1H), 3.92 (qd, $J = 9.1, 6.4$ Hz, 2H), 2.35–2.16 (m, 2H), 1.68 (ddd, $J = 13.6, 10.6, 5.5$ Hz, 1H), 1.51–1.37 (m, 2H), 1.34–1.19 (m, 7H), 1.17–1.07 (m, 1H), 0.87 (t, $J = 7.1$ Hz, 3H), 0.87 (d, $J = 6.3$ Hz, 3H).

¹³C NMR (126 MHz, CDCl₃): δ [ppm] = 173.6 (s), 124.2 (q, $J = 278.3$ Hz), 40.6 (q, $J = 34.6$ Hz), 36.8 (s), 34.3 (s), 32.6 (s), 32.5 (s), 32.2 (s), 26.7 (s), 22.8 (s), 19.4 (s), 14.2 (s).

HR-MS (EI, 70 eV): calculated for C₁₂H₂₂F₃NO [M⁺]: 253.1654; measured: 253.1652.

3-Cyclohexyl-N-(2,2,2-trifluoroethyl)propanamide (S03)



Prepared according to the standard procedure from 3-cyclohexylpropanoic acid (310 mg, 1.98 mmol, 1.00 equiv) and 2,2,2-trifluoroethylamine hydrochloride (323 mg, 2.38 mmol, 1.20 equiv). Purification *via* flash column chromatography (15 g silica gel, P/Et₂O = 2/1) provided amide **S03** (360 mg, 1.52 mmol, 76%) as a white solid.

TLC: $R_f = 0.24$ (P/Et₂O = 2/1) [KMnO₄].

M.p.: $\vartheta_m = 73\text{--}74$ °C.

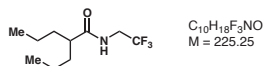
IR (ATR): ν (cm⁻¹) = 3290 (m), 2920 (s), 2854 (m), 1659 (s), 1552 (s), 1439 (w), 1428 (w), 1398 (w), 1376 (w), 1240 (m), 1149 (vs).

¹H NMR (500 MHz, CDCl₃): δ [ppm] = 5.69 (bs, 1H), 3.92 (qd, $J = 9.1, 6.5$ Hz, 2H), 2.31–2.20 (m, 2H), 1.74–1.67 (m, 4H), 1.64 (dt, $J = 13.2, 2.7$ Hz, 1H), 1.57–1.52 (m, 2H), 1.32–1.07 (m, 4H), 0.95–0.84 (m, 2H).

¹³C NMR (126 MHz, CDCl₃): δ [ppm] = 173.6 (s), 124.2 (q, $J = 278.3$ Hz), 40.6 (q, $J = 34.6$ Hz), 37.4 (s), 34.1 (s), 33.1 (s), 32.9 (s), 26.6 (s), 26.3 (s).

HR-MS (EI, 70 eV): calculated for C₁₁H₁₈F₃NO [M⁺]: 237.1341; measured: 237.1338.

2-Propyl-N-(2,2,2-trifluoroethyl)pentanamide (S04)



Prepared according to the standard procedure from 2-(*n*-propyl)pentanoic acid (500 mg, 3.47 mmol, 1.00 equiv) and 2,2,2-trifluoroethylamine hydrochloride (564 mg, 4.16 mmol, 1.20 equiv). Purification *via* flash column chromatography (20 g silica gel, P/Et₂O = 2/1) provided amide **S04** (460 mg, 2.04 mmol, 59%) as a white solid.

TLC: $R_f = 0.21$ (P/Et₂O = 2/1) [KMnO₄].

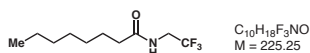
M.p.: $\vartheta_m = 76\text{--}77$ °C.

IR (ATR): ν (cm⁻¹) = 2929 (m), 1782 (w), 1656 (s), 1552 (s), 1469 (w), 1392 (m), 1255 (m), 1147 (vs), 1021 (m), 849 (w), 704 (s).

¹H NMR (400 MHz, CDCl₃): δ [ppm] = 5.92 (bs, 1H), 3.92 (qd, $J = 9.1, 6.4$ Hz, 2H), 2.29–2.03 (m, 1H), 1.60 (dtd, $J = 12.8, 9.4, 5.4$ Hz, 2H), 1.40 (dddd, $J = 12.9, 9.1, 6.5, 4.9$ Hz, 2H), 1.35–1.20 (m, 4H), 0.89 (t, $J = 7.2$ Hz, 6H).

¹³C NMR (101 MHz, CDCl₃): δ [ppm] = 176.5 (s), 124.3 (q, $J = 278.5$ Hz), 47.7 (s), 40.4 (q, $J = 34.6$ Hz), 35.3 (s), 20.8 (s), 14.2 (s).

HR-MS (EI, 70 eV): calculated for C₁₀H₁₈F₃NO [M⁺]: 225.1340; measured: 225.1335.

N-(2,2,2-Trifluoroethyl)octanamide (S05)

Prepared according to the standard procedure from octanoic acid (200 mg, 1.39 mmol, 1.00 equiv) and 2,2,2-trifluoroethylamine (137 mg, 1.39 mmol, 1.00 equiv). Purification *via* flash column chromatography (10 g silica gel, P/Et₂O = 2/1) provided amide **S05** (302 mg, 1.34 mmol, 97%) as a crystalline white solid.

TLC: $R_f = 0.20$ (P/Et₂O = 2/1) [KMnO₄].

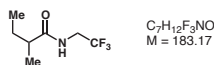
M.p.: $\vartheta_m = 46\text{--}47\text{ }^\circ\text{C}$.

IR (ATR): ν (cm⁻¹) = 3295 (w), 2919 (m), 2847 (w), 1649 (m), 1559 (m), 1400 (m), 1178 (s), 1145 (vs), 836 (m), 667 (s).

¹H NMR (400 MHz, CDCl₃): δ [ppm] = 6.01 (bs, 1H), 3.90 (qd, $J = 9.1, 6.4$ Hz, 2H), 2.24 (t, $J = 7.6$ Hz, 2H), 1.64 (p, $J = 7.4$ Hz, 2H), 1.29 (ddq, $J = 11.0, 7.1, 4.1, 3.3$ Hz, 8H), 0.86 (t, $J = 6.7$ Hz, 3H).

¹³C NMR (101 MHz, CDCl₃): δ [ppm] = 173.6 (s), 124.3 (q, $J = 278.3$ Hz), 40.6 (q, $J = 34.7$ Hz), 36.5 (s), 31.8 (s), 29.2 (s), 29.1 (s), 25.6 (s), 22.7 (s), 14.2 (s).

HR-MS (EI, 70 eV): calculated for C₁₀H₁₈F₃NO [M⁺]: 225.1340; measured: 225.1335.

2-Methyl-N-(2,2,2-trifluoroethyl)butanamide (S06)

2-Methylbutyryl chloride (500 mg, 4.15 mmol, 1.00 equiv.) was dissolved in CH₂Cl₂ (20 mL, 0.2 M) and cooled to 0 °C before 2,2,2-trifluoroethylamine hydrochloride (674 mg, 4.98 mmol, 1.20 equiv) was added, followed by dropwise addition of NEt₃ (420 mg, 4.15 mmol, 1.00 equiv). The reaction mixture was stirred for one hour at 0 °C and then for one hour at room temperature, after which saturated NH₄Cl (50 mL) was added, then the mixture was extracted with CH₂Cl₂ (3 × 50 mL) and the combined organic layers were washed with brine (100 mL), dried (Na₂SO₄) and the solvent was removed *in vacuo*. The crude product was purified by flash column chromatography (15 g silica gel, P/Et₂O = 2/1) to provide amide **S07** (533 mg, 2.91 mmol, 71%) as a white solid.

TLC: $R_f = 0.21$ (P/Et₂O = 2/1) [KMnO₄].

M.p.: $\vartheta_m = 34\text{--}35\text{ }^\circ\text{C}$.

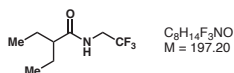
IR (ATR): ν (cm⁻¹) = 3295 (m), 2967 (w), 2935 (w), 1660 (s), 1554 (m), 1460 (w), 1430 (w), 1395 (w), 1230 (m), 1141 (vs).

¹H NMR (500 MHz, CDCl₃): δ [ppm] = 5.79 (bs, 1H), 3.93 (dddd, *J* = 47.3, 15.1, 9.1, 6.3 Hz, 2H), 2.18 (h, *J* = 6.9 Hz, 1H), 1.73–1.61 (m, 1H), 1.47 (ddd, *J* = 13.7, 7.6, 6.4 Hz, 1H), 1.16 (d, *J* = 6.9 Hz, 3H), 0.90 (t, *J* = 7.4 Hz, 3H).

¹³C NMR (126 MHz, CDCl₃): δ [ppm] = 176.8 (s), 124.3 (q, *J* = 278.2 Hz), 43.2 (s), 40.5 (q, *J* = 34.5 Hz), 27.4 (s), 17.5 (s), 11.8 (s).

HR-MS (EI, 70 eV): calculated for C₇H₁₂F₃NO [M⁺]: 183.0871; measured: 183.0864.

2-Ethyl-*N*-(2,2,2-trifluoroethyl)butanamide (S07)



Prepared according to the standard procedure from 2-ethylbutyric acid (230 mg, 1.98 mmol, 1.00 equiv) and 2,2,2-trifluoroethylamine hydrochloride (322 mg, 2.38 mmol, 1.20 equiv). Purification *via* flash column chromatography (8 g silica gel, P/Et₂O = 5/1) provided amide **S08** (164 mg, 831 μmol, 42%) as a crystalline white solid.

TLC: *R*_f = 0.27 (P/Et₂O = 2/1) [KMnO₄].

M.p.: *m* = 68–69 °C.

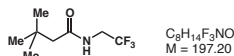
IR (ATR): ν (cm⁻¹) = 3295 (m), 2965 (w), 2931 (w), 1659 (s), 1553 (s), 1461 (w), 1429 (w), 1395 (w), 1228 (m), 1148 (vs).

¹H NMR (400 MHz, CDCl₃): δ [ppm] = 5.77 (bs, 1H), 3.95 (qd, *J* = 9.1, 6.4 Hz, 2H), 1.94 (tt, *J* = 9.0, 5.2 Hz, 1H), 1.63 (ddq, *J* = 13.6, 9.1, 7.4 Hz, 2H), 1.58–1.43 (m, 2H), 0.89 (t, *J* = 7.4 Hz, 6H).

¹³C NMR (101 MHz, CDCl₃): δ [ppm] = 176.1 (s), 124.3 (q, *J* = 278.4 Hz), 51.5 (s), 40.4 (q, *J* = 34.6 Hz), 25.8 (s), 12.0 (s).

HR-MS (EI, 70 eV): calculated for C₈H₁₄F₃NO [M⁺]: 197.1027; measured: 197.1019.

3,3-Dimethyl-*N*-(2,2,2-trifluoroethyl)butanamide (S08)



Prepared according to the standard procedure from 2,2-dimethylbutyric acid (400 mg, 3.44 mmol, 1.00 equiv) and 2,2,2-trifluoroethylamine hydrochloride (600 mg, 4.13 mmol, 1.20 equiv). Purification *via* flash column chromatography (20 g silica gel, P/Et₂O = 5/1) provided amide **S09** (470 mg, 2.38 mmol, 69%) as a crystalline white solid.

TLC: *R*_f = 0.41 (P/Et₂O = 3/1) [KMnO₄].

M.p.: $\varnothing_m = 65\text{--}66\text{ }^\circ\text{C}$.

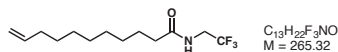
IR (ATR): ν (cm^{-1}) = 3272 (m), 2961 (m), 1655 (s), 1560 (s), 1392 (w), 1368 (w), 1345 (w), 1256 (s), 1156 (vs).

$^1\text{H NMR}$ (500 MHz, CDCl_3): δ [ppm] = 5.64 (bs, 1H), 3.92 (qd, $J = 9.1, 6.5$ Hz, 2H), 2.12 (s, 2H), 1.04 (s, 9H).

$^{13}\text{C NMR}$ (126 MHz, CDCl_3): δ [ppm] = 171.8 (s), 124.3 (q, $J = 277.5$ Hz), 50.5 (s), 40.5 (q, $J = 34.6$ Hz), 31.1 (s), 29.8 (s).

HR-MS (EI, 70 eV): calculated for $\text{C}_8\text{H}_{14}\text{F}_3\text{NO}$ [M^+]: 197.1027; measured: 197.1019.

***N*-(2,2,2-Trifluoroethyl)undec-10-enamide (S09)**



Prepared according to the standard procedure from undec-10-enoic acid (1.00 g, 5.43 mmol, 1.00 equiv) and 2,2,2-trifluoroethylamine hydrochloride (882 mg, 6.51 mmol, 1.20 equiv). Purification *via* flash column chromatography (50 g silica gel, $\text{P/Et}_2\text{O} = 2/1$) provided amide **S09** (1.25 g, 4.71 mmol, 87%) as a white solid.

TLC: $R_f = 0.17$ ($\text{P/Et}_2\text{O} = 2/1$) [KMnO_4].

M.p.: $\varnothing_m = 43\text{--}44\text{ }^\circ\text{C}$.

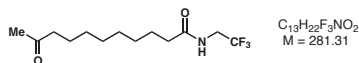
IR (ATR): ν (cm^{-1}) = 3302 (s), 2914 (s), 2848 (s), 1661 (vs), 1558 (s), 1471 (w), 1461 (w), 1435 (w), 1400 (m), 1291 (w), 1267 (w), 1253 (m), 1228 (w), 1159 (vs), 993 (w), 926 (m), 837 (w), 667 (m).

$^1\text{H NMR}$ (500 MHz, CDCl_3): δ [ppm] = 5.80 (ddt, $J = 16.9, 10.2, 6.7$ Hz, 1H), 5.70 (bs, 1H), 4.99 (dq, $J = 17.1, 1.7$ Hz, 1H), 4.93 (ddt, $J = 10.2, 2.3, 1.2$ Hz, 1H), 3.92 (qd, $J = 9.1, 6.4$ Hz, 2H), 2.28–2.21 (m, 2H), 2.07–1.99 (m, 2H), 1.70–1.60 (m, 2H), 1.36 (h, $J = 6.6, 5.8$ Hz, 2H), 1.33–1.25 (m, 8H).

$^{13}\text{C NMR}$ (101 MHz, CDCl_3): δ [ppm] = 173.3 (s), 139.3 (s), 124.3 (q, $J = 278.4$ Hz), 114.3 (s), 40.7 (q, $J = 34.6$ Hz), 36.6 (s), 33.9 (s), 29.41 (s), 29.37 (s), 29.24 (s), 29.17 (s), 29.0 (s), 25.6 (s).

HR-MS (ESI, 3 eV): calculated for $\text{C}_{13}\text{H}_{23}\text{F}_3\text{NO}$ [$\text{M}+\text{H}^+$]: 266.1732; measured: 266.1724.

10-Oxo-*N*-(2,2,2-trifluoroethyl)undecanamide (130a)



A suspension of palladium(II) chloride (40.1 mg, 226 μmol , 0.20 equiv) and copper(I) chloride (44.8 mg, 452 μmol , 0.40 equiv) in $\text{DMF}/\text{H}_2\text{O}$ (5/1, 12 mL, 0.1 M) was purged with oxygen until the color of the reaction mixture was black. Alkene **S09** (300 mg, 1.13 mmol, 1.00 equiv) was added and the reaction mixture was stirred at $40\text{ }^\circ\text{C}$ while oxygen was bubbled through the suspension by a pump drive for 36 h.

Then, HCl (1 M, 25 mL) was added and the reaction mixture was extracted with CH₂Cl₂ (4 × 25 mL). The combined organic layers were washed with H₂O (3 × 30 mL), brine (30 mL) and dried (Na₂SO₄) and the solvent was removed *in vacuo*. The crude product was purified *via* flash column chromatography (25 g silica gel, P/Et₂O = 2/1 → 1/1) to provide oxoamide **130a** (258 mg, 917 μmol, 81%) as a white powder.

TLC: *R*_f = 0.18 (P/Et₂O = 1/1) [KMnO₄].

M.p.: *m* = 76–77 °C.

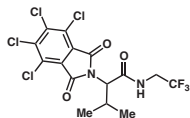
IR (ATR): ν (cm⁻¹) = 3298 (s), 2918 (s), 2848 (s), 1704 (s), 1653 (vs), 1560 (m), 1470 (w), 1429 (w), 1404 (m), 1377 (m), 1285 (w), 1267 (m), 1254 (m), 1231 (m), 1184 (s), 1158 (vs), 837 (w), 715 (w), 669 (m).

¹H NMR (400 MHz, CDCl₃): δ [ppm] = 5.83 (bs, 1H), 3.92 (qd, *J* = 9.1, 6.4 Hz, 2H), 2.41 (t, *J* = 7.4 Hz, 2H), 2.24 (t, *J* = 7.5 Hz, 2H), 2.13 (s, 3H), 1.64 (p, *J* = 7.3 Hz, 2H), 1.55 (p, *J* = 7.4 Hz, 2H), 1.36–1.22 (m, 8H).

¹³C NMR (101 MHz, CDCl₃): δ [ppm] = 209.6 (s), 173.5 (s), 124.3 (q, *J* = 278.4 Hz), 43.8 (s), 40.6 (q, *J* = 34.6 Hz), 36.4 (s), 30.0 (s), 29.2 (s), 29.12 (s), 29.09 (s), 25.5 (s), 23.8 (s).

HR-MS (ESI, 3 eV): calculated for C₁₃H₂₃F₃NO₂ [M+H⁺]: 282.1681; measured: 282.1674.

3-Methyl-2-(4,5,6,7-tetrachloro-1,3-dioxoisindolin-2-yl)-N-(2,2,2-trifluoroethyl)butan-amide (131a)



C₁₅H₁₁Cl₄F₃N₂O₃
M = 466.07

DL-Valine (1.00 g, 8.54 mmol, 1.00 equiv) was dissolved in acetic acid (43 mL, 0.2 M) and tetrachlorophthalic acid anhydride (2.68 g, 9.39 mmol, 1.10 equiv) was added. The reaction mixture was stirred at 140 °C for two hours, after which H₂O (40 mL) was added slowly and the mixture was cooled to 0 °C. Then, the resulting suspension was filtered and the filter residue was washed with cold H₂O (4 × 10 mL) and then dried in high vacuum to provide protected DL-valine (2.76 g, 7.17 mmol, 84%) as an off-white solid.

The protected amino acid (500 mg, 1.30 mmol, 1.00 equiv) was then converted with 2,2,2-trifluoroethylamine hydrochloride (211 mg, 1.56 mmol, 1.20 equiv) according to the standard procedure. Purification *via* flash column chromatography (18 g silica gel, P/EtOAc = 10/1) provided amide **131a** (450 mg, 966 μmol, 74%) as a white solid.

TLC: *R*_f = 0.19 (P/EtOAc = 10/1) [UV, KMnO₄].

M.p.: *m* = 201–202 °C.

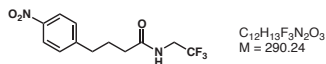
IR (ATR): ν (cm⁻¹) = 3406 (w), 3375 (w), 2930 (w), 2360 (m), 1781 (m), 1719 (vs), 1678 (m), 1539 (m), 1386 (s), 1346 (s), 1258 (m), 1168 (vs), 1148 (vs), 1096 (s), 1000 (m), 954 (m), 833 (m), 741 (vs), 667 (m).

¹H NMR (400 MHz, DMSO-*d*₆): δ [ppm] = 8.72 (t, *J* = 6.3 Hz, 1H), 4.42 (d, *J* = 8.3 Hz, 1H), 3.97 (dq, *J* = 15.0, 9.8, 6.6 Hz, 1H), 3.80 (dq, *J* = 19.4, 9.7, 5.8 Hz, 1H), 2.71 (dp, *J* = 8.4, 6.7 Hz, 1H), 1.02 (d, *J* = 6.7 Hz, 3H), 0.83 (d, *J* = 6.8 Hz, 3H).

¹³C NMR (101 MHz, DMSO-*d*₆): δ [ppm] = 167.9 (s), 163.0 (s), 138.5 (s), 128.3 (s), 127.9 (s), 124.6 (q, *J* = 279.2 Hz), 59.0 (s), 27.5 (s), 20.4 (s), 19.2 (s).

HR-MS (ESI, 3 eV): calculated for C₁₅H₁₂Cl₃³⁷ClF₃N₂O₃ [M+H⁺]: 466.9519; measured: 466.9524.

4-(4-Nitrophenyl)-*N*-(2,2,2-trifluoroethyl)butanamide (**132a**)



Prepared according to the standard procedure from 4-(4-nitrophenyl)butanoic acid (300 mg, 1.68 mmol, 1.00 equiv) and 2,2,2-trifluoroethylamine hydrochloride (274 mg, 2.02 mmol, 1.20 equiv). Purification *via* flash column chromatography (15 g silica gel, P/Et₂O = 1/1) provided amide **132a** (355 mg, 1.37 mmol, 81%) as a crystalline white solid.

TLC: *R*_f = 0.24 (P/Et₂O = 1/1) [UV, KMnO₄].

M.p.: *m* = 148–149 °C.

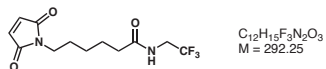
IR (ATR): ν (cm⁻¹) = 3284 (w), 3088 (w), 2930 (w), 1679 (m), 1654 (s), 1603 (m), 1559 (s), 1508 (vs), 1466 (w), 1431 (m), 1399 (w), 1346 (s), 1305 (m), 1286 (m), 1266 (m), 1250 (m), 1225 (m), 1149 (vs), 1108 (m), 1028 (m), 995 (m), 890 (w), 851 (s), 833 (m), 751 (m), 701 (s), 678 (s).

¹H NMR (400 MHz, CDCl₃): δ [ppm] = 8.15 (dd, *J* = 6.5, 2.0 Hz, 2H), 7.38–7.31 (m, 2H), 5.68 (bs, 1H), 3.93 (p, *J* = 8.8 Hz, 2H), 2.78 (t, *J* = 7.2 Hz, 2H), 2.27 (t, *J* = 6.6 Hz, 2H), 2.10–1.97 (m, 2H).

¹³C NMR (126 MHz, CDCl₃): δ [ppm] = 172.3 (s), 149.3 (s), 146.7 (s), 129.4 (s), 124.2 (q, *J* = 278.4 Hz), 123.9 (s), 40.7 (q, *J* = 34.8 Hz), 35.2 (s), 34.9 (s), 26.3 (s).

HR-MS (ESI): calculated for C₁₂H₁₄F₃N₂O₃ [M+H⁺]: 291.0957; measured: 291.0948.

6-(2,5-Dioxo-2,5-dihydro-1*H*-pyrrol-1-yl)-*N*-(2,2,2-trifluoroethyl)hexanamide (**133a**)



6-Maleimidohexanoic acid (500 mg, 2.37 mmol, 1.00 equiv) was dissolved in CH₂Cl₂ (24 mL, 0.1 M), two drops of DMF were added and the reaction mixture was cooled to 0 °C before thionyl chloride (885 mg, 7.10 mmol, 3.00 equiv) was added dropwise. The reaction mixture was stirred for one hour at 0 °C and

then for one hour at room temperature before the solvent was removed *in vacuo*. The residue was dried in high vacuum for one hour and then dissolved in THF (18 mL) and cooled to $-78\text{ }^{\circ}\text{C}$. In a separate flask, 2,2,2-trifluoroethylamine (281 mg, 2.84 mmol, 1.20 equiv) was dissolved in THF (2.9 mL) and cooled to $-78\text{ }^{\circ}\text{C}$ before *n*-butyllithium (2.39 M in hexane, 1.1 mL, 2.60 mmol, 1.10 equiv) was added dropwise and the reaction mixture was stirred at $-78\text{ }^{\circ}\text{C}$ for one hour. The resulting yellow solution was added to the solution of the acid chloride dropwise via cannula at $-78\text{ }^{\circ}\text{C}$ and the orange reaction mixture was stirred at $-78\text{ }^{\circ}\text{C}$ for 90 min, after which HCl (1 M, 25 mL) was added to the cold mixture and the resulting slurry was allowed to slowly warm to room temperature. After extraction ($3 \times 25\text{ mL}$) the combined organic layers were washed with water (50 mL) and brine (50 mL), dried (Na_2SO_4) and the solvent was removed *in vacuo*. Purification *via* flash column chromatography (20 g silica gel, $\text{CH}_2\text{Cl}_2/\text{EtOAc} = 10/1$) provided amide **133a** (219 mg, 749 μmol , 32%) as a white powder.

TLC: $R_f = 0.14$ ($\text{CH}_2\text{Cl}_2/\text{EtOAc} = 10/1$) [UV, KMnO_4].

M.p.: $\Delta_m = 119\text{--}120\text{ }^{\circ}\text{C}$.

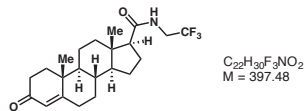
IR (ATR): ν (cm^{-1}) = 3307 (s), 3087 (w), 2937 (w), 2858 (w), 1697 (vs), 1658 (vs), 1552 (s), 1469 (w), 1446 (m), 1415 (s), 1375 (m), 1296 (m), 1273 (m), 1248 (m), 1210 (m), 1159 (vs), 1143 (vs), 1172 (w), 1001 (w), 990 (w), 833 (vs), 697 (s), 669 (m).

^1H NMR (400 MHz, CDCl_3): δ [ppm] = 6.68 (s, 2H), 5.90 (bs, 1H), 3.90 (qd, $J = 9.1, 6.5\text{ Hz}$, 2H), 3.51 (t, $J = 7.2\text{ Hz}$, 2H), 2.24 (t, $J = 7.5\text{ Hz}$, 2H), 1.68 (p, $J = 7.5\text{ Hz}$, 2H), 1.60 (p, $J = 7.4\text{ Hz}$, 2H), 1.35–1.26 (m, 2H).

^{13}C NMR (101 MHz, CDCl_3): δ [ppm] = 172.9 (s), 171.0 (s), 134.2 (s), 124.2 (q, $J = 278.4\text{ Hz}$), 40.6 (q, $J = 34.6\text{ Hz}$), 37.6 (s), 36.2 (s), 28.3 (s), 26.2 (s), 24.8 (s).

HR-MS (ESI, 3 eV): calculated for $\text{C}_{12}\text{H}_{16}\text{F}_3\text{N}_2\text{O}_3$ [$\text{M}+\text{H}^+$]: 293.1113; measured: 293.1106.

(8S,9S,10R,13S,14S,17S)-10,13-Dimethyl-3-oxo-N-(2,2,2-trifluoroethyl)-2,3,6,7,8,9,10,11,12,13,14,15,16,17-tetradecahydro-1H-cyclopenta[*a*]phenanthrene-17-carboxamide (S10)



Progesterone was converted to androst-4-en-3-one-17b-carboxylic acid according to literature^[163].

The carboxylic acid (200 mg, 632 μmol , 1.00 equiv) was dissolved in CH_2Cl_2 (13 mL, 50 mM) and the reaction mixture was cooled to $0\text{ }^{\circ}\text{C}$ before DIPEA (110 μL , 81.7 mg, 632 μmol , 1.00 equiv) and HBTU (264 mg, 695 μmol , 1.10 equiv) was added and the reaction mixture was stirred at $0\text{ }^{\circ}\text{C}$ for 30 min. Then, 2,2,2-trifluoroethylamine hydrochloride (85.7 mg, 632 μmol , 1.00 equiv) and DIPEA (120 μL , 89.9 mg, 695 μmol , 1.10 equiv) was added. The reaction mixture was subsequently stirred at room temperature for

14 h, after which HCl (1 M, 15 mL) was added and the mixture was extracted with CH₂Cl₂ (3 × 15 mL), then the combined organic layers were washed with H₂O (30 mL) and brine (30 mL), dried (Na₂SO₄) and the solvent was removed *in vacuo*. Purification *via* flash column chromatography (30 g silica gel, P/EtOAc = 2/1) provided amide **S10** (211 mg, 531 μmol, 84%) as white solid.

TLC: *R*_f = 0.36 (P/EtOAc = 1/1) [UV, KMnO₄].

M.p.: *m* = 214–215 °C.

[α]_D²⁰: +119.2 (*c* = 0.83, CHCl₃).

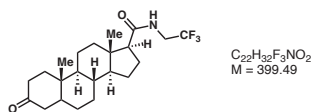
IR (ATR): *ν* (cm⁻¹) = 2953 (w), 2855 (w), 1674 (vs), 1617 (m), 1524 (s), 1436 (w), 1388 (m), 1277 (m), 1221 (s), 1157 (vs), 1133 (vs), 1005 (w), 941 (w), 876 (m), 829 (m), 666 (s).

¹H NMR (400 MHz, CDCl₃): δ [ppm] = 5.73 (s, 1H), 5.70–5.62 (m, 1H), 4.20 (dq, *J* = 14.8, 9.1, 7.3 Hz, 1H), 3.70 (dq, *J* = 14.6, 9.0, 5.3 Hz, 1H), 2.49–2.34 (m, 3H), 2.33–2.22 (m, 2H), 2.21–2.14 (m, 1H), 2.03 (ddd, *J* = 13.7, 5.0, 3.2 Hz, 1H), 1.95 (dt, *J* = 12.0, 3.4 Hz, 1H), 1.87 (dp, *J* = 12.0, 3.0 Hz, 1H), 1.75 (dddd, *J* = 18.7, 15.9, 13.3, 6.3 Hz, 3H), 1.67–1.53 (m, 2H), 1.47 (qd, *J* = 13.1, 4.2 Hz, 1H), 1.34 (dq, *J* = 12.0, 6.1 Hz, 1H), 1.26 (td, *J* = 12.3, 4.1 Hz, 1H), 1.19 (s, 3H), 1.08 (dddd, *J* = 24.9, 17.4, 12.1, 5.7 Hz, 2H), 0.96 (ddd, *J* = 12.3, 10.6, 4.2 Hz, 1H), 0.73 (s, 3H).

¹³C NMR (101 MHz, CDCl₃): δ [ppm] = 199.7 (s), 172.8 (s), 171.1 (s), 124.3 (q, *J* = 278.6 Hz), 124.1 (s), 57.0 (s), 55.7 (s), 53.9 (s), 44.1 (s), 40.5 (q, *J* = 34.4 Hz), 38.8 (s), 38.3 (s), 35.9 (s), 35.8 (s), 34.1 (s), 32.9 (s), 32.1 (s), 24.5 (s), 23.6 (s), 21.1 (s), 17.5 (s), 13.2 (s).

HR-MS (ESI, 3 eV): calculated for C₂₂H₃₁F₃NO₂ [M+H⁺]: 398.2307; measured: 398.2298.

(8R,9S,10S,13S,14S,17S)-10,13-Dimethyl-3-oxo-N-(2,2,2-trifluoroethyl)hexadecahydro-1H-cyclopenta[*a*]phenanthrene-17-carboxamide (134a)



Enone **S10** (175 mg, 440 μmol, 1.00 equiv) was added to a suspension of palladium(0) on charcoal (10% w/w, 23.4 mg, 22.0 μmol, 0.05 equiv) in methanol (2.2 mL, 0.2 M) under argon atmosphere. The flask was subsequently purged with hydrogen and the reaction mixture was stirred at room temperature under hydrogen atmosphere for 24 h. Then, the reaction mixture was filtered through Celite[®] and HCl (1 M, 10 mL) was added to the filtrate before being extracted with CH₂Cl₂ (4 × 10 mL) and the combined organic layers were washed with brine (20 mL), dried (Na₂SO₄) and the solvent was removed *in vacuo*. The crude

product was purified *via* flash column chromatography (30 mg silica gel, CH₂Cl₂/MeCN = 97/3) to provide amide **134a** (123 mg, 308 μmol, 70%) as a white powder.

TLC: $R_f = 0.25$ (CH₂Cl₂/MeCN = 95/5) [KMnO₄].

M.p.: $\Theta_m = 77-79$ °C.

[α]_D²⁰: +50.6 ($c = 0.74$, CHCl₃).

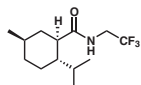
IR (ATR): ν (cm⁻¹) = 3335 (w), 2932 (w), 2866 (w), 1707 (s), 1670 (m), 1534 (m), 1449 (m), 1387 (m), 1271 (m), 1223 (m), 1155 (vs), 1007 (w), 833 (w), 668 (m).

¹H NMR (500 MHz, CDCl₃): δ [ppm] = 5.53 (bs, 1H), 4.20 (dddd, $J = 14.9, 9.3, 7.4, 1.7$ Hz, 1H), 3.70 (ddd, $J = 14.8, 9.1, 5.5$ Hz, 1H), 2.68 (dd, $J = 15.2, 13.3$ Hz, 1H), 2.31 (td, $J = 14.6, 5.4$ Hz, 1H), 2.23–2.14 (m, 3H), 2.04 (dtd, $J = 14.3, 5.1, 2.6$ Hz, 2H), 1.96 (dt, $J = 11.7, 3.1$ Hz, 1H), 1.94–1.69 (m, 4H), 1.59–1.48 (m, 4H), 1.46–1.37 (m, 2H), 1.36–1.22 (m, 3H), 1.03 (s, 4H), 0.70 (s, 4H).

¹³C NMR (126 MHz, CDCl₃): δ [ppm] = 213.3 (s), 172.9 (s), 124.3 (q, $J = 278.5$ Hz), 57.3 (s), 56.3 (s), 44.4 (s), 44.3 (s), 42.4 (s), 40.9 (s), 40.5 (q, $J = 34.6$ Hz), 38.8 (s), 37.3 (s), 37.1 (s), 35.7 (s), 35.1 (s), 26.6 (s), 25.9 (s), 24.6 (s), 23.6 (s), 22.8 (s), 21.3 (s), 13.3 (s).

HR-MS (ESI, 3 eV): calculated for C₂₂H₃₃F₃NO₂ [M+H]⁺: 400.2463; measured: 400.2454.

(1*R*,2*S*,5*R*)-2-isopropyl-5-methyl-*N*-(2,2,2-trifluoroethyl)cyclohexanecarboxamide (**135a**)



C₁₃H₂₂F₃NO
M = 285.32

A solution of (1*R*,2*S*,5*R*)-2-isopropyl-5-methylcyclohexanecarboxylic acid (500 mg, 2.71 mmol, 1.00 equiv) in CH₂Cl₂ (30 mL, 0.1 M) was cooled to 0 °C before DIPEA (470 μL, 351 mg, 2.71 mmol, 1.00 equiv) and HBTU (1.13 g, 2.98 mmol, 1.10 equiv) was added. The reaction mixture was stirred at 0 °C for 30 min, after which 2,2,2-trifluoroethylamine hydrochloride (368 mg, 2.71 mmol, 1.00 equiv) and DIPEA (520 μL, 386 mg, 2.98 mmol, 1.10 equiv) was added. Then, the reaction mixture was allowed to warm to room temperature and stirred for 14 h before HCl (1 M, 50 mL) was added. After extraction with CH₂Cl₂ (3 × 50 mL) the combined organic layers were washed with H₂O (75 mL) and brine (75 mL), dried (Na₂SO₄) and the solvent was removed *in vacuo*. The crude product was purified *via* flash column chromatography (30 g silica gel, P/Et₂O = 5/1) to provide amide **135a** (440 mg, 1.66 mmol, 61%) as a crystalline white solid.

TLC: $R_f = 0.21$ (P/Et₂O = 5/1) [KMnO₄].

M.p.: $\Theta_m = 82-84$ °C.

[α]_D²⁰: -37.3 ($c = 0.62$; CHCl₃).

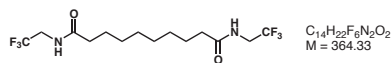
IR (ATR): ν (cm^{-1}) = 3287 (m), 2958 (w), 2930 (m), 2858 (w), 1654 (s), 1549 (m), 1457 (w), 1424 (w), 1393 (w), 1295 (w), 1266 (m), 1238 (w), 1212 (m), 1155 (vs), 898 (w), 833 (w), 689 (w), 669 (w).

^1H NMR (400 MHz, CDCl_3): δ [ppm] = 6.00 (bs, 1H), 4.03–3.78 (m, 2H), 2.10 (td, J = 11.5, 3.4 Hz, 1H), 1.81–1.64 (m, 4H), 1.54 (tt, J = 11.5, 3.1 Hz, 1H), 1.34 (dddd, J = 17.4, 12.8, 6.5, 3.3 Hz, 1H), 1.21 (q, J = 12.1 Hz, 1H), 1.07–0.91 (m, 2H), 0.90 (d, J = 2.2 Hz, 3H), 0.88 (d, J = 1.8 Hz, 3H), 0.77 (d, J = 6.9 Hz, 3H).

^{13}C NMR (101 MHz, CDCl_3): δ [ppm] = 176.3 (s), 124.3 (q, J = 278.5 Hz), 49.8 (s), 44.5 (s), 40.4 (q, J = 34.5 Hz), 39.4 (s), 34.6 (s), 32.4 (s), 28.7 (s), 23.9 (s), 22.4 (s), 21.5 (s), 16.1 (s).

HR-MS (ESI, 3 eV): calculated for $\text{C}_{13}\text{H}_{23}\text{F}_3\text{NO}$ [$\text{M}+\text{H}^+$]: 266.1732; measured: 266.1724.

N^1, N^{10} -Bis(2,2,2-trifluoroethyl)decanediamide (136a)



A suspension of sebacic acid (500 mg, 2.47 mmol, 1.00 equiv) in CH_2Cl_2 (30 mL, 0.1 M) was cooled to 0 °C before EDC·HCl (1.42 g, 7.42 mmol, 3.00 equiv) and DMAP (30.2 mg, 247 μmol , 0.10 equiv) was added, followed by 2,2,2-trifluoroethylamine hydrochloride (804 mg, 5.93 mmol, 2.40 equiv) and NEt_3 (1.7 mL, 1.25 g, 12.4 mmol, 5.00 equiv). The reaction mixture was stirred for 16 h, after which saturated NH_4Cl (50 mL) was added to the now clear pale yellow solution and the mixture was extracted with CH_2Cl_2 (3 \times 50 mL). The combined organic layers were washed with brine (100 mL) and dried (Na_2SO_4), then the solvent was removed *in vacuo*. Purification *via* flash column chromatography (40 g silica gel, P/EtOAc = 1/2) provided diamide **136a** (745 mg, 2.04 mmol, 83%) as a white solid.

TLC: R_f = 0.24 (P/EtOAc = 1/2) [KMnO_4].

M.p.: \varnothing_m = 143–144 °C.

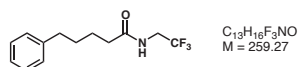
IR (ATR): ν (cm^{-1}) = 3299 (m), 2925 (m), 2850 (m), 1654 (s), 1555(s), 1400 (w), 1269 (m) 1251 (w), 1232 (m), 1154 (vs), 984 (w), 882 (w), 834 (w), 667 (m).

^1H NMR (400 MHz, $\text{DMSO}-d_6$): δ [ppm] = 8.44 (t, J = 6.1 Hz, 2H), 3.87 (qd, J = 9.9, 6.3 Hz, 4H), 2.14 (t, J = 7.4 Hz, 4H), 1.48 (h, J = 6.8 Hz, 4H), 1.27–1.17 (m, 8H).

^{13}C NMR (101 MHz, $\text{DMSO}-d_6$): δ [ppm] = 172.9 (s), 124.8 (q, J = 279.3 Hz), 34.9 (s), 28.6 (s), 28.4 (s), 25.0 (s).

HR-MS (ESI, 3 eV): calculated for $\text{C}_{14}\text{H}_{23}\text{F}_6\text{N}_2\text{O}_2$ [$\text{M}+\text{H}^+$]: 365.1664; measured: 365.1657.

5-Phenyl- N -(2,2,2-trifluoroethyl)pentanamide (37a)



Prepared according to the standard procedure from 5-phenylpentanoic acid (300 mg, 1.68 mmol, 1.00 equiv) and 2,2,2-trifluoroethylamine hydrochloride (274 mg, 2.02 mmol, 1.20 equiv). Purification *via* flash column chromatography (15 g silica gel, P/Et₂O = 1/1) provided amide **37a** (1.25 g, 4.71 mmol, 87%) as a crystalline white solid.

TLC: *R*_f = 0.24 (P/Et₂O = 1/1) [UV, KMnO₄].

M.p.: *m* = 53–54 °C.

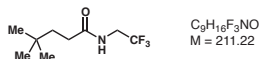
IR (ATR): ν (cm⁻¹) = 3319 (w), 2933 (w), 2858 (w), 1662 (s), 1544 (s), 1497 (w), 1423 (w), 1399 (m), 1275 (m), 1252 (m), 1213 (w), 1154 (vs), 1084 (m), 989 (w), 834 (m), 750 (m), 700 (s), 667 (s).

¹H NMR (400 MHz, CDCl₃): δ [ppm] = 7.31–7.24 (m, 2H), 7.22–7.14 (m, 3H), 5.87 (bs, 1H), 3.89 (qd, *J* = 9.2, 6.5 Hz, 2H), 2.63 (t, *J* = 7.1 Hz, 2H), 2.26 (t, *J* = 7.1 Hz, 2H), 1.81–1.57 (m, 4H).

¹³C NMR (101 MHz, CDCl₃): δ [ppm] = 173.2 (s), 142.1 (s), 128.5 (s), 128.5 (s), 126.0 (s), 124.2 (q, *J* = 278.3 Hz), 40.6 (q, *J* = 34.6 Hz), 36.3 (s), 35.7 (s), 31.0 (s), 25.1 (s).

HR-MS (ESI, 3 eV): calculated for C₁₃H₁₇F₃NO [M+H⁺]: 260.1262; measured: 260.1255.

4,4-Dimethyl-N-(2,2,2-trifluoroethyl)pentanamide (**138a**)



Acrylic acid was converted to 4,4-dimethylpentanoic acid according to literature.^[164]

4,4-Dimethylpentanoic acid (400 mg, 3.07 mmol, 1.00 equiv) was converted according to the standard procedure with 2,2,2-trifluoroethylamine hydrochloride (500 mg, 3.69 mmol, 1.20 equiv). Purification *via* flash column chromatography (45 g silica gel, P/Et₂O = 2/1) provided amide **138a** (492 mg, 3.07 mmol, 76%) as a crystalline white solid.

TLC: *R*_f = 0.22 (P/Et₂O = 2/1) [KMnO₄].

M.p.: *m* = 37–38 °C.

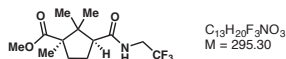
IR (ATR): ν (cm⁻¹) = 3303 (w), 2957 (m), 2869 (w), 1656 (s), 1552 (s), 1397 (m), 1272 (s), 1144 (vs), 833 (m), 666 (s).

¹H NMR (400 MHz, CDCl₃): δ [ppm] = 6.15 (bs, 1H), 3.89 (qd, *J* = 9.1, 6.4 Hz, 2H), 2.29–2.15 (m, 2H), 1.63–1.46 (m, 2H), 0.89 (s, 9H).

¹³C NMR (101 MHz, CDCl₃): δ [ppm] = 174.2 (s), 124.3 (q, *J* = 278.5 Hz), 40.7 (q, *J* = 34.6 Hz), 39.2 (s), 32.1 (s), 30.2 (s), 29.1 (s).

HR-MS (EI, 70 eV): calculated for C₉H₁₆F₃NO [M⁺]: 211.1184; measured: 211.1179.

Methyl 1,2,2-trimethyl-3-((2,2,2-trifluoroethyl)carbamoyl)cyclopentane-1-carb-oxylate (139a)



(1R,3S)-(+)-Camphoric acid was converted to its dimethyl diester according to literature.^[165]

2,2,2-Trifluoroethylamine (468 mg, 4.73 mmol, 2.60 equiv) was dissolved in THF (9 mL, 0.5 M) and cooled to $-78\text{ }^{\circ}\text{C}$ before *n*-butyllithium (2.39 M in hexane, 1.8 mL, 4.36 mmol, 2.4 mmol) was added dropwise and the reaction mixture was stirred at $-78\text{ }^{\circ}\text{C}$ for one hour. A solution of dimethyl (1R,3S)-1,2,2-trimethylcyclopentane-1,3-dicarboxylate (415 mg, 1.82 mmol, 1.00 equiv) in THF (9 mL, 0.1 M final concentration) was added dropwise to the yellow solution and the reaction mixture was stirred at $-78\text{ }^{\circ}\text{C}$ for two hours. Acetic acid (3 mL) was added and the reaction mixture was allowed to warm to room temperature before HCl (1 M, 25 mL) was added and the mixture was extracted with Et₂O (3 × 25 mL). The combined organic layers were washed with saturated NaHCO₃ (2 × 50 mL) and brine (50 mL), dried (Na₂SO₄) and the solvent was removed *in vacuo*. The crude product was purified *via* flash column chromatography (30 g silica gel, P/Et₂O = 2/1) to provide monoamide **139a** (441 mg, 1.49 mmol, 82%) as a crystalline white solid.

TLC: $R_f = 0.35$ (P/Et₂O = 1/2) [KMnO₄].

M.p.: $\text{M.p.} = 89\text{--}90\text{ }^{\circ}\text{C}$.

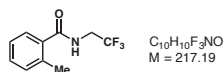
[α]_D²⁰: +12.4 ($c = 1.05$, CHCl₃).

IR (ATR): ν (cm⁻¹) = 3328 (w), 2969 (m), 2886 (w), 1726 (m), 1666 (s), 1538 (m), 1458 (w), 1435 (w), 1395 (w), 1378 (w), 1271 (s), 1238 (m), 1207 (m), 1153 (vs), 1119 (s), 1090 (m), 989 (w), 833 (w), 668 (w).

¹H NMR (400 MHz, CDCl₃): δ [ppm] = 5.81 (t, $J = 6.1$ Hz, 1H), 4.12 (dq, $J = 15.0, 9.2, 7.3$ Hz, 1H), 3.74 (dq, $J = 15.1, 9.2, 5.8$ Hz, 1H), 3.66 (s, 3H), 2.61 (t, $J = 9.3$ Hz, 1H), 2.64–2.55 (m, 1H), 2.22 (dddd, $J = 13.6, 11.8, 9.1, 4.4$ Hz, 1H), 1.80 (dtd, $J = 13.7, 9.6, 6.8$ Hz, 1H), 1.51 (ddd, $J = 13.8, 9.6, 4.4$ Hz, 1H), 1.23 (s, 3H), 1.19 (s, 3H), 0.77 (s, 3H).

¹³C NMR (101 MHz, CDCl₃): δ [ppm] = 176.3 (s), 173.0 (s), 124.2 (q, $J = 278.5$ Hz), 56.5 (s), 54.7 (s), 51.7 (s), 46.8 (s), 40.6 (q, $J = 34.5$ Hz), 32.7 (s), 23.4 (s), 23.1 (s), 21.8 (s), 21.0 (s).

HR-MS (EI, 70 eV): calculated for C₁₃H₂₀O₃NF₃ [M^+]: 295.1390; measured: 295.1393.

2-Methyl-*N*-(2,2,2-trifluoroethyl)benzamide (S11)

Prepared according to the standard procedure from 2-methylbenzoic acid (500 mg, 3.67 mmol, 1.00 equiv) and 2,2,2-trifluoroethylamine hydrochloride (597 mg, 4.41 mmol, 1.20 equiv). Purification *via* flash column chromatography (40 g silica gel, P/Et₂O = 3/1) provided amide **S11** (630 mg, 2.90 mmol, 79%) as a white solid.

TLC: $R_f = 0.24$ (P/Et₂O = 3/1) [UV, KMnO₄].

M.p.: $\vartheta_m = 83\text{--}84$ °C.

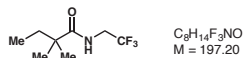
IR (ATR): ν (cm⁻¹) = 3276 (w), 1648 (s), 1528 (m), 1486 (w), 1424 (w), 1393 (w), 1393 (m), 1312 (m), 1263 (s), 1174 (vs), 1047 (m), 968 (w), 832 (w), 782 (w), 720 (m), 692 (s), 656 (s).

¹H NMR (400 MHz, CDCl₃): δ [ppm] = 7.39–7.32 (m, 2H), 7.23 (dd, $J = 13.4, 7.3$ Hz, 2H), 6.07 (bs, 1H), 4.09 (qd, $J = 9.0, 6.5$ Hz, 2H), 2.44 (s, 3H).

¹³C NMR (101 MHz, CDCl₃): δ [ppm] = 170.0 (s), 136.6 (s), 135.1 (s), 131.4 (s), 130.7 (s), 126.8 (s), 126.0 (s), 124.3 (q, $J = 278.5$ Hz), 41.0 (q, $J = 34.7$ Hz), 19.8 (s).

HR-MS (ESI, 3 eV): calculated for XX [M+H⁺]: 218.0793; measured: 218.0785.

2,2-Dimethyl-N-(2,2,2-trifluoroethyl)butanamide (S12)



2,2-Dimethylbutyric acid (500 mg, 4.30 mmol, 1.00 equiv) was dissolved in CH₂Cl₂ (43 mL, 0.1 M), two drops of DMF were added and the reaction mixture was cooled to 0 °C before thionyl chloride (1.54 g, 12.9 mmol, 3.00 equiv) was added dropwise. The reaction mixture was stirred for one hour at 0 °C and then for one hour at room temperature before the solvent was removed *in vacuo*. The residue was dissolved in CH₂Cl₂ (43 mL, 0.1 M) and cooled to 0 °C. NEt₃ (3.0 mL, 2.18 g, 21.5 mmol, 5.00 equiv) was added dropwise, after which 2,2,2-trifluoroethylamine hydrochloride (700 mg, 5.17 mmol, 1.20 equiv) was added and the reaction mixture was stirred at 0 °C for one hour and then at room temperature for one hour. After addition of saturated NH₄Cl (50 mL) the reaction mixture was extracted with CH₂Cl₂ (3 × 50 mL) and the combined organic layers were washed with brine (100 mL), dried (Na₂SO₄) and the solvent was removed *in vacuo*. The crude product was purified via flash column chromatography (15 g silica gel, P/Et₂O = 2/1) to provide amide **S12** (114 mg, 578 μmol, 13%) as a colorless oil.

TLC: $R_f = 0.24$ (P/Et₂O = 2/1) [KMnO₄].

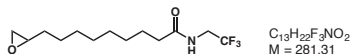
IR (ATR): ν (cm⁻¹) = 3351 (w), 2970 (m), 1656 (s), 1525 (s), 1477 (w), 1424 (w), 1395 (w), 1280 (m), 1152 (vs).

¹H NMR (500 MHz, CDCl₃): δ [ppm] = 5.85 (bs, 1H), 3.93 (qd, $J = 9.1, 6.3$ Hz, 2H), 1.57 (q, $J = 7.5$ Hz, 2H), 1.18 (s, 6H), 0.84 (t, $J = 7.5$ Hz, 3H).

^{13}C NMR (126 MHz, CDCl_3): δ [ppm] = 178.0 (s), 124.3 (q, J = 278.4 Hz), 42.8 (s), 40.7 (q, J = 34.5 Hz), 34.0 (s), 25.0 (s), 9.1 (s).

HR-MS (ESI): calculated for $\text{C}_7\text{H}_{11}\text{F}_3\text{NO}$ [$\text{M}-\text{CH}_3^+$]: 182.0793; measured: 182.0789.

9-(Oxiran-2-yl)-*N*-(2,2,2-trifluoroethyl)nonanamide (S13)



A solution of alkene **S09** (500 mg, 1.88 mmol, 1.00 equiv) in CH_2Cl_2 (19 mL, 0.1 M) was cooled to 0 °C and *m*-CPBA (70% purity, 627 mg, 2.54 mmol, 1.35 equiv) was added slowly. The reaction mixture was then slowly allowed to warm to room temperature and stirred at room temperature for ten hours before Na_2SO_3 (1 M, 5 mL). After stirring for 30 min CH_2Cl_2 (30 mL) was added and the organic layer was washed with saturated NaHCO_3 (3 \times 30 mL) and brine (30 mL), dried (Na_2SO_4) and the solvent was removed *in vacuo*. The crude product was dried under high vacuum for 30 min to provide epoxide **S13** (492 mg, 1.75 mmol, 93%) as a white powdery solid without any further purification.

TLC: R_f = 0.30 (P/Et₂O = 1/1) [KMnO_4].

M.p.: m = 83–84 °C.

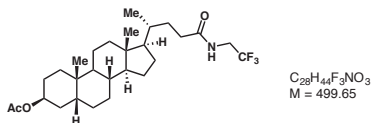
IR (ATR): ν (cm^{-1}) = 3309 (w), 2927 (w), 2851 (w), 1654 (vs), 1556 (s), 1435 (w), 1399 (m), 1289 (m), 1272 (m), 1253 (m), 1228 (m), 1166 (s), 1151 (vs), 990 (w), 947 (w), 887 (w), 832 (s), 724 (w), 693 (m), 669 (s).

^1H NMR (400 MHz, CDCl_3): δ [ppm] = 5.73 (bs, 1H), 3.92 (qd, J = 9.1, 6.4 Hz, 2H), 2.90 (tdd, J = 5.2, 4.0, 2.7 Hz, 1H), 2.74 (dd, J = 5.0, 4.0 Hz, 1H), 2.46 (dd, J = 5.0, 2.7 Hz, 1H), 2.30–2.20 (m, 2H), 1.65 (p, J = 7.2 Hz, 2H), 1.56–1.48 (m, 2H), 1.44 (ddt, J = 12.4, 6.0, 3.8 Hz, 2H), 1.39–1.26 (m, 8H).

^{13}C NMR (101 MHz, CDCl_3): δ [ppm] = 173.5 (s), 124.2 (q, J = 278.5 Hz), 52.6 (s), 47.2 (s), 40.6 (q, J = 34.6 Hz), 36.4 (s), 32.5 (s), 29.40 (s), 29.39 (s), 29.24 (s), 29.15 (s), 26.0 (s), 25.5 (s).

HR-MS (ESI, 3 eV): calculated for $\text{C}_{13}\text{H}_{23}\text{F}_3\text{NO}_2$ [$\text{M}+\text{H}^+$]: 282.1671; measured: 282.1674.

(3S,5R,8R,10S,13R,14S,17R)-10,13-dimethyl-17-((R)-5-oxo-5-((2,2,2-trifluoroethyl)-amino)pentan-2-yl)hexadecahydro-1H-cyclopenta[*a*]phenanthren-3-yl acetate (S14)



Lithocholic acid was converted to the acetate according to literature.^[166] *O*-Acetylithocholic acid (420 mg, 1.00 mmol, 1.00 equiv) was converted according to the standard procedure with 2,2,2-trifluoroethylamine hydrochloride (163 mg, 1.20 mmol, 1.20 equiv). Purification *via* flash column chromatography (40 g silica gel, P/Et₂O = 3/2) provided amide **S14** (342 mg, 684 μmol, 68%) as a crystalline white solid.

TLC: *R*_f = 0.22 (P/Et₂O = 3/2) [KMnO₄].

M.p.: *m* = 137–138 °C.

[α]_D²⁰: +37.7 (*c* = 1.03, CHCl₃).

IR (ATR): *v* (cm⁻¹) = 3294 (w), 2935 (m), 2855 (w), 1739 (s), 1655 (s), 1555 (m), 1447 (m), 1379 (m), 1244 (s), 1157 (vs), 1026 (s), 833 (w), 670 (m).

¹H NMR (300 MHz, CDCl₃): δ [ppm] = 5.68 (t, *J* = 6.6 Hz, 1H), 4.72 (tt, *J* = 11.3, 4.8 Hz, 1H), 3.92 (qd, *J* = 9.1, 6.4 Hz, 2H), 2.31 (ddd, *J* = 14.9, 10.2, 4.9 Hz, 1H), 2.14 (ddd, *J* = 14.5, 9.5, 6.4 Hz, 1H), 2.03 (s, 3H), 2.00–1.92 (m, 1H), 1.91–1.75 (m, 5H), 1.73–1.62 (m, 1H), 1.62–1.49 (m, 2H), 1.41 (tdd, *J* = 13.5, 6.3, 3.2 Hz, 7H), 1.32–1.00 (m, 10H), 0.92 (s, 3H), 0.92 (d, *J* = 6.3 Hz, 3H), 0.64 (s, 3H).

¹³C NMR (101 MHz, CDCl₃): δ [ppm] = 173.8 (s), 170.8 (s), 124.3 (q, *J* = 278.6 Hz), 74.6 (s), 56.6 (s), 56.2 (s), 42.9 (s), 42.0 (s), 40.7 (q, *J* = 34.7 Hz), 40.5 (s), 40.3 (s), 35.9 (s), 35.5 (s), 35.2 (s), 34.7 (s), 33.4 (s), 32.4 (s), 31.6 (s), 28.4 (s), 27.2 (s), 26.8 (s), 26.5 (s), 24.3 (s), 23.5 (s), 21.6 (s), 21.0 (s), 18.5 (s), 12.2 (s).

HR-MS (EI, 70 eV): calculated for C₂₈H₄₅F₃NO₃ [M+H⁺]: 500.3346; measured: 500.3350.

Preparation of Acetyl Hypobromite

Silver(I) acetate (2.10 g, 12.6 mmol, 1.10 equiv) was stirred in CH₂Cl₂ (dry, stored over 4 Å MS, ACROS, 40 mL) in a 250 mL round-bottom flask wrapped in aluminium foil at 0 °C. Bromine (0.58 mL, 1.81 g, 11.3 mmol, 1.00 equiv) was slowly added to the suspension and the reaction mixture was stirred for 10 min or until the color of the reaction mixture turned from orange-red to green-yellow. The suspension was filtered rapidly and eluted with CH₂Cl₂ (10 mL). The resulting green-yellow solution was stored at –20 °C and used for up to one week. Concentration decreased by approx. 3–5 mM per day.

Titration of Acetyl Hypobromite

A precise amount of triphenyl phosphine (12–16 mg) was dissolved in CH₂Cl₂ (550–600 μL, *ca.* 0.1 M). A solution of acetyl hypobromite was added dropwise at room temperature under stirring until the color of the solution turned from colorless to light yellow.

General Procedure for the Amide Bromination Screening

Amide (1.00 equiv) was dissolved in CH_2Cl_2 (dry, stored over 4 Å MS, ACROS; to give a final concentration of 25 mM once the acetyl hypobromite solution is added) in a reaction vial wrapped with aluminium foil and the laboratory lights were turned off. Freshly titrated acetyl hypobromite solution ($-20\text{ }^\circ\text{C}$, 2.50 equiv) was added and the reaction mixture was stirred for 30 min at room temperature, at which point the aluminium foil was removed and the reaction mixture was irradiated with white LEDs (24 W, approx. 120 units, held at approx. 5 cm distance, figure S1) for 30 min. Then, the solvent was removed *in vacuo* and the residue was dried under high vacuum for 30 min to remove all residual acetic acid.

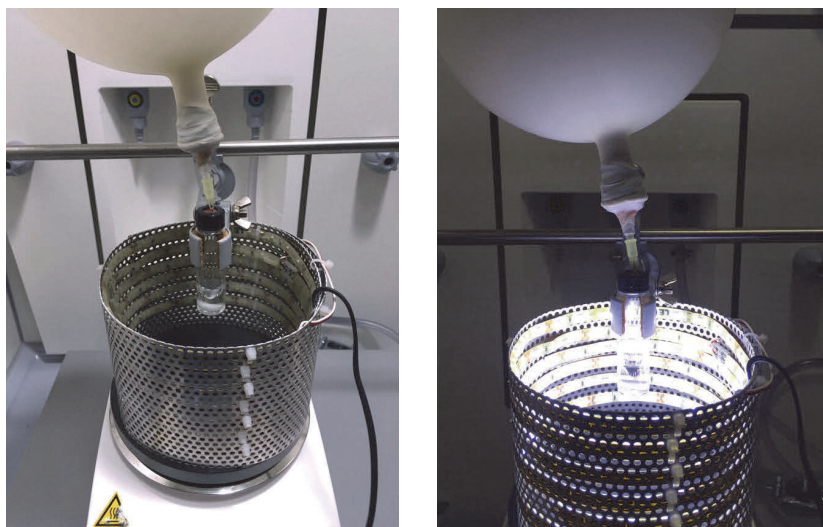
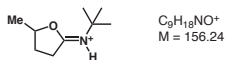


Figure S1. Reaction setup with white LEDs attached to a perforated bent metal plate (left: LEDs switched off; right: LEDs switched on).

2-Methyl-N-(5-methyldihydrofuran-2(3H)-ylidene)propan-2-aminium (S15)



Prepared according to the screening procedure from amide **16** (10.0 mg, 63.6 μmol , 1.00 equiv) to provide the crude product of spontaneously cyclized iminolactone hydrobromide **S15** (18.2 mg) as a dark yellow solid.

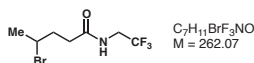
TLC: $R_f = 0.29$ (P/Et₂O = 2/1) [KMnO₄] (deprotonated iminolactone).

IR (ATR): ν (cm⁻¹) = 2973 (m), 2933 (m), 2868 (m), 1683 (vs), 1530 (s), 1454 (m), 1372 (m), 1361 (m), 1198 (vs), 1033 (s), 964 (s), 898 (m), 800 (m), 730 (s), 687 (m).

¹H NMR (300 MHz, CDCl₃): δ [ppm] = 11.30 (bs, 1H), 5.34 (dp, $J = 8.3, 6.3$ Hz, 1H), 3.72 (ddd, $J = 19.0, 9.2, 3.9$ Hz, 1H), 3.50 (dt, $J = 19.0, 9.5$ Hz, 1H), 2.60 (dddd, $J = 13.1, 9.9, 6.5, 3.9$ Hz, 1H), 2.02 (ddd, $J = 18.0, 8.6, 3.7$ Hz, 1H), 1.63 (d, $J = 6.3$ Hz, 3H), 1.54 (s, 9H).

¹³C NMR (126 MHz, UDEFT, CDCl₃): δ [ppm] = 179.1 (s), 90.8 (s), 58.5 (s), 33.0 (s), 29.3 (s), 28.4 (s), 20.5 (s).

4-Bromo-*N*-(2,2,2-trifluoroethyl)pentanamide (S16)



Prepared according to the screening procedure from amide **17** (10.0 mg, 54.6 μ mol, 1.00 equiv) to provide the crude bromide **S16** (16.7 mg) as a pale yellow solid.

TLC: $R_f = 0.18$ (P/Et₂O = 2/1) [KMnO₄].

IR (ATR): ν (cm⁻¹) = 3292 (w), 2961 (w), 2933 (w), 1662 (s), 1547 (m), 1396 (m), 1261 (m), 1152 (vs), 992 (m), 833 (m), 668 (bm).

¹H NMR (300 MHz, CDCl₃): δ [ppm] = 5.88 (bs, 1H), 4.15 (dq, $J = 10.0, 6.6, 3.4$ Hz, 1H), 3.92 (qd, $J = 9.1, 6.4$ Hz, 2H), 2.62–2.36 (m, 2H), 2.32–2.14 (m, 1H), 2.01 (dddd, $J = 14.7, 9.8, 7.7, 5.5$ Hz, 1H), 1.74 (d, $J = 6.6$ Hz, 3H).

¹³C NMR (101 MHz, CDCl₃): δ [ppm] = 172.3 (s), 124.2 (q, $J = 278.4$ Hz), 51.0 (s), 40.7 (q, $J = 34.8$ Hz), 36.2 (s), 34.5 (s), 26.7 (s).

Determination of Ratio of Product/Starting Material of Bromides Using ¹H NMR

In general, the ratio of product/starting material of the crude products from bromination of *N*-substituted pentanamides was determined by comparing the integrals of the methyl signals in δ -position of both species in the ¹H NMR spectra. These signals were chosen due to both signals being isolated, allowing for reliable comparison (figure S2).

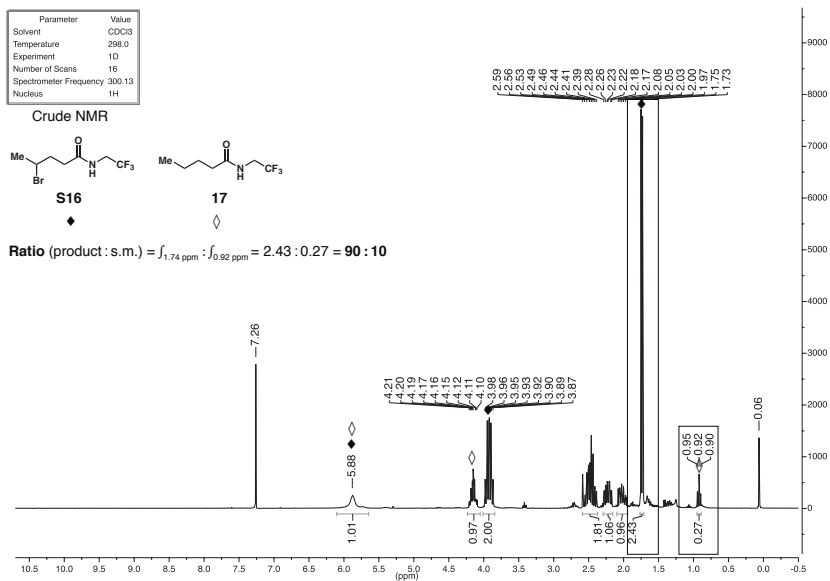


Figure S2. Determination of ratio of product/starting material in A14/A09 using the methyl signal in δ -position.

Optimization of the Synthesis of γ -Bromoamides

Table S1. Optimization of the synthesis of γ -bromoamides.

#	Change from Screening Conditions	ratio products/s.m. ^{a)}
1	1) AcOBr (5.0 eq)	75 : 25
2	1) AcOBr (1.5 eq)	58 : 42
3	1) AcOBr (1.1 eq)	53 : 47
4	1) 60 min	81 : 19
5	2) remove solvent, then (CH ₂ Cl ₂)	82 : 18
6	2) remove solvent, then (THF)	— ^{b)}
7	2) remove solvent, then (dioxane)	19 : 81
8	2) remove solvent, then (MeCN)	76 : 24
9	2) remove solvent, then (PhCF ₃)	83 : 17
10	1) AcOBr (1.2 eq); 2) remove solvent, then (PhCF ₃)	83 : 17
11	1) AcOBr (1.2 eq), 0 °C; 2) remove solvent, then (PhCF ₃), CBr ₄ (1.0 eq)	96 : 4
12	1) AcOBr (1.2 eq), 0 °C; 2) remove solvent, then (CH ₂ Cl ₂), CBr ₄ (1.0 eq)	94 : 6

^{a)} Ratio determined from crude ¹H NMR. ^{b)} Complex product mixture, no bromination product.

General Procedure for the Formation of Volatile Lactones

γ -Bromoamide was prepared according to the general procedure for amide bromination screening from amide (1.00 equiv). The residue was dissolved in CH_2Cl_2 (dry, stored over 4 Å MS, ACROS, 50 mm), the laboratory lights were turned off and silver(I) tetrafluoroborate (1.50 equiv) was added. The reaction mixture was stirred for 30 min or until TLC showed complete consumption of the γ -bromoamide before H_2O (2.5% v/v) was added and the reaction was stirred for another four hours or until TLC showed complete consumption of the iminolactone. Then, a saturated solution of sodium chloride in ammonium hydroxide (25% aq.) was added and the reaction mixture was extracted with CH_2Cl_2 (3 \times). The combined organic layers were dried (Na_2SO_4) and the solvent was removed under reduced pressure (400 mbar, 40 °C, 30 min) to provide the crude product of lactone.

Yield Determination Using ^1H NMR and Internal Standard

A precise amount of crude lactone ($m_{\text{crude,NMR}}$) and a precise amount of dibromomethane (m_{IS} , molar mass $M_{\text{IS}} = 173.83$ g/mol) was weighed into an NMR tube and dissolved in CDCl_3 . Based the relative integrals of the signal of internal standard at 4.93 ppm (s, 2H) (I_{IS}) and of a signal of the lactone (I_{Lactone}) representing a known amount of protons in the lactone (H_{Lactone}), the mass of pure lactone in the weighed amount ($m_{\text{Lactone,NMR}}$, molar mass M_{Lactone}) was determined according to equation 3.

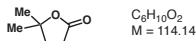
$$\frac{n_{\text{Lactone,NMR}}}{n_{\text{IS}}} = \frac{\frac{I_{\text{Lactone}}}{H_{\text{Lactone}}}}{\frac{I_{\text{IS}}}{2}} \quad (1)$$

$$n = \frac{m}{M} \quad (2)$$

$$m_{\text{Lactone,NMR}} = \frac{2 \cdot I_{\text{Lactone}} \cdot m_{\text{IS}} \cdot M_{\text{Lactone}}}{H_{\text{Lactone}} \cdot I_{\text{IS}} \cdot M_{\text{IS}}} \quad (3)$$

Based on $m_{\text{crude,NMR}}$, $m_{\text{Lactone,NMR}}$ and the total mass of crude lactone obtained (m_{crude}), the total mass of pure lactone in the crude product (m_{Lactone}) was determined according to equation 4.

$$m_{\text{Lactone}} = m_{\text{Lactone,NMR}} \cdot \frac{m_{\text{crude}}}{m_{\text{crude,NMR}}} \quad (4)$$

5,5-Dimethyldihydrofuran-2(3H)-one (121)

Prepared according to the general procedure from **S01** (50.0 mg, 254 μ mol) to provide crude product of **121** (50.8 mg) as a pale yellow oil. The yield of the volatile product was determined with following parameters:

$I_{Lactone} = 3.914$; $H_{Lactone} = 6$; $I_{IS} = 2.000$; $m_{IS} = 9.5$ mg; $m_{crude} = 50.8$ mg; $m_{crude,NMR} = 8.4$ mg.

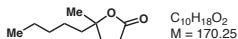
Yield (internal standard): $m_{Lactone} = 24.6$ mg, 216 μ mol, 85%.

TLC: $R_f = 0.24$ (P/Et₂O = 2/1) [KMnO₄].

¹H NMR (500 MHz, CDCl₃): δ [ppm] = 2.62 (dd, $J = 8.6, 7.9$ Hz, 2H), 2.05 (t, $J = 8.2$ Hz, 2H), 1.43 (s, 6H).

¹³C NMR (101 MHz, CDCl₃): δ [ppm] = 176.8 (s), 84.7 (s), 34.8 (s), 29.5 (s), 27.8 (s).

The spectroscopic data matched those reported in the literature.^[102]

5-Methyl-5-pentyldihydrofuran-2(3H)-one (122)

Prepared according to the general procedure from **S02** (36.8 mg, 254 μ mol) to provide crude product of **22** (48.5 mg) as a colorless oil. The yield of the volatile product was determined with following parameters:

$I_{Lactone} = 0.402$; $H_{Lactone} = 1$; $I_{IS} = 2.000$; $m_{IS} = 9.8$ mg; $m_{crude} = 48.5$ mg; $m_{crude,NMR} = 9.3$ mg.

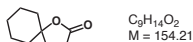
Yield (internal standard): $m_{Lactone} = 20.1$ mg, 118 μ mol, 81%.

TLC: $R_f = 0.43$ (P/Et₂O = 2/1) [KMnO₄].

¹H NMR (500 MHz, CDCl₃): δ [ppm] = 2.84–2.66 (m, 1H), 2.59 (td, $J = 9.5, 7.2$ Hz, 1H), 2.12–1.83 (m, 2H), 1.72–1.55 (m, 2H), 1.33 (s, 3H), 1.32–1.22 (m, 6H), 0.89 (t, $J = 7.0$ Hz, 3H).

¹³C NMR (101 MHz, CDCl₃): δ [ppm] = 177.0 (s), 87.1 (s), 41.1 (s), 33.0 (s), 32.1 (s), 29.3 (s), 25.7 (s), 23.6 (s), 22.6 (s), 14.1 (s).

The spectroscopic data matched those reported in the literature.^[167]

1-Oxaspiro[4.5]decan-2-one (123)

Prepared according to the general procedure from **S03** (50.0 mg, 211 μ mol) to provide crude product of **123** (52.6 mg) as a pale yellow oil. The yield of the volatile product was determined with following parameters:

$I_{Lactone} = 0.868$; $H_{Lactone} = 2$; $I_{IS} = 2.000$; $m_{IS} = 8.6$ mg; $m_{crude} = 52.6$ mg; $m_{crude,NMR} = 8.3$ mg.

Yield (internal standard): $m_{Lactone} = 21.0$ mg, 136 μmol , 65%.

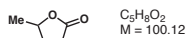
TLC: $R_f = 0.31$ (P/Et₂O = 2/1) [KMnO₄].

¹H NMR (500 MHz, CDCl₃): δ [ppm] = 2.58 (dd, $J = 8.7, 8.0$ Hz, 2H), 2.00 (dd, $J = 8.7, 8.0$ Hz, 2H), 1.84–1.76 (m, 2H), 1.75–1.67 (m, 2H), 1.61–1.46 (m, 6H).

¹³C NMR (101 MHz, CDCl₃): δ [ppm] = 177.0 (s), 86.6 (s), 37.0 (s), 33.1 (s), 28.7 (s), 25.0 (s), 22.7 (s).

The spectroscopic data matched those reported in the literature.^[168]

5-Methyldihydrofuran-2(3H)-one (124)



Prepared according to the general procedure from **117** (100 mg, 546 μmol) to provide crude product of **124** (108 mg) as a pale yellow oil. The yield of the volatile product was determined with following parameters:

$I_{Lactone} = 1.146$; $H_{Lactone} = 3$; $I_{IS} = 2.000$; $m_{IS} = 10.9$ mg; $m_{crude} = 108$ mg; $m_{crude,NMR} = 5.9$ mg.

Yield (internal standard): $m_{Lactone} = 43.9$ mg, 438 μmol , 80%.

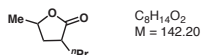
TLC: $R_f = 0.19$ (P/Et₂O = 2/1) [KMnO₄].

¹H NMR (500 MHz, CDCl₃): δ [ppm] = 4.64 (dp, $J = 7.9, 6.3$ Hz, 1H), 2.57–2.52 (m, 2H), 2.36 (dddd, $J = 12.7, 8.2, 6.5, 5.6$ Hz, 1H), 1.83 (dtd, $J = 12.7, 9.4, 7.8$ Hz, 1H), 1.41 (d, $J = 6.2$ Hz, 3H).

¹³C NMR (101 MHz, CDCl₃): δ [ppm] = 177.4 (s), 77.4 (s), 29.8 (s), 29.2 (s), 21.1 (s).

The spectroscopic data matched those reported in the literature.^[169]

5-Methyl-3-propyldihydrofuran-2(3H)-one (125)



Prepared according to the general procedure from **S04** (50.0 mg, 222 μmol) to provide crude product of **125** (55.2 mg) as a colorless oil. The yield of the volatile product was determined with following parameters:

$I_{Lactone} = 0.748$; $H_{Lactone} = 2$; $I_{IS} = 2.000$; $m_{IS} = 7.2$ mg; $m_{crude} = 55.2$ mg; $m_{crude,NMR} = 9.5$ mg.

Yield (internal standard): $m_{Lactone} = 25.6$ mg, 180 μmol , 81%.

TLC: $R_f = 0.48$ (P/Et₂O = 2/1) [KMnO₄].

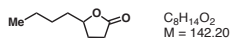
¹H NMR (500 MHz, CDCl₃): (d.r. = 1/1; * denotes signals of the diastereomer) δ [ppm] = 4.66 (dq, $J = 7.3, 6.3, 5.0$ Hz, 1H), 4.51–4.44* (m, 1H), 2.62 (tt, $J = 11.9, 8.8$ Hz, 1H), 2.62* (tt, $J = 11.9, 8.8$ Hz, 1H), 2.47* (ddd, $J = 12.4, 8.5, 5.5$ Hz, 1H), 2.08* (dt, $J = 12.8, 7.4$ Hz, 1H), 2.01 (ddd, $J = 12.8, 9.0, 5.1$ Hz, 1H), 1.89*

(dddd, $J = 9.7, 7.6, 5.8, 3.6$ Hz, 1H), 1.85–1.77 (m, 1H), 1.49–1.40* (m, 3H) 1.41* (d, $J = 6.1$ Hz, 3H), 1.42–1.35 (m, 4H), 1.37 (d, $J = 6.3$ Hz, 3H), 0.94 (t, $J = 7.2$ Hz, 3H), 0.94* (t, $J = 7.2$ Hz, 3H).

$^{13}\text{C NMR}$ (101 MHz, CDCl_3): δ [ppm] = 179.6 (s), 179.2 (s), 75.2 (s), 75.1 (s), 67.0 (s), 41.4 (s), 39.2 (s), 37.1 (s), 35.1 (s), 32.9 (s), 32.5 (s), 21.3 (s), 21.1 (s), 20.7 (s), 13.90 (s), 13.87 (s).

The spectroscopic data matched those reported in the literature.^[170]

5-Butyldihydrofuran-2(3H)-one (126)



Prepared according to the general procedure from **S05** (50.0 mg, 222 μmol) to provide crude product of **126** (37.8 mg) as a colorless oil. The yield was determined with following parameters:

$I_{\text{lactone}} = 0.584$; $H_{\text{lactone}} = 1$; $I_{\text{IS}} = 2.000$; $m_{\text{IS}} = 9.5$ mg; $m_{\text{crude}} = 37.8$ mg; $m_{\text{crude,NMR}} = 8.0$ mg.

Yield (internal standard): $m_{\text{lactone}} = 21.4$ mg, 151 μmol , 68%.

The crude product was purified *via* flash column chromatography (12 g silica gel, $\text{P}/\text{CH}_2\text{Cl}_2 = 1/2$) to provide **26** (20.9 mg, 147 μmol , 66%) as a colorless oil.

TLC: $R_f = 0.19$ ($\text{P}/\text{CH}_2\text{Cl}_2 = 1/2$) [KMnO_4].

$^1\text{H NMR}$ (400 MHz, CDCl_3): δ [ppm] = 4.48 (tt, $J = 7.6, 5.8$ Hz, 1H), 2.58–2.48 (m, 2H), 2.32 (dt, $J = 12.5, 6.7$ Hz, 1H), 1.85 (dtd, $J = 12.8, 9.5, 7.9$ Hz, 1H), 1.79–1.69 (m, 1H), 1.60 (ddt, $J = 13.5, 11.2, 4.9$ Hz, 1H), 1.49–1.29 (m, 4H), 0.91 (t, $J = 7.0$ Hz, 3H).

$^{13}\text{C NMR}$ (101 MHz, CDCl_3): δ [ppm] = 177.4 (s), 81.2 (s), 35.4 (s), 29.0 (s), 28.2 (s), 27.5 (s), 22.6 (s), 14.0 (s).

The spectroscopic data matched those reported in the literature.^[171]

3-Methyldihydrofuran-2(3H)-one (127)



Prepared according to the general procedure from **S06** (50.0 mg, 273 μmol) to provide crude product of **127** (32.9 mg) as a pale yellow oil. The yield of the volatile product was determined with following parameters:

$I_{\text{lactone}} = 2.575$; $H_{\text{lactone}} = 3$; $I_{\text{IS}} = 2.000$; $m_{\text{IS}} = 6.8$ mg; $m_{\text{crude}} = 32.9$ mg; $m_{\text{crude,NMR}} = 5.8$ mg.

Yield (internal standard): $m_{\text{lactone}} = 19.1$ mg, 190 μmol , 70%.

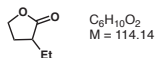
TLC: $R_f = 0.26$ ($\text{P}/\text{Et}_2\text{O} = 2/1$) [KMnO_4].

$^1\text{H NMR}$ (500 MHz, CDCl_3): δ [ppm] = 4.34 (td, $J = 8.8, 2.7$ Hz, 1H), 4.18 (ddd, $J = 9.8, 9.1, 6.6$ Hz, 1H), 2.60 (ddq, $J = 10.4, 8.6, 7.1$ Hz, 1H), 2.43 (dddd, $J = 12.6, 8.7, 6.6, 2.7$ Hz, 1H), 1.92 (dtd, $J = 12.6, 10.1, 8.4$ Hz, 1H), 1.29 (d, $J = 7.1$ Hz, 3H).

$^{13}\text{C NMR}$ (101 MHz, CDCl_3): δ [ppm] = 180.3 (s), 66.4 (s), 34.3 (s), 30.8 (s), 15.3 (s).

The spectroscopic data matched those reported in the literature.^[172]

3-Ethylidihydrofuran-2(3H)-one (128)



Prepared according to the general procedure from **S09** (50.0 mg, 254 μmol) to provide crude product of **128** (34.5 mg) as a pale yellow oil. The yield of the volatile product was determined with following parameters:

$I_{\text{Lactone}} = 2.015$; $H_{\text{Lactone}} = 3$; $I_{\text{IS}} = 2.000$; $m_{\text{IS}} = 8.4$ mg; $m_{\text{crude}} = 34.5$ mg; $m_{\text{crude,NMR}} = 5.8$ mg.

Yield (internal standard): $m_{\text{Lactone}} = 22.0$ mg, 193 μmol , 76%.

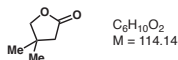
TLC: $R_f = 0.38$ (P/Et₂O = 2/1) [KMnO_4].

$^1\text{H NMR}$ (500 MHz, CDCl_3): δ [ppm] = 4.34 (td, $J = 8.8, 3.1$ Hz, 1H), 4.19 (td, $J = 9.2, 6.8$ Hz, 1H), 2.48 (dtd, $J = 9.8, 8.7, 4.8$ Hz, 1H), 2.39 (dddd, $J = 12.1, 8.8, 6.8, 3.1$ Hz, 1H), 1.99–1.85 (m, 2H), 1.55–1.49 (m, 1H), 1.01 (t, $J = 7.5$ Hz, 3H).

$^{13}\text{C NMR}$ (101 MHz, CDCl_3): δ [ppm] = 179.6 (s), 66.6 (s), 40.7 (s), 28.1 (s), 23.5 (s), 11.7 (s).

The spectroscopic data matched those reported in the literature.^[173]

4,4-Dimethyldihydrofuran-2(3H)-one (129)



Prepared according to the general procedure from **S08** (50.0 mg, 254 μmol) to provide crude product of **129** (31.2 mg) as a pale yellow oil. The yield of the volatile product was determined with following parameters: $I_{\text{Lactone}} = 6.583$; $H_{\text{Lactone}} = 6$; $I_{\text{IS}} = 2.000$; $m_{\text{IS}} = 7.6$ mg; $m_{\text{crude}} = 31.2$ mg; $m_{\text{crude,NMR}} = 6.5$ mg.

Yield (internal standard): $m_{\text{Lactone}} = 26.3$ mg, 230 μmol , 91%.

TLC: $R_f = 0.33$ (P/Et₂O = 2/1) [KMnO_4].

$^1\text{H NMR}$ (500 MHz, CDCl_3): δ [ppm] = 3.98 (s, 2H), 2.33 (s, 2H), 1.19 (s, 6H).

$^{13}\text{C NMR}$ (101 MHz, CDCl_3): δ [ppm] = 177.1 (s), 79.7 (s), 43.2 (s), 36.7 (s), 25.9 (s).

The spectroscopic data matched those reported in the literature.^[174]

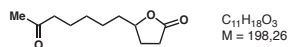
General Optimized Procedure for the Formation of Lactones

Amide (1.00 equiv) was dissolved in CH_2Cl_2 (dry, stored over 4 Å MS, ACROS, enough to give a final concentration of 50 mM once the acetyl hypobromite solution is added) in a round-bottom flask wrapped with aluminium foil, cooled to 0 °C and the laboratory lights were turned off. Freshly titrated acetyl hypobromite solution (-20 °C, 1.20 equiv) was added and the reaction mixture was stirred for 10 min at 0 °C or until TLC showed complete consumption of the starting material. The solvent was then removed *in vacuo* and the residue was placed under high vacuum for one minute before being dissolved in trifluorotoluene (50 mM). Carbon tetrabromide (1.00 equiv) was added to the reaction mixture, the aluminium foil was removed and the reaction mixture was irradiated with white LEDs (24 W, approx. 120 units, held at approx. 5 cm distance, figure S1) for 15 min or until TLC showed complete consumption of the *N*-bromide. Then, the solvent was removed *in vacuo*.

After drying the residue under high vacuum for 30 min, it was dissolved in CH_2Cl_2 (50 mM), the laboratory lights were turned off and silver(I) tetrafluoroborate (1.50 equiv) was added. The reaction mixture was stirred for 30 min or until TLC showed complete consumption of the γ -bromoamide before H_2O (2.5% v/v) was added and the reaction was stirred for another four hours or until TLC showed complete consumption of the iminolactone. The reaction mixture was then filtered through Celite[®] and the solvent was removed *in vacuo*. The crude reaction mixture was subsequently purified by flash column chromatography.

In an alternate procedure, silver(I) acetate (1.50 equiv) was used for cyclization instead of silver(I) tetrafluoroborate. For hydrolysis, acetic acid (83% aq., 2.5% v/v of total reaction volume) was added. Addition of acetic acid was crucial as upon addition of H_2O alone, iminolactone was not hydrolyzed. The use of silver(I) acetate slightly increased yield compared to silver(I) tetrafluoroborate, but was not sufficient for cyclization in several cases.

5-(6-Oxoheptyl)dihydrofuran-2(3H)-one (130b)



Prepared according to the optimized procedure from **130a** (70.0 mg, 249 μmol , 1.00 equiv), using silver(I) tetrafluoroborate (72.7 mg, 373 μmol , 1.50 equiv) for cyclization. Purification *via* flash column chromatography (12 g silica gel, CH_2Cl_2 (3% MeCN)) provided recovered amide **130a** (29.6 mg, 105 μmol) and lactone **30b** (24.1 mg, 122 μmol , 49%, 85% brsm), which was isolated as a pale yellow oil.

TLC: R_f = 0.24 (CH_2Cl_2 (6% MeCN)) [KMnO_4].

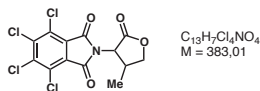
IR (ATR): ν (cm^{-1}) = 2934 (w), 2860 (w), 1767 (vs), 1711 (vs), 1458 (w), 1419 (w), 1356 (m), 1173 (vs), 1015 (w), 969 (w), 915 (m), 723 (w).

¹H NMR (400 MHz, CDCl₃): δ [ppm] = 4.47 (tdd, *J* = 8.0, 6.6, 5.2 Hz, 1H), 2.52 (dd, *J* = 9.4, 7.0 Hz, 2H), 2.43 (t, *J* = 7.3 Hz, 2H), 2.31 (dq, *J* = 13.3, 6.8 Hz, 1H), 2.13 (s, 3H), 1.84 (dtd, *J* = 12.8, 9.5, 8.0 Hz, 1H), 1.72 (dddd, *J* = 13.2, 9.9, 7.7, 5.2 Hz, 1H), 1.65–1.53 (m, 3H), 1.52–1.44 (m, 1H), 1.43–1.37 (m, 1H), 1.37–1.30 (m, 2H).

¹³C NMR (101 MHz, CDCl₃): δ [ppm] = 209.0 (s), 177.3 (s), 81.0 (s), 43.6 (s), 35.5 (s), 30.1 (s), 29.0 (s), 28.9 (s), 28.2 (s), 25.3 (s), 23.6 (s).

HR-MS (EI, 70 eV): calculated for C₁₁H₁₈O₃ [M⁺]: 198.1250; measured: 189.1253.

4,5,6,7-Tetrachloro-2-(4-methyl-2-oxotetrahydrofuran-3-yl)isoindoline-1,3-dione (**131b**)



Prepared according to the optimized procedure from **131a** (150 mg, 322 μmol, 1.00 equiv), using silver(I) tetrafluoroborate (94.0 mg, 4.83 μmol, 1.50 equiv) for cyclization. Purification *via* flash column chromatography (60 g silica gel, P/Et₂O = 2/1 (3% CH₂Cl₂)) provided recovered amide **131a** (74.7 mg, 160 μmol) and lactone **131b** (56.6 mg, 148 μmol, 46%, 91% brsm) as an inseparable mixture of diastereomers (d.r. = 7/1), which was isolated as a white solid. NMR data are given for the major diastereomer.

TLC: *R*_f = 0.24 (P/Et₂O = 2/1 (3% CH₂Cl₂)) [UV, KMnO₄].

M.p.: *m* = 224–225 °C.

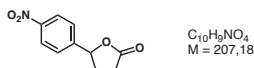
IR (ATR): ν (cm⁻¹) = 2922 (w), 2361 (w), 1773 (s), 1721 (vs), 1478 (w), 1390 (s), 1367 (s), 1251 (m), 1191 (s), 1004 (s), 904 (m), 738 (s).

¹H NMR (400 MHz, CDCl₃): δ [ppm] = 4.70–4.59 (m, 2H), 3.97 (dd, *J* = 10.4, 9.1 Hz, 1H), 3.17 (dddq, *J* = 11.5, 10.4, 8.1, 6.6 Hz, 1H), 1.22 (d, *J* = 6.6 Hz, 3H).

¹³C NMR (101 MHz, CDCl₃): δ [ppm] = 171.0 (s), 162.5 (s), 140.9 (s), 130.4 (s), 127.3 (s), 71.9 (s), 55.2 (s), 34.5 (s), 15.0 (s).

HR-MS (ESI, 3 eV): calculated for C₁₃H₇Cl₄CINaO₄ [M+Na⁺]: 405.8997; measured: 405.8992.

5-(4-Nitrophenyl)dihydrofuran-2(3H)-one (**132b**)



Prepared according to the optimized procedure from **132a** (70.0 mg, 241 μmol, 1.00 equiv), using silver(I) acetate (60.4 mg, 362 μmol, 1.50 equiv) for cyclization. Purification *via* flash column chromatography (12 g silica gel, CH₂Cl₂) provided lactone **132b** (46.3 mg, 233 μmol, 93%) as a yellow oil.

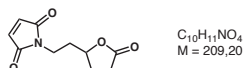
TLC: $R_f = 0.39$ (CH_2Cl_2 (3% MeCN)) [UV, KMnO_4].

^1H NMR (400 MHz, CDCl_3): δ [ppm] = 8.29–8.24 (m, 2H), 7.66–7.42 (m, 2H), 5.60 (dd, $J = 8.3, 6.7$ Hz, 1H), 2.89–2.65 (m, 3H), 2.27–2.08 (m, 1H).

^{13}C NMR (101 MHz, CDCl_3): δ [ppm] = 176.0 (s), 148.0 (s), 146.7 (s), 126.1 (s), 124.3 (s), 79.7 (s), 31.0 (s), 28.8 (s).

The spectroscopic data matched those reported in the literature.^[111]

1-(2-(5-Oxotetrahydrofuran-2-yl)ethyl)-1H-pyrrole-2,5-dione (**133b**)



Prepared according to the optimized procedure from **133a** (70.0 mg, 240 μmol , 1.00 equiv), using silver(I) tetrafluoroborate (70.0 mg, 359 μmol , 1.50 equiv) for cyclization. Purification *via* flash column chromatography (12 g silica gel, CH_2Cl_2 (6% MeCN)) provided lactone **133b** (37.8 mg, 181 μmol , 75%) as a white solid.

TLC: $R_f = 0.28$ (CH_2Cl_2 (6% MeCN)) [UV, KMnO_4].

M.p.: $\varnothing_m = 79$ – 80 °C.

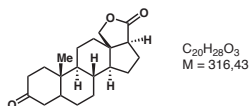
IR (ATR): ν (cm^{-1}) = 3087 (w), 2924 (w), 2853 (w), 1763 (s), 1700 (vs), 1441 (m), 1404 (m), 1368 (m), 1368 (m), 1332 (w), 1183 (s), 1146 (m), 994 (w), 922 (m), 838 (s), 692 (s).

^1H NMR (400 MHz, CDCl_3): δ [ppm] = 6.71 (s, 2H), 4.49 (tdd, $J = 8.3, 6.5, 4.5$ Hz, 1H), 3.79–3.61 (m, 2H), 2.52 (dd, $J = 9.7, 6.6$ Hz, 2H), 2.37 (dq, $J = 13.2, 6.6$ Hz, 1H), 2.04 (dq, $J = 15.5, 7.4$ Hz, 1H), 1.96–1.83 (m, 2H).

^{13}C NMR (101 MHz, CDCl_3): δ [ppm] = 176.6 (s), 170.7 (s), 134.4 (s), 78.7 (s), 34.7 (s), 34.4 (s), 28.7 (s), 28.1 (s).

HR-MS (ESI): calculated for $\text{C}_{10}\text{H}_{12}\text{NO}_4$ [$\text{M}+\text{MeOH}^+$]: 242.1028; measured: 242.1021.

(3aS,5aS,5bR,11aS,11bS,13aS)-11a-Methyltetradecahydronaphtho[2',1':4,5]indeno[1,7a-c]furan-3,9(1H,5bH)-dione (**34b**)



Prepared according to the optimized procedure from **34a** (66.5 mg, 166 μmol , 1.00 equiv), using silver(I) tetrafluoroborate (48.6 mg, 250 μmol , 1.50 equiv) for cyclization. Purification *via* flash column chromatography (12 g silica gel, CH_2Cl_2) provided amide **34a** (20.5 mg, 51 μmol) and lactone **34b** (13.5 mg, 42.7 μmol , 26%, 37% brsm), which was isolated as a white solid.

TLC: $R_f = 0.15$ (CH_2Cl_2 (3% MeCN)) [KMnO_4].

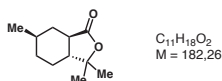
^1H NMR (400 MHz, CDCl_3): δ [ppm] = 4.09 (d, $J = 9.6$ Hz, 1H), 3.98 (d, $J = 9.6$ Hz, 1H), 2.66 (dd, $J = 15.3, 13.3$ Hz, 1H), 2.51 (dd, $J = 11.9, 3.4$ Hz, 1H), 2.33 (td, $J = 14.6, 5.4$ Hz, 1H), 2.25–1.97 (m, 6H), 1.95–1.80 (m, 2H), 1.75 (dq, $J = 13.9, 3.6$ Hz, 1H), 1.66–1.52 (m, 2H), 1.44 (dd, $J = 19.7, 9.3$ Hz, 4H), 1.34–1.19 (m, 5H), 0.98 (s, 3H).

^{13}C NMR (101 MHz, CDCl_3): δ [ppm] = 212.5 (s), 180.6 (s), 72.3 (s), 55.3 (s), 51.6 (s), 48.9 (s), 44.1 (s), 42.3 (s), 40.0 (s), 37.2 (s), 37.0 (s), 36.5 (s), 35.0 (s), 34.9 (s), 30.0 (s), 26.7 (s), 26.3 (s), 26.1 (s), 22.7 (s), 21.9 (s).

HR-MS (EI, 70 eV): calculated for $\text{C}_{11}\text{H}_{18}\text{O}_3$ [M^+]: 316.2033; measured: 316.2038.

The spectroscopic data matched those reported in the literature.^[175]

(3a*R*,6*R*,7a*R*)-3,3,6-Trimethylhexahydroisobenzofuran-1(3*H*)-one (135b)



Prepared according to the optimized procedure from **135a** (80.0 mg, 302 μmol , 1.00 equiv), using silver(I) acetate (75.5 mg, 452 μmol , 1.50 equiv) for cyclization to provide crude product of **135b** (70.5 mg) as a pale yellow oil. The yield was determined with following parameters:

$I_{\text{Lactone}} = 1.258$; $H_{\text{Lactone}} = 2$; $I_{\text{IS}} = 2.000$; $m_{\text{IS}} = 6.1$ mg; $m_{\text{crude}} = 70.5$ mg; $m_{\text{crude,NMR}} = 6.1$ mg.

Yield (internal standard): $m_{\text{Lactone}} = 35.5$ mg, 195 μmol , 65%.

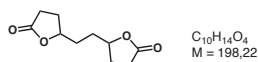
TLC: $R_f = 0.22$ ($\text{P}/\text{CH}_2\text{Cl}_2 = 4/1$ (2% MeCN)) [KMnO_4].

^1H NMR (500 MHz, CDCl_3): δ [ppm] = 2.22 (ddd, $J = 13.7, 11.7, 3.3$ Hz, 1H), 2.14 (dtd, $J = 12.6, 3.6, 1.3$ Hz, 1H), 1.89–1.82 (m, 1H), 1.78 (dp, $J = 14.5, 3.6$ Hz, 1H), 1.70–1.65 (m, 1H), 1.47–1.37 (m, 1H), 1.43 (s, 3H), 1.26 (s, 3H), 1.25–1.18 (m, 1H), 0.99 (d, $J = 6.6$ Hz, 3H), 1.03–0.92 (m, 2H).

^{13}C NMR (101 MHz, CDCl_3): δ [ppm] = 176.7 (s), 85.7 (s), 52.5 (s), 44.3 (s), 34.4 (s), 33.9 (s), 32.8 (s), 27.5 (s), 25.8 (s), 22.1 (s), 20.9 (s).

The spectroscopic data matched those reported in the literature.^[176]

5,5'-(Ethane-1,2-diyl)bis(dihydrofuran-2(3*H*)-one) (136b)



Diamide **136a** (100 mg, 274 μmol , 1.00 equiv) was dissolved in CH_2Cl_2 (2.4 mL, 30 mM final concentration) in a round-bottom flask wrapped with aluminium foil, cooled to 0 $^\circ\text{C}$ and the laboratory lights were turned off. Acetyl hypobromite solution (–20 $^\circ\text{C}$, 102 mM, 6.7 mL, 2.50 equiv) was added and the reaction mixture

was stirred for 10 min at 0 °. The solvent was then removed *in vacuo* and the residue was placed under high vacuum for one minute before being dissolved in trifluorotoluene (5.5 mL, 50 mM). Carbon tetrabromide (182 mg, 549 μmol , 2.00 equiv) was added to the reaction mixture, the aluminium foil was removed and the reaction mixture was irradiated with white LEDs for 15 min. Then, the solvent was removed *in vacuo*.

The residue was dissolved in CH_2Cl_2 (5.5 mL, 50 mM), the laboratory lights were turned off and silver(I) acetate (137 mg, 823 μmol , 3.00 equiv) was added. The reaction mixture was stirred for 14 h before AcOH (83% aq, 270 μL) was added and the reaction was stirred for another four hours. The reaction mixture was then filtered through Celite[®] and the solvent was removed *in vacuo*. Purification of the crude product *via* flash column chromatography (30 g silica gel, P/ CH_2Cl_2 /MeCN = 10/10/1 (0.5% MeOH)) provided **136b** (20.0 mg, 101 μmol , 37%) as a white crystalline solid.

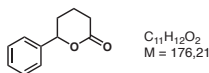
TLC: R_f = 0.21 (P/ CH_2Cl_2 /MeCN = 10/10/1 (0.5% MeOH)) [KMnO_4].

¹H NMR (500 MHz, CDCl_3): δ [ppm] = 4.61–4.43 (m, 2H), 2.58–2.50 (m, 4H), 2.36 (dq, J = 13.4, 6.8 Hz, 2H), 1.88 (dddd, J = 12.3, 10.0, 7.5, 1.8 Hz, 4H), 1.84–1.71 (m, 2H).

¹³C NMR (126 MHz, CDCl_3): δ [ppm] = 177.0 (s), 80.7 (s), 79.8 (s), 32.4 (s), 31.4 (s), 28.9 (s), 28.8 (s), 28.2 (s), 28.0 (s).

The spectroscopic data matched those reported in the literature.^[177]

6-Phenyltetrahydro-2H-pyran-2-one (137b)



Prepared according to the optimized procedure from **137a** (70.0 mg, 270 μmol , 1.00 equiv), using silver(I) acetate (67.6 mg, 405 μmol , 1.50 equiv) for cyclization. Purification *via* flash column chromatography (20 g silica gel, P/ CH_2Cl_2 = 2/1 (3% MeCN)) provided lactone **137b** (29.8 mg, 169 μmol , 63%) as a colorless oil.

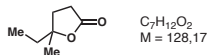
TLC: R_f = 0.48 (CH_2Cl_2 (3% MeCN)) [UV, KMnO_4].

¹H NMR (400 MHz, CDCl_3): δ [ppm] = 7.44–7.29 (m, 5H), 5.36 (dd, J = 10.4, 3.4 Hz, 1H), 2.72 (dtd, J = 17.9, 6.4, 1.1 Hz, 1H), 2.58 (dt, J = 17.8, 7.8 Hz, 1H), 2.25–2.13 (m, 1H), 2.07–1.94 (m, 2H), 1.93–1.82 (m, 1H).

¹³C NMR (101 MHz, CDCl_3): δ [ppm] = 171.4 (s), 139.9 (s), 128.7 (s), 128.4 (s), 125.8 (s), 81.8 (s), 30.7 (s), 29.7 (s), 18.7 (s).

HR-MS (EI, 70 eV): calculated for $\text{C}_{11}\text{H}_{12}\text{O}_2$ [M^+]: 176.0832; measured: 176.0833.

The spectroscopic data matched those reported in the literature.^[111]

5-Ethyl-5-methyldihydrofuran-2(3H)-one (138b)

Prepared according to the optimized procedure from **138a** (100 mg, 473 μ mol, 1.00 equiv), using silver(I) tetrafluoroborate (138 mg, 710 μ mol, 1.50 equiv) for cyclization. Purification *via* flash column chromatography (8 g silica gel, P/Et₂O = 1/1) and provided recovered amide **138a** (24.2 mg, 115 μ mol) and a solution of the volatile lactone **138b** in Et₂O (46.9 mg, 94% solution, 344 μ mol, 73%, 96% brsm), which was isolated as a colorless oil.

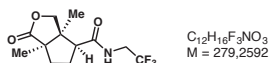
TLC: R_f = 0.23 (P/Et₂O = 1/1) [KMnO₄].

¹H NMR (400 MHz, CDCl₃): δ [ppm] = 2.69–2.50 (m, 2H), 2.09 (ddd, J = 12.8, 9.4, 7.9 Hz, 1H), 1.96 (ddd, J = 12.9, 9.5, 6.6 Hz, 1H), 1.70 (h, J = 7.2 Hz, 2H), 1.38 (s, 3H), 0.97 (t, J = 7.5 Hz, 3H).

¹³C NMR (101 MHz, CDCl₃): δ [ppm] = 177.0 (s), 87.3 (s), 33.8 (s), 32.6 (s), 29.4 (s), 25.3 (s), 8.3 (s).

HR-MS (EI, 70 eV): calculated for C₇H₁₂O₂ [M⁺]: 128.0832; measured: 128.0833.

The spectroscopic data matched those reported in the literature.^[178]

3a,6a-Dimethyl-1-oxo-N-(2,2,2-trifluoroethyl)hexahydro-1H-cyclopenta[c]furan-4-carboxamide (139b)

Prepared according to the optimized procedure from **139a** (50.0 mg, 169 μ mol, 1.00 equiv), using silver(I) tetrafluoroborate (49.4 mg, 254 μ mol, 1.50 equiv) for cyclization. Purification *via* flash column chromatography (12 g silica gel, P/EtOAc = 2/1) and provided recovered amide **139a** (30.8 mg, 104 μ mol) and lactone **139b** (12.5 mg, 44.8 μ mol, 26%, 69% brsm), which was isolated as a yellow oil.

TLC: R_f = 0.21 (P/EtOAc = 2/1) [KMnO₄].

[α]_D²⁰: +13.8 (c = 0.51, CHCl₃).

IR (ATR): ν (cm⁻¹) = 3337 (w), 2974 (w), 2361 (w), 1772 (m), 1721 (vs), 1538 (m), 1391 (s), 1368 (s), 1271 (m), 1154 (vs), 1005 (m), 904 (w), 833 (w), 738 (s), 654 (m).

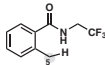
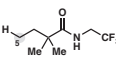
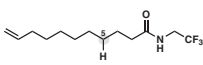
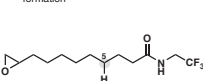
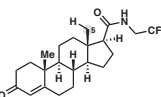
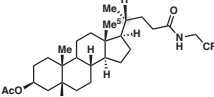
¹H NMR (400 MHz, CDCl₃): δ [ppm] = 6.50–6.31 (m, 1H), 4.47 (d, J = 10.3 Hz, 1H), 4.03 (dq, J = 14.8, 9.1, 6.9 Hz, 1H), 3.87 (d, J = 10.4 Hz, 1H), 3.85–3.73 (m, 1H), 2.60 (dd, J = 11.4, 7.6 Hz, 1H), 2.29 (ddd, J = 13.7, 8.3, 2.8 Hz, 1H), 2.08–1.86 (m, 2H), 1.67 (ddd, J = 13.7, 10.2, 8.3 Hz, 1H), 1.21 (s, 3H), 1.17 (s, 3H).

¹³C NMR (101 MHz, CDCl₃): δ [ppm] = 182.3 (s), 172.3 (s), 124.1 (q, J = 278.4 Hz), 73.9 (s), 55.4 (s), 52.5 (s), 52.0 (s), 40.6 (q, J = 34.8 Hz), 37.7 (s), 27.3 (s), 21.2 (s), 18.8 (s).

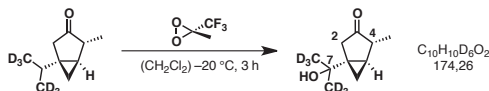
HR-MS (EI, 70 eV): calculated for $C_{12}H_{16}F_3NNaO_3$ [$M+Na^+$]: 302.0980; measured: 302.0974.

Unsuccessful Lactonization Attempts

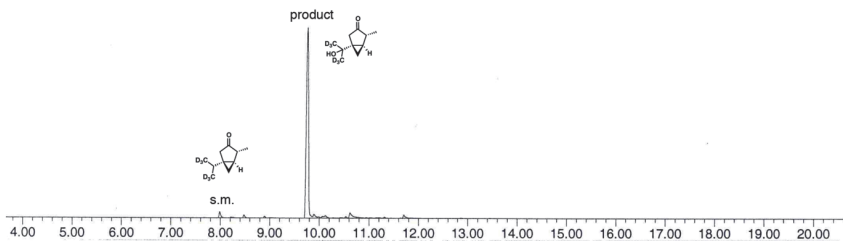
Table S2. Unsuccessful Lactonization Substrates.

Substrate (comment)		
 <p>S11</p> <ul style="list-style-type: none"> • γ-bromination successful • no lactone formation when subjected to cyclization conditions, presumably lactame formation 	 <p>S12</p> <ul style="list-style-type: none"> • no <i>N</i>-bromination observed (TLC), presumably due to steric bulk of the α-quaternary carbon center 	 <p>S09</p> <ul style="list-style-type: none"> • side reactions of alkene during bromination
 <p>S13</p> <ul style="list-style-type: none"> • γ-bromination successful • no cyclization observed with $AgOAc$ • side reactions of epoxide with $AgBF_4$ 	 <p>S10</p> <ul style="list-style-type: none"> • side reactions of enone during bromination 	 <p>S14</p> <ul style="list-style-type: none"> • <i>N</i>-bromination observed (TLC) • <i>H</i>-abstraction not successful (for detailed discussion see chapter 3)

(-)- α -7-hydroxy Thujone- d_6 (144- d_6)



In a 10 mL reaction-vial, 10 mg of (-)- α -Thujone- d_6 (0.063 mmol, 1.0 equiv) was dissolved in 0.7 mL of dry dichloromethane and cooled to $-20\text{ }^\circ\text{C}$ with a cryostat. ~ 0.27 mL of a 0.7 M TFDO solution (0.189 mmol, 3.0 equiv) was added using a mantle-cooled syringe. The reaction mixture was stirred at $-20\text{ }^\circ\text{C}$ until reaction control by GC-MS-analysis of an aliquot indicated clean conversion of the starting material to a single product. (>90% conversion). The reaction was quenched after 3 h at $-20\text{ }^\circ\text{C}$ with 0.1 mL of a saturated Na_2SO_4 solution. After warming up to room temperature, 5 mL of water were added and the reaction mixture was extracted with dichloromethane (3×10 mL). All organic phases were combined, dried over Na_2SO_4 , filtrated and concentrated under reduced pressure to yield the product. To remove residual solvent traces a column chromatography (1 g silica gel, $\varnothing = 0.8$ cm, $h = 15$ cm, pent:Et $_2$ O = 2:1) was performed and an analytically pure sample of the volatile product was isolated as a colorless oil.



TLC: $R_f = 0.2$ (pent:Et₂O = 1:1, [KMnO₄])

IR (ATR): ν (cm⁻¹) = 3446 (br), 2964 (w), 2929 (w), 2872 (w), 2227 (w), 1731 (s), 1455 (m), 1371 (w), 1264 (w), 1212 (w), 1156 (m), 1097 (m), 1051 (s), 940, 811 (m), 700 (w).

¹H-NMR (500 MHz, CDCl₃, 300 K): δ [ppm] = 2.78 (ddd, $J = 19.0, 2.9, 1.3$ Hz, 1H), 2.29 (q, $J = 7.5$ Hz, 1H), 2.18 (d, $J = 18.8$ Hz, 1H), 1.34 (dd, $J = 8.5, 4.2$ Hz, 1H), 1.18 (d, $J = 7.5$ Hz, 4H), 1.14 – 1.10 (m, 2H), 0.11 (dd, $J = 5.9, 4.7$ Hz, 1H).

¹³C-NMR (101 MHz, CDCl₃, 300 K): δ [ppm] = 220.8 (s), 69.9 (s), 47.4 (s), 41.2 (s), 33.3 (s), 23.6 (s), 18.4 (s), 16.4 (s).

HR-MS (EI, 70 eV): ber.: (C₁₀H₁₀²H₆O₂): 174.1527; gef.: 174.1521.

(-)- α -7-hydroxy Thujone (144)

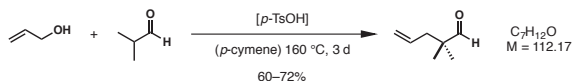
The reaction was performed as described above with 10 mg (-)- α -Thujone in <90% conversion. An analytically pure sample of the volatile title compound was obtained after column chromatography as a colorless oil.

TLC: $R_f = 0.2$ (pent:Et₂O = 1:1, [KMnO₄])

¹H-NMR (500 MHz, CDCl₃): δ [ppm] = 2.78 (ddd, $J = 18.8, 2.8, 1.3$ Hz, 1H), 2.29 (qd, $J = 7.5, 1.3$ Hz, 1H), 2.18 (d, $J = 18.8$ Hz, 1H), 1.34 (dd, $J = 8.5, 4.3$ Hz, 1H), 1.31 (s, 3H, CH₃), 1.21 (s, 3H), 1.18 (d, $J = 7.5$ Hz, 3H), 1.12 (ddd, $J = 8.4, 5.7, 2.6$ Hz, 1H), 0.11 (dd, $J = 5.7, 4.3$ Hz, 1H).

¹³C-NMR (101 MHz, CDCl₃): δ [ppm] = 220.8 (s), 70.1 (s), 47.5 (s), 41.3 (s), 33.3 (s), 27.7 (s), 27.5 (s), 23.6 (s), 18.4 (s), 16.4 (s).

The data obtained matched those reported in the literature.

2,2-Dimethylpent-4-enal (S21)

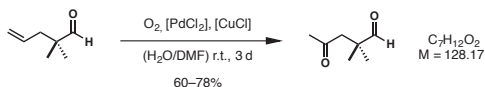
According to a modified literature procedure,^[179] a solution of isobutyraldehyde (137 mL, 108 g, 1.50 mol, 1.5 equiv) in *p*-cymene (230 mL) was treated with 2-propen-1-ol (68.4 mL, 58.1 g, 1.00 mol, 1.0 equiv) and *p*-toluene sulfonic acid (340 mg, 1.79 mmol, 0.002 equiv). The reaction mixture was stirred at reflux at 140 °C for three days under removal of H₂O by a DEAN-STARK trap. Distillation (normal pressure, 160 °C) and collection of the fraction with a boiling point of 118–120 °C afforded product **S21** (67.3 g, 0.60 mol, 60%) in a purity of 89% (*para*-cymene) as a colorless liquid.

TLC: *R*_f = 0.58 (P/Et₂O = 2/1) [KMnO₄].

¹H NMR (500 MHz, CDCl₃): δ [ppm] = 9.46 (s, 1H), 5.69 (ddt, *J* = 16.4, 10.7, 7.4 Hz, 1H), 5.07 (d, *J* = 1.2 Hz, 1H), 5.06 – 5.02 (m, 1H), 2.20 (dt, *J* = 7.4, 1.2 Hz), 1.04 (s, 6H).

¹³C NMR (75 MHz, CDCl₃) δ [ppm] = 205.1 (s), 133.2 (s), 118.3 (s), 45.5 (s), 41.4 (s), 21.1 (s).

The spectroscopic data matched those reported in the literature.^[180]

2,2-Dimethyl-4-oxopentenal (S22)

According to a modified literature procedure,^[123] a suspension of palladium chloride (482 mg, 2.72 mmol, 0.01 equiv) and copper(I) chloride (5.00 g, 50.5 mmol, 0.2 equiv) in DMF (125 mL) and H₂O (50 mL) was saturated with oxygen. 2,2-Dimethylpent-4-enal (**S21**) (28.0 g, 250 mmol, 1.0 equiv) was added and oxygen was bubbled through the dark suspension under stirring at room temperature for three days using a pump-drive setup for the oxygen gas circulation. The green reaction mixture was then acidified with HCl (1 M, 120 mL) and diluted with Et₂O (80 mL). After separation of the two phases, the aqueous layer was extracted with Et₂O (3 × 80 mL). The aqueous layer was then saturated with sodium chloride and extracted with Et₂O (5 × 80 mL). The combined organic layers were washed with H₂O (2 × 100 mL), lithium chloride solution (5%, 2 × 100 mL) and brine (1 × 100 mL), dried (Na₂SO₄), filtered and concentrated under reduced pressure. Product **S22** (19.3 g, 150 mmol, 60%) was afforded as a yellow solution in Et₂O (41%) and was used without further purification in the next step.

Without the pump-drive system, the reaction time increased from several days to weeks and the reaction required higher catalyst loading, as well as repeated addition of catalyst and oxygen to drive the reaction to completion.

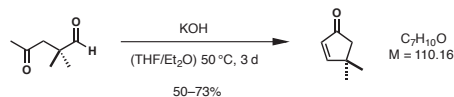
TLC: $R_f = 0.58$ (P/Et₂O = 10/1) [KMnO₄].

¹H NMR (360 MHz, CDCl₃): δ [ppm] = 9.57 (s, 1H), 2.73 (s, 2H), 2.14 (s, 3H), 1.13 (s, 6H)

¹³C NMR (90.6 MHz, CDCl₃) δ [ppm] = 206.5 (s), 205.0 (s), 51.7 (s), 44.6 (s), 30.7 (s), 22.4 (s, 2C).

The spectroscopic data matched those reported in the literature.^[181]

4,4-Dimethylcyclopent-2-en-1-one (104)



According to the literature procedure,^[123] a solution of 2,2-Dimethyl-4-oxopentanal (**S22**) (41% in Et₂O, 19.3 g, 150 mmol, 1.0 equiv) in Et₂O (250 mL) and THF (50 mL) was treated with an aqueous KOH solution (5%, 100 mL, 5.00 g, 89.1 mmol, 0.6 equiv) and stirred at 50 °C for three days. After cooling to room temperature, the reaction mixture was extracted with Et₂O (3 × 100 mL). The combined organic layers were washed with brine (3 × 100 mL), dried (Na₂SO₄), filtered and concentrated under reduced pressure (500 mbar, 40 °C). Vacuum distillation (100 mbar, oil bath: 130 °C) and collection of the fraction at 88–91 °C afforded product **104** (8.22 g, 74.7 mmol, 50%) as a colorless liquid.

TLC: $R_f = 0.31$ (P/Et₂O = 5/1) [UV, KMnO₄].

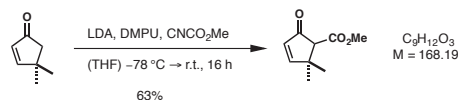
B.p.: $\vartheta_b = 88$ –91 °C (100 mbar)

¹H NMR (500 MHz, CDCl₃): δ [ppm] = 7.45 (d, $J = 5.5$ Hz, 1 H), 5.99 (d, $J = 5.5$ Hz, 1 H), 2.24 (s, 2 H), 1.23 (s, 6 H).

¹³C NMR (101 MHz, CDCl₃): δ [ppm] = 210.2 (s), 174.0 (s), 131.2 (s), 50.0 (s), 41.6 (s), 28.1 (s, 2C).

The spectroscopic data matched those reported in the literature.^[182]

Methyl 2,2-dimethyl-5-oxocyclopent-3-ene-1-carboxylate (S23)



To a stirred solution of diisopropylamine (11.7 mL, 8.14 g, 83.1 mmol, 1.2 equiv) in THF (120 mL) was added drop-wise *n*-butyl lithium solution (2.21 M in pentane, 34.4 mL, 4.88 g, 76.2 mmol, 1.1 equiv) at –78 °C. The reaction mixture was allowed to warm to 0 °C, stirred for 2 hours and was then cooled to –

78 °C. A solution of 4,4-Dimethylcyclopent-2-en-1-one (**104**) (7.63 g, 69.3 mmol, 1.0 equiv) in THF (100 mL) was slowly added at -78 °C. After stirring at 0 °C for 10 min, DMPU (9.22 mL, 9.77 g, 76.2 mmol, 1.1 equiv) and methyl cyanofornate (7.36 mL, 7.07 g, 83.1 mmol, 1.2 equiv) were successively added at -78 °C. The reaction was allowed to warm to room temperature and stirred for 14 h. After addition of sat. NH₄Cl solution (200 mL), the aqueous phase was extracted with CH₂Cl₂ (4 × 150 mL). The combined organic layers were dried over Na₂SO₄, filtered and concentrated under reduced pressure. After column chromatography (500 g silica, Ø 9.5 cm, pent/Et₂O = 5/1 → 2/1 → 1/1), ester **S23** (7.20 g, 42.81 mmol, 63%) was obtained as colorless oil.

TLC: $R_f = 0.24$ (P/Et₂O = 5/1) [KMnO₄].

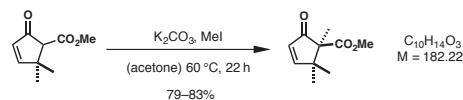
IR (ATR): ν (cm⁻¹) = 2964 (br), 1737 (s), 1704 (s), 1590 (w), 1434 (w), 1320 (m), 1253 (m), 1143 (s), 1030 (m), 808 (m), 763(m).

¹H NMR (400 MHz, CDCl₃): δ [ppm] = 7.44 (d, $J = 5.6$ Hz, 1H), 6.06 (d, $J = 5.6$ Hz, 1H), 3.73 (s, 3H), 3.15 (s, 1H), 1.36 (s, 3H), 1.18 (s, 3H).

¹³C NMR (101 MHz, CDCl₃): δ [ppm] = 203.5 (s), 172.6 (s), 169.5 (s), 62.6 (s), 52.2 (s), 45.2 (s), 29.0 (s), 23.8 (s, 2C).

HR-MS (EI, 70 eV): m/z calculated for C₉H₁₂O₃ [M⁺]: 168.0786; measured: 168.0768.

Methyl-1,2,2-trimethyl-5-oxocyclopent-3-ene-1-carboxylate (**103**)



To a solution of methyl 2,2-dimethyl-5-oxocyclopent-3-ene-1-carboxylate (**S23**) (7.20 g, 42.81 mmol, 1.0 equiv) in anhydrous acetone (50 mL) was added freshly ground anhydrous potassium carbonate (23.9 g, 173 mmol, 4.0 equiv) and methyl iodide (12.9 mL, 208 mmol, 4.8 equiv). The white suspension was heated under reflux for 40 h and after cooling to room temperature treated with triethylamine (7 mL) and concentrated under reduced pressure. H₂O (300 mL) was added to the reaction mixture. After dilution with Et₂O (250 mL) and phase separation, the aqueous layer was extracted with Et₂O (3 × 100 mL). The combined organic layers were dried (Na₂SO₄), filtered and concentrated under reduced pressure. After column chromatography (500 g silica, Ø 9.5 cm, pent/Et₂O = 2/1 → 1/1) methyl-1,2,2-trimethyl-5-oxocyclopent-3-ene-1-carboxylate (**103**) (6.15 g, 33.5 mmol, 79%) was obtained as a yellow oil.

Especially on larger scales, the described reaction conditions lead to formation of methyl enol ether by O-methylation as a side product, typically in a product to starting material mixture in ratio of more than 10:1, which was easily separable by column chromatography.

TLC: $R_f = 0.40$ (P/Et₂O = 2/1) [KMnO₄].

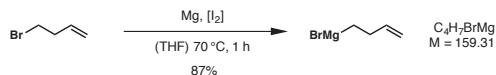
IR (ATR): ν (cm⁻¹) = 2952 (br), 1736 (s), 1709 (s), 1678 (m), 1607 (m), 1536 (w), 1398 (m), 1230 (m), 1096 (m), 1063 (m), 799 (w).

¹H NMR (400 MHz, CDCl₃): δ [ppm] = 7.39 (d, $J = 5.8$ Hz, 1H), 6.10 (d, $J = 5.8$ Hz, 1H), 3.66 (s, 3H), 1.33 (s, 3H), 1.15 (d, $J = 4.2$ Hz, 6H).

¹³C NMR (101 MHz, CDCl₃): δ [ppm] = 207.6 (s), 172.7 (s), 171.3 (s), 129.6 (s), 61.0 (s), 52.0 (s), 47.7 (s), 25.1 (s), 24.7 (s), 17.2 (s).

HR-MS (EI, 70 eV): m/z calculated for C₁₀H₁₄O₃ [M⁺]: 182.0943; measured: 182.0937.

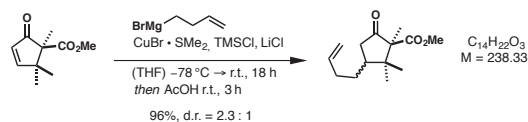
But-3-en-1-ylmagnesium bromide (S24)



A dried three-necked flask equipped with a reflux condenser was charged with magnesium turnings (2.92 g, 120 mmol, 1.2 equiv). A small crystal of iodine was added and treated with the heat gun until the iodine vapors were evenly distributed inside the flask. A solution of 4-bromobut-1-ene (13.5 g, 100 mmol, 1.0 equiv) in THF (100 mL) was first added portion-wise until the formation of a grey slurry and then drop-wise through a dropping funnel over the course of 30 min, so that the reaction mixture was continuously boiling. The dark reaction mixture was cooled down to room temperature and was titrated with menthol/1,10-phenanthroline in THF. The estimated concentration of but-3-en-1-yl magnesium bromide solution (S24) was 0.87 M (87.0 mmol, 87 %). The material was used without further purification in the next step.

In some attempts the initiation had to be accelerated by external heating with a heat gun. In case the final concentration was too low, after complete addition of the alkyl halide, the reaction mixture was further refluxed for 1–2 hours. The quality of magnesium was crucial for this reaction and best results were obtained with sharp-edged magnesium turnings with a shiny, metallic surface.

Methyl 3-(but-3-en-1-yl)-1,2,2-trimethyl-5-oxocyclopentane-1-carboxylate (102)



A 500 mL-SCHLENK flask was charged with lithium chloride (1.82 g, 43.0 mmol, 2.15 equiv) and repeatedly dried with the heat gun *in vacuo* over the course of two hours. Copper(I) bromide dimethyl sulfide complex

(8.84 g, 43.0 mmol, 2.15 equiv) was added and the flask dried *in vacuo* at room temperature for one hour. THF (35 mL) was added, the resulting brown suspension was stirred at $-78\text{ }^{\circ}\text{C}$ for 30 min and then slowly treated with alkyl magnesium bromide solution **S24** (0.87 M in THF, 46 mL, 40.0 mmol, 2.0 equiv). A solution of enone **103** (3.64 g, 20.0 mmol, 1.0 equiv) and trimethylsilyl chloride (6.35 mL, 5.43 g, 50.0 mmol, 2.5 equiv) in THF (45 mL) was added. The reaction mixture was allowed to warm to room temperature and was stirred for 18 hours. After the addition of glacial acetic acid (20 mL), and stirring for three hours at room temperature, saturated NHCO_3 solution (150 mL) was carefully added under strong gas evolution. The reaction mixture was filtered over Celite[®] and the aqueous phase was extracted with dichloromethane (3 \times 150 mL). The combined organic layers were washed with H_2O (2 \times 100 mL) and brine (1 \times 100 mL), dried (Na_2SO_4), filtered and concentrated under reduced pressure. After column chromatography (150 g silica, \varnothing 3.5 cm, P/Et₂O = 5/1) besides recovered starting material (0.16 g, 0.88 mmol, 4%) the two diastereomers of methyl 3-(but-3-en-1-yl)-1,2,2-trimethyl-5-oxocyclopentane-1-carboxylate (**101**) (3.16 g, 13.3 mmol, 66%) and (*iso*-**102**) (1.44 g, 6.04 mmol, 30%) were obtained as colorless oils.

Depending on scale the diastereomeric ratio of this reaction can fluctuate. Key factors for optimal results include: High concentration of GRIGNARD reagent, protection from light during formation of the cuprate, relatively fast addition of the enone/TMSCl solution.

Diastereomer **102**

TLC: $R_f = 0.54$ (P/Et₂O = 5/1) [KMnO_4].

IR (ATR): ν (cm^{-1}) = 3077 (w), 2973 (br), 2933 (m), 1743 (s), 1724 (s), 1640 (w), 1456 (m), 1391 (w), 1375 (w), 1277 (s), 1234 (m), 1224 (m), 1074 (m), 910 (m).

¹H NMR (400 MHz, CDCl_3): δ [ppm] = 5.84 – 5.73 (m, 1H), 5.03 (dq, $J = 17.1, 1.7$ Hz, 1H), 4.98 (dq, $J = 10.3, 1.9, 1.4$ Hz, 1H), 3.69 (s, 3H), 2.50 (dd, $J = 18.6, 7.5$ Hz, 1H), 2.14 (s, 1H), 2.09 (dd, $J = 18.6, 12.5$ Hz, 1H), 2.04 – 1.90 (m, 2H), 1.69 – 1.60 (m, 1H), 1.36 – 1.27 (m, 1H), 1.27 (s, 3H), 1.10 (s, 3H), 0.85 (s, 3H).

¹³C NMR (101 MHz, CDCl_3): δ [ppm] = 214.8 (s), 172.1 (s), 138.2 (s), 115.3 (s), 64.4 (s), 51.9 (s), 44.6 (s), 42.3 (s), 41.9 (s), 33.0 (s), 28.8 (s), 21.9 (s), 20.3 (s), 17.5 (s).

HR-MS (ESI): m/z calculated for $\text{C}_{14}\text{H}_{23}\text{O}_3^+$ [$\text{M}+\text{H}^+$]: 239.1642; measured: 239.1642.

Diastereomer *iso*-**102**

TLC: $R_f = 0.89$ (P/Et₂O = 2/1) [KMnO_4].

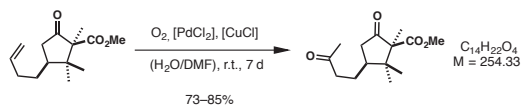
IR (ATR): ν (cm^{-1}) = 3077 (w), 2974 (br), 1750 (s), 1731 (s), 1640 (w), 1455 (m), 1393 (w), 1373 (w), 1254 (s), 1192 (m), 1113 (m), 1088 (m), 910 (m).

¹H NMR (400 MHz, CDCl₃): δ [ppm] = 5.81 (ddt, *J* = 17.0, 10.2, 6.7 Hz, 1H), 5.08 – 4.94 (m, 2H), 3.66 (s, 3H), 2.75 (dd, *J* = 19.1, 8.6 Hz, 1H), 2.27 (tdd, *J* = 11.3, 8.6, 3.0 Hz, 1H), 2.20 – 2.07 (m, 1H), 2.07 – 1.94 (m, 1H), 1.85 (dd, *J* = 19.1, 11.3, 1H), 1.70 – 1.56 (m, 1H), 1.34 – 1.18 (m, 1H), 1.13 (s, 3H), 1.01 (s, 3H), 0.74 (s, 3H).

¹³C NMR (101 MHz, CDCl₃): δ [ppm] = 215.8 (s), 172.6 (s), 138.5 (s), 115.0 (s), 64.9 (s), 52.0 (s), 45.4 (s), 42.8 (s), 42.3 (s), 33.1 (s), 29.3 (s), 22.9 (s), 18.5 (s), 14.0 (s).

HR-MS (ESI): *m/z* calculated for C₁₄H₂₃O₃⁺ [M+H⁺]; 239.1642; measured: 239.1642.

Methyl 1,2,2-trimethyl-5-oxo-3-(3-oxobutyl)cyclopentane-1-carboxylate (**101**)



According to a modified literature procedure,^[179] a suspension of palladium chloride (120 mg, 0.67 mmol, 0.05 equiv) and copper(I) chloride (0.33 g, 3.38 mmol, 0.25 equiv) in DMF (80 mL) and H₂O (80 mL) was saturated with oxygen for two hours at room temperature. Methyl 3-(but-3-en-1-yl)-1,2,2-trimethyl-5-oxocyclopentane-1-carboxylate (**102**) (2.6 g, 10.9 mmol, 1.0 equiv) was added and oxygen was bubbled through the dark suspension under stirring at room temperature for 18 h using a pump-drive setup for the oxygen gas circulation. The green reaction mixture was then acidified with HCl (1 M, 20 mL) and diluted with Et₂O (100 mL). After separation of the two layers, the aqueous layer was extracted with Et₂O (6 × 100 mL). The combined organic layers were washed with H₂O (1 × 100 mL), lithium chloride solution (5%, 2 × 100 mL) and brine (1 × 100 mL), dried (Na₂SO₄), filtered and concentrated under reduced pressure. After column chromatography (100 g silica, Ø 3.5 cm, pent/Et₂O = 1/1) methyl 1,2,2-trimethyl-5-oxo-3-(3-oxobutyl)cyclopentane-1-carboxylate (**101**) (2.52 g, 9.91 mmol, 73%) was obtained as a white solid. A single crystal suitable for X-ray crystallography was obtained by slow evaporation at room temperature of a solution of 10 mg pure material in CH₂Cl₂ (0.1 mL) overlaid with pentane (1 mL).

This reaction was performed on smaller scale without the pump-drive system with reaction times from 1–7 days and yields from 80–85%. For multi-gram scale however, a pump-drive system is necessary for optimal results with short reaction times and economic reaction conditions in respect to catalyst loading.

TLC: *R_f* = 0.19 (P/Et₂O = 5/1) [KMnO₄].

M.p.: *T_m* = 61–62 °C.

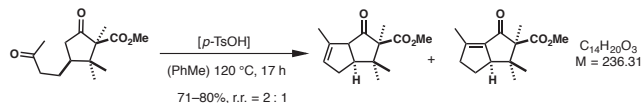
IR (ATR): ν (cm⁻¹) = 2948 (br), 1754 (s), 1718 (s), 1707 (s), 1455 (w), 1409 (w), 1364 (m), 1272 (s), 1212 (m), 1163 (w), 1065 (s), 1045 (m), 985 (w).

¹H NMR (360 MHz, CDCl₃): δ [ppm] = 3.69 (s, 3H), 2.56 – 2.36 (m, 3H), 2.16 (s, 3H), 2.10 (dd, *J* = 18.5, 12.3 Hz, 1H), 1.97 – 1.81 (m, 2H), 1.51 – 1.37 (m, 1H), 1.26 (s, 3H), 1.13 (s, 3H), 0.87 (s, 3H).

¹³C NMR (91 MHz, CDCl₃): δ [ppm] = 214.3 (s), 208.0 (s), 172.0 (s), 64.4 (s), 52.0 (s), 44.7 (s), 42.7 (s), 42.4 (s), 41.8 (s), 30.2 (s), 23.4 (s), 21.9 (s), 20.2 (s), 17.5 (s).

HR-MS (ESI): *m/z* calculated for C₁₄H₂₃O₄⁺ [*M*+H⁺]: 255.1591; measured: 255.1591.

Methyl 2,3,3,6-tetramethyl-1-oxo-1,2,3,3a,4,6a-hexahydropentalene-2-carboxylate (**100**)



To a solution of ketone **101** (2.52 g, 9.91 mmol, 1.0 equiv) in toluene (100 mL) was added *p*-toluene sulfonic acid (314 mg, 1.98 mmol, 0.2 equiv) and the reaction mixture was heated at reflux for 17 h. H₂O (50 mL) and dichloromethane (100 mL) was added and after phase separation the aqueous layer was extracted with dichloromethane (3 × 50 mL). The combined organic layers were dried (Na₂SO₄), filtered and concentrated under reduced pressure. After column chromatography (100 g silica, Ø 4 cm, P/Et₂O = 10/1) the two regioisomers methyl 2,3,3,6-tetramethyl-1-oxo-1,2,3,3a,4,6a-hexahydropentalene-2-carboxylate (**100**) (1.16 g, 4.91 mmol, 50%) and methyl 2,3,3,6-tetramethyl-1-oxo-1,2,3,3a,4,5-hexahydropentalene-2-carboxylate (*iso*-**100**) (501 mg, 2.12 mmol, 21%) were obtained as a colorless oil.

On smaller scale, the yield of this reaction turned out to be higher (up to 80%, *r.r.* = 2:1).

Regioisomer **100**:

TLC: *R_f* = 0.89 (P/Et₂O = 1/1) [KMnO₄].

IR (ATR): ν (cm⁻¹) = 3037 (w), 2938 (br), 2861 (w), 1745 (s), 1727 (s), 1455 (m), 1434 (m), 1394 (w), 1373 (w), 1284 (w), 1252 (m), 1193 (w), 1101 (m).

¹H NMR (360 MHz, CDCl₃): δ [ppm] = 5.32 – 5.27 (m, 1H), 3.58 (s, 3H), 3.23 (d, *J* = 9.1 Hz, 1H), 2.76 (td, *J* = 9.1, 4.5 Hz, 1H), 2.50 – 2.36 (m, 1H), 2.35 – 2.22 (m, 1H), 1.81 (p, *J* = 2.2 Hz, 3H), 1.25 (s, 3H), 1.04 (s, 3H), 0.98 (s, 3H).

¹³C NMR (91 MHz, CDCl₃): δ [ppm] = 214.4 (s), 172.6 (s), 138.0 (s), 126.3 (s), 62.7 (s), 61.5 (s), 51.6 (s), 49.1 (s), 43.3 (s), 33.7 (s), 26.8 (s), 21.2 (s), 16.7 (s), 15.1 (s).

HR-MS (EI, 70 eV): *m/z* calculated for C₁₄H₂₀O₃ [*M*⁺]: 236.1412; measured: 236.1407.

Regioisomer *iso*-**100**:

TLC: *R_f* = 0.77 (P/Et₂O = 1/1) [UV, KMnO₄].

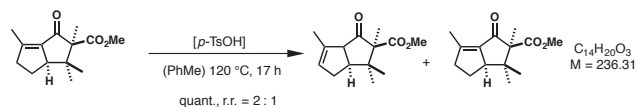
IR (ATR): ν (cm^{-1}) = 3403 (m), 2970 (m), 2952 (m), 2861 (w), 1726 (s), 1708 (s), 1455 (m), 1435 (m), 1375 (m), 1269 (m), 1101 (m).

$^1\text{H NMR}$ (400 MHz, CDCl_3): δ [ppm] = 3.70 (s, 3H), 3.25 – 3.13 (m, 1H), 2.91 – 2.73 (m, 1H), 2.61 – 2.47 (m, 1H), 2.12 – 2.04 (m, 3H), 1.95 (dtd, J = 12.6, 7.6, 1.4 Hz, 1H), 1.75 (dtd, J = 12.6, 10.4, 9.3 Hz, 1H), 1.60 – 1.53 (m, 1H), 1.35 (s, 3H), 1.08 (s, 3H),

$^{13}\text{C NMR}$ (101 MHz, CDCl_3): δ [ppm] = 199.2 (s), 172.1 (s), 152.5 (s), 137.8 (s), 69.1 (s), 55.4 (s), 51.5 (s), 43.4 (s), 42.5 (s), 25.0 (s), 22.4 (s), 21.5 (s), 17.3 (s), 15.5 (s).

HR-MS (EI, 70 eV): m/z calculated for $\text{C}_{14}\text{H}_{20}\text{O}_3$ [M^+]: 236.1412; measured: 236.1407

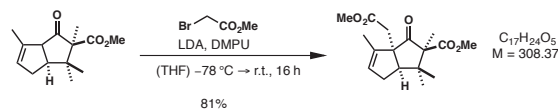
Acidic equilibration of *iso*-14 to Methyl 2,3,3,6-tetramethyl-1-oxo-1,2,3,3a,4,6a-hexahydropentalene-2-carboxylate (**100**)



To a solution of ketone *iso*-**100** (501 mg, 2.12 mmol, 1.0 equiv) in toluene (25 mL) was added *p*-toluene sulfonic acid (73.1 mg, 0.42 mmol, 0.2 equiv) and the reaction mixture was heated reflux for 17 h. H_2O (20 mL) and dichloromethane (50 mL) was added and after phase separation the aqueous layer was extracted with dichloromethane (3 \times 50 mL). The combined organic layers were dried (Na_2SO_4), filtered and concentrated under reduced pressure. After column chromatography (100 g silica, \varnothing 4 cm, $\text{P/Et}_2\text{O}$ = 10/1) the two regioisomers methyl 2,3,3,6-tetramethyl-1-oxo-1,2,3,3a,4,6a-hexahydropentalene-2-carboxylate (**100**) (322 mg, 1.36 mmol, 64%) and methyl 2,3,3,6-tetramethyl-1-oxo-1,2,3,3a,4,5-hexahydropentalene-2-carboxylate (*iso*-**100**) (181 mg, 0.76 mmol, 36%) were obtained as colorless oils respectively.

Spectroscopic data of the material obtained from the acidic equilibration matched those obtained from reaction **101** \rightarrow **100**.

Methyl 6a-(2-methoxy-2-oxoethyl)-2,3,3,6-tetramethyl-1-oxo-1,2,3,3a,4,6a-hexahydro-pentalene-2-carboxylate (**150**)



To a solution of diisopropylamine (1.03 mL, 745 mg, 7.36 mmol, 1.5 equiv) in THF (20 mL) was added drop-wise *n*-butyl lithium solution (2.27 M in pentane, 3.24 mL, 472 mg, 7.36 mmol, 1.5 equiv) at $-78\text{ }^{\circ}\text{C}$. The reaction mixture was allowed to warm to $0\text{ }^{\circ}\text{C}$, stirred for 30 min and then cooled to $-78\text{ }^{\circ}\text{C}$. A solution of ketone **100** (1.16 g, 4.91 mmol, 1.0 equiv) in THF (25 mL) was slowly added at $-78\text{ }^{\circ}\text{C}$ and stirred for 20 min. After stirring at $0\text{ }^{\circ}\text{C}$ for 10 min and subsequent cooling to $-78\text{ }^{\circ}\text{C}$, DMPU (0.89 mL, 944 mg, 7.36 mmol, 1.5 equiv) and methyl bromoacetate (1.09 mL, 1.76 g, 11.5 mmol, 2.3 equiv) were successively added. The reaction was allowed to slowly warm to room temperature for 16 h. After addition of satd. NH_4Cl solution (5 mL), H_2O (20 mL) and Et_2O (50 mL), the phases were separated and the aqueous layer was extracted with Et_2O ($3 \times 50\text{ mL}$). The combined organic layers were dried (Na_2SO_4), filtered and concentrated under reduced pressure. After column chromatography (100 g silica, $\varnothing 4\text{ cm}$, pent/ Et_2O = 10/1 \rightarrow 5/1), methyl 6a-(2-methoxy-2-oxoethyl)-2,3,3,6-tetramethyl-1-oxo-1,2,3,3a,4,6a-hexahydro-pentalene-2-carboxylate (**150**) (1.23 g, 3.99 mmol, 81%) was obtained as a white crystalline solid.

TLC: $R_f = 0.55$ (P/ Et_2O = 2/1) [KMnO_4].

M.p.: $\varnothing_m = 44\text{--}46\text{ }^{\circ}\text{C}$.

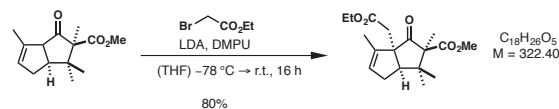
IR (ATR): ν (cm^{-1}) = 2950 (m), 2924 (br), 2857 (w), 1730 (s), 1436 (m), 1375 (w), 1248 (w), 1210 (w), 1114 (w).

^1H NMR (400 MHz, CDCl_3): δ [ppm] = 5.45 – 5.31 (m, 1H), 3.61 (s, 3H), 3.55 (s, 3H), 2.97 (d, $J = 14.2\text{ Hz}$, 1H), 2.80 (dd, $J = 8.2, 3.2\text{ Hz}$, 1H), 2.54 – 2.35 (m, 2H), 2.34 (d, $J = 14.2\text{ Hz}$, 1H), 1.65 (td, $J = 2.3, 1.6\text{ Hz}$, 3H), 1.28 (s, 3H), 1.13 (s, 3H), 0.98 (s, 3H).

^{13}C NMR (101 MHz, CDCl_3): δ [ppm] = 213.2 (s), 171.8 (s), 171.4 (s), 139.4 (s), 129.0 (s), 66.1 (s), 61.9 (s), 52.9 (s), 51.6 (s), 51.4 (s), 42.1 (s), 39.6 (s), 33.0 (s), 27.2 (s), 21.0 (s), 17.1 (s), 12.4 (s).

HR-MS (EI, 70 eV): m/z calculated for $\text{C}_{17}\text{H}_{24}\text{O}_5$ [M^+]: 308.1624; measured: 308.1629.

Ethyl 6a-(2-methoxy-2-oxoethyl)-2,3,3,6-tetramethyl-1-oxo-1,2,3,3a,4,6a-hexahydro-pentalene-2-carboxylate (**151**)



Following the same procedure as for compound **150**, starting from **100** (0.95 g, 4.00 mmol, 1.0 equiv) with ethyl bromoacetate (1.34 g, 8.00 mmol, 2.0 equiv) afforded ethyl ester **151** (1.04 g, 3.23 mmol, 80%) as a colorless oil.

TLC: $R_f = 0.18$ (P/ Et_2O = 10/1) [KMnO_4].

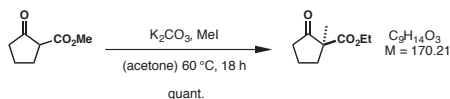
IR (ATR): ν (cm⁻¹) = 2947 (br), 1725 (s), 1446 (w), 1369 (w), 1309 (w), 1247 (m), 1204 (m), 1112 (m), 1031 (m), 806 (w).

¹H NMR (500 MHz, CDCl₃): δ [ppm] = 5.39 – 5.35 (m, 1H), 4.13 – 4.01 (m, 2H), 3.55 (s, 3H), 2.97 (d, J = 14.0 Hz, 1H), 2.82 (dd, J = 8.5, 3.0 Hz, 1H), 2.52 – 2.38 (m, 1H), 2.29 (d, J = 14.0 Hz, 1H), 1.65 (q, J = 2.0 Hz, 3H), 1.28 (s, 3H), 1.21 (t, J = 7.1 Hz, 3H), 1.14 (s, 3H), 0.98 (s, 3H).

¹³C NMR (91 MHz, CDCl₃): δ [ppm] = 213.4 (s), 172.1 (s), 171.2 (s), 139.5 (s), 129.2 (s), 66.3 (s), 62.0 (s), 60.6 (s), 53.0 (s), 51.6 (s), 42.2 (s), 39.9 (s), 33.3 (s), 27.4 (s), 21.2 (s), 17.2 (s), 14.3 (s), 12.6 (s).

HR-MS (ESI): m/z calculated for C₁₈H₂₇O₅⁺ [M+H⁺]: 323.1853; measured: 323.1853.

Ethyl-1-methyl-2-oxocyclopentan-1-carboxylat (S26)



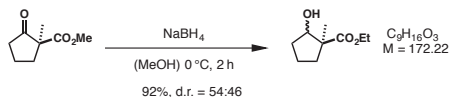
According to a modified literature procedure,^[145] a solution of ethyl 2-oxocyclopentan-1-carboxylate (22.3 mL, 23.3 g, 150 mmol, 1.0 equiv) in anhydrous acetone (200 mL) was added freshly grinded anhydrous potassium carbonate (51.8 g, 375 mmol, 2.5 equiv) and methyl iodide (18.7 mL, 42.6 g, 300 mmol, 2.0 equiv). The white suspension was refluxed for 18 h and after cooling to room temperature was treated with triethylamine (41.8 mL, 30.4 g, 300 mmol, 2.0 equiv) and concentrated under reduced pressure. Water (200 mL) was added to the reaction mixture. After dilution with Et₂O (250 mL) and phase separation, the aqueous layer was extracted with Et₂O (3 × 100 mL). The combined organic layers were washed with 1 M HCl (50 mL), water (50 mL), and brine (50 mL), dried over Na₂SO₄, filtered and concentrated under reduced pressure. After removal of all volatiles *in vacuo*, the crude product **S26** (25.5 g, 150 mmol, quant.) was isolated as yellow oil and used in the next step without further purification.

TLC: R_f = 0.24 (P/Et₂O = 10/1) [KMnO₄].

¹H NMR (360 MHz, CDCl₃): δ [ppm] = 4.15 (q, J = 7.0 Hz, 2H), 2.41 (m, 3H), 1.93 (m, 3H), 1.30 (s, 3H), 1.24 (t, J = 7.0 Hz, 3H).

¹³C NMR (90.6 MHz, CDCl₃): δ [ppm] = 216.0 (s), 172.5 (s), 61.5 (s), 56.1 (s), 37.8 (s), 36.4 (s), 19.7 (s), 19.6 (s), 14.2 (s).

The spectroscopic data matched those reported in the literature.^[145]

Ethyl 2-hydroxy-1-methylcyclopentane-1-carboxylate (**S27**)

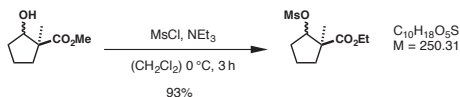
According to the literature procedure,^[145] a solution of crude **S26** (25.5 g 150 mmol, 1.0 equiv) in methanol (150 mL) was cooled to 0 °C and treated with sodium borohydride (3.4 g, 90 mmol, 0.6 equiv). The white suspension was stirred for 2 hours at 0 °C. Saturated ammonium chloride solution (100 mL) was added to the reaction mixture and after dilution with Et₂O (100 mL) and phase separation, the aqueous layer was extracted with Et₂O (3 × 100 mL). The combined organic layers were washed with water (150 mL), and brine (150 mL), dried over Na₂SO₄, filtered and concentrated under reduced pressure. After removal of all volatiles *in vacuo*, the crude product **S27** (23.7 g, 138 mmol, 92%, d.r. = 54:46) was isolated as yellow liquid and used in the next step without further purification.

TLC: $R_f = 0.19$ (P/Et₂O = 5/1) [KMnO₄].

¹H NMR (360 MHz, CDCl₃): δ [ppm] = 4.33 (t, $J = 7.5$ Hz, 0.5H), 4.16 (virt. dq, $J = 7.1$ Hz, $J = 8.1$ Hz, 2H), 3.98 (virt. dd, $J = 5.6$, 3.2 Hz, 0.5H), 2.07 (m, 3H), 1.65 (m, 3H), 1.27 (virt. td, $J = 7.1$, 4.0 Hz, 3H), 1.20 (virt. d, $J = 5.9$ Hz, 3H).

¹³C NMR (90.6 MHz, CDCl₃) δ [ppm] = 177.9 (s), 177.4 (s), 80.1 (s), 77.0 (s), 60.8 (s), 60.7 (s), 54.2 (s), 52.1 (s), 33.8 (s), 33.4 (s), 32.1 (s), 30.9 (s), 22.5 (s), 20.6 (s), 19.1 (s), 17.4 (s), 14.3 (s).

The spectroscopic data matched those reported in the literature.^[145]

Ethyl 1-methyl-2-((methylsulfonyl)oxy)cyclopentane-1-carboxylate (**S28**)

According to the literature procedure,^[145] a solution of crude **S27** (23.8 g 138 mmol, 1.0 equiv) in dichloromethane (250 mL) was cooled to 0 °C and treated with triethylamine (57.7 mL, 42.0 g, 415 mmol, 3.0 equiv). methanesulfonyl chloride (13.9 mL, 20.6 g, 1.3 equiv) was added drop-wise and the reaction mixture was stirred for 2 hours at 0 °C. Water (50 mL) was added and the reaction mixture was extracted with dichloromethane (3 × 100 mL). The combined organic layers were washed with water (2 × 200 mL) and brine (150 mL), dried over Na₂SO₄, filtered and concentrated under reduced pressure. After removal of all volatiles *in vacuo*, the crude product **S28** (32.2 g, 129 mmol, 93%, d.r. ≈ 1:1) was isolated as orange oil and used in the next step without further purification.

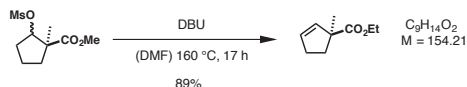
TLC: $R_f = 0.55$ (P/Et₂O = 1/1) [KMnO₄].

$^1\text{H NMR}$ (360 MHz, CDCl_3): δ [ppm] = 5.28 (m, 0.5 H), 4.88 (t, $J = 3.4$ Hz, 0.5H), 4.16 (m, 2H), 3.00 (virt. d, $J = 22.4$ Hz, 3H), 2.35 – 1.70 (m, 6H), 1.31 (s, 1.5H), 1.30 – 1.25 (m, 3H), 1.24 (s, 1.5H).

$^{13}\text{C NMR}$ (90.6 MHz, CDCl_3) δ [ppm] = 175.6 (s), 174.0 (s), 90.0 (s), 86.1 (s), 61.2 (s), 61.0 (s), 54.5 (s), 52.7 (s), 38.5 (s), 38.2 (s), 35.2 (s), 32.2 (s), 31.3 (s), 22.7 (s), 20.4 (s), 20.3 (s), 18.4 (s), 14.3 (s), 14.2 (s).

The spectroscopic data matched those reported in the literature.^[145]

Ethyl 1-methylcyclopent-2-ene-1-carboxylate (**S29**)



According to the literature procedure,^[145] a solution of crude **S28** (32.2 g 129 mmol, 1.0 equiv) in dimethylformamide (250 mL) was treated with DBU (28.8 mL, 29.4 g, 193 mmol, 1.5 equiv) heated to 160 °C and stirred under reflux for 17 hours. After cooling to room temperature, diethyl ether (400 mL) was added and after phase separation, the organic layer was washed with water (3 × 100 mL). The combined aqueous layers were extracted with diethyl ether (3 × 100 mL) and all combined organic layers were washed with water (2 × 150 mL) and brine (150 mL), dried over Na_2SO_4 , filtered and concentrated under reduced pressure. After removal of all volatiles under reduced pressure (600 mbar, 40 °C) the crude product **S29** (17.7 g, 115 mmol, 89%) was isolated as dark oil and used in the next step without further purification.

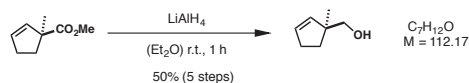
TLC: $R_f = 0.88$ (P/Et₂O = 5/1) [KMnO_4].

$^1\text{H NMR}$ (360 MHz, CDCl_3): δ [ppm] = 5.72 (virt. ddt, $J = 24.2, 5.6, 2.1$ Hz, 2H), 4.12 (q, $J = 7.1$ Hz, 2H), 2.48 – 2.32 (m, 2H), 1.79 – 1.61 (m, 4H), 1.30 (s, 3H), 1.24 (t, $J = 7.1$ Hz, 3H).

$^{13}\text{C NMR}$ (90.6 MHz, CDCl_3) δ [ppm] = 177.2 (s), 135.3 (s), 131.7 (s), 60.6 (s), 55.7 (s), 35.2 (s), 31.9 (s), 24.8 (s), 14.3 (s).

The spectroscopic data matched those reported in the literature (except for a proposed signal at 89.3 ppm which was mistakenly assigned by the authors).^[145]

(1-Methylcyclopent-2-en-1-yl)methanol (**152**)



According to the literature procedure,^[145] a solution of crude **S28** (17.7 g 115 mmol, 1.0 equiv) in diethyl ether (250 mL) was cooled to 0 °C and carefully treated with LiAlH_4 (5.68 g, 150 mmol, 1.3 equiv). The

reaction mixture was stirred for 1 hour at room temperature. Water (50 mL) was added dropwise and the reaction mixture was filtered. After phase separation, the aqueous layer was extracted with dichloromethane (3 × 100 mL) and the combined organic layers were dried over Na₂SO₄, filtered and concentrated under reduced pressure (750 mbar, 40 °C). After column chromatography (325 g silica, Ø 8 cm, pent/Et₂O = 5/1 → 2/1) product **152** (12.9 g, 70% in Et₂O, 8.35 g, 74.4 mmol, 50% over 5 steps) as a yellow solution in diethylether.

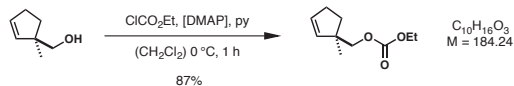
TLC: *R*_f = 0.26 (P/Et₂O = 5/1) [KMnO₄].

¹H NMR (360 MHz, CDCl₃): δ [ppm] = 5.80 (dt, *J* = 5.7, 2.3 Hz, 1H), 5.45 (dt, *J* = 5.6, 2.2 Hz, 1H), 3.41 (q, *J* = 10.5 Hz, 2H), 2.39 (tt, *J* = 7.0, 2.3 Hz, 2H), 1.96 – 1.87 (m, 1H), 1.61 – 1.54 (m, 1H), 1.06 (s, 3H).

¹³C NMR (90.6 MHz, CDCl₃) δ [ppm] = 136.6 (s), 132.4 (s), 70.7 (s), 51.7 (s), 33.7 (s), 32.4 (s), 23.5 (s).

The spectroscopic data matched those reported in the literature.^[145]

Ethyl ((1-methylcyclopent-2-en-1-yl)methyl) carbonate (**S30**)



A solution of alcohol **152** (12.9 g, 74.4 mmol, 1.0 equiv) in dichloromethane (500 mL) was cooled to 0 °C and treated with DMAP (0.91 g, 7.44 mmol, 0.1 equiv), pyridine (18.1 mL, 17.7 g, 223 mmol, 3.0 equiv) and ethyl chloroformate (14.2 mL, 16.2 g, 149 mmol, 2.0 equiv). The reaction mixture was stirred for 30 min at 0 °C and then warmed up to room temperature. After stirring for 30 min, NH₄Cl solution (100 mL) was added. The layers were separated and the aqueous layer was extracted with Et₂O (3 × 50 mL). The combined organic layers were washed with 1 M HCl (200 mL), H₂O (200 mL) and saturated NaHCO₃ solution (200 mL), dried (Na₂SO₄), filtered and concentrated under reduced pressure (750 mbar, 40 °C). After column chromatography (400 g silica, Ø 8 cm, pent/Et₂O = 5/1) carbonate **S30** was isolated as yellow solution (16.8 g, 71% in Et₂O, 11.9 g, 64.4 mmol, 87%).

TLC: *R*_f = 0.89 (P/Et₂O = 5/1) [KMnO₄].

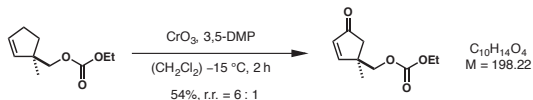
IR (ATR): ν (cm⁻¹) = 2957 (br), 1742 (s), 1463 (w), 1398 (w), 1384 (w), 1372 (m), 1247 (s), 1089 (w), 1007 (m), 790 (m).

¹H NMR (360 MHz, CDCl₃): δ [ppm] = 5.73 (dt, *J* = 4.8, 2.3 Hz, 1H), 5.51 (dt, *J* = 5.5, 2.1 Hz, 1H), 4.18 (q, *J* = 7.2 Hz, 2H), 3.99 (d, *J* = 10.3 Hz, 1H), 3.93 (d, *J* = 10.3 Hz, 1H), 2.38 (tt, *J* = 7.2, 2.2 Hz, 2H), 1.86 (dt, *J* = 13.5, 7.0 Hz, 1H), 1.59 (dt, *J* = 13.5, 7.4 Hz, 1H), 1.30 (t, *J* = 7.2 Hz, 3H), 1.10 (s, 2H).

¹³C NMR (91 MHz, CDCl₃): δ [ppm] = 155.6 (s), 136.2 (s), 131.6 (s), 74.6 (s), 64.0 (s), 49.2 (s), 34.2 (s), 31.8 (s), 23.6 (s), 14.4 (s).

HR-MS (EI, 70 eV): m/z calculated for C_7H_{11} [$M-O-CO_2Et^+$]: 95.0855; measured: 95.0849.

Ethyl ((1-methyl-4-oxocyclopent-2-en-1-yl)methyl) carbonate (149)



According to the modified literature procedure,^[146] a suspension of freshly ground chromium(VI) oxide (96.6 g, 966 mmol, 15.0 equiv) in dichloromethane (500 mL) was cooled to $-15\text{ }^{\circ}\text{C}$ and treated with 3,5-dimethylpyrazol (92.2 g, 966 mmol, 15.0 equiv). After stirring at $-15\text{ }^{\circ}\text{C}$ for 15 min, a solution of olefin **S30** (11.9 g, 64.4 mmol, 1.0 equiv) in dichloromethane (80 mL) was added drop-wise over the course of 60 min, so that the temperature of the reaction mixture did not exceed $-14\text{ }^{\circ}\text{C}$. After complete addition, the reaction mixture was stirred for 60 min at $-15\text{ }^{\circ}\text{C}$ and then filtered through a plug of Celite[®] two times, the filter residue was rinsed with Et₂O after both filtration steps. After Filtration, all volatiles were removed under reduces pressure. Colum chromatography (500 g silica, \varnothing 8 cm, pent/Et₂O = 5/1 \rightarrow 1/1 \rightarrow 1/2) yielded starting material **149** (1.14 g, 6.19 mmol), undesired regioisomer *iso*-**149** (1.03 g, 5.20 mmol, 8%) and enone **18** (5.92 g, 29.9 mmol, 46%) as a yellow oil (54%, r.r. = 6:1).

TLC: R_f = 0.24 (P/Et₂O = 2/1) [UV, KMnO₄].

IR (ATR): ν (cm^{-1}) = 2977 (br), 1742 (s), 1713 (s), 1588 (w), 1464 (w), 1374 (m), 1344 (w), 1248 (s), 1189 (w), 1089 (w), 1004 (m), 788 (m).

¹H NMR (360 MHz, CDCl₃): δ [ppm] = 7.45 (d, J = 5.6 Hz, 1H), 6.14 (d, J = 5.6 Hz, 1H), 4.18 (q, J = 7.1 Hz, 2H), 4.14 (d, J = 10.6 Hz, 1H), 4.03 (d, J = 10.6 Hz, 1H), 2.43 (d, J = 18.5 Hz, 1H), 2.16 (d, J = 18.5 Hz, 1H), 1.30 (t, J = 7.1 Hz, 2H), 1.28 (s, 3H).

¹³C NMR (91 MHz, CDCl₃): δ [ppm] = 208.2 (s), 168.2 (s), 155.2 (s), 134.0 (s), 72.6 (s), 64.5 (s), 45.5 (s), 45.3 (s), 23.1 (s), 14.4 (s).

HR-MS (EI, 70 eV): m/z calculated for $C_{10}H_{14}O_4$ [M^+]: 198.0892; measured: 198.0888.

(2-(But-3-en-1-yl)-1-methyl-4-oxocyclopentyl)methyl ethyl carbonate (153)



A 500 mL-SCHLENK flask was charged with lithium chloride (1.82 g, 43.0 mmol, 2.15 equiv) and repeatedly dried with a heat gun *in vacuo* over the course of two hours. Copper(I) bromide dimethyl sulfide complex

(8.84 g, 43.0 mmol, 2.15 equiv) was added and the flask was dried *in vacuo* at room temperature for one hour. THF (50 mL) was added, the resulting brown suspension was stirred at $-78\text{ }^{\circ}\text{C}$ for 30 min and then slowly treated with alkyllmagnesium bromide solution **S24** (0.69 M in THF, 58 mL, 6.37 g, 40.0 mmol, 2.0 equiv). A solution of enone **149** (3.96 g, 20.0 mmol, 1.0 equiv) and trimethylsilyl chloride (6.36 mL, 5.43 g, 50.0 mmol, 2.5 equiv) in THF (45 mL) was added. The reaction mixture was allowed to warm to room temperature and was stirred for 20 h. After the addition of glacial acetic acid (12 mL) and stirring for three hours at room temperature, saturated NHCO_3 solution (150 mL) was carefully added under strong gas evolution. The reaction mixture was filtered over Celite[®], rinsed and extracted with dichloromethane (3 \times 150 mL). The combined organic layers were washed with H_2O (2 \times 100 mL) and brine (1 \times 100 mL), dried (Na_2SO_4), filtered and concentrated under reduced pressure. After column chromatography (150 g silica, \varnothing 3.5 cm, pent/Et $_2$ O = 5/1) product **153** (3.64 g, 14.31 mmol, 72%) was isolated as a colorless oil. The product was obtained as an inseparable mixture of diastereomers (d.r. \approx 1 : 1).

Depending on the scale, the reaction gave higher yields (up to 87%, d.r. \approx 1 : 1).

TLC: $R_f = 0.37$ (P/Et $_2$ O = 2/1) [KMnO_4].

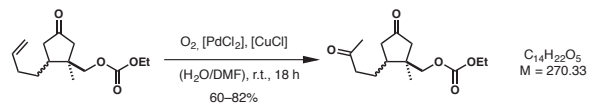
IR (ATR): ν (cm^{-1}) = 2961 (w), 2931 (br), 1741 (s), 1464 (w), 1402 (w), 1375 (w), 1249 (s), 1173 (w), 1089 (w), 1004 (m), 874 (w), 789 (s).

^1H NMR (360 MHz, CDCl_3): δ [ppm] = 5.85 – 5.72 (m, 2H), 5.08 – 4.95 (m, 4H), 4.19 (dq, $J = 14.1, 7.1$ Hz, 4H), 4.13 – 4.04 (m, 2H), 4.03 (s, 2H), 2.56 – 2.35 (m, 4H), 2.24 – 1.91 (m, 10H), 1.80 – 1.61 (m, 2H), 1.42 – 1.31 (m, 2H), 1.32 (t, $J = 7.1$ Hz, 3H), 1.29 (t, $J = 7.1$ Hz, 3H), 1.18 (s, 3H), 0.96 (s, 3H).

^{13}C NMR (91 MHz, CDCl_3): δ [ppm] = 216.8 (s), 216.5 (s), 155.3 (s), 155.2 (s), 138.1 (s), 137.9 (s), 115.4 (s), 115.3 (s), 72.3 (s), 71.8 (s), 64.38 (s), 64.36 (s), 50.5 (s), 45.3 (s), 43.5 (s), 42.4 (s), 42.3 (s), 41.9 (s), 40.2 (s), 33.0 (s), 32.8 (s), 29.2 (s), 28.5 (s), 23.3 (s), 14.4 (s).

HR-MS (ESI): m/z calculated for $\text{C}_{14}\text{H}_{23}\text{O}_4^+$ [$\text{M}+\text{H}^+$]: 255.1591; measured: 255.1591.

Ethyl ((1-methyl-4-oxo-2-(3-oxobutyl)cyclopentyl)methyl) carbonate (**S31**)



According to a modified literature procedure,^[123] a suspension of palladium chloride (126 mg, 0.72 mmol, 0.05 equiv) and copper(I) chloride (284 g, 2.86 mmol, 0.2 equiv) in DMF (75 mL) and H_2O (75 mL) was saturated with oxygen for two hours at room temperature. Carbonate **153** (3.64 g, 14.3 mmol, 1.0 equiv) was added and oxygen was bubbled through the dark suspension under stirring at room temperature for

18 h using a pump-drive setup for the oxygen gas circulation. The green reaction mixture was then acidified with HCl (1 M, 20 mL) and diluted with Et₂O (100 mL). After separation of the two phases, the aqueous layer was extracted with Et₂O (6 × 100 mL). The combined organic layers were washed with H₂O (100 mL), lithium chloride solution (5%, 2 × 100 mL) and brine (100 mL), dried (Na₂SO₄), filtered and concentrated under reduced pressure. After column chromatography (100 g silica, Ø 3.5 cm, pent/Et₂O = 1/2) product **S31** (2.31 g, 8.55 mmol, 60%) was isolated as a colorless oil. The product was obtained as an inseparable mixture of diastereomers (d.r. ≈ 1:1).

This reaction was performed on a smaller scale without the pump-drive system with reaction times from 1–7 days and yields from 75–82%. For multi-gram scale however, a pump-drive system is necessary for optimal results with short reaction times and economic reaction conditions in respect to catalyst loading.

TLC: R_f = 0.21 (P/Et₂O = 1/2) [UV, CAM].

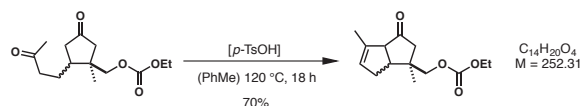
IR (ATR): ν (cm⁻¹) = 2961 (br), 1739 (s), 1714 (m), 1674 (m), 1465 (w), 1376 (m), 1248 (s), 1166 (m), 1089 (w), 1002 (m), 873 (w), 790 (m).

¹H NMR (360 MHz, CDCl₃): δ [ppm] = 4.21 (q, J = 7.1 Hz, 2H), 4.17 (q, J = 7.1 Hz, 2H), 4.14 – 4.04 (m, 4H), 2.57 – 2.35 (m, 8H), 2.16 (s, 3H), 2.15 (s, 3H), 2.13 – 1.84 (m, 8H), 1.53 – 1.40 (m, 2H), 1.32 (t, J = 7.1 Hz, 3H), 1.29 (t, J = 7.1 Hz, 3H), 1.20 (s, 3H), 0.98 (s, 3H).

¹³C NMR (91 MHz, CDCl₃): δ [ppm] = 216.0 (s), 215.7 (s), 207.8 (s), 207.7 (s), 71.7 (s), 71.6 (s), 64.3 (s), 64.2 (s), 50.4 (s), 50.1 (s), 45.2 (s), 43.2 (s), 42.5 (s), 42.4 (s), 42.2 (s), 42.0 (s), 41.8 (s), 39.9 (s), 30.0 (s), 30.0 (s), 23.5 (s), 23.2 (s), 23.0 (s), 17.4 (s), 14.3 (s), 14.2 (s).

HR-MS (ESI): m/z calculated for C₁₄H₂₃O₅⁺ [M+H⁺]: 271.1540; measured: 271.1540.

1,4-Dimethyl-3-oxo-1,2,3,3a,6,6a-hexahydropentalen-1-yl)methyl ethyl carbonate (**148**)



A solution of ketone **S31** (1.29 g, 4.76 mmol, 1.0 equiv) in toluene (50 mL) was treated with *p*-toluene sulfonic acid (163 mg, 0.95 mmol, 0.2 equiv) and the reaction mixture was stirred under reflux for 18 h. H₂O (50 mL) and dichloromethane (100 mL) was added and after phase separation the aqueous layer was extracted with dichloromethane (3 × 100 mL). The combined organic layers were dried (Na₂SO₄), filtered and concentrated under reduced pressure. After column chromatography (100 g silica, Ø 4.5 cm, pent/Et₂O = 10/1) ketone **148** (848 mg, 3.36 mmol, 70%) was isolated as a crystalline solid. The product was obtained as an inseparable mixture of diastereomers (d.r. ≈ 1:1).

TLC: $R_f = 0.71$ (P/Et₂O = 1/1) [KMnO₄].

M.p.: $\vartheta_m = 49\text{--}42$ °C.

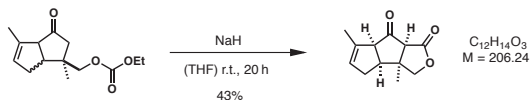
IR (ATR): ν (cm⁻¹) = 2965 (w), 2937 (br), 1734 (s), 1465 (w), 1448 (w), 1367 (m), 1248 (s), 1175 (w), 1121 (w), 1003 (m), 875 (w), 790 (m).

¹H NMR (360 MHz, CDCl₃): δ [ppm] = 5.39 – 5.33 (m, 2H), 4.20 (q, $J = 7.1$ Hz, 2H), 4.19 (q, $J = 7.1$ Hz, 2H), 4.15 (s, 2H), 4.15 (s, 2H), 3.96 (d, $J = 10.7$ Hz, 1H), 3.91 (d, $J = 10.7$ Hz, 1H), 3.15 (t, $J = 10.3$ Hz, 2H), 2.98 – 2.82 (m, 2H), 2.55 – 2.35 (m, 4H), 2.30 (d, $J = 17.0$ Hz, 1H), 2.27 (dt, $J = 17.0, 1.1$ Hz, 1H), 2.18 (d, $J = 17.0$ Hz, 1H), 2.02 (dt, $J = 17.0, 1.5$ Hz, 1H), 1.77 (s, 6H), 1.32 (t, $J = 7.1$ Hz, 3H), 1.31 (t, $J = 7.1$ Hz, 3H), 1.14 (s, 3H), 1.11 (s, 3H).

¹³C NMR (91 MHz, CDCl₃): δ [ppm] = δ 215.5 (s), 214.8 (s), 155.4 (s), 155.3 (s), 137.4 (s), 136.6 (s), 126.9 (s), 126.5 (s), 75.0 (s), 73.0 (s), 64.4 (s), 64.3 (s), 62.5 (s), 61.8 (s), 49.3 (s), 47.6 (s), 46.8 (s), 46.5 (s), 40.8 (s), 40.2 (s), 33.6 (s), 33.3 (s), 25.6 (s), 19.7 (s), 15.2 (s), 15.2 (s), 14.4 (s).

HR-MS (EI): m/z calculated for C₁₄H₂₀O₄ [M⁺]: 252.1356; measured: 252.1354.

3a,6-Dimethyl-3a,4,6a,7a-tetrahydropentaleno[1,2-c]furan-1,7(3H,3bH)-dione (154)



According to a modified literature procedure for a related ring closure,^[34] to a solution of carbonate **148** (504 mg, 2.00 mmol, 1.0 equiv) in freshly distilled THF (100 mL) was added 50 μ L H₂O at room temperature. The reaction mixture was heated to 30 °C and treated portion-wise with sodium hydride (60% dispersion of paraffin oil, 479 mg, 20.0 mmol, 10 equiv). After stirring for 3 hours at 30 °C, satd. NH₄Cl solution (50 mL) and dichloromethane (250 mL) was added. After separation of the two layers, the aqueous layer was extracted with CH₂Cl₂ (3 \times 250 mL). The combined organic layers were dried (Na₂SO₄), filtered and concentrated under reduced pressure. After column chromatography (100 g silica, \varnothing 3.5 cm, pent/Et₂O = 2/1 \rightarrow 1/1 \rightarrow 1/2) the desired diastereomer **154** (175 mg, 0.85 mmol, 43%, >99% de,) was isolated as a crystalline solid.

Since the reaction conditions were optimized during summer time, reproduction with dry THF during winter led to lower yields. Therefore "summer conditions" were applied using dry THF and addition of H₂O (500 ppm were found to be optimal for this reaction) and elevated temperature (30 °C). The undesired diastereomer was separable by column chromatography.

TLC: $R_f = 0.22$ (P/Et₂O = 1/1) [KMnO₄].

M.p.: $\vartheta_m = 72\text{--}74$ °C.

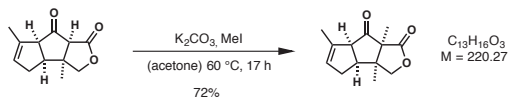
IR (ATR): ν (cm^{-1}) = 3458 (br), 2966 (br), 1774 (s), 1725 (s), 1454 (w), 1374 (m), 1266 (m), 1236 (m), 1160 (s), 1015 (s), 911 (w), 732 (s).

$^1\text{H NMR}$ (360 MHz, CDCl_3): δ [ppm] = 5.43 (s, 1H), 4.24 (d, $J = 9.5$ Hz, 1H), 4.02 (d, $J = 9.5$ Hz, 1H), 3.52 (dtt, $J = 9.5, 2.7, 1.4$ Hz, 1H), 3.07 (s, 1H), 2.91 (td, $J = 9.2, 2.6$ Hz, 1H), 2.62 (dddt, $J = 16.6, 9.2, 4.9, 2.4$ Hz, 1H), 2.19 (dp, $J = 17.6, 2.4$ Hz, 1H), 1.84 – 1.77 (m, 2H), 1.42 (s, 3H).

$^{13}\text{C NMR}$ (91 MHz, CDCl_3): δ [ppm] = 206.8 (s), 170.1 (s), 137.1 (s), 127.0 (s), 75.2 (s), 64.0 (s), 62.3 (s), 47.7 (s), 46.5 (s), 33.6 (s), 25.8 (s), 14.8 (s).

HR-MS (ESI): m/z calculated for $\text{C}_{12}\text{H}_{18}\text{NO}_3^+$ [$\text{M}+\text{NH}_4^+$]: 224.1281; measured: 224.1282.

3a,6,7a-Trimethyl-3a,4,6a,7a-tetrahydropentaleno[1,2-*cl*furan-1,7(3H,3bH)-dione (S32)



To a stirring solution of lactone **154** (0.24 g, 1.17 mmol, 1.0 equiv) in anhydrous acetone (15 mL) was added freshly ground anhydrous potassium carbonate (0.48 g, 3.52 mmol, 3.0 equiv) and methyl iodide (0.29 mL, 0.66 g, 4.49 mmol, 4.0 equiv). The white suspension was heated at reflux for 17 h and after cooling to room temperature was treated with satd. NH_4Cl solution (10 mL). After dilution with dichloromethane (50 mL) and phase separation, the aqueous layer was extracted with dichloromethane (3×50 mL). The combined organic layers were dried (Na_2SO_4), filtered and concentrated under reduced pressure. After column chromatography (20 g silica, \varnothing 2 cm, pent/Et $_2$ O = 2/1 \rightarrow 1/1) the title compound **S32** (185 mg, 0.84 mmol, 72%) was obtained as a yellow oil.

TLC: $R_f = 0.13$ (P/Et $_2$ O = 2/1) [KMnO_4].

IR (ATR): ν (cm^{-1}) = 2937 (w), 2928 (br), 1772 (s), 1730 (s), 1448 (w), 1373 (w), 1269 (m), 1194 (m), 1078 (m), 1011 (s), 800 (w), 734 (s).

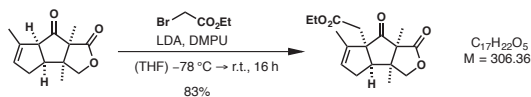
$^1\text{H NMR}$ (500 MHz, CDCl_3): δ [ppm] = 5.41 (s, 1H), 4.14 (d, $J = 9.7$ Hz, 1H), 3.94 (d, $J = 9.7$ Hz, 1H), 3.52 (dq, $J = 9.9, 2.8, 1.3$ Hz, 1H), 2.84 (td, $J = 9.5, 2.2$ Hz, 1H), 2.63 (dddd, $J = 17.5, 9.5, 5.1, 2.5$ Hz, 1H), 2.22 – 2.15 (m, 1H), 1.87 – 1.79 (m, 3H), 1.27 (s, 3H), 1.23 (s, 3H).

$^{13}\text{C NMR}$ (91 MHz, CDCl_3): δ [ppm] = 210.8 (s), 173.8 (s), 137.5(s), 126.9 (s), 73.5 (s), 62.1 (s), 61.8 (s), 50.4 (s), 44.6 (s), 33.1 (s), 21.0 (s), 14.8 (s), 14.2 (s).

HR-MS (ESI): m/z calculated for $\text{C}_{13}\text{H}_{17}\text{O}_3^+$ [M^+]: 221.1172; measured: 221.1172.

Ethyl 2-(3a,6,7a-trimethyl-1,7-dioxo-3a,3b,4,7,7a-hexahydropentaleno[1,2-c]furan-6a-(1H)-yl)

acetate (155)



To a solution of diisopropylamine (0.16 mL, 118 mg, 1.18 mmol, 1.55 equiv) in THF (2.5 mL) was added drop-wise *n*-butyl lithium solution (2.50 M in pentane, 0.45 mL, 72.9 mg, 1.14 mmol, 1.5 equiv) at $-78\text{ }^\circ\text{C}$. The reaction mixture was allowed to warm to $0\text{ }^\circ\text{C}$, stirred for 30 min and then cooled to $-78\text{ }^\circ\text{C}$. A solution of ketone **S32** (167 mg, 0.76 mmol, 1.0 equiv) in THF (5 mL) was slowly added at $-78\text{ }^\circ\text{C}$ and stirred for 20 min. After stirring at $0\text{ }^\circ\text{C}$ for 10 min and subsequent cooling to $-78\text{ }^\circ\text{C}$, DMPU (0.14 mL, 145 mg, 1.14 mmol, 1.5 equiv) and ethyl bromoacetate (0.17 mL, 253 mg, 1.52 mmol, 2.0 equiv) were added successively. The reaction was allowed to slowly warm to room temperature and stirred for 16 h. After addition of satd. NH_4Cl solution (5 mL), H_2O (10 mL) and Et_2O (25 mL), the phases were separated and the aqueous layer was extracted with Et_2O ($3 \times 25\text{ mL}$). The combined organic layers were dried (Na_2SO_4), filtered and concentrated under reduced pressure. Column chromatography (20 g silica, $\varnothing\ 2\text{ cm}$, pent/ $\text{Et}_2\text{O} = 2/1$) afforded title compound **155** (192 mg, 0.63 mmol, 83%) as a colorless oil.

TLC: $R_f = 0.20$ (P/ $\text{Et}_2\text{O} = 2/1$) [KMnO_4].

M.p.: $\varnothing_m = 69\text{--}70\text{ }^\circ\text{C}$.

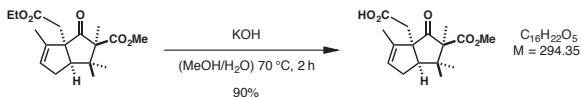
IR (ATR): ν (cm^{-1}) = 2992 (br), 1777 (s), 1725 (s), 1451 (w), 1405 (w), 1369 (m), 1341 (m), 1263 (w), 1195 (s), 1165 (s), 1078 (m), 1018 (s), 988 (m), 809 (w).

$^1\text{H NMR}$ (500 MHz, CDCl_3): δ [ppm] = 5.51 (s, 1H), 4.37 (d, $J = 9.8\text{ Hz}$, 1H), 4.08 (qd, $J = 7.1, 4.0\text{ Hz}$, 2H), 3.90 (d, $J = 9.8\text{ Hz}$, 1H), 2.85 (d, $J = 16.1\text{ Hz}$, 1H), 2.78 (dd, $J = 8.3, 1.1\text{ Hz}$, 1H), 2.65 (ddp, $J = 15.7, 7.6, 2.6\text{ Hz}$, 1H), 2.51 (d, $J = 16.1\text{ Hz}$, 1H), 2.32 (ddq, $J = 17.8, 2.8, 1.5\text{ Hz}$, 1H), 1.62 – 1.59 (m, 3H), 1.36 (s, 3H), 1.26 (s, 3H), 1.23 (t, $J = 7.1\text{ Hz}$, 3H).

$^{13}\text{C NMR}$ (91 MHz, CDCl_3): δ [ppm] = 209.8 (s), 174.5 (s), 171.0 (s), 139.6 (s), 129.6 (s), 74.4 (s), 67.4 (s), 61.0 (s), 60.8 (s), 51.3 (s), 48.6 (s), 38.8 (s), 33.1 (s), 22.7 (s), 15.6 (s), 14.3 (s), 12.1 (s).

HR-MS (ESI): m/z calculated for $\text{C}_{17}\text{H}_{23}\text{O}_5^+$ [$\text{M}+\text{H}^+$]: 307.1540; measured: 307.1540.

2-(2-(Methoxycarbonyl)-1,1,2,4-tetramethyl-3-oxo-2,3,6,6a-tetrahydropentalen-3a(1H)-yl)acetic acid (156)



A solution of ester **151** (100 mg, 0.31 mmol, 1.0 equiv) in methanol (5 mL) and H₂O (1 mL) was treated with potassium hydroxide (348 mg, 6.20 mmol, 20 equiv). The reaction mixture was heated to 70 °C and stirred for two hours, cooled to room temperature and extracted with dichloromethane (10 mL). The aqueous layer was acidified with HCl (1 M) to pH 2 and the resulting white suspension was extracted with dichloromethane (3 × 25 mL). The combined organic layers were dried (Na₂SO₄), filtered and after removal of all volatiles *in vacuo*, acid **156** (82 mg, 0.28 mmol, 90%) was obtained as crystalline solid.

TLC: $R_f \approx 0.15$ (EtOAc/MeOH = 10/1) [KMnO₄].

M.p.: $\varnothing_m = 120\text{--}122$ °C.

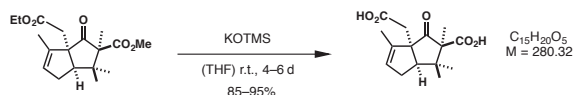
IR (ATR): ν (cm⁻¹) = 2949 (br), 1725 (s), 1698 (s), 1449 (w), 1411 (w), 1314 (w), 1218 (m), 1113 (m), 1063 (w), 1019 (w), 955 (m), 803 (w).

¹H NMR (500 MHz, CDCl₃): δ [ppm] = 5.43 (s, 1H), 3.57 (s, 3H), 3.01 (d, $J = 14.3$ Hz, 1H), 2.82 (dd, $J = 8.6, 2.9$ Hz, 1H), 2.58 – 2.43 (m, 2H), 2.38 (d, $J = 14.3$ Hz, 1H), 1.68 (s, 3H), 1.30 (s, 3H), 1.18 (s, 3H), 1.00 (s, 3H).

¹³C NMR (126 MHz, CDCl₃): δ [ppm] = 213.3 (s), 177.0 (s), 172.0 (s), 139.0 (s), 129.7 (s), 66.1 (s), 61.9 (s), 53.0 (s), 51.6 (s), 42.2 (s), 39.5 (s), 33.3 (s), 27.6 (s), 21.1 (s), 17.2 (s), 12.5 (s).

HR-MS (EI, 70 eV): calculated for C₁₆H₂₂O₅ [M⁺]; measured: 294.1464.

6a-(Carboxymethyl)-2,3,3,6-tetramethyl-1-oxo-1,2,3,3a,4,6a-hexahydropentalene-2-carboxylic acid (**157**)



A solution of diester **151** (50 mg, 0.16 mmol, 1.0 equiv) in tetrahydrofuran (5 mL) was treated with potassium trimethylsilanolate (199 mg, 1.55 mmol, 10 equiv) and the reaction mixture was stirred at room temperature for four days or until LC-MS analysis of an aliquot showed full conversion of the starting material to the diacid. H₂O (5 mL) was added, followed by acidification with 1 M HCl (0.5 mL) and the reaction mixture was extracted with dichloromethane (3 × 15 mL). The combined organic layers were dried (Na₂SO₄), filtered and after removal of all volatiles *in vacuo*, acid **157** (40 mg, 0.14 mmol, 92%) was obtained as crystalline solid.

Alternative methods for reaction control have been tested. However, presumably because of the high polarity of the diacid, only LC-MS analysis allowed for following the reaction progression. In some attempts the reaction time was even longer, on which additional KOTMS was added to drive the reaction to completion. Reaction at higher than room temperature led to rapid decarboxylation.

TLC: $R_f \approx 0.10$ (EtOAc/MeOH = 10/1) [KMnO₄].

M.p.: $\varnothing_m = 83\text{--}84$ °C.

IR (ATR): ν (cm^{-1}) = 2972 (w), 2920 (br), 1707 (s), 1443 (w), 1371 (w), 1214 (m), 1168 (w), 1083 (m), 1027 (w), 937 (m), 808 (m).

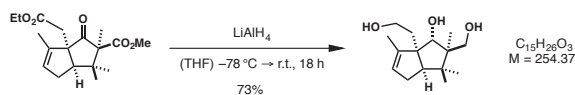
^1H NMR (500 MHz, CDCl_3): δ [ppm] = 5.45 (s, 1H), 2.94 (d, J = 14.3 Hz, 1H), 2.87 (dd, J = 9.5, 2.4 Hz, 1H), 2.56 (ddt, J = 17.8, 9.5, 2.4 Hz, 1H), 2.47 (d, J = 14.3 Hz, 1H), 2.36 (dq, J = 17.8, 2.3 Hz, 1H), 1.67 – 1.62 (m, 3H), 1.14 (s, 3H), 0.98 (s, 3H), 0.92 (s, 3H).

^{13}C NMR (101 MHz, CDCl_3): δ [ppm] = 218.3 (s), 176.6 (s), 138.7 (s), 129.8 (s), 81.9 (s), 63.5 (s), 51.4 (s), 42.1 (s), 39.5 (s), 33.1 (s), 25.3 (s), 22.0 (s), 19.2 (s), 12.4 (s).

Presumably because of hydrogen bonding of the β -keto carboxylic acid, relaxation of the carbonyl carbon is very slow, so that in a regular ^{13}C NMR spectrum the carbon was not visible. However, using the UDEFT experiment the carbon signal was detected.

HR-MS (EI, 70 eV): m/z calculated for $\text{C}_{14}\text{H}_{18}\text{O}_3$ [$\text{M}-\text{CO}_2\text{H}^+$]: 234.1252; measured: 234.1250.

6a-(2-Hydroxyethyl)-2-(hydroxymethyl)-2,3,3,6-tetramethyl-1,2,3,3a,4,6a-hexahydropentalen-1-ol (158)



A solution of diester **151** (100 mg, 0.31 mmol, 1.0 equiv) in freshly distilled tetrahydrofuran (2.5 mL) was cooled to $-78\text{ }^\circ\text{C}$ and carefully treated with lithium aluminium hydride solution (1.0 M in THF, 0.62 mL, 24 mg, 0.62 mmol, 2.0 equiv). The reaction was allowed to slowly warm to room temperature and stirred for 18 h. According to a literature work-up procedure,^[183] the reaction mixture was diluted with diethylether (2 mL), cooled to $0\text{ }^\circ\text{C}$, treated with H_2O (24 μL), aqueous potassium hydroxide solution (15%, 24 μL), H_2O (72 μL), warmed to room temperature and stirred for 15 min. Anhydrous MgSO_4 was added, stirred for 15 min, filtered and after removal of all volatiles, alcohol **158** (58 mg, 0.23 mmol, 73%) was obtained as a crystalline solid.

Because of the hydrophilicity of the product, usual aqueous work-up and extraction of the product with a variety of solvents was not successful.

TLC: R_f = 0.39 (P/acetone = 2/1) [KMnO_4].

M.p.: \varnothing_m = 144–147 $^\circ\text{C}$.

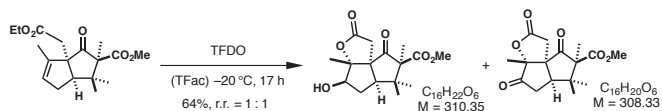
IR (ATR): ν (cm^{-1}) = 3312 (br), 2974 (w), 2919 (br), 1443 (w), 1377 (w), 1261 (w), 1124 (w), 1124 (w), 1067 (m), 1050 (m), 1033 (s), 1011 (s), 956 (m), 801 (w), 696 (m).

^1H NMR (500 MHz, Acetone- d_6): δ [ppm] = 5.15 (s, 1H), 3.90 (d, J = 4.5 Hz, 1H), 3.63 (d, J = 4.5 Hz, 1H), 3.62 – 3.56 (m, 2H), 3.56 – 3.47 (m, 2H), 3.44 – 3.36 (m, 2H), 2.43 (d, J = 8.1 Hz, 1H), 2.17 – 2.08 (m, 1H), 2.02 – 1.93 (m, 1H), 1.74 – 1.67 (m, 1H), 1.66 – 1.64 (m, 3H), 1.06 (s, 3H), 0.91 (s, 3H), 0.74 (s, 3H).

^{13}C NMR (126 MHz, Acetone- d_6): δ [ppm] = 144.3 (s), 123.5 (s), 80.8 (s), 68.6 (s), 60.1 (s), 58.6 (s), 56.1 (s), 50.8 (s), 41.8 (s), 35.5 (s), 30.5 (s), 24.5 (s), 18.4 (s), 12.8 (s), 11.7 (s).

HR-MS (ESI): m/z calculated for $\text{C}_{15}\text{H}_{27}\text{O}_3^+$ [$\text{M}+\text{H}^+$]: 255.1955; measured: 255.1955.

Methyl 4-hydroxy-3a,6,6,7-tetramethyl-2,8-dioxooctahydro-5H-pentaleno[1,6a-b]furan-7-carboxylate (159) and Methyl 3a,6,6,7-tetramethyl-2,4,8-trioxooctahydro-5H-penta-leno[1,6a-b]furan-7-carboxylate (160)



A solution of ester **151** (10 mg, 0.03 mmol, 1.0 equiv) in dichloromethane (0.75 mL) was cooled to -20 °C and treated with a freshly prepared TFDO-solution (0.38 M in trifluoroacetone, 0.45 mL, 5.0 equiv). The reaction mixture was stirred at -20 °C for 17 h and warmed up to room temperature. After removal of all volatiles *in vacuo*, separation of the product mixture by column chromatography (2 g, \varnothing 0.8 cm, pent/Et $_2$ O = 1/2) afforded alcohol **159** (3 mg, 0.01 mmol, 32%) and ketone **160** (3 mg, 0.01 mmol, 32%) as crystalline solids.

Alcohol 159

TLC: R_f = 0.16 (P/Et $_2$ O = 1/2) [KMnO_4].

M.p.: \varnothing_m = 129–130 °C.

IR (ATR): ν (cm^{-1}) = 3446 (br), 2955 (br), 1754 (s), 1736 (s), 1706 (s), 1436 (w), 1385 (w), 1261 (s), 1185 (m), 1112 (s), 1091 (m), 1043 (m), 1022 (m), 970 (m).

^1H NMR (500 MHz, CDCl_3): δ [ppm] = 4.08 (s, 1H), 3.68 (s, 3H), 3.04 (d, J = 18.1 Hz, 1H), 2.70 – 2.65 (m, 1H), 2.62 (d, J = 18.1 Hz, 1H), 2.17 (b, 1H), 2.08 (ddd, J = 14.2, 9.6, 4.9 Hz, 1H), 1.93 (ddd, J = 14.2, 8.1, 3.9 Hz, 1H), 1.53 (s, 3H), 1.25 (s, 3H), 1.08 (s, 3H), 1.03 (s, 3H).

^{13}C NMR (91 MHz, CDCl_3): δ [ppm] = 216.3 (s), 174.1 (s), 172.9 (s), 95.4 (s), 79.2 (s), 63.7 (s), 61.9 (s), 58.6 (s), 52.2 (s), 44.8 (s), 41.3 (s), 33.5 (s), 28.2 (s), 22.7 (s), 20.0 (s), 18.2 (s).

HR-MS (EI, 70 eV): m/z calculated for $\text{C}_{16}\text{H}_{22}\text{O}_6$ [M^+]: 310.1416; measured: 310.1411.

Ketone 160

TLC: R_f = 0.52 (P/Et $_2$ O = 1/2) [KMnO_4].

M.p.: \varnothing_m = 176–178 °C.

IR (ATR): ν (cm^{-1}) = 2961 (br), 1794 (s), 1754 (s), 1736 (s), 1696 (s), 1434 (w), 1413 (w), 1378 (w), 1274 (s), 1226 (s), 1172 (m), 1105 (s), 1087 (s), 1048 (m), 1025 (m), 930 (s), 821 (w).

$^1\text{H NMR}$ (500 MHz, CDCl_3): δ [ppm] = 3.55 (s, 3H), 3.44 – 3.36 (m, 1H), 2.87 (dd, J = 20.4, 12.3 Hz, 1H), 2.65 (t, J = 5.6 Hz, 1H), 2.61 (d, J = 17.6 Hz, 1H), 2.46 (dd, J = 20.4, 5.5 Hz, 1H), 1.43 (s, 3H), 1.22 (s, 3H), 1.12 (s, 3H), 1.04 (s, 3H).

$^{13}\text{C NMR}$ (126 MHz, CDCl_3): δ [ppm] = 211.7 (s), 207.0 (s), 173.0 (s), 172.2 (s), 90.7 (s), 63.1 (s), 62.1 (s), 52.1 (s), 51.0 (s), 43.4 (s), 42.6 (s), 37.6 (s), 28.6 (s), 21.6 (s), 15.6 (s), 15.0 (s).

HR-MS (EI, 70 eV): calculated for $\text{C}_{16}\text{H}_{20}\text{O}_6$ [M^+]: 308.1260; measured: 308.1254.

(3-(Methoxycarbonyl)-1a,3,4,4-tetramethyl-2-oxohexahydro-pentaleno[1,2-*b*]oxiren-1b(1a*H*)-yl)acetic acid (161**)**



A solution of carboxylic acid **156** (11.0 mg, 37.4 μmol , 1.0 equiv) in dichloromethane (0.2 mL) was treated with DMSO solution (0.06 M in acetone, 0.99 mL, 59.8 μmol , 1.6 equiv) and stirred at room temperature for two hours. After removing all volatiles *in vacuo*, product **161** (11.5 mg, 37.4 μmol , quant.) was isolated as a crystalline white solid.

TLC: $R_f \approx 0.28$ (P/Et₂O+AcOH = 2/1) [KMnO_4].

M.p.: $\Delta_m = 138$ °C.

IR (ATR): ν (cm^{-1}) = 3453 (br), 2945 (br), 1727 (s), 1700 (s), 1431 (w), 1414 (w), 1398 (w), 1374 (w), 1294 (w), 1230 (m), 1186 (m), 1115 (m), 1053 (m), 946 (w), 839 (w).

$^1\text{H NMR}$ (500 MHz, CDCl_3): δ [ppm] = 3.65 (s, 3H), 3.31 (s, 1H), 3.11 (d, J = 13.9 Hz, 1H), 2.65 (dd, J = 9.9, 6.5 Hz, 1H), 2.37 (d, J = 13.9 Hz, 1H), 2.24 (dd, J = 15.4, 9.9 Hz, 1H), 1.73 (ddd, J = 15.4, 6.5, 2.1 Hz, 1H), 1.51 (s, 3H), 1.18 (s, 3H), 1.12 (s, 3H), 0.96 (s, 3H).

$^{13}\text{C NMR}$ (126 MHz, CDCl_3): δ [ppm] = 214.5 (s), 174.7 (s), 173.1 (s), 71.2 (s), 65.8 (s), 62.9 (s), 61.6 (s), 51.91 (s), 51.87 (s), 42.3 (s), 38.9 (s), 30.4 (s), 28.2 (s), 21.5 (s), 15.9 (s), 13.4 (s).

HR-MS (EI, 70 eV): m/z calculated for $\text{C}_{16}\text{H}_{22}\text{O}_6$ [M^+]: 310.1416; measured: 310.1411.

Methyl 1b-(2-amino-2-oxoethyl)-1a,3,4,4-tetramethyl-2-oxooctahydro-pentaleno[1,2-b]-oxirene-3-carboxylate (162)



A solution of carboxylic acid **156** (50 mg, 0.17 mmol, 1.0 equiv) in dichloromethane (1 mL) was treated with thionyl chloride (1 mL, 13.8 mmol, 81 equiv) and stirred at 50 °C for two hours. All volatiles were removed under reduced pressure and the resulting oil was dissolved in 5 mL dichloromethane and treated with NH_4OH (25%, 3 mL) at room temperature. The reaction mixture was acidified with 1 M HCl (10 mL) and extracted with dichloromethane (3×15 mL). The combined organic layers were dried (Na_2SO_4), filtered and after removal of all volatiles *in vacuo*, the crude amide was isolated and used in the next step without further purification.

To a solution of the crude amide (10 mg, 34.1 μmol , 1.0 equiv) in dichloromethane (1 mL) was added *m*-chloroperoxybenzoic acid (70%, 7.1 mg, 40.9 μmol , 1.2 equiv). The reaction mixture was stirred for 18 h at room temperature and, after addition of aqueous NaHCO_3 solution (10 mL), was extracted with dichloromethane (3×10 mL). The combined organic layers were dried (Na_2SO_4), filtered and concentrated under reduced pressure. Column chromatography (1 g silica, \varnothing 0.8 cm, $P/\text{EtOAc} = 1/5$) afforded product **162** (4.2 mg, 16.7 μmol , 49% over 2 steps) as white crystalline solid. A single crystal suitable for X-ray crystallography was obtained by slow evaporation at room temperature of a solution of the pure material (4.2 mg) in CDCl_3 (0.5 mL).

TLC: $R_f = 0.30$ ($P/\text{EtOAc} = 1/5$) [CAM , KMnO_4].

M.p.: $\varnothing_m = 146\text{--}148$ °C.

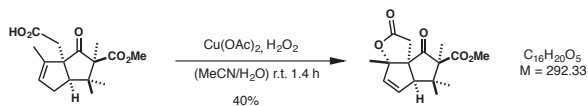
IR (ATR): ν (cm^{-1}) = 3361 (br), 2929 (br), 1728 (s), 1667 (s), 1617 (w), 1445 (m), 1395 (m), 1372 (w), 1261 (s), 1235 (s), 1185 (m), 1116 (s), 1085 (m), 1051 (m), 952 (m), 841 (w).

$^1\text{H NMR}$ (500 MHz, CDCl_3): δ [ppm] = 6.76 (b, 1H), 5.40 (b, 1H), 3.66 (s, 3H), 3.34 (d, $J = 2.1$ Hz, 1H), 3.03 (d, $J = 14.8$ Hz, 1H), 2.58 (dd, $J = 9.9, 6.1$ Hz, 1H), 2.40 (d, $J = 14.8$ Hz, 1H), 2.22 (dd, $J = 15.4, 9.9$ Hz, 1H), 1.80 (ddd, $J = 15.4, 6.1, 2.3$ Hz, 1H), 1.48 (s, 3H), 1.19 (s, 3H), 1.09 (s, 3H), 0.96 (s, 3H).

$^{13}\text{C NMR}$ (126 MHz, CDCl_3): δ [ppm] = 216.1 (s), 173.1 (s), 172.6 (s), 71.7 (s), 66.1 (s), 63.3 (s), 61.2 (s), 52.5 (s), 51.9 (s), 42.2 (s), 40.6 (s), 30.5 (s), 28.0 (s), 21.6 (s), 16.1 (s), 13.9 (s).

HR-MS (EI, 70 eV): calculated for $\text{C}_{14}\text{H}_{19}\text{O}_4$ [$\text{M}^+ - \text{CH}_2\text{CONH}_2$]: 251.1283; measured: 251.1280.

Methyl 3a,6,6,7-tetramethyl-2,8-dioxo-1,2,3a,5a,7,8-hexahydro-6H-pentaleno[1,6a-b]-furan-7-carboxylate (163)



Following a modified literature procedure,^[97] a solution of acid **156** (10.0 mg, 34.0 μmol , 1.0 equiv) in acetonitrile (0.25 mL) was treated with copper(II) acetate (0.6 mg, 3.40 μmol , 0.1 equiv) and hydrogen peroxide solution (35% in H_2O , 3 μL , 1.0 equiv) at room temperature. After 10 min another portion of copper(II) acetate (0.6 mg, 3.40 μmol , 0.1 equiv) as well as hydrogen peroxide solution (35% in H_2O , 3 μL , 1.0 equiv) was added and this process is repeated 10 times in total. After addition of 1 M HCl (0.5 mL) the reaction mixture was extracted with dichloromethane ($3 \times 10 \text{ mL}$). The combined organic layers were dried (Na_2SO_4), filtered and concentrated under reduced pressure. Column chromatography (1 g silica, \varnothing 0.8 cm, P/Et $_2$ O = 1/5) afforded product **163** (4.0 mg, 14.7 μmol , 40%) as white crystalline solid.

TLC: $R_f = 0.21$ (P/Et $_2$ O = 2/1) [UV, KMnO_4].

M.p.: $\varnothing_m = 111\text{--}121 \text{ }^\circ\text{C}$.

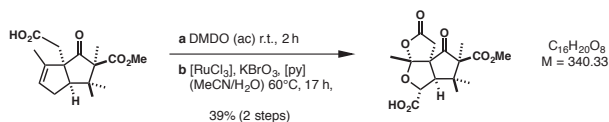
IR (ATR): ν (cm^{-1}) = 2922 (br), 1774 (s), 1747 (m), 1720 (s), 1433 (w), 1377 (w), 1243 (s), 1227 (s), 1112 (m), 1086 (m), 936 (m), 917 (m), 760 (m).

$^1\text{H NMR}$ (300 MHz, CDCl_3): δ [ppm] = 6.13 (dd, $J = 5.8, 2.4 \text{ Hz}$, 1H), 5.82 (dd, $J = 5.8, 2.4 \text{ Hz}$, 1H), 3.53 (s, 3H), 3.34 (d, $J = 17.7 \text{ Hz}$, 1H), 3.09 (t, $J = 2.4 \text{ Hz}$, 1H), 2.59 (d, $J = 17.7 \text{ Hz}$, 1H), 1.55 (s, 3H), 1.33 (s, 3H), 1.23 (s, 3H), 0.95 (s, 3H).

$^{13}\text{C NMR}$ (75 MHz, CDCl_3): δ [ppm] = 212.0 (s), 173.4 (s), 171.4 (s), 137.4 (s), 134.6 (s), 99.0 (s), 65.3 (s), 62.1 (s), 61.6 (s), 51.6 (s), 41.8 (s), 40.5 (s), 27.8 (s), 21.7 (s), 20.4 (s), 16.7 (s).

HR-MS (EI, 70 eV): calculated for $\text{C}_{16}\text{H}_{20}\text{O}_5$ [M]: 292.1311; measured: 251.1305.

7-(Methoxycarbonyl)-3a,6,6,7-tetramethyl-2,8-dioxohexahydro-3aH,5H-cyclopenta[c]-furo[2,3-b]furan-5-carboxylic acid (164)



A solution of carboxylic acid **156** (10 mg, 33.9 μmol , 1.0 equiv) in dichloromethane (0.2 mL) was treated with DMDO solution (0.06 M in acetone, 0.90 mL, 54 μmol , 1.6 equiv) and stirred at room temperature for

two hours. After removing all volatiles *in vacuo*, the crude epoxide (11 mg) was isolated and used in the subsequent step without any further purification.

Following a modified literature procedure,^[149] a solution of RuCl₃ (0.70 mg, 3.4 μmol, 0.1 equiv) and KBrO₃ (17.0 mg, 101 μmol, 3.0 equiv) in H₂O (0.4 mL) was treated with pyridine (0.5 μL, 0.54 mg, 0.2 equiv) at room temperature. A solution of the crude epoxide (11 mg, 33.9 μmol, 1.0 equiv) in acetonitrile (0.4 mL) was added and the reaction mixture was stirred at 60°C for 17 h, cooled to room temperature and quenched with aqueous sodium sulfite solution (0.5 mL). The reaction mixture was washed with dichloromethane (3 × 10 mL), the resulting aqueous phase was acidified with 1 M HCl (2 mL) and extracted with dichloromethane (3 × 10 mL). The combined organic layers were dried (Na₂SO₄), filtered and concentrated under reduced pressure. Column chromatography (1 g silica, Ø 0.8 cm, EtOAc/MeOH = 10/1) afforded product **164** (4.3 mg, 16.7 μmol, 39% over 2 steps) as a white crystalline solid. A single crystal suitable for X-ray crystallography was obtained by slow evaporation at room temperature of a solution of the pure material (4.3 mg) in dichloromethane (0.5 mL).

TLC: R_f = 0.10 (EtOAc/MeOH = 10/1) [KMnO₄].

M.p.: *m* = 208–210 °C.

IR (ATR): ν (cm⁻¹) = 2954 (w), 2992 (br), 2852 (w), 1732 (s), 1454 (w), 1389 (w), 1264 (m), 1233 (m), 1186 (m), 1129 (m), 1101 (m), 927 (m).

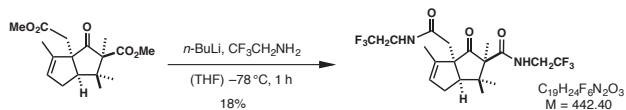
¹H NMR (500 MHz, CDCl₃): δ [ppm] = 4.80 (s, 1H), 3.70 (s, 3H), 3.26 (d, *J* = 17.7 Hz, 1H), 2.99 (s, 1H), 2.71 (d, *J* = 17.7 Hz, 1H), 1.67 (s, 3H), 1.30 (s, 3H), 1.28 (s, 3H), 1.07 (s, 3H).

¹³C NMR (126 MHz, CDCl₃): δ [ppm] = 210.1 (s), 170.9 (s), 170.6 (s), 119.5 (s), 65.4 (s), 63.2 (s), 60.5 (s), 52.3 (s), 42.4 (s), 42.2 (s), 29.7 (s), 27.6 (s), 21.7 (s), 20.4 (s), 16.5 (s).

The signal of the carboxylic acid carbon is not visible in the ¹³C NMR spectra.

HR-MS (ESI): *m/z* calculated for C₁₆H₂₁O₈⁺ [M+H⁺]: 341.1231; measured: 341.1233.

2,3,3,6-Tetramethyl-1-oxo-6a-(2-oxo-2-((2,2,2-trifluoroethyl)amino)ethyl)-N-(2,2,2-trifluoroethyl)-1,2,3,3a,4,6a-hexahydropentalene-2-carboxamide (165)



A solution of trifluoroethylamine (0.54 mL, 0.68 g, 11.0 equiv) in THF (6 mL) was cooled to -78 °C and treated with *n*-butyllithium solution (2.23 M in hexane, 2.78 mL, 10.0 equiv). After stirring for 30 min, a solution of the methyl ester **150** (0.20 g, 0.65 mmol, 1.0 equiv) in tetrahydrofuran (4 mL) was added drop-

wise at $-78\text{ }^{\circ}\text{C}$ and the reaction mixture was stirred for one hour. Aqueous NH_4Cl (1 mL) was added to the reaction mixture at $-78\text{ }^{\circ}\text{C}$, which was then warmed to room temperature, acidified with 1 M HCl (2 mL) and extracted with dichloromethane ($3 \times 10\text{ mL}$). The combined organic layers were dried (Na_2SO_4), filtered and concentrated under reduced pressure. Column chromatography (20 g silica, $\varnothing 2.5\text{ cm}$, $\text{P/Et}_2\text{O} = 5/1 \rightarrow 1/1 \rightarrow \text{P/EtOAc} = 1/1$) afforded product **164** (50 mg, 0.62 mmol, 18%) as a white crystalline solid.

Along with the desired product also mono amide and elimination product were isolated.

TLC: $R_f = 0.71$ ($\text{P/EtOAc} = 1/1$) [KMnO_4].

M.p.: $\Delta_m = 177\text{ }^{\circ}\text{C}$.

IR (ATR): ν (cm^{-1}) = 3375 (br), 3287 (br), 2923 (br), 1727 (m), 1654 (m), 1527 (m), 1394 (w), 1269 (m), 1145 (s), 978 (m), 670 (m).

$^1\text{H NMR}$ (500 MHz, $\text{DMSO-}d_6$): 8.62 – 8.56 (m, 1H), 7.98 (t, $J = 6.3\text{ Hz}$, 1H), 5.30 (s, 1H), 3.99 – 3.72 (m, 4H), 2.86 (d, $J = 7.3\text{ Hz}$, 1H), 2.55 (d, $J = 13.2\text{ Hz}$, 1H), 2.36 (d, $J = 13.2\text{ Hz}$, 1H), 2.36 – 2.30 (m, 1H), 2.13 (d, $J = 16.8\text{ Hz}$, 1H), 1.67 (s, 3H), 1.29 (s, 3H), 1.10 (s, 3H), 0.66 (s, 3H).

$^{13}\text{C NMR}$ (126 MHz, $\text{DMSO-}d_6$): δ [ppm] = 219.9 (s), 171.9 (s), 169.8 (s), 140.0 (s), 128.4 (s), 126.2 (d, $J = 279.9\text{ Hz}$), 123.6 (q, $J = 279.9\text{ Hz}$), 65.4 (s), 62.6 (s), 50.5 (s), 42.6 (s), 41.8 (s), 31.3 (s), 23.6 (s), 21.3 (s), 19.6 (s), 13.1 (s).

Due to signal overlapping of the $\text{DMSO-}d_6$ peak, the CF_3 quartets at $\sim 40\text{ ppm}$ are not listed. However, they are visible if the sample is dissolved in CDCl_3 (due to the bad solubility in chloroform, then, the other CF_3 -quartets at $\sim 124\text{ ppm}$ are not well resolved).

$^{13}\text{C NMR}$ (126 MHz, CDCl_3): δ [ppm] = 222.6 (s), 172.0 (s), 169.3 (s), 139.3 (s), 130.1 (s), 124.9 (d, $J = 279.7\text{ Hz}$), 123.84 (d, $J = 279.7\text{ Hz}$), 65.1 (s), 62.2 (s), 49.8 (s), 42.8 (s), 42.2 (s), 40.6 (q, $J = 35.0\text{ Hz}$), 39.9 (q, $J = 34.6\text{ Hz}$), 31.2 (s), 22.8 (s), 20.7 (s), 20.2 (s), 12.6 (s).

HR-MS (ESI): m/z calculated for $\text{C}_{19}\text{H}_{25}\text{F}_6\text{N}_2\text{O}_5^+$ [$\text{M}+\text{H}^+$]: 443.1764; measured: 443.1758.

3a,6,6,7-Tetramethyl-2,8-dioxo-N-(2,2,2-trifluoroethyl)octahydro-5H-pentaleno[1,6a-b]-furan-7-carboxamide (166)



A solution of trifluoroethylamine (0.19 mL, 0.26 g, 8.0 equiv) in THF (4 mL) was cooled to $-78\text{ }^{\circ}\text{C}$ and treated with n -butyllithium solution (2.10 M in hexane, 1.08 mL, 7.0 equiv). After stirring for 30 min, a

solution of the methyl ester **150** (0.10 g, 0.32 mmol, 1.0 equiv) in THF (2 mL) was added drop-wise at $-78\text{ }^{\circ}\text{C}$ and the reaction mixture was stirred for one hour. Aqueous NH_4Cl (1 mL) was added to the reaction mixture at $-78\text{ }^{\circ}\text{C}$, which was then warmed to room temperature, acidified with 1 M HCl (1 mL) and extracted with dichloromethane ($3 \times 10\text{ mL}$). The combined organic layers were dried (Na_2SO_4), filtered and all volatiles were removed *in vacuo*.

The crude product mixture was dissolved in dichloromethane (4 mL), treated with trifluoroacetic acid (2.0 mL, 2.96 g, 80.0 equiv) and stirred at room temperature for three days. Removal of all volatiles *in vacuo* and column chromatography (10 g silica, \varnothing 2 cm, P/EtOAc = 4/1 \rightarrow 2/1) afforded product **166** (60 mg, 0.17 mmol, 51% over 2 steps) as white crystalline solid.

TLC: $R_f = 0.31$ (P/EtOAc = 2/1) [KMnO_4].

M.p.: $\varnothing_m = 151\text{--}152\text{ }^{\circ}\text{C}$.

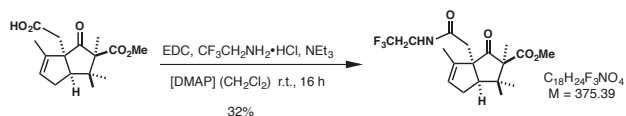
IR (ATR): ν (cm^{-1}) = 3361 (br), 2975 (br), 1751 (s), 1724 (s), 1678 (s), 1522 (m), 1273 (s), 1154 (s), 956 (m), 665 (m).

$^1\text{H NMR}$ (500 MHz, CDCl_3): δ [ppm] = 8.05 (s, 1H), 4.09 (dq, $J = 14.8, 9.0, 6.8\text{ Hz}$, 1H), 3.79 (dq, $J = 15.0, 9.0, 5.9\text{ Hz}$, 1H), 3.15 (d, $J = 17.9\text{ Hz}$, 1H), 2.69 (d, $J = 17.9\text{ Hz}$, 1H), 2.46 (d, $J = 8.1\text{ Hz}$, 1H), 2.19 (dd, $J = 13.8, 7.5\text{ Hz}$, 1H), 2.14 – 1.98 (m, 1H), 1.92 – 1.76 (m, 2H), 1.51 (s, 3H), 1.36 (s, 3H), 1.30 (s, 3H).

$^{13}\text{C NMR}$ (126 MHz, CDCl_3): δ [ppm] = δ 221.4 (s), 172.9 (s), 171.1 (s), 124.0 (q, $J = 278.4\text{ Hz}$), 97.7 (s), 62.9 (s), 62.1 (s), 57.6 (s), 46.0 (s), 43.1 (s), 40.0 (s), 39.9 (q, $J = 34.6\text{ Hz}$), 23.6 (s), 23.1 (s), 22.2 (s), 21.6 (s), 20.2 (s).

HR-MS (ESI): m/z calculated for $\text{C}_{17}\text{H}_{23}\text{F}_3\text{NO}_4 + [\text{M} + \text{H}^+]$: 362.1574; measured: 362.1572.

Methyl 2,3,3,6-tetramethyl-1-oxo-6a-(2-oxo-2-((2,2,2-trifluoroethyl)amino)ethyl)-1,2,3,3a,4,6a-hexahydropentalene-2-carboxylate (**167**)



To a solution of acid **156** (182 mg, 0.62 mmol, 1.0 equiv) in dichloromethane (10 mL) was added EDC·HCl (237 mg, 1.24 mmol, 2.0 equiv), DMAP (1 spatula tip) and trifluoroethyl-amine hydrochloride (168 mg, 1.24 mmol, 2.0 equiv). After drop-wise addition of trimethylamine (0.25 mL, 1.85 mmol, 3.0 equiv) the reaction mixture was stirred at room temperature for 16 h. Aqueous NH_4Cl solution (5 mL) was added and after acidification with 1 M HCl (2 mL), the reaction mixture was extracted with dichloromethane ($3 \times 10\text{ mL}$). The combined organic layers were dried (Na_2SO_4), filtered and concentrated under reduced

pressure. Column chromatography (10 g silica, \varnothing 1.5 cm, P/EtOAc = 2/1) afforded product **167** (75 mg, 0.62 mmol, 32%) as a colorless oil.

TLC: R_f = 0.22 (P/EtOAc = 2/1) [KMnO_4].

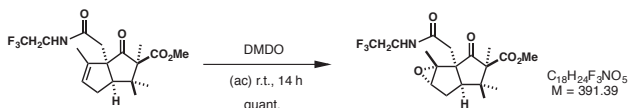
IR (ATR): ν (cm^{-1}) = 3344 (br), 2952 (w), 2924 (br), 1727 (s), 1667 (m), 1536 (w), 1433 (w), 1395 (w), 1375 (w), 1278 (m), 1220 (w), 1159 (s), 1115 (w).

$^1\text{H NMR}$ (500 MHz, CDCl_3): δ [ppm] = 6.36 (s, 1H), 5.48 – 5.35 (m, 1H), 4.09 – 3.91 (m, 1H), 3.75 – 3.60 (m, 1H), 3.56 (s, 3H), 2.85 (dd, J = 8.4, 2.0 Hz, 1H), 2.66 (d, J = 14.1 Hz, 1H), 2.53 (ddt, J = 17.7, 8.3, 2.4 Hz, 1H), 2.44 (d, J = 14.1 Hz, 1H), 2.41 – 2.34 (m, 1H), 1.63 (s, 3H), 1.22 (s, 3H), 1.02 (s, 3H), 0.97 (s, 3H).

$^{13}\text{C NMR}$ (126 MHz, CDCl_3): δ [ppm] = 215.2 (s), 171.8 (s), 170.4 (s), 139.2 (s), 129.9 (s), 124.0 (q, J = 278.5 Hz), 66.5 (s), 62.4 (s), 52.2 (s), 51.6 (s), 42.1 (s), 41.0 (s), 40.5 (q, J = 34.6 Hz), 32.6 (s), 26.3 (s), 21.4 (s), 17.1 (s), 12.4 (s).

HR-MS (ESI): m/z calculated for $\text{C}_{18}\text{H}_{25}\text{F}_3\text{NO}_4^+$ [$\text{M}+\text{H}^+$]: 376.1730; measured: 376.1729.

Methyl 1a,3,4,4-tetramethyl-2-oxo-1b-(2-oxo-2-((2,2,2-trifluoroethyl)amino)ethyl)octa-hydro-pentaleno[1,2-*b*]oxirene-3-carboxylate (**168**)



A solution of amide **167** (10.0 mg, 26.6 μmol , 1.0 equiv) in dichloromethane (0.2 mL) was treated with DMDO solution (0.06 M in acetone, 0.71 mL, 42.6 μmol , 1.6 equiv) and stirred at room temperature for 14 h. After removing all volatiles *in vacuo*, product **168** (10.4 mg, 26.6 μmol , quant.) was isolated as a crystalline white solid.

TLC: R_f = 0.19 (P/EtOAc = 1/2) [KMnO_4].

M.p.: Θ_m = 133–134 $^\circ\text{C}$.

IR (ATR): ν (cm^{-1}) = 3281 (br), 2933 (br), 1743 (m), 1709 (m), 1663 (m), 1556 (w), 1257 (m), 1154 (s), 1108 (m), 959 (w), 833(w).

$^1\text{H NMR}$ (400 MHz, CDCl_3): δ [ppm] = 7.59 (s, 1H), 4.13 – 3.99 (m, 1H), 3.77 – 3.65 (m, 1H), 3.66 (s, 3H), 3.38 (d, J = 2.2 Hz, 1H), 3.10 (d, J = 15.4 Hz, 1H), 2.46 (d, J = 15.5 Hz, 1H), 2.41 (dd, J = 9.9, 6.1 Hz, 1H), 2.20 (dd, J = 15.5, 9.9 Hz, 1H), 1.81 (ddd, J = 15.5, 6.1, 2.2 Hz, 1H), 1.48 (s, 3H), 1.18 (s, 3H), 1.09 (s, 3H), 0.91 (s, 3H).

¹³C NMR (101 MHz, CDCl₃): δ [ppm] = 215.9 (s), 173.2 (s), 170.5 (s), 124.4 (q, *J* = 278.7 Hz), 72.3 (s), 66.9 (s), 63.4 (s), 60.9 (s), 52.8 (s), 52.0 (s), 42.3 (s), 41.3 (s), 40.8 (q, *J* = 34.2 Hz), 30.6 (s), 28.3 (s), 21.5 (s), 16.1 (s), 13.9 (s).

HR-MS (ESI): *m/z* calculated for C₁₈H₂₅F₃NO₅⁺ [M+H⁺]: 392.1679; measured: 392.1676.

8.3 Neurite Outgrowth Assay

Cell culture, transfection and morphological analysis. N2a cells were cultured in Dulbecco's modified Eagle's medium (DMEM, INVITROGEN, Karlsruhe, Germany) with 10% heat-inactivated FCS at 37 °C under a humidified 5% CO₂ atmosphere at 37 °C. N2a cells were plated at a density of 35×10^3 cells/well on glass cover slips (24-well plate, polylysine-coated) in medium containing serum. 24 h later a transient transfection was performed—including treatment with compounds or DMSO—by addition of a transfection cocktail containing 800 ng of DNA (encoding myr-Venus together with plasmid pRK5) and 1.5 μ l of lipofectamine 2000 transfection reagent per well (INVITROGEN, Karlsruhe, Germany) in 100 μ l of Opti-MEM medium (INVITROGEN, Karlsruhe, Germany). 100 μ l transfection mix were added to 400 μ l DMEM (containing compounds or DMSO) without FCS to induce differentiation. After additional 24–36 h, N2a cells were fixed with paraformaldehyde solution (4%) and mounted with Vectashield (VECTOR, Burlingame, USA). At least 25 cells from each run were arbitrarily chosen and analyzed using a fluorescence microscope (Axioplan 2, CARL ZEISS, Jena, Germany). The total length of neurites was determined using *ImageJ* software with a *NeuronJ* plugin (NIH, Bethesda, USA). Each condition was performed in triplicate. Given values represent the mean of the data.

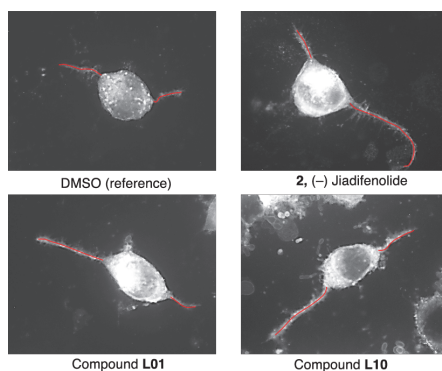


Figure S4. Morphological analysis of N2a cells with tracing of NeuronJ marked in red.

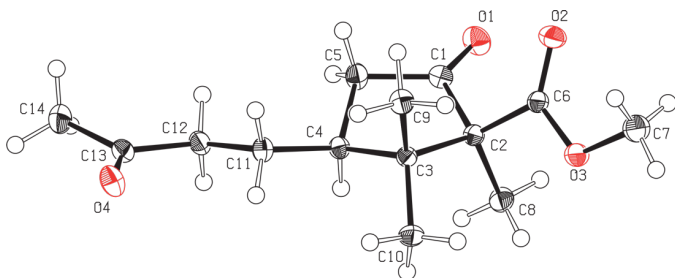
8.4 X-Ray Crystallographic Data

Compound 101 (CCDC 1512693)

A clear colourless block-like specimen of $C_{14}H_{22}O_4$, approximate dimensions 0.140 mm \times 0.340 mm \times 0.720 mm, was used for the X-ray crystallographic analysis. The X-ray intensity data were measured on a Bruker Kappa APEX II CCD system equipped with a graphite monochromator and a Mo fine-focus tube ($\lambda = 0.71073 \text{ \AA}$).

A total of 2693 frames were collected. The total exposure time was 14.96 hours. The frames were integrated with the Bruker SAINT software package using a narrow-frame algorithm. The integration of the data using an orthorhombic unit cell yielded a total of 40130 reflections to a maximum θ angle of 28.32° (0.75 \AA resolution), of which 3435 were independent (average redundancy 11.683, completeness = 99.9%, $R_{\text{int}} = 2.65\%$, $R_{\text{sig}} = 1.34\%$) and 3275 (95.34%) were greater than $2\sigma(F^2)$. The final cell constants of $a = 12.9623(3) \text{ \AA}$, $b = 9.7509(2) \text{ \AA}$, $c = 10.9430(2) \text{ \AA}$, volume = $1383.13(5) \text{ \AA}^3$, are based upon the refinement of the XYZ-centroids of 134 reflections above $20 \sigma(I)$ with $5.246^\circ < 2\theta < 44.65^\circ$. Data were corrected for absorption effects using the multi-scan method (SADABS). The ratio of minimum to maximum apparent transmission was 0.798. The calculated minimum and maximum transmission coefficients (based on crystal size) are 0.9394 and 0.9879.

The structure was solved and refined using the Bruker SHELXTL Software Package in conjunction with SHELXL, using the space group $Pc2_1$, with $Z = 4$ for the formula unit, $C_{14}H_{22}O_4$. The final anisotropic full-matrix least-squares refinement on F^2 with 168 variables converged at $R1 = 2.89\%$, for the observed data and $wR2 = 7.59\%$ for all data. The goodness-of-fit was 1.065. The largest peak in the final difference electron density synthesis was $0.269 \text{ e}/\text{\AA}^3$ and the largest hole was $-0.151 \text{ e}/\text{\AA}^3$ with an RMS deviation of $0.034 \text{ e}/\text{\AA}^3$. On the basis of the final model, the calculated density was $1.221 \text{ g}/\text{cm}^3$ and $F(000)$, 552 e $^-$.



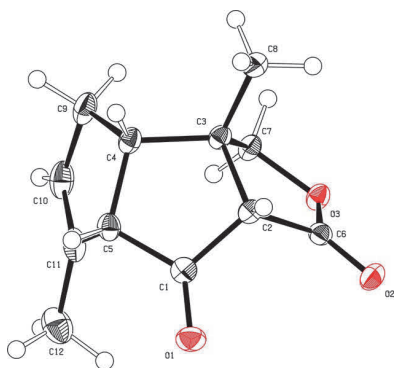
Sample and crystal data for compound **101**.

Identification code	RicJo1 AP7137-123	
Chemical formula	C ₁₄ H ₂₂ O ₄	
Formula weight	254.32	
Temperature	123(2) K	
Wavelength	0.71073 Å	
Crystal size	0.140 x 0.340 x 0.720 mm	
Crystal habit	clear colourless block	
Crystal system	orthorhombic	
Space group	<i>P</i> c a 2 ₁	
Unit cell dimensions	a = 12.9623(3) Å	α = 90°
	b = 9.7509(2) Å	β = 90°
	c = 10.9430(2) Å	γ = 90°
Volume	1383.13(5) Å ³	
Z	4	
Density (calculated)	1.221 g/cm ³	
Absorption coefficient	0.088 mm ⁻¹	
F(000)	552	

Data collection and structure refinement for compound **101**.

Diffractometer	Bruker Kappa APEX II CCD
Radiation source	fine-focus tube, Mo
Theta range for data collection	2.09 to 28.32°
Index ranges	-17<=h<=17, -13<=k<=13, -14<=l<=14
Reflections collected	40130
Independent reflections	3435 [R(int) = 0.0265]
Coverage of independent reflections	99.9%
Absorption correction	multi-scan
Max. and min. transmission	0.9879 and 0.9394
Structure solution technique	direct methods
Structure solution program	SHELXS-97 (Sheldrick, 1990)
Refinement method	Full-matrix least-squares on F ²
Refinement program	SHELXL-97 (Sheldrick, 1997)
Function minimized	Σ w(F _o ² - F _c ²) ²
Data / restraints / parameters	3435 / 1 / 168

Goodness-of-fit on F^2	1.065	
Final R indices	3275 data; $I > 2\sigma(I)$	R1 = 0.0289, wR2 = 0.0743
	all data	R1 = 0.0315, wR2 = 0.0759
Weighting scheme	$w = 1/[\sigma^2(F_o^2) + (0.0453P)^2 + 0.1909P]$ where $P = (F_o^2 + 2F_c^2)/3$	
Absolute structure parameter	0.0(6)	
Largest diff. peak and hole	0.269 and -0.151 $e\text{\AA}^{-3}$	
R.M.S. deviation from mean	0.034 $e\text{\AA}^{-3}$	

Compound 154 (CCDC 1512694)**Crystal Data and Details of the Structure Determination for: compound 154**

Formula	C12 H14 O3		
Formula Weight	206.23		
Crystal System	Monoclinic		
Space group	P21/n (No. 14)		
a, b, c [Angstrom]	10.5017(3)	9.3872(3)	10.7387(3)
alpha, beta, gamma [deg]	90	100.4498(12)	90
V [Ang**3]	1041.08(5)		
Z	4		
D(calc) [g/cm**3]	1.316		
Mu(MoKa) [/mm]	0.094		
F(000)	440		
Crystal Size [mm]	0.43 x 0.43 x 0.53		

Data Collection

Temperature (K)	100
Radiation [Angstrom]	MoK α 0.71073
Theta Min-Max [Deg]	2.5, 25.4
Dataset	-12: 12 ; -11: 11 ; -12: 12
Tot., Uniq. Data, R(int)	18199, 1904, 0.030
Observed data [$I > 2.0 \sigma(I)$]	1852

Refinement

Nref, Npar	1904, 192
R, wR2, S	0.0337, 0.0829, 1.03
$w = 1/[\sigma^2(F_o^2) + (0.0367P)^2 + 0.5612P]$ where $P = (F_o^2 + 2F_c^2)/3$	
Max. and Av. Shift/Error	0.00, 0.00
Min. and Max. Resd. Dens. [e/Ang^3]	-0.23, 0.33

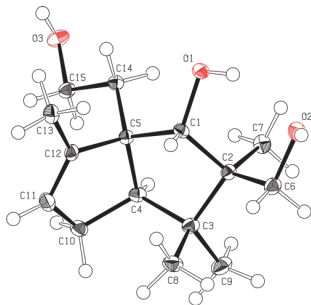
Compound 158 (CCDC 1512695)

A clear colourless fragment-like specimen of C₁₅H₂₆O₃, approximate dimensions 0.180 mm x 0.236 mm x 0.264 mm, was used for the X-ray crystallographic analysis. The X-ray intensity data were measured on a Bruker Kappa APEX II CCD system equipped with a graphite monochromator and a Mo fine-focus tube ($\lambda = 0.71073 \text{ \AA}$).

A total of 2096 frames were collected. The total exposure time was 17.47 hours. The frames were integrated with the Bruker SAINT software package using a narrow-frame algorithm. The integration of the data using an orthorhombic unit cell yielded a total of 26392 reflections to a maximum θ angle of 27.16° (0.78 Å resolution), of which 3021 were independent (average redundancy 8.736, completeness = 100.0%, $R_{\text{int}} = 3.96\%$, $R_{\text{sig}} = 2.81\%$) and 2693 (89.14%) were greater than $2\sigma(F^2)$. The final cell constants of $a = 7.43840(10) \text{ \AA}$, $b = 9.5575(2) \text{ \AA}$, $c = 19.1157(4) \text{ \AA}$, volume = 1358.98(4) Å³, are based upon the refinement of the XYZ-centroids of 111 reflections above $20 \sigma(I)$ with $6.960^\circ < 2\theta < 54.21^\circ$. Data were corrected for absorption effects using the multi-scan method (SADABS). The ratio of minimum to maximum apparent transmission was 0.860. The calculated minimum and maximum transmission coefficients (based on crystal size) are 0.9780 and 0.9850.

The structure was solved and refined using the Bruker SHELXTL Software Package in conjunction with SHELXL, using the space group P 21 21 21, with Z = 4 for the formula unit, C₁₅H₂₆O₃. The final anisotropic full-matrix least-squares refinement on F² with 179 variables converged at R1 = 3.33%, for the observed

data and $wR2 = 7.84\%$ for all data. The goodness-of-fit was 1.057. The largest peak in the final difference electron density synthesis was $0.246 \text{ e}/\text{\AA}^3$ and the largest hole was $-0.167 \text{ e}/\text{\AA}^3$ with an RMS deviation of $0.038 \text{ e}/\text{\AA}^3$. On the basis of the final model, the calculated density was $1.243 \text{ g}/\text{cm}^3$ and $F(000)$, 560 e⁻.



Sample and crystal data for compound **158**.

Identification code	RicJo2 AP7199-123	
Chemical formula	$\text{C}_{15}\text{H}_{26}\text{O}_3$	
Formula weight	254.36	
Temperature	123(2) K	
Wavelength	0.71073 Å	
Crystal size	0.180 x 0.236 x 0.264 mm	
Crystal habit	clear colourless fragment	
Crystal system	orthorhombic	
Space group	$P 2_1 2_1 2_1$	
Unit cell dimensions	$a = 7.43840(10) \text{ \AA}$	$\alpha = 90^\circ$
	$b = 9.5575(2) \text{ \AA}$	$\beta = 90^\circ$
	$c = 19.1157(4) \text{ \AA}$	$\gamma = 90^\circ$
Volume	$1358.98(4) \text{ \AA}^3$	
Z	4	
Density (calculated)	$1.243 \text{ g}/\text{cm}^3$	
Absorption coefficient	0.084 mm^{-1}	
F(000)	560	

Data collection and structure refinement for compound **158**.

Diffractometer Bruker Kappa APEX II CCD

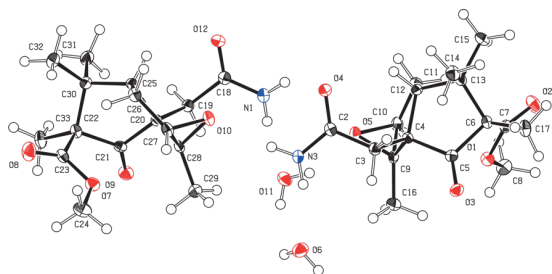
Radiation source	fine-focus tube, Mo	
Theta range for data collection	2.13 to 27.16°	
Index ranges	-9<=h<=9, -11<=k<=12, -24<=l<=24	
Reflections collected	26392	
Independent reflections	3021 [R(int) = 0.0396]	
Coverage of independent reflections	100.0%	
Absorption correction	multi-scan	
Max. and min. transmission	0.9850 and 0.9780	
Structure solution technique	direct methods	
Structure solution program	SHELXS-97 (Sheldrick, 2008)	
Refinement method	Full-matrix least-squares on F ²	
Refinement program	SHELXL-2014/7 (Sheldrick, 2014)	
Function minimized	$\Sigma w(F_o^2 - F_c^2)^2$	
Data / restraints / parameters	3021 / 0 / 179	
Goodness-of-fit on F²	1.057	
Final R indices	2693 data; l>2σ(I)	R1 = 0.0333, wR2 = 0.0744
	all data	R1 = 0.0419, wR2 = 0.0784
Weighting scheme	w=1/[σ ² (F _o ²)+(0.0388P) ² +0.2690P] where P=(F _o ² +2F _c ²)/3	
Absolute structure parameter	0.5(0)	
Largest diff. peak and hole	0.246 and -0.167 eÅ ⁻³	
R.M.S. deviation from mean	0.038 eÅ ⁻³	

Compound 162 (CCDC 1512696)

A clear pale yellow block-like specimen of C₁₆H₂₃NO_s, approximate dimensions 0.174 mm x 0.423 mm x 0.503 mm, was used for the X-ray crystallographic analysis. The X-ray intensity data were measured on a Bruker Kappa APEX II CCD system equipped with a graphite monochromator and a Mo fine-focus tube (λ = 0.71073 Å).

A total of 6088 frames were collected. The total exposure time was 33.82 hours. The frames were integrated with the Bruker SAINT software package using a narrow-frame algorithm. The integration of the data using a triclinic unit cell yielded a total of 55031 reflections to a maximum θ angle of 25.40° (0.83 Å resolution), of which 5916 were independent (average redundancy 9.302, completeness = 99.6%, R_{int} = 4.31%, R_{sig} = 2.59%) and 4737 (80.07%) were greater than 2σ(F²). The final cell constants of \underline{a} = 7.100(8) Å, \underline{b}

= 14.62(2) Å, c = 16.372(18) Å, α = 68.52(4)°, β = 82.17(4)°, γ = 88.73(6)°, volume = 1566.5(5) Å³, are based upon the refinement of the XYZ-centroids of 114 reflections above 20 $\sigma(I)$ with $7.299^\circ < 2\theta < 41.90^\circ$. Data were corrected for absorption effects using the multi-scan method (SADABS). The ratio of minimum to maximum apparent transmission was 0.893. The calculated minimum and maximum transmission coefficients (based on crystal size) are 0.9500 and 0.9820. The structure was solved and refined using the Bruker SHELXTL Software Package in conjunction with SHELXL, with $Z = 2$ for the formula unit, C₁₆H₂₃NO₅. The final anisotropic full-matrix least-squares refinement on F^2 with 443 variables converged at $R1 = 3.51\%$, for the observed data and $wR2 = 8.70\%$ for all data. The goodness-of-fit was 1.034. The largest peak in the final difference electron density synthesis was 0.262 e/Å³ and the largest hole was -0.220 e/Å³ with an RMS deviation of 0.042 e/Å³. On the basis of the final model, the calculated density was 1.347 g/cm³ and $F(000)$, 704 e⁻.



Sample and crystal data for compound **162**.

Identification code	RicJo3 AP7267-123	
Chemical formula	C ₁₆ H ₂₃ NO ₅	
Formula weight	309.36	
Temperature	123(2) K	
Wavelength	0.71073 Å	
Crystal size	0.174 x 0.423 x 0.503 mm	
Crystal habit	clear pale yellow block	
Crystal system	triclinic	
Space group	$P - 1$	
Unit cell dimensions	$a = 7.100(8)$ Å	$\alpha = 68.52(4)^\circ$
	$b = 14.62(2)$ Å	$\beta = 82.17(4)^\circ$
	$c = 16.372(18)$ Å	$\gamma = 88.73(6)^\circ$
Volume	1566.5(5) Å ³	

Z	2
Density (calculated)	1.347 g/cm ³
Absorption coefficient	0.103 mm ⁻¹
F(000)	704

Data collection and structure refinement for compound **162**.

Diffractometer	Bruker Kappa APEX II CCD	
Radiation source	fine-focus tube, Mo	
Theta range for data collection	1.47 to 25.40°	
Index ranges	-8<=h<=8, -17<=k<=17, -19<=l<=19	
Reflections collected	55031	
Independent reflections	5916 [R(int) = 0.0431]	
Coverage of independent reflections	99.6%	
Absorption correction	multi-scan	
Max. and min. transmission	0.9820 and 0.9500	
Structure solution technique	direct methods	
Structure solution program	SHELXS-97 (Sheldrick, 2008)	
Refinement method	Full-matrix least-squares on F ²	
Refinement program	SHELXL-97 (Sheldrick, 2008) and SHELXLE (Huebschle, 2011)	
Function minimized	$\sum w(F_o^2 - F_c^2)^2$	
Data / restraints / parameters	5916 / 9 / 443	
Goodness-of-fit on F²	1.034	
Δ/σ_{\max}	0.001	
Final R indices	4737 data; I>2σ(I)	R1 = 0.0351, wR2 = 0.0804
	all data	R1 = 0.0488, wR2 = 0.0870
Weighting scheme	w=1/[σ ² (F _o ²)+(0.0400P) ² +0.6089P] where P=(F _o ² +2F _c ²)/3	
Largest diff. peak and hole	0.262 and -0.220 eÅ ⁻³	
R.M.S. deviation from mean	0.042 eÅ ⁻³	

8.5 DFT-Calculations and Computational Details

In order to better understand the unsuccessful conversion of compound **S14**, DFT calculations were performed to obtain several reaction profiles. Specifically, two structures were investigated, with either a trifluorethyl amide or a methyl substituent (Figure S3): Compound **S01** experimentally produced lactone

21 (Table 2 in the manuscript) in good yields and **S19**, a substrate analogue of **S14** that does not convert at all (see previous chapter). Additionally, **S17** and **S18**, carrying methyl amide substituents instead of the electron-withdrawing group were investigated, to gauge the influence of this groups.

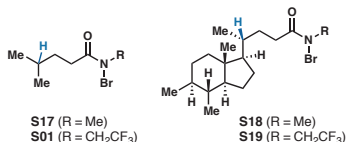
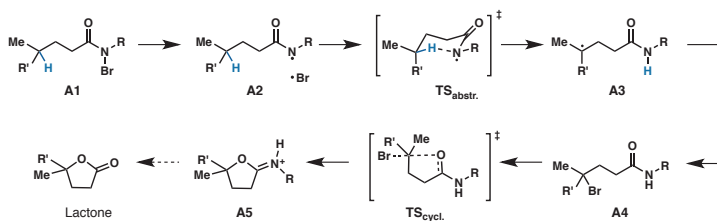


Figure S3. *N*-brominated starting material for the DFT study.

The calculated stationary points alongside the proposed mechanism are shown in Scheme S1. In our case, we leave out the *N*-bromination, since it is already accomplished in the previous step and focus on the behavior of the radical obtained through a photoreaction.



Scheme S1. The photoreaction with 1,5-H abstraction and cyclization mechanism (R = Me or CH₂CF₃).

The first step is the homolytic cleavage of the N–Br bond of **A1** leading to a nitrogen centered radical **A2** and a Br radical. The *N*-radical undergoes 1,5-hydrogen shift (*via* TS_{abstr.}) to produce a carbon centered radical at the γ position of **A3**. Here, the Br-radical can recombine leading to compound **A4**. In a cyclization reaction, the iminium lactone **A5** is formed *via* heterolytic cleavage of the C–Br bond (TS_{cycl.}).

Table S3. Calculated ΔG values in kcal/mol of the intermediates and transition states.

entry	substrate	R	A1	A2	TS1	A3	A4	TS2	A5
1	S17	Me	0.0	+33.6	+43.8	+24.7	–27.2	+3.7	–20.3
2	S18	Me	0.0	+33.7	+46.3	+21.0	–24.6	+3.4	–26.1

3	S01	CHCF ₃	0.0	+33.1	+41.1	+23.5	-28.3	+5.2	-18.5
4	S19	CHCF ₃	0.0	+32.3	+43.2	+18.1	-27.3	+3.8	-24.3

From Table S3, the following observations can be made: First of all, the C-centered radical is more stable than the N-centered radical (**A2** vs **A3**) and also the subsequent bromo compound is more stable when Br is bound to the γ -carbon rather than to the amide (**A1** vs. **A4**). A comparison of the two different substrates **S17** and **S18** shows a higher barrier (**TS_{abstr.}**) for the sterically more demanding substituent during the H transfer. Together with the energy difference at **A4** (γ -bromo compound) that also sees the smaller substituent with the better exergonicity of the formation, this hints at the steric hindrance during this part of the mechanism. These calculations indicate that compound **S14** failed to be converted under the conditions described due to a energetically disfavored transition state for the H-abstraction.

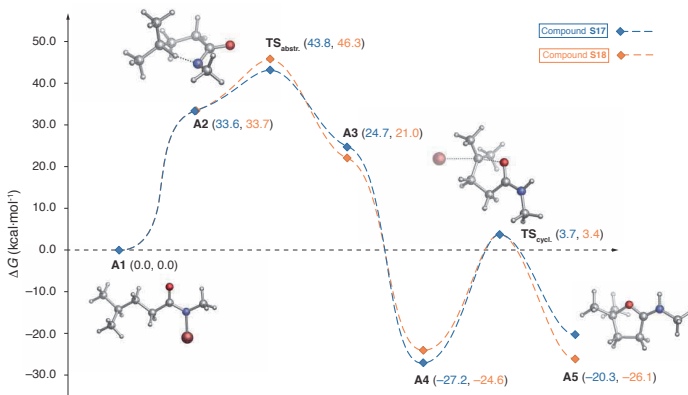


Figure S4. Gibbs free-energy diagram computed for substrate **S17** and substrate **S18**. Optimized structures of transition states identified for 1,5-H abstraction (**TS_{abstr.}**) and cyclization (**TS_{cycl.}**).

Figure 5 shows the ΔG values for the $-\text{CH}_2\text{CF}_3$ substituted substrates **S01** and **S19**. The main difference to **S17** and **S18** is that the barrier for the H transfer in the intermediate radical is lowered while the barrier height for the cyclization is increased.

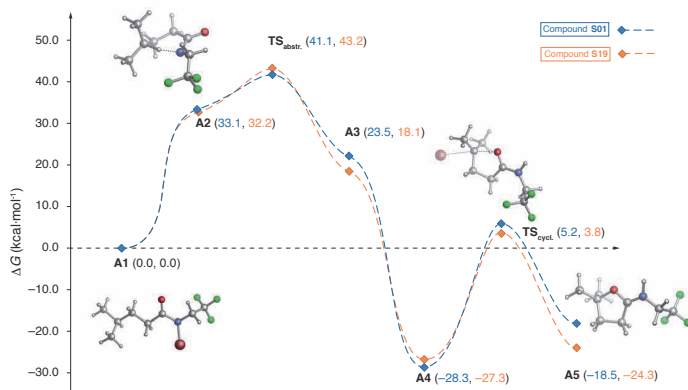


Figure S5. Gibbs free-energy diagram computed for substrate **S01** and substrate **S19**. Optimized structures of transition states identified for 1,5-H abstraction ($\text{TS}_{\text{abstr.}}$) and cyclization ($\text{TS}_{\text{cycl.}}$).

Computational Details

The calculations have been conducted using the Gaussian 09 C.01 package.^[184] The B3LYP hybrid density functional^[185] has been used together with the triple- ζ basis set 6-311+G**.^[186] Free energy values are reported in kcal/mol and given as differences to the starting material A1 as long not stated otherwise. The energies values are reported for 298.15 K and 1 atm. Frequency calculations have been carried out in order to check if the number of negative frequencies is either 0 (ground state) or 1 (transition state).

XYZ Coordinates and Absolute Energies (in a.u.) of all Calculated Species

Bromine radical (to be added to A2, A3 and $\text{TS}_{\text{abstr.}}$):

Center Number	Atomic Number	Atomic Type	Coordinates (Angstroms)		
			X	Y	Z
1	35	0	0.000000	0.000000	0.000000
HF= -2574.1057349 / NImag =0					
Sum of electronic and thermal Enthalpies=			-2574.103374		
Sum of electronic and thermal Free Energies=			-2574.122565		

Calculations according starting with compound **S17**:

S17-A1

Center Number	Atomic Number	Atomic Type	Coordinates (Angstroms)		
			X	Y	Z

Experimental Section

1	6	0	-4.590909	0.326786	-0.495456
2	6	0	-3.244711	-0.385719	-0.303169
3	1	0	-5.391669	-0.388983	-0.703179
4	1	0	-4.869021	0.884793	0.405282
5	1	0	-4.551143	1.036797	-1.326583
6	6	0	-2.126734	0.647428	-0.069946
7	1	0	-3.016394	-0.923787	-1.234066
8	6	0	-0.717288	0.050206	-0.056137
9	1	0	-2.175379	1.409706	-0.853266
10	1	0	-2.306983	1.176622	0.871830
11	1	0	-0.599482	-0.661334	0.767676
12	1	0	-0.533272	-0.524056	-0.970198
13	6	0	0.357789	1.113965	0.085509
14	8	0	0.112349	2.285698	0.314434
15	7	0	1.682563	0.738259	-0.111120
16	35	0	2.200832	-1.088435	-0.102352
17	6	0	-3.341616	-1.420727	0.827703
18	1	0	-2.425790	-2.008154	0.933996
19	1	0	-3.537863	-0.929352	1.787300
20	1	0	-4.158991	-2.123839	0.643011
21	6	0	2.782478	1.664994	0.157254
22	1	0	3.601277	1.461076	-0.532707
23	1	0	2.404034	2.672003	-0.006677
24	1	0	3.140766	1.578730	1.187746

HF= -2979.402784 / NImag = 0
Sum of electronic and thermal Enthalpies= -2979.185023
Sum of electronic and thermal Free Energies= -2979.240552

S17-A2

Center Number	Atomic Number	Atomic Type	Coordinates (Angstroms)		
			X	Y	Z
1	6	0	3.442966	-0.895274	0.044175
2	6	0	2.333988	0.108586	-0.300919
3	1	0	4.426372	-0.513979	-0.245893
4	1	0	3.468203	-1.093847	1.121255
5	1	0	3.288862	-1.850455	-0.465991
6	6	0	0.956142	-0.476273	0.063592
7	1	0	2.352410	0.265955	-1.388477
8	6	0	-0.230698	0.364928	-0.408432
9	1	0	0.863398	-1.476944	-0.368038
10	1	0	0.897977	-0.614224	1.150215
11	1	0	-0.241556	1.358112	0.055119
12	1	0	-0.175370	0.552997	-1.487870
13	6	0	-1.578850	-0.274303	-0.143413
14	8	0	-1.734744	-1.425419	0.238898
15	7	0	-2.666634	0.520156	-0.485983
16	6	0	2.601165	1.460860	0.375867
17	1	0	1.876302	2.223642	0.079998
18	1	0	2.559843	1.363789	1.466684
19	1	0	3.594376	1.837605	0.114943
20	6	0	-3.841997	0.436935	0.336372
21	1	0	-3.896383	1.355457	0.941442
22	1	0	-4.735387	0.429008	-0.293651
23	1	0	-3.830953	-0.427622	1.007520

HF=-405.2243323 / NImag = 0
Sum of electronic and thermal Enthalpies= -405.011780
Sum of electronic and thermal Free Energies= -405.064383

S17-TS1

Center Number	Atomic Number	Atomic Type	Coordinates (Angstroms)		
			X	Y	Z
1	6	0	2.501137	0.849723	-0.763070
2	6	0	1.439293	0.108560	0.029754
3	1	0	2.732105	1.821503	-0.318049
4	1	0	3.433861	0.269249	-0.784615
5	1	0	2.189146	1.009874	-1.798261
6	6	0	0.977558	-1.205279	-0.607746
7	1	0	0.379046	0.725872	-0.134304
8	6	0	-0.419047	-1.623582	-0.124288
9	1	0	0.956919	-1.075123	-1.693967
10	1	0	1.701394	-2.004449	-0.399674
11	1	0	-0.831561	-2.418717	-0.750656
12	1	0	-0.381645	-2.037663	0.888712
13	6	0	-1.455622	-0.500340	-0.078245
14	8	0	-2.627645	-0.717811	0.209864

Experimental Section

15	7	0	-1.003107	0.747217	-0.416706
16	6	0	1.725043	0.037793	1.521365
17	1	0	0.905906	-0.416919	2.083272
18	1	0	2.624543	-0.565463	1.704120
19	1	0	1.908600	1.031309	1.939317
20	6	0	-1.732045	1.915849	0.038866
21	1	0	-2.019379	1.859069	1.094125
22	1	0	-1.125354	2.805793	-0.136675
23	1	0	-2.648581	2.011292	-0.553122

HF=-405.2076378 / NImag = 1 (-1239.5927 cm⁻¹)

Sum of electronic and thermal Enthalpies= -404.999928

Sum of electronic and thermal Free Energies= -405.048162

S17-A3

Center Number	Atomic Number	Atomic Type	Coordinates (Angstroms)		
			X	Y	Z
1	6	0	3.226429	-0.201023	-1.102809
2	6	0	2.213664	0.135556	-0.055392
3	1	0	3.894087	0.642357	-1.309110
4	1	0	3.873753	-1.041378	-0.793068
5	1	0	2.755806	-0.502673	-2.043709
6	6	0	0.945790	-0.665793	0.040882
7	6	0	-0.327821	0.194963	-0.037955
8	1	0	0.907332	-1.415445	-0.753728
9	1	0	0.912552	-1.230919	0.982926
10	1	0	-0.309280	0.976345	0.731111
11	1	0	-0.363215	0.724299	-0.996775
12	6	0	-1.606459	-0.618564	0.137757
13	8	0	-1.602586	-1.808795	0.414509
14	7	0	-2.783530	0.064781	-0.019564
15	6	0	2.654497	0.942455	1.125838
16	1	0	1.810711	1.323622	1.709024
17	1	0	3.266436	0.339193	1.819833
18	1	0	3.273309	1.796500	0.830060
19	6	0	-2.951252	1.453146	-0.419997
20	1	0	-2.652552	1.629686	-1.459396
21	1	0	-4.005045	1.715187	-0.322688
22	1	0	-2.380959	2.128389	0.222859
23	1	0	-3.606634	-0.512701	0.073582

HF= -405.237325 / NImag = 0

Sum of electronic and thermal Enthalpies= -405.024228

Sum of electronic and thermal Free Energies= -405.078598

S17-A4

Center Number	Atomic Number	Atomic Type	Coordinates (Angstroms)		
			X	Y	Z
1	6	0	2.340178	1.771318	0.256502
2	6	0	1.333723	0.781107	-0.322844
3	1	0	3.358066	1.530756	-0.053975
4	1	0	2.098259	2.776772	-0.107191
5	1	0	2.302724	1.785663	1.346670
6	6	0	-0.076648	1.086384	0.194310
7	6	0	-1.196109	0.153431	-0.263035
8	1	0	-0.057630	1.115910	1.285651
9	1	0	-0.314618	2.107660	-0.125200
10	1	0	-1.273178	0.132214	-1.356169
11	1	0	-0.981761	-0.874014	0.045228
12	6	0	-2.551686	0.582963	0.289992
13	8	0	-2.717782	1.634898	0.890388
14	7	0	-3.593185	-0.273413	0.060368
15	6	0	1.433822	0.711729	-1.843579
16	1	0	0.805281	-0.072027	-2.266395
17	1	0	1.114682	1.673417	-2.263114
18	1	0	2.461940	0.527765	-2.159174
19	6	0	-3.538001	-1.580223	-0.578179
20	1	0	-2.957216	-2.304298	0.002627
21	1	0	-4.555451	-1.960309	-0.670088
22	1	0	-3.113546	-1.521692	-1.584032
23	1	0	-4.469988	0.033770	0.455611
24	35	0	1.885866	-1.061632	0.385853

HF= -2979.4477086 / NImag = 0

Sum of electronic and thermal Enthalpies= -2979.228923

Sum of electronic and thermal Free Energies= -2979.283926

S17-TS2

Center Number	Atomic Number	Atomic Type	Coordinates (Angstroms)		
			X	Y	Z

```

-----
  1      6      0      0.616807      1.788213      -0.923223
  2      6      0      0.170758      0.718322      0.015171
  3      1      0      0.362716      2.773350      -0.527465
  4      1      0      1.703514      1.712559      -1.009165
  5      1      0      0.178951      1.659490      -1.913053
  6      6      0      -0.221880      -0.649849      -0.494244
  7      6      0      -1.621725      -1.054987      -0.003876
  8      1      0      0.529267      -1.357108      -0.144654
  9      1      0      -2.034109      -1.861428      -0.613384
  10     1      0      -1.597135      -1.423412      1.028292
  11     6      0      -2.472107      0.191733      -0.036193
  12     8      0      -1.876867      1.282543      -0.064245
  13     7      0      -3.810722      0.120823      -0.006878
  14     6      0      0.331377      0.960056      1.480542
  15     1      0      -0.115662      0.174417      2.090435
  16     1      0      1.404578      0.973161      1.686576
  17     1      0      -0.093386      1.929511      1.748669
  18     6      0      -4.610223      -1.102231      0.002377
  19     1      0      -5.636756      -0.837487      0.251830
  20     1      0      -4.607823      -1.596607      -0.972911
  21     1      0      -4.249055      -1.800263      0.759064
  22     1      0      -4.289332      1.010970      -0.032950
  23     1      0      -0.186224      -0.652983      -1.584436
  24     35     0      3.061783      -0.483366      -0.012802
HF=-2979.3958087 / NImag = 1 (-308.0005 cm-1)
Sum of electronic and thermal Enthalpies= -2979.178775
Sum of electronic and thermal Free Energies= -2979.234641

```

S17-A5

```

-----
Center      Atomic      Atomic      Coordinates (Angstroms)
Number      Number      Type          X          Y          Z
-----
  1      6      0      2.910030      1.738170      -0.999459
  2      6      0      2.509832      0.662945      -0.002865
  3      1      0      2.432604      2.688626      -0.754424
  4      1      0      3.993836      1.878907      -0.974768
  5      1      0      2.618634      1.455862      -2.013008
  6      6      0      3.051259      -0.743581      -0.339027
  7      6      0      1.895515      -1.686484      0.029548
  8      1      0      3.266678      -0.813328      -1.407461
  9      1      0      3.969305      -0.963740      0.206026
  10     1      0      1.798532      -2.548510      -0.631641
  11     1      0      1.971258      -2.070212      1.052272
  12     6      0      0.695318      -0.779783      -0.061505
  13     8      0      1.038196      0.490002      -0.139931
  14     7      0      -0.542926      -1.113781      -0.062426
  15     6      0      2.775524      1.081171      1.441019
  16     1      0      2.484189      0.300367      2.148464
  17     1      0      3.840063      1.286689      1.578818
  18     1      0      2.212680      1.984604      1.681665
  19     6      0      -1.024880      -2.490234      0.003277
  20     1      0      -2.106076      -2.430408      0.126103
  21     1      0      -0.803065      -3.030379      -0.920765
  22     1      0      -0.595650      -3.026592      0.852651
  23     1      0      -1.354992      -0.343145      -0.070724
  24     35     0      -3.003105      0.651842      0.007351
HF=-2979.4354151 / NImag = 0
Sum of electronic and thermal Enthalpies= -2979.218222
Sum of electronic and thermal Free Energies= -2979.272845

```

Calculations according starting with compound S18:

S18-A1

```

-----
Center      Atomic      Atomic      Coordinates (Angstroms)
Number      Number      Type          X          Y          Z
-----
  1      6      0      -0.027449      1.774455      -0.853693
  2      6      0      1.394550      1.952422      -0.265206
  3      6      0      2.261695      0.689034      -0.255176
  4      1      0      1.910875      2.723579      -0.845562
  5      1      0      1.335319      2.344657      0.751396
  6      1      0      1.783541      -0.111262      0.319871
  7      1      0      2.395703      0.287527      -1.263220
  8      6      0      3.628421      0.945537      0.356434
  9      8      0      3.928987      1.988699      0.911057
  10     7      0      4.599434      -0.042739      0.231698

```

Experimental Section

11	35	0	4.146516	-1.813750	-0.281713
12	6	0	5.882052	0.059226	0.928015
13	1	0	6.659818	-0.403953	0.320851
14	1	0	6.096354	1.118195	1.057233
15	1	0	5.847139	-0.423225	-1.909752
16	6	0	-0.894634	0.804778	-0.015214
17	6	0	-2.404670	0.606796	-0.384727
18	6	0	-0.943608	1.202097	1.494451
19	6	0	-2.902306	-0.115725	0.901319
20	6	0	-2.303139	0.704674	2.053238
21	1	0	-0.103176	0.771096	2.043565
22	6	0	-4.184309	-0.738505	-1.620367
23	1	0	-2.953192	1.547234	2.310621
24	6	0	-4.731062	-1.338917	-0.309563
25	1	0	-4.794059	0.131472	-1.893213
26	1	0	-0.854810	2.287002	1.602956
27	1	0	-2.181287	0.113509	2.963309
28	1	0	-4.329663	-1.464860	-2.427994
29	1	0	-0.441422	-0.193417	-0.088950
30	6	0	-2.700530	-0.332498	-1.569885
31	1	0	-2.425884	0.123339	-2.524389
32	1	0	-2.083202	-1.234223	-1.465397
33	6	0	-3.087153	1.975186	-0.597409
34	1	0	-2.880060	2.671184	0.218970
35	1	0	-2.730666	2.440718	-1.520361
36	1	0	-4.171367	1.888336	-0.679788
37	6	0	-4.401935	-0.448216	0.919723
38	1	0	-2.380075	-1.086115	0.906017
39	1	0	-0.489274	2.767091	-0.782637
40	6	0	0.048144	1.412077	-2.347199
41	1	0	0.331254	0.366575	-2.503203
42	1	0	-0.904958	1.568439	-2.854280
43	1	0	0.790168	2.036890	-2.854565
44	1	0	-4.213449	-2.296583	-0.146179
45	6	0	-6.229998	-1.635380	-0.457901
46	1	0	-6.631737	-2.187453	0.394314
47	1	0	-6.804316	-0.707458	-0.557006
48	1	0	-6.418186	-2.235592	-1.353295
49	1	0	-4.975272	0.485045	0.830617
50	6	0	-4.806857	-1.115632	2.243048
51	1	0	-4.278745	-2.066568	2.378954
52	1	0	-4.566082	-0.477733	3.096827
53	1	0	-5.878548	-1.321070	2.285070

HF= -3409.5310659/ Nimag = 0

Sum of electronic and thermal Enthalpies= -3409.031828

Sum of electronic and thermal Free Energies= -3409.111631

S18-A2

Center Number	Atomic Number	Atomic Type	Coordinates (Angstroms)		
			X	Y	Z
1	6	0	1.133531	1.370840	0.737965
2	6	0	2.586051	0.846950	0.873863
3	6	0	3.206793	0.296322	-0.412899
4	1	0	3.214987	1.665083	1.236494
5	1	0	2.633158	0.077184	1.648500
6	1	0	2.647797	-0.562544	-0.803038
7	1	0	3.192330	1.036679	-1.220228
8	6	0	4.649894	-0.135723	-0.251411
9	8	0	5.333068	0.089205	0.737879
10	7	0	5.203477	-0.719465	-1.385447
11	6	0	6.155132	-1.779191	-1.195540
12	1	0	6.987342	-1.659534	-1.894329
13	1	0	6.518322	-1.844847	-0.165102
14	1	0	5.661766	-2.727791	-1.459125
15	6	0	0.137651	0.249321	0.357251
16	6	0	-1.393101	0.570866	0.274974
17	6	0	0.198547	-0.961292	1.342383
18	6	0	-1.969336	-0.875563	0.237852
19	6	0	-1.210262	-1.613219	1.351134
20	1	0	0.968168	-1.676067	1.040950
21	6	0	-3.403641	1.221783	-1.152110
22	1	0	-1.702178	-1.470159	2.318912
23	6	0	-4.006334	-0.195180	-1.061827
24	1	0	-3.870398	1.854266	-0.388239
25	1	0	0.473446	-0.620898	2.345125
26	1	0	-1.165632	-2.690692	1.178752
27	1	0	-3.688532	1.663889	-2.114393
28	1	0	0.413569	-0.112256	-0.642648
29	6	0	-1.872673	1.278891	-1.007001

Experimental Section

30	1	0	-1.553196	2.323662	-1.035097
31	1	0	-1.409538	0.787986	-1.872797
32	6	0	-1.846658	1.352461	1.526630
33	1	0	-1.511201	0.877939	2.451738
34	1	0	-1.440838	2.367699	1.514668
35	1	0	-2.932229	1.442920	1.585829
36	6	0	-3.502040	-0.961409	0.191591
37	1	0	-1.615476	-1.302461	-0.714201
38	1	0	0.861404	1.721462	1.741426
39	6	0	1.090090	2.590558	-0.198788
40	1	0	1.179580	2.304744	-1.251102
41	1	0	0.160409	3.151188	-0.092949
42	1	0	1.910738	3.277388	0.030795
43	1	0	-3.651065	-0.761137	-1.936503
44	1	0	-3.913362	-0.467208	1.082585
45	6	0	-3.977787	-2.422179	0.209156
46	1	0	-3.615391	-2.944007	0.098097
47	1	0	-5.067189	-2.496629	0.211722
48	1	0	-3.607714	-2.964430	-0.668746
49	6	0	-5.537116	-0.113949	-1.144069
50	1	0	-5.847283	0.462415	-2.021017
51	1	0	-6.004178	-1.098194	-1.220176
52	1	0	-5.948937	0.385243	-0.259725

HF= -835.3525428/ NImag = 0

Sum of electronic and thermal Enthalpies= -834.858565

Sum of electronic and thermal Free Energies= -834.935372

S18-TS1

Center Number	Atomic Number	Atomic Type	Coordinates (Angstroms)		
			X	Y	Z
1	6	0	1.632849	0.616000	0.149260
2	6	0	2.294467	0.214118	1.488305
3	6	0	3.461887	-0.790895	1.325933
4	1	0	2.687935	1.116584	1.966291
5	1	0	1.563468	-0.204797	2.182404
6	1	0	4.054630	-0.845926	2.239404
7	1	0	3.072269	-1.791570	1.118191
8	6	0	4.394414	-0.413546	0.182957
9	8	0	5.604455	-0.265975	0.316523
10	7	0	3.759029	-0.309014	-1.031992
11	6	0	4.391430	0.474357	-2.077671
12	1	0	4.783325	1.435531	-1.727010
13	1	0	5.233865	-0.098801	-2.480572
14	1	0	3.677533	0.632265	-2.888135
15	6	0	0.350594	-0.101847	-0.305221
16	6	0	-1.060840	0.315736	0.258521
17	6	0	0.369888	-1.647515	-0.122874
18	6	0	-1.916576	-0.824953	-0.366927
19	6	0	-1.113931	-2.107325	-0.090889
20	1	0	0.935598	-2.122235	-0.927235
21	6	0	-3.138491	1.773466	0.028391
22	1	0	-1.372553	-2.525526	0.887220
23	6	0	-3.990207	0.585325	-0.464028
24	1	0	-3.298937	1.901819	1.105589
25	1	0	0.866652	-1.923781	0.808749
26	1	0	-1.318121	-2.885930	-0.828518
27	1	0	-3.514666	2.692125	-0.435424
28	1	0	0.277171	0.096870	-1.383364
29	6	0	-1.630972	1.648487	-0.259932
30	1	0	-1.113481	2.505378	0.180150
31	1	0	-1.466134	1.705181	-1.343383
32	6	0	-1.078311	0.293198	1.800291
33	1	0	-0.712829	-0.652031	2.207037
34	1	0	-0.451653	1.092930	2.204122
35	1	0	-2.083233	0.443403	2.197100
36	6	0	-3.408406	-0.780348	-0.004646
37	1	0	-1.869275	-0.656848	-1.454297
38	6	0	1.643223	2.123174	-0.082130
39	1	0	1.226832	2.390304	-1.056651
40	1	0	1.059393	2.645137	0.684322
41	1	0	2.662577	2.516891	-0.027335
42	1	0	-3.949639	0.585128	-1.563989
43	6	0	-5.453847	0.788211	-0.047878
44	1	0	-6.119518	0.045623	-0.492567
45	1	0	-5.562697	0.727241	1.040785
46	1	0	-5.811232	1.774476	-0.359014
47	1	0	-3.513831	-0.849240	1.086923
48	6	0	-4.162631	-1.967969	-0.621678

Experimental Section

```

49      1      0      -4.102642    -1.942331    -1.715833
50      1      0      -3.741086    -2.919363    -0.288706
51      1      0      -5.219026    -1.967979    -0.345582
52      1      0      2.463242     0.184314    -0.637618
HF= -835.3327785 / Nimag = 1 (-965.1355 cm-1)
Sum of electronic and thermal Enthalpies=      -834.843334
Sum of electronic and thermal Free Energies=     -834.915322

```

S18-A3

Center Number	Atomic Number	Atomic Type	Coordinates (Angstroms)		
			X	Y	Z
1	6	0	-1.135553	0.963174	-0.570828
2	6	0	-2.511084	0.395183	-0.786503
3	6	0	-3.319107	0.231211	0.533123
4	1	0	-3.078870	1.056233	-1.452042
5	1	0	-2.479353	-0.583789	-1.266681
6	1	0	-2.767147	-0.423513	1.214753
7	1	0	-3.434367	1.199268	1.031072
8	6	0	-4.669034	-0.427178	0.281578
9	8	0	-4.766249	-1.503058	-0.290850
10	7	0	-5.758203	0.271618	0.722917
11	6	0	-7.117349	-0.231727	0.599595
12	1	0	-7.798371	0.586870	0.357775
13	1	0	-7.136590	-0.965949	-0.204348
14	1	0	-7.457301	-0.718181	1.520050
15	6	0	-0.037924	0.062786	-0.060291
16	6	0	1.463748	0.434883	-0.326756
17	6	0	-0.128447	-1.417593	-0.550054
18	6	0	2.146845	-0.877287	-0.154492
19	6	0	1.309248	-1.999729	-0.478968
20	1	0	-0.831898	-1.993100	0.055344
21	6	0	3.584229	1.619733	0.442788
22	1	0	1.679806	-2.244730	-1.479561
23	6	0	4.278245	0.287063	0.790266
24	1	0	3.895666	1.928519	-0.562621
25	1	0	-0.503678	-1.453306	-1.575039
26	1	0	1.349292	-2.921755	0.104648
27	1	0	3.956801	2.397906	1.118575
28	1	0	-0.127883	0.043780	1.044279
29	6	0	2.047052	1.583116	0.517203
30	1	0	1.654889	2.554527	0.205376
31	1	0	1.739078	1.442318	1.561754
32	6	0	1.675077	0.697868	-1.832996
33	1	0	1.285407	-0.116198	-2.447466
34	1	0	1.154230	1.608569	-2.139419
35	1	0	2.728481	0.822553	-2.088229
36	6	0	3.674257	-0.905308	-0.001049
37	1	0	1.954495	-0.920149	1.238428
38	6	0	-1.049615	2.447135	-0.355879
39	1	0	-0.944085	2.707953	0.710343
40	1	0	-0.191583	2.899903	-0.861433
41	1	0	-1.947506	2.950635	-0.725408
42	1	0	4.085905	0.083514	1.854761
43	6	0	5.795958	0.428053	0.606773
44	1	0	6.342454	-0.442028	0.976446
45	1	0	6.051361	0.559997	-0.450669
46	1	0	6.170944	1.302500	1.147279
47	1	0	3.927110	-0.774966	-1.062620
48	6	0	4.253968	-2.253978	0.452718
49	1	0	4.047363	-2.429796	1.514795
50	1	0	3.817563	-3.081826	-0.111284
51	1	0	5.335748	-2.301885	0.311188
52	1	0	-5.603639	1.124827	1.235064

```

HF= -835.3710852 / Nimag = 0
Sum of electronic and thermal Enthalpies=      -834.876342
Sum of electronic and thermal Free Energies=     -834.955599

```

S18-A4

Center Number	Atomic Number	Atomic Type	Coordinates (Angstroms)		
			X	Y	Z
1	6	0	-1.044021	0.862297	0.432681
2	6	0	-2.417434	0.305843	-0.012746
3	6	0	-2.779782	-1.086031	0.546505
4	1	0	-3.185231	1.017176	0.302908

Experimental Section

5	1	0	-2.464370	0.258449	-1.100233
6	1	0	-2.016540	-1.822631	0.281436
7	1	0	-2.851505	-1.065087	1.637845
8	6	0	-4.079448	-1.582421	-0.081784
9	8	0	-4.190367	-1.725743	-1.289844
10	7	0	-5.092488	-1.848790	0.794655
11	6	0	-6.396666	-2.336847	0.373195
12	1	0	-7.192229	-1.675860	0.727127
13	1	0	-6.407569	-2.355402	-0.715272
14	1	0	-6.581326	-3.348365	0.746674
15	6	0	0.117316	0.011484	-0.131906
16	6	0	1.626746	0.205963	0.260940
17	6	0	0.131701	-0.121833	-1.685710
18	6	0	2.260535	-0.813825	-0.736026
19	6	0	1.584090	-0.498379	-2.077474
20	1	0	-0.578203	-0.883290	-2.015597
21	6	0	3.540999	-0.413269	1.831415
22	1	0	2.084169	0.337899	-2.575739
23	6	0	4.201636	-1.318625	0.772429
24	1	0	4.018917	0.573261	1.801983
25	1	0	-0.174198	0.815573	-2.152439
26	1	0	1.613222	-1.343159	-2.768295
27	1	0	3.759659	-0.817179	2.826404
28	1	0	-0.117614	-0.984694	0.268591
29	6	0	2.017559	-0.253600	1.680565
30	1	0	1.661379	0.444895	2.442122
31	1	0	1.535142	-1.218253	1.888111
32	6	0	2.125000	1.643085	0.010782
33	1	0	1.854111	2.008714	-0.979810
34	1	0	1.693398	2.337792	0.733707
35	1	0	3.210083	1.710126	0.102112
36	6	0	3.791506	-0.917547	-0.671370
37	1	0	1.883242	-1.801596	-0.424431
38	6	0	-0.993256	1.068506	1.945235
39	1	0	-0.920021	0.100111	2.450767
40	1	0	-0.137253	1.669133	2.246250
41	1	0	-1.897880	1.571765	2.293324
42	1	0	3.823289	-2.340272	0.930230
43	6	0	5.721826	-1.342259	0.984861
44	1	0	6.219296	-2.078624	0.350347
45	1	0	6.161293	-0.361988	0.769006
46	1	0	5.963428	-1.589844	2.022999
47	1	0	4.227856	0.065942	-0.891902
48	6	0	4.323825	-1.906573	-1.719552
49	1	0	3.938552	-2.916160	-1.535727
50	1	0	4.021702	-1.614493	-2.727988
51	1	0	5.414430	-1.959469	-1.711865
52	35	0	-1.053122	2.762585	-0.359335
53	1	0	-4.922377	-1.713277	1.777997

HF= -3409.571662 / NIMag = 0

Sum of electronic and thermal Enthalpies= -3409.071224

Sum of electronic and thermal Free Energies= -3409.150799

S18-TS2

Center Number	Atomic Number	Atomic Type	Coordinates (Angstroms)		
			X	Y	Z
1	6	0	1.309282	-0.521559	-0.227026
2	6	0	2.327269	-0.976018	0.805706
3	6	0	1.813563	-2.215908	1.541670
4	1	0	3.272847	-1.193159	0.308368
5	1	0	2.534353	-0.134824	1.473593
6	1	0	2.618862	-2.791279	2.003096
7	1	0	1.097556	-1.965660	2.331830
8	6	0	1.082245	-3.002539	0.477396
9	8	0	0.679407	-2.364204	-0.517867
10	7	0	0.884901	-4.315152	0.608896
11	6	0	0.157786	-5.128490	-0.364817
12	1	0	-0.908496	-5.167158	-0.129129
13	1	0	0.284750	-4.693177	-1.354420
14	1	0	0.565813	-6.138888	-0.359313
15	6	0	0.080820	0.147642	0.340147
16	6	0	-1.316224	0.193821	-0.370251
17	6	0	0.412942	1.664186	0.644874
18	6	0	-1.993445	1.281627	0.517891
19	6	0	-0.949791	2.403540	0.590173
20	1	0	0.881997	1.747991	1.625803
21	6	0	-3.630145	-0.840394	-0.597369
22	1	0	-1.004883	3.047691	-0.292336

Experimental Section

23	6	0	-4.288156	0.313381	0.187460
24	1	0	-3.724555	-0.638935	-1.671026
25	1	0	1.138369	2.078024	-0.055343
26	1	0	-1.085990	3.047186	1.460984
27	1	0	-4.201764	-1.758273	-0.418865
28	1	0	-0.116862	-0.326842	1.307571
29	6	0	-2.152921	-1.092842	-0.247256
30	1	0	-1.751218	-1.881600	-0.888108
31	1	0	-2.090091	-1.459560	0.786709
32	6	0	-1.229297	0.625196	-1.847266
33	1	0	-0.592125	1.499262	-1.990411
34	1	0	-0.835699	-0.187199	-2.462051
35	1	0	-2.212863	0.876179	-2.244807
36	6	0	-3.442293	1.615445	0.131340
37	1	0	-2.050219	0.843064	0.527670
38	6	0	1.907354	-0.130502	-1.501330
39	1	0	1.223065	0.224937	-2.261950
40	1	0	2.618688	0.708530	-1.206103
41	1	0	2.567415	-0.905266	-1.892657
42	1	0	-4.325178	0.012306	1.245779
43	6	0	-5.732159	0.511977	-0.294409
44	1	0	-6.282314	1.224044	0.323830
45	1	0	-5.752586	0.878528	-1.326703
46	1	0	-6.281443	-0.434043	-0.270033
47	1	0	-3.460447	1.993119	-0.899759
48	6	0	-4.013269	2.717152	1.037160
49	1	0	-4.038322	2.389891	2.082950
50	1	0	-3.404923	3.622994	0.987167
51	1	0	-5.029543	2.993949	0.749943
52	35	0	4.154971	2.027751	-0.142944
53	1	0	1.230886	-4.757709	1.446946

HF= -3409.5264963 / NImag = 1 (-150.3741 cm⁻¹)
Sum of electronic and thermal Enthalpies= -3409.028161
Sum of electronic and thermal Free Energies= -3409.106207

S18-A5

Center Number	Atomic Number	Atomic Type	Coordinates (Angstroms)		
			X	Y	Z
1	6	0	0.274350	-0.904778	0.324103
2	6	0	0.966475	-0.947882	-1.057755
3	6	0	2.470918	-0.896015	-0.745539
4	1	0	0.693141	-1.849040	-1.604840
5	1	0	0.683465	-0.091572	-1.667299
6	1	0	2.921985	-1.888362	-0.651339
7	1	0	3.088843	-0.352437	-1.461904
8	6	0	2.496217	-0.235259	0.598007
9	8	0	1.321020	-0.227307	1.188718
10	7	0	3.534690	0.285371	1.150294
11	6	0	3.548441	0.926507	2.460914
12	1	0	4.485285	1.475010	2.545069
13	1	0	2.707374	1.613456	2.566030
14	1	0	3.497581	0.179082	3.256091
15	6	0	-0.966320	-0.005192	0.504043
16	6	0	-2.341487	-0.394077	-0.141141
17	6	0	-0.742821	1.482565	0.085501
18	6	0	-3.112581	0.937662	0.108391
19	6	0	-2.131538	2.032677	-0.333223
20	1	0	-0.324205	2.045595	0.921066
21	6	0	-4.600737	-1.548090	0.116121
22	1	0	-2.183689	2.188107	-1.415351
23	6	0	-5.345835	-0.202917	0.234373
24	1	0	-4.658270	-1.895946	-0.922265
25	1	0	-0.026256	1.577506	-0.732921
26	1	0	-2.344132	2.995554	0.134109
27	1	0	-5.134348	-2.300001	0.707426
28	1	0	-1.143285	-0.011672	1.586269
29	6	0	-3.129824	-1.511661	0.568741
30	1	0	-2.685267	-2.495454	0.392563
31	1	0	-3.088822	-1.339562	1.651801
32	6	0	-2.196859	-0.714341	-1.643710
33	1	0	-1.635188	0.051524	-2.181637
34	1	0	-1.683137	-1.668118	-1.790758
35	1	0	-3.167075	-0.800924	-2.132600
36	6	0	-4.553719	0.960588	-0.423500
37	1	0	-3.197686	1.021302	1.203565
38	6	0	0.112222	-2.301219	0.918467

Experimental Section

39	1	0	-0.253794	-2.249339	1.945360
40	1	0	-0.594021	-2.885407	0.327761
41	1	0	1.066569	-2.834040	0.919692
42	1	0	-5.420938	0.038382	1.305532
43	6	0	-6.771542	-0.349920	-0.315207
44	1	0	-7.383399	0.533893	-0.125009
45	1	0	-6.758368	-0.522395	-1.397093
46	1	0	-7.277664	-1.202270	0.147586
47	1	0	-4.539466	0.795645	-1.509679
48	6	0	-5.212662	2.325168	-0.171527
49	1	0	-5.260983	2.544134	0.901158
50	1	0	-4.651708	3.130916	-0.650737
51	1	0	-6.229970	2.362474	-0.565530
52	1	0	4.445416	0.283233	0.548187
53	35	0	5.947567	0.269963	-0.752413

HF= -3409.5736723/ NImag = 0
 Sum of electronic and thermal Enthalpies= -3409.074309
 Sum of electronic and thermal Free Energies= -3409.153135

Calculations according starting with compound S01:

S01-A1

Center Number	Atomic Number	Atomic Type	Coordinates (Angstroms)		
			X	Y	Z
1	6	0	-5.250033	-1.359828	0.556423
2	6	0	-4.154668	-0.286587	0.485513
3	1	0	-6.164796	-0.962101	1.005079
4	1	0	-5.502826	-1.726444	-0.444365
5	1	0	-4.928775	-2.218271	1.153244
6	6	0	-2.860292	-0.889917	-0.090323
7	1	0	-3.943452	0.042240	1.512800
8	6	0	-1.653772	0.050547	-0.030609
9	1	0	-2.616732	-1.805038	0.456966
10	1	0	-3.030343	-1.198282	-1.127646
11	1	0	-1.815839	0.943146	-0.642763
12	1	0	-1.500510	0.417042	0.990462
13	6	0	-0.378599	-0.621584	-0.499097
14	8	0	-0.333896	-1.752346	-0.941820
15	7	0	0.818817	0.096803	-0.388274
16	35	0	0.847419	1.941619	0.043627
17	6	0	-4.646228	0.932611	-0.308978
18	1	0	-3.923138	1.752714	-0.304486
19	1	0	-4.840628	0.662746	-1.353142
20	1	0	-5.578724	1.320981	0.110585
21	6	0	2.058977	-0.454526	-0.908427
22	1	0	1.801594	-1.320463	-1.519008
23	1	0	2.585454	0.278726	-1.521091
24	6	0	3.011198	-0.932421	0.182326
25	9	0	3.456975	0.077515	0.960817
26	9	0	2.445354	-1.841957	0.994040
27	9	0	4.095336	-1.505811	-0.389530

HF= -3316.5496544/ NImag = 0
 Sum of electronic and thermal Enthalpies= -3316.323577
 Sum of electronic and thermal Free Energies= -3316.388476

S01-A2

Center Number	Atomic Number	Atomic Type	Coordinates (Angstroms)		
			X	Y	Z
1	6	0	-0.870247	0.310267	-0.273791
2	8	0	-1.693222	-0.552561	0.272641
3	6	0	-3.116110	-0.117706	0.139723
4	6	0	-3.041018	0.942606	-0.978657
5	6	0	-1.600502	1.471337	-0.897264
6	6	0	-3.908413	-1.359800	-0.231019
7	6	0	-3.526796	0.456383	1.492327
8	7	0	0.396992	0.071100	-0.229969
9	6	0	1.423720	0.904584	-0.823755
10	6	0	1.911126	1.992807	0.124867
11	9	0	0.905854	2.856809	0.442725
12	9	0	2.881289	2.715541	-0.467929
13	9	0	2.389977	1.506564	1.273555
14	35	0	1.723578	-2.603942	-0.000075
15	1	0	-3.860753	-2.102059	0.567646

Experimental Section

16	1	0	-4.955731	-1.091173	-0.392178
17	1	0	-3.518925	-1.810549	-1.145664
18	1	0	-3.216771	0.473992	-1.949312
19	1	0	-3.785228	1.727062	-0.841174
20	1	0	-1.175383	1.747247	-1.863005
21	1	0	-1.503834	2.341068	-0.242205
22	1	0	-2.948639	1.348441	1.746924
23	1	0	-4.584744	0.729462	1.472061
24	1	0	-3.376128	-0.284858	-2.279058
25	1	0	2.266101	0.244205	-1.046199
26	1	0	1.097146	1.389205	-1.746210
27	1	0	0.779859	-0.964355	0.041806

HF= -742.3730628/ NImag = 0
Sum of electronic and thermal Enthalpies= -742.152087
Sum of electronic and thermal Free Energies= -742.213201

S01-TS1

Center Number	Atomic Number	Atomic Type	Coordinates (Angstroms)		
			X	Y	Z
1	6	0	-1.830967	-2.343313	-0.602618
2	6	0	-1.960058	-0.980410	0.055621
3	1	0	-1.310004	-3.054820	0.042906
4	1	0	-2.827660	-2.755136	-0.812180
5	1	0	-1.291338	-2.281183	-1.550438
6	6	0	-2.559975	0.101181	-0.847571
7	1	0	-0.832467	-0.521251	0.113849
8	6	0	-2.180949	1.517705	-0.393111
9	1	0	-2.196929	-0.057724	-1.867065
10	1	0	-3.652561	0.002017	-0.882278
11	1	0	-2.424195	2.257454	-1.159957
12	1	0	-2.748617	1.818219	0.493747
13	6	0	-0.710941	1.719352	-0.032498
14	8	0	-0.261824	2.822309	0.247068
15	7	0	0.078688	0.590896	-0.092577
16	6	0	-2.524551	-1.033357	1.467275
17	1	0	-2.526915	-0.056961	1.957388
18	1	0	-3.562286	-1.390775	1.440748
19	1	0	-1.958594	-1.725849	2.095933
20	6	0	1.294247	0.549131	0.679184
21	1	0	1.685255	1.565694	0.789874
22	1	0	1.138548	0.140724	1.685436
23	6	0	2.346546	-0.307135	-0.000688
24	9	0	2.685747	0.155435	-1.216748
25	9	0	1.931768	-1.587305	-0.158810
26	9	0	3.472643	-0.345249	0.749999

HF= -742.3592516/ NImag = 1 (-975.3294 cm⁻¹)
Sum of electronic and thermal Enthalpies= -742.142973
Sum of electronic and thermal Free Energies= -742.20044

S01-A3

Center Number	Atomic Number	Atomic Type	Coordinates (Angstroms)		
			X	Y	Z
1	6	0	-4.657323	-0.252852	-0.736016
2	6	0	-3.352927	-0.546209	-0.065662
3	1	0	-5.074083	-1.142118	-1.220380
4	1	0	-5.418932	0.094290	-0.014796
5	1	0	-4.561670	0.534832	-1.489697
6	6	0	-2.413148	0.584045	0.249152
7	6	0	-0.982956	0.350358	-0.270434
8	1	0	-2.788237	1.520118	-0.171152
9	1	0	-2.354262	0.749031	1.334909
10	1	0	-0.576977	-0.581190	0.135780
11	1	0	-1.003669	0.226799	-1.359899
12	6	0	-0.038580	1.494409	0.078953
13	8	0	-0.390796	2.480633	0.698406
14	7	0	1.267135	1.398077	-0.369046
15	6	0	-3.212603	-1.838713	0.676456
16	1	0	-2.173708	-2.065809	0.933325
17	1	0	-3.771944	-1.817652	1.628571
18	1	0	-3.610064	-2.682729	0.102938
19	6	0	1.912134	0.279599	-1.006988
20	1	0	2.615570	0.628609	-1.767663
21	1	0	1.182550	-0.359462	-1.502777

Experimental Section

22	1	0	1.848341	2.174336	-0.081296
23	6	0	2.707051	-0.594997	-0.040343
24	9	0	3.305719	-1.607254	-0.706187
25	9	0	3.674879	0.108510	0.585938
26	9	0	1.927581	-1.141755	0.915527

HF= -742.3877789 / NImag = 0
Sum of electronic and thermal Enthalpies= -742.165986
Sum of electronic and thermal Free Energies= -742.228422

S01-A4

Center Number	Atomic Number	Atomic Type	Coordinates (Angstroms)		
			X	Y	Z
1	6	0	-3.715783	1.131193	0.997970
2	6	0	-2.447743	0.320341	0.745534
3	1	0	-4.548892	0.486259	1.281062
4	1	0	-3.530400	1.833314	1.819124
5	1	0	-4.004169	1.705896	0.116647
6	6	0	-1.314624	1.236454	0.268670
7	6	0	0.011985	0.559622	-0.073621
8	1	0	-1.658360	1.811700	-0.593005
9	1	0	-1.144430	1.967696	1.067401
10	1	0	0.411454	0.013465	0.786108
11	1	0	-0.145621	-0.178264	-0.866739
12	6	0	1.060472	1.570630	-0.519791
13	8	0	0.872828	2.773179	-0.500057
14	7	0	2.264166	1.071213	-0.978997
15	6	0	-2.083903	-0.535872	1.954789
16	1	0	-1.247262	-1.205261	1.754655
17	1	0	-1.805432	0.124192	2.784880
18	1	0	-2.933265	-1.142350	2.272627
19	6	0	2.720854	-0.295146	-0.993392
20	1	0	3.328632	-0.480394	-1.882685
21	1	0	1.880806	-0.988217	-1.020873
22	1	0	2.930164	1.792195	-1.222976
23	35	0	-2.900477	-0.974809	-0.776707
24	6	0	3.581170	-0.662356	0.213401
25	9	0	4.003779	-1.941471	0.117184
26	9	0	4.675309	0.123295	0.303152
27	9	0	2.907258	-0.543496	1.377507

HF= -3316.598001 / NImag = 0
Sum of electronic and thermal Enthalpies= -3316.370656
Sum of electronic and thermal Free Energies= -3316.433598

S01-TS2

Center Number	Atomic Number	Atomic Type	Coordinates (Angstroms)		
			X	Y	Z
1	6	0	-2.056550	1.485255	1.411892
2	6	0	-1.585693	0.861222	0.146173
3	1	0	-2.092781	2.572134	1.323342
4	1	0	-3.072226	1.112450	1.580054
5	1	0	-1.434402	1.194068	2.258266
6	6	0	-0.938284	-0.502038	0.160464
7	6	0	0.405726	-0.494204	-0.586098
8	1	0	-1.640981	-1.194832	-0.304514
9	1	0	1.013290	-1.352594	-0.296763
10	1	0	0.264032	-0.549835	-1.671795
11	6	0	1.068443	0.825059	-0.264014
12	8	0	0.352321	1.726760	0.190410
13	7	0	2.380480	1.047101	-0.497640
14	6	0	-1.999243	1.485249	-1.142641
15	1	0	-1.504568	1.045560	-2.009211
16	1	0	-3.073153	1.293444	-1.239938
17	1	0	-1.830889	2.563312	-1.116135
18	6	0	3.353038	0.097615	-0.994732
19	1	0	4.041161	0.597941	-1.678731
20	1	0	2.864373	-0.706278	-1.543247
21	1	0	2.709272	1.968865	-0.238014
22	1	0	-0.796450	-0.826529	1.192033
23	35	0	-4.280883	-0.818880	-0.004435
24	6	0	4.187538	-0.526977	0.121267
25	9	0	3.421721	-1.215262	0.991498
26	9	0	5.093011	-1.375667	-0.397498
27	9	0	4.851094	0.414510	0.822237

HF= -3316.541403/ NImag = 1 (-322.1048 cm⁻¹)

Experimental Section

Sum of electronic and thermal Enthalpies= -3316.316147
 Sum of electronic and thermal Free Energies= -3316.380185

S01-A5

Center Number	Atomic Number	Atomic Type	Coordinates (Angstroms)		
			X	Y	Z
1	6	0	-0.870247	0.310267	-0.273791
2	8	0	-1.693222	-0.552561	0.272641
3	6	0	-3.116110	-0.117706	0.139723
4	6	0	-3.041018	0.942606	-0.978657
5	6	0	-1.600502	1.471337	-0.897264
6	6	0	-3.908413	-1.359800	-0.231019
7	6	0	-3.526796	0.456383	1.492327
8	7	0	0.396992	0.071100	-0.229969
9	6	0	1.423720	0.904584	-0.823755
10	6	0	1.911126	1.992807	0.124867
11	9	0	0.905854	2.856809	0.442725
12	9	0	2.881289	2.715541	-0.467929
13	9	0	2.389977	1.506564	1.273555
14	35	0	1.723578	-2.603942	-0.000075
15	1	0	-3.860753	-2.102059	0.567646
16	1	0	-4.955731	-1.091173	-0.392178
17	1	0	-3.518925	-1.810549	-1.145664
18	1	0	-3.216771	0.473992	-1.949312
19	1	0	-3.785228	1.727062	-0.841174
20	1	0	-1.175383	1.747247	-1.863005
21	1	0	-1.503834	2.341068	-0.242205
22	1	0	-2.948639	1.348441	1.746924
23	1	0	-4.584744	0.729462	1.472061
24	1	0	-3.376128	-0.284858	2.279058
25	1	0	2.266101	0.244205	-1.046199
26	1	0	1.097146	1.389205	-1.746210
27	1	0	0.779859	-0.964355	0.041806

HF= -3316.581776/ NImag = 0

Sum of electronic and thermal Enthalpies= -3316.356501
 Sum of electronic and thermal Free Energies= -3316.418285

Calculations according starting with compound **S19**:

S19-A1

Center Number	Atomic Number	Atomic Type	Coordinates (Angstroms)		
			X	Y	Z
1	6	0	-1.042448	1.779166	-0.781416
2	6	0	0.376307	1.918237	-0.175136
3	6	0	1.223556	0.641466	-0.203976
4	1	0	0.909566	2.701034	-0.723085
5	1	0	0.312113	2.274242	0.854563
6	1	0	0.727128	-0.175859	0.329607
7	1	0	1.366559	0.280531	-1.226565
8	6	0	2.585398	0.851876	0.426895
9	8	0	2.929235	1.883317	0.969997
10	7	0	3.506622	-0.201600	0.361681
11	35	0	3.017831	-1.929494	-0.243319
12	6	0	4.788419	-0.103528	1.039493
13	1	0	4.741298	0.757592	1.706656
14	1	0	4.991412	-1.003922	1.621114
15	6	0	-1.931009	0.797601	0.020056
16	6	0	-3.440469	0.634637	-0.368234
17	6	0	-1.987315	1.149961	1.540838
18	6	0	-3.960907	-0.117700	0.891271
19	6	0	-3.359462	0.657848	2.072631
20	1	0	-1.158893	0.688714	2.083918
21	6	0	-5.229066	-0.644588	-1.658783
22	1	0	-3.998064	1.502820	2.350010
23	6	0	-5.798551	-1.274045	-0.371456
24	1	0	-5.821735	0.242989	-1.912064
25	1	0	-1.882173	2.229498	1.683079
26	1	0	-3.255242	0.037503	2.965251
27	1	0	-5.378338	-1.344513	-2.488652
28	1	0	-1.493254	-0.205233	-0.080615
29	6	0	-3.739406	-0.265307	-1.582609
30	1	0	-3.447319	0.212403	-2.521104
31	1	0	-3.138315	-1.180115	-1.497803
32	6	0	-4.099240	2.019381	-0.546634
33	1	0	-3.883277	2.689648	0.288750

Experimental Section

34	1	0	-3.732207	2.503657	-1.455703
35	1	0	-5.184374	1.952912	-0.634473
36	6	0	-5.465436	-0.427273	0.887478
37	1	0	-3.453624	-1.095827	0.871241
38	1	0	-1.490177	2.775848	-0.683364
39	6	0	-0.958384	1.463339	-2.285031
40	1	0	-0.686784	0.419926	-2.472527
41	1	0	-1.905676	1.646743	-2.793699
42	1	0	-0.205503	2.095244	-2.766872
43	1	0	-5.299604	-2.245456	-0.232721
44	6	0	-7.301244	-1.538069	-0.541890
45	1	0	-7.720806	-2.109278	0.288818
46	1	0	-7.857349	-0.596849	-0.616274
47	1	0	-7.492277	-2.105900	-1.457532
48	1	0	-6.023681	0.517086	0.824128
49	6	0	-5.891065	-1.129952	2.185815
50	1	0	-5.378925	-2.092923	2.295089
51	1	0	-5.647572	-0.523437	3.061415
52	1	0	-6.966083	-1.319642	2.212987
53	6	0	5.959687	0.120473	0.089402
54	9	0	6.153598	-0.920168	-0.749909
55	9	0	7.096163	0.272343	0.808447
56	9	0	5.802757	1.219647	-0.667587

HF= -3746.678033/ NImag = 0
 Sum of electronic and thermal Enthalpies= -3746.170388
 Sum of electronic and thermal Free Energies= -3746.258434

S19-A2

Center Number	Atomic Number	Atomic Type	Coordinates (Angstroms)		
			X	Y	Z
1	6	0	-0.554592	2.046358	0.184522
2	6	0	0.917208	1.960522	0.661453
3	6	0	1.819060	1.034681	-0.159531
4	1	0	1.346929	2.966158	0.641867
5	1	0	0.949736	1.648089	1.708254
6	1	0	1.455130	0.000253	-0.163941
7	1	0	1.854319	1.327588	-1.215166
8	6	0	3.251024	1.011685	0.323414
9	8	0	3.731977	1.789714	1.129779
10	7	0	4.057716	0.069443	-0.326242
11	6	0	5.049674	-0.578296	0.475478
12	1	0	5.485015	0.118264	1.202894
13	1	0	4.600284	-1.404659	1.046334
14	6	0	-1.287662	0.687139	0.292278
15	6	0	-2.823977	0.615096	-0.011336
16	6	0	-1.173733	0.054764	1.716387
17	6	0	-3.142870	-0.794840	0.566345
18	6	0	-2.441752	-0.813282	1.932663
19	1	0	-0.262043	-0.540328	1.812348
20	6	0	-4.696554	0.164217	-1.680460
21	1	0	-3.085493	-0.380231	2.704975
22	6	0	-5.067654	-1.171638	-1.004543
23	1	0	-5.358292	0.950787	-1.297763
24	1	0	-1.108750	0.838854	2.476549
25	1	0	-2.196580	-1.825947	2.259376
26	1	0	-4.916553	0.089884	-2.751379
27	1	0	-0.815888	-0.000706	-0.422923
28	6	0	-3.229316	0.590857	-1.497181
29	1	0	-3.082115	1.564092	-1.971696
30	1	0	-2.578179	-0.115903	-2.027705
31	6	0	-3.569950	1.742571	0.734957
32	1	0	-3.272986	1.808459	1.784305
33	1	0	-3.361716	2.713147	0.275900
34	1	0	-4.651727	1.604469	0.714778
35	6	0	-4.616760	-1.216500	0.481601
36	1	0	-2.590773	-1.499787	-0.075822
37	1	0	-1.039460	2.735702	0.886597
38	6	0	-0.630082	2.686186	-1.212050
39	1	0	-0.319376	1.992818	-1.999543
40	1	0	-1.640800	3.017522	-1.452812
41	1	0	0.019717	3.565406	-1.266795
42	1	0	-4.511423	-1.967704	-1.522814
43	1	0	-5.226173	-0.497493	1.046558
44	6	0	-4.834173	-2.602649	1.107684
45	1	0	-4.518394	-2.619293	2.153562
46	1	0	-5.884356	-2.900834	1.082940
47	1	0	-4.257539	-3.366535	0.573369
48	6	0	-6.566048	-1.449006	-1.189796

Experimental Section

49	1	0	-6.844837	-1.374475	-2.245293
50	1	0	-6.850435	-2.445948	-0.847296
51	1	0	-7.169632	-0.719717	-0.637898
52	6	0	6.159755	-1.168330	-0.379098
53	9	0	6.807947	-0.227764	-1.089481
55	9	0	5.699518	-2.090787	-1.246312
55	9	0	7.070644	-1.779556	0.415457

HF= -1172.501281 / Nimag = 0
 Sum of electronic and thermal Enthalpies= -1171.999133
 Sum of electronic and thermal Free Energies= -1172.084437

S19-TS1

Center Number	Atomic Number	Atomic Type	Coordinates (Angstroms)		
			X	Y	Z
1	6	0	-0.757438	-1.000753	-0.628678
2	6	0	-1.076405	-2.462418	-0.233350
3	6	0	-2.244190	-2.593360	0.774856
4	1	0	-1.344088	-3.019037	-1.136716
5	1	0	-0.199361	-2.960666	0.182894
6	1	0	-2.585328	-3.626675	0.840533
7	1	0	-1.919047	-2.281091	1.771432
8	6	0	-3.438038	-1.731597	0.396932
9	8	0	-4.570171	-2.169285	0.241687
10	7	0	-3.133258	-0.385032	0.312492
11	6	0	-3.996352	0.451361	-0.482439
12	1	0	-3.785611	0.386758	-1.557627
13	1	0	-5.036077	0.139778	-0.336925
14	6	0	0.377956	-0.250973	0.090842
15	6	0	1.885236	-0.475100	-0.314107
16	6	0	0.389267	-0.412729	1.638247
17	6	0	2.560642	0.349987	0.821336
18	6	0	1.835601	-0.088975	2.104226
19	1	0	-0.351894	0.244488	2.097669
20	6	0	3.861129	0.216902	-1.765591
21	1	0	2.312054	-0.972837	2.540597
22	6	0	4.564792	0.911641	-0.581916
23	1	0	4.270258	-0.794620	-1.875949
24	1	0	0.122668	-1.431119	1.927240
25	1	0	1.853689	0.687754	2.870960
26	1	0	4.125058	0.742548	-2.689912
27	1	0	0.196291	0.810109	-0.123338
28	6	0	2.327090	0.145912	-1.651893
29	1	0	1.935560	-0.416012	-2.504454
30	1	0	1.912722	1.159353	-1.726131
31	6	0	2.264841	-1.968483	-0.269316
32	1	0	1.989020	-2.439072	0.676600
33	1	0	1.766255	-2.517348	-1.072949
34	1	0	3.337147	-2.118384	-0.399234
35	6	0	4.096738	0.347885	0.787960
36	1	0	2.259474	1.392837	0.636898
37	6	0	-0.817309	-0.777846	-2.136681
38	1	0	-0.651394	0.268589	-2.403037
39	1	0	-0.060995	-1.378467	-2.653472
40	1	0	-1.788319	-1.084935	-2.538012
41	1	0	4.268077	1.971268	-0.598859
42	6	0	6.086705	0.846491	-0.773442
43	1	0	6.625133	1.442858	-0.034152
44	1	0	6.446155	-0.185855	-0.697804
45	1	0	6.368123	1.221163	-1.762139
46	1	0	4.455092	-0.687182	0.875513
47	6	0	4.676464	1.141881	1.968546
48	1	0	4.367407	2.192355	1.922282
49	1	0	4.334150	0.736941	2.923826
50	1	0	5.767983	1.115698	1.979196
51	1	0	-1.728462	-0.437418	-0.201963
52	6	0	-3.862937	1.907471	-0.080182
53	9	0	-2.597338	2.363997	-0.246384
54	9	0	-4.665542	2.679744	-0.850428
55	9	0	-4.200488	2.127808	1.202811

HF= -1172.485197 / Nimag = 1 (-582.2053 cm⁻¹)
 Sum of electronic and thermal Enthalpies= -1171.986753
 Sum of electronic and thermal Free Energies= -1172.067029

S19-A3

Center	Atomic	Atomic	Coordinates (Angstroms)		
--------	--------	--------	-------------------------	--	--

Experimental Section

Number	Number	Type	X	Y	Z
1	6	0	0.184159	-0.778581	0.215687
2	6	0	-1.146781	-0.129913	0.470410
3	6	0	-1.937632	0.172727	-0.838135
4	1	0	-1.761584	-0.792167	1.091308
5	1	0	-1.049540	0.810706	1.013313
6	1	0	-1.355730	0.857613	-1.461442
7	1	0	-2.088632	-0.747799	-1.410223
8	6	0	-3.257706	0.857422	-0.532415
9	8	0	-3.323266	1.917252	0.065683
10	7	0	-4.383344	0.192753	-0.968171
11	6	0	-5.712558	0.698727	-0.728647
12	1	0	-5.617828	1.664603	-0.231155
13	1	0	-6.272745	0.829999	-1.658884
14	6	0	1.380350	0.048472	-0.185180
15	6	0	2.816451	-0.417223	0.256226
16	6	0	1.340905	1.541024	0.266934
17	6	0	3.638675	0.831599	-0.168592
18	6	0	2.814460	2.026312	0.338187
19	1	0	0.743258	2.147323	-0.417610
20	6	0	4.921249	-1.763449	-0.240271
21	1	0	3.089028	2.281710	1.366607
22	6	0	5.741359	-0.489451	-0.529096
23	1	0	5.094644	-2.066507	0.799291
24	1	0	0.868363	1.629189	1.246974
25	1	0	2.980213	2.923250	-0.262120
26	1	0	5.313367	-2.581676	-0.854841
27	1	0	1.416047	0.042871	-1.292476
28	6	0	3.408831	-1.626035	-0.491534
29	1	0	2.917382	-2.559027	-0.204136
30	1	0	3.231758	-1.496519	-1.567370
31	6	0	2.831827	-0.659047	1.780166
32	1	0	2.447390	0.198771	2.335925
33	1	0	2.201061	-1.515187	2.033969
34	1	0	3.834185	-0.866700	2.157837
35	6	0	5.136458	0.761297	0.165484
36	1	0	3.577609	0.855973	-1.268250
37	6	0	0.169409	-2.248177	-0.095784
38	1	0	0.430571	-2.452305	-1.145778
39	1	0	0.889095	-2.813177	0.506841
40	1	0	-0.815887	-2.684532	0.090398
41	1	0	5.685530	-0.300228	-1.612009
42	6	0	7.214592	-0.727547	-0.169417
43	1	0	7.858531	0.096246	-0.484423
44	1	0	7.337165	-0.854077	0.912133
45	1	0	7.588342	-1.636182	-0.651157
46	1	0	5.253758	0.641784	1.251627
47	6	0	5.858374	2.054968	-0.241074
48	1	0	5.794431	2.214507	-1.323641
49	1	0	5.415257	2.925082	0.249163
50	1	0	6.915904	2.034352	0.030523
51	1	0	-4.277815	-0.671065	-1.476402
52	6	0	-6.526559	-0.225901	0.161887
53	9	0	-6.642160	-1.463207	-0.388963
54	9	0	-7.777137	0.254997	0.327452
55	9	0	-5.983900	-0.388174	1.381369
HF=			-1172.522974	/ NImag = 0	
Sum of electronic and thermal Enthalpies=				-1172.019548	
Sum of electronic and thermal Free Energies=				-1172.107093	

S19-A4

Center Number	Atomic Number	Atomic Type	Coordinates (Angstroms)		
			X	Y	Z
1	6	0	0.149610	0.999057	0.372672
2	6	0	-1.240240	0.598991	-0.179841
3	6	0	-1.746634	-0.785793	0.274582
4	1	0	-1.960764	1.355359	0.141350
5	1	0	-1.228654	0.620129	-1.269066
6	1	0	-1.036517	-1.569765	-0.002618
7	1	0	-1.868892	-0.822698	1.360451
8	6	0	-3.048939	-1.132601	-0.434063
9	8	0	-3.140896	-1.166429	-1.647739
10	7	0	-4.110408	-1.422015	0.391921
11	6	0	-5.412414	-1.767201	-0.126247
12	1	0	-5.334535	-1.834980	-1.211784
13	1	0	-5.763283	-2.725026	0.267794
14	6	0	1.264253	0.091000	-0.198324

Experimental Section

15	6	0	2.755475	0.113711	0.296615
16	6	0	1.368188	0.084224	-1.754613
17	6	0	3.365825	-0.870326	-0.748893
18	6	0	2.806081	-0.386824	-2.094182
19	1	0	0.619903	-0.581553	-2.190321
20	6	0	4.501077	-0.807162	1.915963
21	1	0	3.404872	0.439519	-2.489336
22	6	0	5.157292	-1.668580	0.818046
23	1	0	5.058284	0.132078	2.010755
24	1	0	1.173454	1.080409	-2.154267
25	1	0	2.808973	-1.171972	-2.852572
26	1	0	4.616463	-1.316392	2.879350
27	1	0	0.918895	-0.909035	0.100146
28	6	0	3.009986	-0.500248	1.688883
29	1	0	2.663003	0.158067	2.489422
30	1	0	2.434402	-1.431563	1.775666
31	6	0	3.389524	1.516477	0.210137
32	1	0	3.232397	1.985817	-0.761320
33	1	0	2.960403	2.185691	0.957969
34	1	0	4.465384	1.478676	0.386540
35	6	0	4.875700	-1.112557	-0.604955
36	1	0	2.888980	-1.843751	-0.548773
37	6	0	0.133298	1.090134	1.897730
38	1	0	0.097166	0.086033	2.333120
39	1	0	1.019816	1.588801	2.284284
40	1	0	-0.742515	1.646192	2.239101
41	1	0	4.691623	-2.665212	0.859735
42	6	0	6.653743	-1.836619	1.116357
43	1	0	7.134177	-2.552375	0.446223
44	1	0	7.180869	-0.880830	1.020034
45	1	0	6.806252	-2.194473	2.139117
46	1	0	5.403863	-0.155538	-0.711242
47	6	0	5.392404	-2.052134	-1.705171
48	1	0	4.907074	-3.032891	-1.641690
49	1	0	5.191100	-1.645869	-2.699127
50	1	0	6.470572	-2.208626	-1.633031
51	35	0	0.346122	2.942574	-0.270308
52	1	0	-3.983017	-1.380956	1.390807
53	6	0	-6.463101	-0.723557	-0.218209
54	9	0	-7.675127	-1.105716	-0.236125
55	9	0	-6.570416	-0.560268	1.563137
56	9	0	-6.188986	0.484011	-0.304223

HF= -3746.722776 / NIMag = 0

Sum of electronic and thermal Enthalpies= -3746.213979

Sum of electronic and thermal Free Energies= -3746.301891

S19-TS2

Center Number	Atomic Number	Atomic Type	Coordinates (Angstroms)		
			X	Y	Z
1	6	0	-0.079391	1.221147	0.176115
2	6	0	-0.749394	2.073020	-0.893700
3	6	0	-1.617943	1.173548	-1.776799
4	1	0	-1.358932	2.839642	-0.415183
5	1	0	0.024318	2.619651	-1.439460
6	1	0	-2.430714	1.714977	-2.265419
7	1	0	-1.045349	0.666830	-2.561245
8	6	0	-2.129866	0.129660	-0.817309
9	8	0	-1.498012	-0.006805	0.252636
10	7	0	-3.196896	-0.622131	-1.110506
11	6	0	-3.738039	-1.640879	-0.227176
12	1	0	-3.776918	-2.608962	-0.730989
13	1	0	-3.099488	-1.720033	0.650779
14	6	0	1.065850	0.364443	-0.322310
15	6	0	1.555555	-0.953672	0.370049
16	6	0	2.372444	1.239908	-0.444014
17	6	0	2.879193	-1.152319	-0.430278
18	6	0	3.549438	0.228639	-0.387602
19	1	0	2.359668	1.806671	-1.374969
20	6	0	1.419990	-3.494713	0.472632
21	1	0	4.123965	0.355536	0.534622
22	6	0	2.787851	-3.654342	-0.222078
23	1	0	1.562051	-3.558789	1.557722
24	1	0	2.435064	1.991115	0.342422
25	1	0	4.243216	0.381102	-1.215948
26	1	0	0.788588	-4.350223	0.207178
27	1	0	0.803750	0.058679	-1.342144
28	6	0	0.675526	-2.193182	0.126096
29	1	0	-0.248313	-2.136399	0.708346

Experimental Section

30	1	0	0.385492	-2.220107	-0.933641
31	6	0	1.815953	-0.781132	1.880052
32	1	0	2.368506	0.131926	2.105946
33	1	0	0.875008	-0.754636	2.434389
34	1	0	2.395511	-1.613903	2.278892
35	6	0	3.685616	-2.399426	-0.038328
36	1	0	2.569557	-1.319323	-1.474710
37	6	0	-0.060922	1.862975	1.501482
38	1	0	0.440533	1.306110	2.284302
39	1	0	0.475749	2.835590	1.314563
40	1	0	-1.064646	2.155108	1.813130
41	1	0	2.598949	-3.746105	-1.302760
42	6	0	3.459655	-4.951688	0.248790
43	1	0	4.363241	-5.182114	-0.318814
44	1	0	3.736103	-4.887279	1.306949
45	1	0	2.779960	-5.801954	0.137405
46	1	0	3.964915	-2.329570	1.021379
47	6	0	4.984938	-2.491538	-0.853043
48	1	0	4.770089	-2.581428	-1.924043
49	1	0	5.601343	-1.601017	-0.711712
50	1	0	5.589236	-3.352474	-0.560682
51	35	0	1.221068	4.799664	0.187256
52	1	0	-3.671022	-0.448942	-1.986090
53	6	0	-5.150344	-1.288965	0.221617
54	9	0	-5.653493	-2.274453	0.982924
55	9	0	-5.189396	-0.147277	0.927071
56	9	0	-5.967233	-1.131320	-0.848543

HF= -3746.671653 / Nimag = 1 (-137.0132 cm⁻¹)

-3746.164457

Sum of electronic and thermal Enthalpies=

-3746.250727

Sum of electronic and thermal Free Energies=

-3746.250727

S19-A5

Center Number	Atomic Number	Atomic Type	Coordinates (Angstroms)		
			X	Y	Z
1	6	0	-0.291626	-0.979073	0.520493
2	6	0	0.245295	-1.831647	-0.650822
3	6	0	1.776189	-1.734862	-0.544399
4	1	0	-0.102911	-2.860669	-0.574870
5	1	0	-0.088460	-1.437755	-1.608845
6	1	0	2.234312	-2.552016	0.021384
7	1	0	2.306870	-1.705055	-1.495707
8	6	0	1.970144	-0.467029	0.227457
9	8	0	0.869401	-0.025317	0.778008
10	7	0	3.106235	0.132123	0.375358
11	6	0	3.318418	1.302968	1.204907
12	1	0	2.587171	1.358264	2.012139
13	1	0	4.323240	1.236955	1.625839
14	6	0	-1.479266	-0.029332	0.267494
15	6	0	-2.924431	-0.598645	0.054454
16	6	0	-1.269855	0.961622	-0.919389
17	6	0	-3.635492	0.713359	-0.396750
18	6	0	-2.686868	1.320980	-1.440875
19	1	0	-0.726966	1.844302	-0.579952
20	6	0	-5.162894	-1.259696	1.079646
21	1	0	-2.864681	0.886316	-2.429494
22	6	0	-5.862415	-0.008513	0.511663
23	1	0	-5.341322	-2.104397	0.403544
24	1	0	-0.665405	0.524259	-1.717081
25	1	0	-2.818442	2.399309	-1.542916
26	1	0	-5.643112	-1.533706	2.025082
27	1	0	-1.537817	0.571170	1.183258
28	6	0	-3.651128	-1.097216	1.318415
29	1	0	-3.248646	-2.052713	1.667337
30	1	0	-3.488984	-0.374517	2.128152
31	6	0	-2.951570	-1.685220	-1.040752
32	1	0	-2.438988	-1.371548	-1.951990
33	1	0	-2.474946	-2.604698	-0.689956
34	1	0	-3.970883	-1.947672	-1.323510
35	6	0	-5.125659	0.555545	-0.734664
36	1	0	-3.597079	1.378828	0.480203
37	6	0	-0.417371	-1.795722	1.803051
38	1	0	-0.670243	-1.157490	2.651384
39	1	0	-1.197215	-2.549886	1.693779
40	1	0	0.518142	-2.314671	2.027761
41	1	0	-5.812868	0.774832	1.283069
42	6	0	-7.343250	-0.316617	0.249955
43	1	0	-7.912848	0.575889	-0.015611
44	1	0	-7.455088	-1.040780	-0.564683

Experimental Section

45	1	0	-7.811066	-0.747782	1.139932
46	1	0	-5.233549	-0.167658	-1.554654
47	6	0	-5.727503	1.886854	-1.209424
48	1	0	-5.661523	2.648172	-0.423944
49	1	0	-5.201445	2.268364	-2.087541
50	1	0	-6.778718	1.781722	-1.484124
51	1	0	3.992371	-0.410814	-0.014067
52	35	0	5.417806	-1.626601	-0.511399
53	6	0	3.233274	2.600759	0.408463
54	9	0	4.148582	2.663542	-0.568275
55	9	0	2.017899	2.759461	-0.165142
56	9	0	3.430749	3.650670	1.234525

HF= -3746.718913 / Nimag = 0
Sum of electronic and thermal Enthalpies= -3746.211368
Sum of electronic and thermal Free Energies= -3746.297171

9 Bibliographic Data of Complete Publications

Title..... Synthesis of Lactones via C–H Functionalization of Nonactivated C(sp³)–H Bonds
Author names **Johannes Richers**, Michael Heilmann, Markus Drees, and Konrad Tiefenbacher
Published in Organic Letters, American Chemical Society
Publication date December 5, 2016
Published in *Org. Lett.*, **2016**, *18*, 6472–6475
DOI 10.1021/acs.orglett.6b03371
Hyperlink <http://pubs.acs.org/doi/abs/10.1021/acs.orglett.6b03371>

Title..... Synthesis and Neurotrophic Activity Studies of *Illicium* Sesquiterpene
Natural Product Analogs
Author names **Johannes Richers**, Alexander Pöthig, Eberhardt Herdtweck, Claudia Sippel,
Felix Hausch, and Konrad Tiefenbacher
Published in Chemistry – A European Journal, John Wiley & Sons, Inc.
Publication date February 7, 2017
Citation *Chem. Eur. J.* **2017**, *23*, 3178–3183
DOI 10.1002/chem.201605362
Hyperlink <http://onlinelibrary.wiley.com/doi/10.1002/chem.201605362/abstract>

Title..... A six-step total synthesis of α -thujone and D₆- α -thujone, enabling facile access to
isotopically labelled metabolites
Author names Irene Thamm, **Johannes Richers**, Michael Rychlika and Konrad Tiefenbacher
Published in Chemical Communications, Royal Society of Chemistry
Publication date September 12, 2016
Citation *Chem. Commun.* **2016**, *52*, 11701–11703
DOI 10.1039/C6CC05376A
Hyperlink <http://pubs.rsc.org/en/content/articlelanding/2016/cc/c6cc05376a#!divAbstract>

10 Publication Summaries

10.1 Synthesis of Lactones via C–H Functionalization of Non-Activated C(sp³)–H Bonds

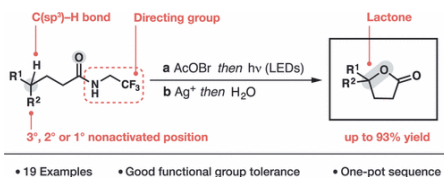
Johannes Richers,^{a†} Michael Heilmann,^{b†} Markus Drees,^a and Konrad Tiefenbacher*^{b,c}

^a Department of Chemistry, Technical University of Munich, Lichtenbergstraße 4, 85747 Garching, Germany

^b Department of Chemistry, University of Basel, St. Johans-Ring 19, 4056 Basel, Switzerland

^c Department of Biosystems Science and Engineering, ETH Zurich, Mattenstrasse 26, 4058 Basel, Switzerland

[†]these authors contributed equally. * Corresponding authors



Abstract: An electron-deficient amide is utilized as a directing group to functionalize nonactivated C(sp³)–H bonds through radical 1,5-hydrogen abstraction. The γ -bromoamides formed are subsequently converted to γ -lactones under mild conditions. The method described is not limited to tertiary and secondary positions but also allows functionalization of primary nonactivated sp³-hybridized positions in a one-pot sequence. In addition, the broad functional group tolerance renders this method suitable for the late-stage introduction of γ -lactones into complex carbon frameworks.

Author contributions: J. R. jointly conceived the study with K. T., developed the concept, designed and carried out the experiments, interpreted data and prepared the manuscript and supporting information. M. H. contributed equally, carried out the experiments, interpreted data, prepared the supporting information and edited the manuscript. M. D. performed the DFT calculations and prepared supporting information. K. T. conceived, developed and supervised the study, interpreted data and edited the manuscript. All authors reviewed the results and approved the final version of the manuscript.

10.2 A Six-Step Total Synthesis of α -Thujone and D₆- α -Thujone, enabling facile Access to Isotopically Labelled Metabolites

Irene Thamm,^a Johannes Richers,^b Michael Rychlik,^a and Konrad Tiefenbacher*^{c,d}

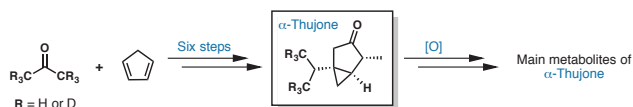
^a Analytical Food Chemistry, Technical University of Munich, Alte Akademie 10, 85354 Freising, Germany

^b Department of Chemistry, Technical University of Munich, Lichtenbergstraße 4, 85747 Garching, Germany

^c Department of Chemistry, University of Basel, St. Johannisring 19, CH-4056 Basel, Switzerland. E-mail: konrad.tiefenbacher@unibas.ch

^d Department of Biosystems Science and Engineering, ETH Zürich, Mattenstrasse 26, CH-4058 Basel, Switzerland. E-mail: tkonrad@ethz.ch

* Corresponding authors



Abstract: The short synthesis of α -Thujone relies on the functionalization of the readily available dimethylfulvene. Furthermore, the three main metabolites of the natural product were also synthesized. Since *d*-acetone can be used as a starting material, the route developed allows for the facile incorporation of isotopic labels which are required for detecting and quantifying trace amounts *via* GC/MS analysis.

Author contributions: I. T. designed and carried out the experiments, interpreted data and prepared the manuscript and supporting information. J. R. designed and carried out the experiments, interpreted data, prepared supporting information and edited the manuscript. M. R. conceived, developed and supervised the study. K. T. conceived, developed and supervised the study, interpreted data and wrote the manuscript. All authors reviewed the results and approved the final version of the manuscript.

10.3 Synthesis and Neurotrophic Activity Studies of *Illicium* Sesquiterpene Natural Product Analogs

Johannes Richers,^a Alexander Pöthig,^b Eberhardt Herdtweck,^b Claudia Sippel,^c Felix Hausch,^d and Konrad Tiefenbacher^{*c,e,f}

^a Department Chemistry, Technical University of Munich, Lichtenbergstraße 4, 85747 Garching, Germany

^b Catalysis Research Center, Technical University of Munich, Ernst-Otto-Fischer-Str. 1, 85747 Garching, Germany

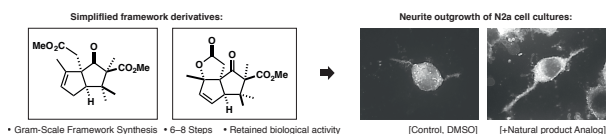
^c Department of Translational Research in Psychiatry, Max-Planck-Institute of Psychiatry, Kraepelinstr. 2–10, 80804 Munich, Germany

^d Clemens-Schöpf-Institute of Organic Chemistry and Biochemistry, TU Darmstadt, Alarich-Weiss-Str. 4, 64287 Darmstadt, Germany

^e Department of Chemistry, University of Basel, St. Johannisring 19, CH-4056 Basel, Switzerland. E-mail: konrad.tiefenbacher@unibas.ch

^f Department of Biosystems Science and Engineering, ETH Zürich, Mattenstrasse 26, CH-4058 Basel, Switzerland. E-mail: tkonrad@ethz.ch

* Corresponding authors



Abstract: Neurotrophic natural products hold potential as privileged structures for the development of therapeutic agents against neurodegeneration. However, only a few studies have been conducted to investigate a common pharmacophoric motif and structure–activity relationships (SARs). Here, an investigation of structurally more simple analogues of neurotrophic sesquiterpenes of the illicium family is presented. A concise synthetic route enables preparation of the carbon framework of (\pm)-Merrilactone A and (\pm)-Anislactone A/B on a gram scale. This has allowed access to a series of structural analogues by modification of the core structure, including variation of oxidation levels and alteration of functional groups. In total, 15 derivatives of the natural products have been synthesized and tested for their neurite outgrowth activities. Our studies indicate that the promising biological activity can be retained by structurally simpler natural product analogues, which are accessible by a straightforward synthetic route.

Author contributions: J. R. jointly conceived the study with K. T., developed the concept, designed and carried out experiments, assisted in the neurite outgrowth experiments, interpreted data, and prepared the manuscript and supporting information. A. P. and E. H. conducted the x-ray experiments and resolved crystal structures. C. S. performed the neurite outgrowth experiments, collected and analyzed data. F. H. supervised the neurite outgrowth experiments, interpreted data and edited the manuscript. K. T. conceived, developed and supervised the study, carried out experiments, interpreted data and edited the manuscript. All authors reviewed the results and approved the final version of the manuscript.

11 Reprint Permissions

11.1 American Chemical Society

**RightsLink**[®]**ACS Publications**
Most Trusted. Most Cited. Most Read.

Title: Synthesis of Lactones via C–H Functionalization of Nonactivated C(sp³)–H Bonds
Author: Johannes Richers, Michael Heilmann, Markus Drees, et al
Publication: Organic Letters
Publisher: American Chemical Society
Date: Dec 1, 2016
Copyright © 2016, American Chemical Society

PERMISSION/LICENSE IS GRANTED FOR YOUR ORDER AT NO CHARGE

This type of permission/license, instead of the standard Terms & Conditions, is sent to you because no fee is being charged for your order. Please note the following:

- Permission is granted for your request in both print and electronic formats, and translations.
- If figures and/or tables were requested, they may be adapted or used in part.
- Please print this page for your records and send a copy of it to your publisher/graduate school.
- Appropriate credit for the requested material should be given as follows: "Reprinted (adapted) with permission from (COMPLETE REFERENCE CITATION). Copyright (YEAR) American Chemical Society." Insert appropriate information in place of the capitalized words.
- One-time permission is granted only for the use specified in your request. No additional uses are granted (such as derivative works or other editions). For any other uses, please submit a new request.

[BACK](#)[CLOSE WINDOW](#)

Copyright © 2017 [Copyright Clearance Center, Inc.](#) All Rights Reserved. [Privacy statement](#). [Terms and Conditions](#).
Comments? We would like to hear from you. E-mail us at customer-care@copyright.com

11.2 Royal Society of Chemistry

This article is licensed under a Creative Commons Attribution-NonCommercial 3.0 Unported Licence. Material from this article can be used in other publications provided that the correct acknowledgement is given with the reproduced material and it is not used for commercial purposes.

11.3 John Wiley & Sons, Inc.

**JOHN WILEY AND SONS LICENSE
TERMS AND CONDITIONS**

Apr 28, 2017

This Agreement between Johannes Richers ("You") and John Wiley and Sons ("John Wiley and Sons") consists of your license details and the terms and conditions provided by John Wiley and Sons and Copyright Clearance Center.

License Number	4097811476558
License date	
Licensed Content Publisher	John Wiley and Sons
Licensed Content Publication	Chemistry - A European Journal
Licensed Content Title	Synthesis and Neurotrophic Activity Studies of Illicium Sesquiterpene Natural Product Analogues
Licensed Content Author	Johannes Richers, Alexander Pöthig, Eberhardt Herdtweck, Claudia Sippel, Felix Hausch, Konrad Tiefenbacher
Licensed Content Date	Feb 7, 2017
Licensed Content Pages	6
Type of use	Dissertation/Thesis
Requestor type	Author of this Wiley article
Format	Print and electronic
Portion	Full article
Will you be translating?	No
Title of your thesis / dissertation	Studies toward the Synthesis and Biological Activity of Illicium Sesquiterpeneoids via C-H Functionalization
Expected completion date	May 2017
Expected size (number of pages)	200
Requestor Location	Johannes Richers Lilienthalstr. 10 Berlin, 10965 Germany Attn: Johannes Richers
Publisher Tax ID	EU826007151

12 Index of Abbreviations

ac.....	acetone
Ac.....	acetyl
ATR	attenuated total reflection
BDE.....	bond dissociation energy
Bu.....	butyl
CAM.....	ceric ammonium nitrate
cat.....	catalyst
d	doublet
DMDO.....	dimethyldioxirane
DMAP	4-dimethylaminopyridine
DMF.....	<i>N,N</i> -dimethyl formamide
DMSO.....	dimethyl sulfoxide
d.r.....	diastereomeric ratio
EDC	1-ethyl-3-(3-dimethylaminopropyl)carbodiimide
ee.....	enantiomeric excess
EI.....	electron ionization
ESI.....	electron spray ionization
Et.....	ethyl
Et ₂ O.....	diethyl ether
EtOAc.....	ethyl acetate
EtOH	ethanol
<i>et al.</i>	<i>et alii</i> , and co-workers
EWG	electron withdrawing group
eq.....	equivalents
FG	functional group
GC.....	gas chromatography
HRMS.....	high resolution mass spectrometry
HV	high vacuum
IR.....	infrared spectroscopy
<i>J</i>	coupling constant

LDA	lithium diisopropylamide
L _n	ligand
m	multiplet
M	molar, m/L
Me	methyl
MeCN	acetonitrile
MeOH	methanol
MS	mass spectrometry
NMR	nuclear magnetic resonance
NOE	nuclear OVERHAUSER effect
py	pyridine
quant.	quantitative (yield > 99%)
R _t	retention factor
r.r.	regioisomeric ratio
r.t.	room temperature
SAR	structure–activity relationship
SET	single electron transfer
s.m.	starting material
TFac	trifluoroacetone
TFA	trifluoroacetic acid
TFDO	methyl(trifluoromethyl)dioxirane
THF	tetrahydrofuran
TLC	thin layer chromatography
TMS	trimethylsilyl
Ts	tosyl
<i>p</i> TsOH	<i>para</i> -toluenesulfonic acid
UV	ultraviolet
virt	virtual

13 References

- [1] K. C. Nicolaou, *Proc. R. Soc. A* **2014**, *470*, 1–17.
- [2] C. G. Wermuth, C. R. Ganellin, P. Lindberg, L. A. Mitscher, *Pure Appl. Chem.* **1998**, *70*, 1129–1143.
- [3] GBD 2015 Disease and Injury Incidence and Prevalence Collaborators, *Lancet* **2016**, *388*, 1545–1602.
- [4] C. P. Ferri, M. Prince, C. Brayne, H. Brodaty, L. Fratiglioni, M. Ganguli, K. Hall, K. Hasegawa, H. Hendrie, Y. Huang, A. Jorm, C. Mathers, P. R. Menezes, E. Rimmer, M. Sczuzfca, *The Lancet* **2005**, *366*, 2112–2117.
- [5] "Fact Sheet: Dementia", World Health Organization, **2016**, who.int/mediacentre/factsheets/fs362/en/ (09.04.2017)
- [6] "Alzheimer's disease brain diagram", Stanford Healthcare, stanfordhealthcare.org/medical-conditions/brain-and-nerves/alzheimers-disease (09.04.17)
- [7] K. Senior, *Nat. Rev. Neurol.* **2009**, *5*, 405–405.
- [8] G. Krabbe, A. Halle, V. Matyash, J. L. Rinnenthal, G. D. Eom, U. Bernhardt, K. R. Miller, S. Prokop, H. Kettenmann, F. L. Heppner, *PLoS One* **2013**, *8*, 1–8.
- [9] J. H. Lee, S. K. Jeong, B. C. Kim, K. W. Park, A. Dash, *Acta. Neurol. Scand.* **2015**, *131*, 259–267.
- [10] M. J. O'Neil, *The Merck Index: An Encyclopedia of Chemicals, Drugs, and Biologicals*, **2006**, Merck & Co., Whitehouse Station, NJ, USA.
- [11] P. Kása, Z. Rakoncay, K. Gulya, *Prog. Neurobiol.* **1997**, *52*, 511–535.
- [12] D. M. Robinson, G. M. Keating, *Drugs* **2006**, *66*, 1515–1534.
- [13] A. C.-H. M. Prince, M. Knapp, M. Guerchet, M. Karagiannidou, **2016**, Alzheimer's Disease International, London.
- [14] T. J. Schmidt, in *Current Organic Chemistry*, **1999**, 3, Bentham Science Publisher BV, Hilversum, 577–608.
- [15] N. J. White, *Antimicrob. Agents and Chemother.* **1997**, *41*, 1413–1422.
- [16] A. Wesolowska, A. Nikiforuk, K. Michalska, W. Kisiel, E. Chojnacka-Wojcik, *J. Ethnopharmacol.* **2006**, *107*, 254–258.
- [17] K. Ehrenberger, E. Benkoe, D. Felix, *Acta Oto-Laryngologica.* **1982**, *93*, 269–273.
- [18] T. Gulder, T. A. M. Gulder, *Nachr. Chem.* **2014**, *62*, 765–768.
- [19] *Illicium merrillianum* A.C.Sm. **1918**, *Herbarium Catalogue: Royal Botanic Garden Edinburgh*, E00003599.
- [20] a) J.-M. Huang, R. Yokoyama, C.-S. Yang, Y. Fukuyama, *Tetrahedron Lett.* **2000**, *41*, 6111–6114; b) J.-M. Huang, C.-S. Yang, M. Tanaka, Y. Fukuyama, *Tetrahedron* **2001**, *57*, 4691–4698.
- [21] I. Kouno, K. Mori, N. Kawano, S. Sato, *Tetrahedron Lett.* **1989**, *30*, 7451–7452.
- [22] D. Urabe, M. Inoue, *Tetrahedron* **2009**, *65*, 6271–6289.
- [23] J.-M. Huang, C.-S. Yang, M. Tanaka, Y. Fukuyama, *Tetrahedron* **2001**, 4691–4698.
- [24] X. Tian, R. Yue, H. Zeng, H. Li, L. Shan, W. He, Y. Shen, W. Zhang, *Sci. Rep.* **2015**, *5*, 1–9.
- [25] a) P. M. Joyner, R. H. Cichewicz, *Nat. Prod. Rep.* **2011**, *28*, 26–47; b) P. Williams, A. Sorribas, M. J. Howes, *Nat. Prod. Rep.* **2011**, *28*, 48–77.
- [26] a) K. Harada, H. Kato, Y. Fukuyama, *Tetrahedron Lett.* **2005**, *46*, 7407–7410; b) K. Harada, H. Ito, H. Hioki, Y. Fukuyama, *Tetrahedron Lett.* **2007**, *48*, 6105–6108.
- [27] V. B. Birman, S. J. Danishefsky, *J. Am. Chem. Soc.* **2002**, *124*, 2080–2081.
- [28] Z. Meng, S. J. Danishefsky, *Angew. Chem. Int. Ed.* **2005**, *44*, 1511–1513; *Angew. Chem.* **2005**, *117*, 1535–1537.
- [29] M. Inoue, T. Sato, M. Hirama, *J. Am. Chem. Soc.* **2003**, *125*, 10772–10773.
- [30] M. Inoue, T. Sato, M. Hirama, *Angew. Chem. Int. Ed.* **2006**, *45*, 4843–4848; *Angew. Chem.* **2006**, *118*, 4961–4966.
- [31] M. Inoue, N. Lee, S. Kasuya, T. Sato, M. Hirama, M. Moriyama, Y. Fukuyama, *J. Org. Chem.* **2007**, *72*, 3065–3075.
- [32] G. Mehta, S. R. Singh, *Angew. Chem. Int. Ed.* **2006**, *45*, 953–955; *Angew. Chem.* **2006**, *118*, 967–969.
- [33] W. He, J. Huang, X. Sun, A. J. Frontier, *J. Am. Chem. Soc.* **2007**, *129*, 498–499.
- [34] W. He, J. Huang, X. Sun, A. J. Frontier, *J. Am. Chem. Soc.* **2008**, *130*, 300–308.

- [35] J. Chen, P. Gao, F. Yu, Y. Yang, S. Zhu, H. Zhai, *Angew. Chem. Int. Ed.* **2012**, *51*, 5897–5899; *Angew. Chem.* **2012**, *124*, 5999–6001.
- [36] K. C. Nicolaou, D. Vourloumis, N. Winssinger, P. S. Baran, *Angew. Chem. Int. Ed.* **2000**, *39*, 44–122; *Angew. Chem.* **2000**, *112*, 46–126.
- [37] J. I. Seeman, *Angew. Chem. Int. Ed.* **2016**, *55*, 12898–12912; *Angew. Chem.* **2016**, *128*, 13090–13104.
- [38] R. B. Woodward, M. P. Cava, W. D. Ollis, A. Hunger, H. U. Daeniker, K. Schenker, *J. Am. Chem. Soc.* **1954**, *76*, 4749–4751.
- [39] R. B. Woodward, *Pure Appl. Chem.* **1973**, *33*, 145–178.
- [40] E. J. Corey, X.-M. Cheng, *The Logic of Chemical Synthesis*, **1995**, Wiley, New York.
- [41] P. Wang, S. Dong, J. H. Shieh, E. Peguero, R. Hendrickson, M. A. Moore, S. J. Danishefsky, *Science* **2013**, *342*, 1357–1360.
- [42] a) K. C. Nicolaou, R. J. Aversa, *Isr. J. Chem.* **2011**, *51*, 359–377; b) K. C. Nicolaou, J. H. Seo, T. Nakamura, R. J. Aversa, *J. Am. Chem. Soc.* **2011**, *133*, 214–219.
- [43] D. MacMillan, A. Walji, *Synlett* **2007**, *2007*, 1477–1489.
- [44] M. Glasenapp-Breiling, Jagtap, P.G., Kingston, D.G.I., Montforts, F.-P., Samala, L., Yuan, H., *Progress in the Chemistry of Organic Natural Products*, **2002**, *84*, Springer: Vienna.
- [45] R. Hoffmann, *Synthesis* **2006**, *2006*, 3531–3541.
- [46] T. Gaich, P. S. Baran, *J. Org. Chem.* **2010**, *75*, 4657–4673.
- [47] a) M. E. Wolff, *Chem. Rev.* **1963**, *63*, 55–64; b) A. W. Hofmann, *Ber. dtsch. chem. Ges.* **1879**, *12*, 984–990.
- [48] A. W. Hofmann, *Ber. dtsch. chem. Ges.* **1881**, *14*, 2725–2736.
- [49] A. W. Hofmann, *Ber. dtsch. chem. Ges.* **1883**, *16*, 558–560.
- [50] E. Lellmann, *Liebigs Ann.* **1890**, *259*, 193–208.
- [51] K. Löffler, C. Freytag, *Ber. dtsch. chem. Ges.* **1909**, *42*, 3427–3431.
- [52] S. Wawzonek, P. J. Thelen, *J. Am. Chem. Soc.* **1950**, *72*, 2118–2120.
- [53] E. J. Corey, W. R. Hertler, *J. Am. Chem. Soc.* **1960**, *82*, 1657–1668.
- [54] H. J. H. Fenton, *J. Chem. Soc., Trans.* **1894**, *65*, 899–910.
- [55] J. H. Merz, W. A. Waters, *J. Chem. Soc.* **1949**, 15.
- [56] M. S. Kharasch, H. S. Isbell, *J. Am. Chem. Soc.* **1931**, *53*, 3053–3059.
- [57] J. Chatt, J. M. Davidson, *J. Chem. Soc.* **1965**, 843.
- [58] A. E. Shilov, G. B. Shul'pin, *Chem. Rev.* **1997**, *97*, 2879–2932.
- [59] R. H. Crabtree, *J. Chem. Soc., Dalton Trans.* **2001**, 2437–2450.
- [60] J. A. Labinger, A. M. Herring, D. K. Lyon, G. A. Luinstra, J. E. Bercaw, I. T. Horvath, K. Eller, *Organometallics* **1993**, *12*, 895–905.
- [61] a) M. Lersch, M. Tilsel, *Chem. Rev.* **2005**, *105*, 2471–2526; b) R. A. Periana, G. Bhalla, W. J. Tenn, K. J. H. Young, X. Y. Liu, O. Mironov, C. J. Jones, V. R. Ziatdinov, *J. Mol. Catal. A: Chem.* **2004**, *220*, 7–25.
- [62] R. Breslow, *Acc. Chem. Res.* **1980**, *13*, 170–177.
- [63] R. Breslow, *Chem. Soc. Rev.* **1972**, *1*, 553–580.
- [64] T. Bruckl, R. D. Baxter, Y. Ishihara, P. S. Baran, *Acc. Chem. Res.* **2012**, *45*, 826–839.
- [65] D. C. Haines, D. R. Tomchick, M. Machius, J. A. Peterson, *Biochemistry* **2001**, *40*, 13456–13465.
- [66] a) J. C. Lewis, P. S. Coelho, F. H. Arnold, *Chem. Soc. Rev.* **2011**, *40*, 2003–2021; b) J. A. McIntosh, C. C. Farwell, F. H. Arnold, *Curr. Opin. Chem. Biol.* **2014**, *19*, 126–134.
- [67] K. Zhang, B. M. Shafer, M. D. Demars, 2nd, H. A. Stern, R. Fasan, *J. Am. Chem. Soc.* **2012**, *134*, 18695–18704.
- [68] C. J. Moody, J. L. O'Connell, *Chem. Commun.* **2000**, 1311–1312.
- [69] N. Takaishi, Y. Fujikura, Y. Inamoto, *Synthesis* **1983**, 1983, 293–294.
- [70] D. M. Camaioni, J. T. Bays, W. J. Shaw, J. C. Linehan, J. C. Birnbaum, *J. Org. Chem.* **2001**, *66*, 789–795.
- [71] R. Curci, L. D'Accolti, C. Fusco, *Acc. Chem. Res.* **2006**, *39*, 1–9.
- [72] a) R. Bernardi, B. Novo, G. Resnati, *J. Chem. Soc., Perkin Trans. 1* **1996**, 2517–2521; b) V. A. Petrov, D. D. DesMarteau, *J. Org. Chem.* **1993**, *58*, 4754–4755; c) N. D. Litvinas, B. H. Brodsky, J. Du Bois, *Angew. Chem. Int. Ed.* **2009**, *48*, 4513–4516; *Angew. Chem.* **2009**, *121*, 4583–4586.

- [73] a) E. V. Avzyanova, N. N. Kabalnova, V. V. Shereshevets, *Russ. Chem. Bull.* **1996**, *45*, 360–362; b) Z. Cohen, E. Keinan, Y. Mazur, T. H. Varkony, *J. Org. Chem.* **1975**, *40*, 2141–2142.
- [74] a) A. D. R. Curci, M. F. Rubino, *Pure Appl. Chem.* **1995**, *67*, 811; b) R. W. Murray, R. Jeyaraman, L. Mohan, *J. Am. Chem. Soc.* **1986**, *108*, 2470–2472; c) R. Mello, L. Cassidei, M. Fiorentino, C. Fusco, R. Curci, *Tetrahedron Lett.* **1990**, *31*, 3067–3070.
- [75] R. Mello, M. Fiorentino, C. Fusco, R. Curci, *J. Am. Chem. Soc.* **1989**, *111*, 6749–6757.
- [76] W. Adam, Y. Y. Chan, D. Cremer, J. Gauss, D. Scheutzow, M. Schindler, *J. Org. Chem.* **1987**, *52*, 2800–2803.
- [77] R. Mello, M. Fiorentino, O. Sciacovelli, R. Curci, *J. Org. Chem.* **1988**, *53*, 3890–3891.
- [78] a) D. Yang, M.-K. Wong, X.-C. Wang, Y.-C. Tang, *J. Am. Chem. Soc.* **1998**, *120*, 6611–6612; b) M.-K. Wong, N.-W. Chung, L. He, X.-C. Wang, Z. Yan, Y.-C. Tang, D. Yang, *J. Org. Chem.* **2003**, *68*, 6321–6328.
- [79] Y. Tu, Z.-X. Wang, Y. Shi, *J. Am. Chem. Soc.* **1996**, *118*, 9806–9807.
- [80] a) W. Adam, G. Asensio, R. Curci, M. E. Gonzalez-Nunez, R. Mello, *J. Org. Chem.* **1992**, *57*, 953–955; b) R. Vanni, S. J. Garden, J. T. Banks, K. U. Ingold, *Tetrahedron Lett.* **1995**, *36*, 7999–8002.
- [81] P. A. Wender, M. K. Hilinski, A. V. Mayweg, *Org. Lett.* **2005**, *7*, 79–82.
- [82] W. Adam, F. Precht, M. J. Richter, A. K. Smerz, *Tetrahedron Lett.* **1995**, *36*, 4991–4994.
- [83] a) F. R. van Heerden, J. T. Dixon, C. W. Holzappel, *Tetrahedron Lett.* **1992**, *33*, 7399–7402; b) P. Bovicelli, P. Lupattelli, V. Fiorini, E. Mincione, *Tetrahedron Lett.* **1993**, *34*, 6103–6104; c) J. Hu, T. Lan, Y. Sun, H. Chen, J. Yao, Y. Rao, *Chem. Commun.* **2015**, *51*, 14929–14932.
- [84] T. Horiguchi, Q. Cheng, T. Oritani, *Tetrahedron Lett.* **2000**, *41*, 3907–3910.
- [85] P. Bovicelli, P. Lupattelli, E. Mincione, T. Prencipe, R. Curci, *J. Org. Chem.* **1992**, *57*, 5052–5054.
- [86] K. Chen, P. S. Baran, *Nature* **2009**, *459*, 824–828.
- [87] J. Schreiber, A. Eschenmoser, *Helv. Chim. Acta* **1955**, *38*, 1529–1536.
- [88] K. Chen, A. Eschenmoser, P. S. Baran, *Angew. Chem. Int. Ed.* **2009**, *48*, 9705–9708; *Angew. Chem.* **2009**, *121*, 9885–9888.
- [89] B.-J. Li, Z.-J. Shi, in *Homogeneous Catalysis for Unreactive Bond Activation*, **2014**, John Wiley & Sons, Inc., Hoboken, New Jersey, 441–573.
- [90] W. A. Herrmann, R. W. Fischer, W. Scherer, M. U. Rauch, *Angew. Chem. Int. Ed.* **1993**, *32*, 1157–1160.
- [91] S. Lee, P. L. Fuchs, *J. Am. Chem. Soc.* **2002**, *124*, 13978–13979.
- [92] D. H. R. Barton, S. Bévière, W. Chavasiri, D. R. Hill, B. Hu, T. L. Wang, C. Bardin, in *The Activation of Dioxigen and Homogeneous Catalytic Oxidation*, **1993**, Springer US, Boston, MA, 448–448.
- [93] D. H. R. Barton, D. Doller, *Acc. Chem. Res.* **1992**, *25*, 504–512.
- [94] a) C. Djerassi, R. R. Engle, *J. Am. Chem. Soc.* **1953**, *75*, 3838–3840; b) P. H. J. Carlsen, T. Katsuki, V. S. Martin, K. B. Sharpless, *J. Org. Chem.* **1981**, *46*, 3936–3938.
- [95] J. R. Frost, S. M. Huber, S. Breitenlechner, C. Bannwarth, T. Bach, *Angew. Chem. Int. Ed.* **2015**, *54*, 691–695; *Angew. Chem.* **2015**, *127*, 701–705.
- [96] a) K. J. Fraunhofer, N. Prabakaran, L. E. Sirois, M. C. White, *J. Am. Chem. Soc.* **2006**, *128*, 9032–9033; b) J. M. Lee, S. Chang, *Tetrahedron Lett.* **2006**, *47*, 1375–1379.
- [97] C. M. Rasik, M. K. Brown, *Angew. Chem. Int. Ed.* **2014**, *53*, 14522–14526; *Angew. Chem.* **2014**, *126*, 14750–14754
- [98] L.-C. Kao, A. Sen, *J. Chem. Soc., Chem. Commun.* **1991**, 1242.
- [99] a) R. C. Larock, T. R. Hightower, *J. Org. Chem.* **1993**, *58*, 5298–5300; b) N. Basicckes, A. Sen, *Polyhedron* **1995**, *14*, 197–202; c) B. D. Dangel, J. A. Johnson, D. Sames, *J. Am. Chem. Soc.* **2001**, *123*, 8149–8150.
- [100] L. V. Desai, K. L. Hull, M. S. Sanford, *J. Am. Chem. Soc.* **2004**, *126*, 9542–9543.
- [101] M. S. Chen, M. C. White, *Science* **2007**, *318*, 783–787.
- [102] M. A. Bigi, S. A. Reed, M. C. White, *Nat. Chem.* **2011**, *3*, 216–222.
- [103] M. P. S. P. Renaud, *Radicals in Organic Synthesis*, **2001**, Wiley-VCH Verlag GmbH, Weinheim.
- [104] E. I. Troyanskii, I. V. Svitani'ko, G. I. Nikishin, *Russ. Chem. Bull.* **1982**, *31*, 2432–2437.
- [105] a) R. S. Neale, *Synthesis* **1971**, *1971*, 1–15; b) A. Martin, I. Perez-Martin, E. Suarez, *Org. Lett.* **2005**, *7*, 2027–2030; c) Z. I. Watts, C. J. Easton, *J. Am. Chem. Soc.* **2009**, *131*, 11323–11325; d) T. Liu, T. S. Mei, J. Q. Yu, *J. Am. Chem. Soc.* **2015**, *137*, 5871–5874.

- [106] G. I. Nikishin, I. V. Svitan'ko, E. I. Troyanskii, *J. Chem. Soc., Perkin Trans. 2* **1983**, 595.
- [107] a) G. Majetich, K. Wheless, *Tetrahedron* **1995**, *51*, 7095–7129; b) R. Kundu, Z. T. Ball, *Org. Lett.* **2010**, *12*, 2460–2463.
- [108] R. Hernandez, S. M. Velazquez, E. Suarez, M. S. Rodriguez, *J. Org. Chem.* **1994**, *59*, 6395–6403.
- [109] M.-K. Wong, N.-W. Chung, L. He, D. Yang, *J. Am. Chem. Soc.* **2002**, *125*, 158–162.
- [110] S. Kasuya, S. Kamijo, M. Inoue, *Org. Lett.* **2009**, *11*, 3630–3632.
- [111] T. Dohi, N. Takenaga, A. Goto, A. Maruyama, Y. Kita, *Org. Lett.* **2007**, *9*, 3129–3132.
- [112] a) J. I. Concepción, C. G. Francisco, R. Hernández, J. A. Salazar, E. Suárez, *Tetrahedron Lett.* **1984**, *25*, 1953–1956; b) R. L. Dorta, C. G. Francisco, R. Freire, E. Suárez, *Tetrahedron Lett.* **1988**, *29*, 5429–5432; c) C. G. Francisco, C. C. González, E. Suárez, *Tetrahedron Lett.* **1996**, *37*, 1687–1690; d) C. G. Francisco, R. Freire, A. J. Herrera, I. Pérez-Martín, E. Suárez, *Tetrahedron* **2007**, *63*, 8910–8920.
- [113] Y. L. Chow, T. W. Mojelsky, L. J. Magdzinski, M. Tichý, *Can. J. Chem.* **1985**, *63*, 2197–2202.
- [114] K. Chen, J. M. Richter, P. S. Baran, *J. Am. Chem. Soc.* **2008**, *130*, 7247–7249.
- [115] H. M. Davies, D. Morton, *J. Org. Chem.* **2016**, *81*, 343–350.
- [116] a) P. L. Fuchs, *Handbook of Reagents for Organic Synthesis, Reagents for Direct Functionalization of C-H Bonds*, **2006**, John Wiley & Sons, Inc., Hoboken; b) E. M. Simmons, J. F. Hartwig, *Nature* **2012**, *483*, 70–73.
- [117] H. Chen, *Science* **2000**, *287*, 1995–1997.
- [118] J. Wencel-Delord, F. Glorius, *Nat. Chem.* **2013**, *5*, 369–375.
- [119] M. Christmann, *Angew. Chem. Int. Ed.* **2008**, *47*, 2740–2742; *Angew. Chem.* **2008**, *120*, 2780–2783.
- [120] T. Gulder, T. A. M. Gulder, *Nachr. Chem.* **2014**, *62*, 534–537.
- [121] a) H. M. Davies, D. Morton, *Angew. Chem. Int. Ed.* **2014**, 10256–10259; *Angew. Chem.* **2014**, *126*, 10422–10424; b) P. Baran, Y. Ishihara, *Synlett* **2010**, *2010*, 1733–1745; c) J. Yamaguchi, A. D. Yamaguchi, K. Itami, *Angew. Chem. Int. Ed.* **2012**, *51*, 8960–9009; *Angew. Chem.* **2012**, *124*, 9092–9142.
- [122] P. D. Magnus, M. S. Nobbs, *Synth. Commun.* **1980**, *10*, 273–278.
- [123] F. A. D. Pauley, T. Hudlicky, *Org. Synth.* **1989**, *67*, 121–124.
- [124] M. Kubo, C. Okada, J. M. Huang, K. Harada, H. Hioki, Y. Fukuyama, *Org. Lett.* **2009**, *11*, 5190–5193.
- [125] a) Z. Paryzek, I. Skiera, *Org. Prep. Proced. Int.* **2007**, *39*, 203–296; b) S. Gil, M. Parra, P. Rodriguez, J. Segura, *Mini. Rev. Org. Chem.* **2009**, *6*, 345–358.
- [126] a) T. Newhouse, P. S. Baran, *Angew. Chem. Int. Ed.* **2011**, *50*, 3362–3374; *Angew. Chem.* **2011**, *123*, 3422–3435; b) K. Godula, D. Sames, *Science* **2006**, *312*, 67–72; c) H. M. Davies, J. R. Manning, *Nature* **2008**, *451*, 417–424; *PMC3033428*; d) M. C. White, *Science* **2012**, *335*, 807–809.
- [127] a) L. R. Reddy, B. V. S. Reddy, E. J. Corey, *Org. Lett.* **2006**, *8*, 2819–2821; b) Q. Qin, S. Yu, *Org. Lett.* **2015**, *17*, 1894–1897; c) R. K. Quinn, Z. A. Konst, S. E. Michalak, Y. Schmidt, A. R. Szklarski, A. R. Flores, S. Nam, D. A. Horne, C. D. Vanderwal, E. J. Alexanian, *J. Am. Chem. Soc.* **2016**, *138*, 696–702; d) E. A. Wappes, S. C. Fosu, T. C. Chopko, D. A. Nagib, *Angew. Chem. Int. Ed.* **2016**, *55*, 9974–9978; *Angew. Chem.* **2016**, *128*, 10128–10132.
- [128] a) D. H. R. Barton, A. L. J. Beckwith, A. Goosen, *J. Chem. Soc.* **1965**, 181; b) R. S. Neale, N. L. Marcus, R. G. Schepers, *J. Am. Chem. Soc.* **1966**, *88*, 3051–3058; c) T. C. Joseph, J. N. S. Tam, M. Kitadani, Y. L. Chow, *Can. J. Chem.* **1976**, *54*, 3517–3525.
- [129] C. J. M. Stirling, *J. Chem. Soc.* **1960**, 255–262.
- [130] N. M. Donahue, J. S. Clarke, J. G. Anderson, *J. Phys. Chem. A* **1998**, *102*, 3923–3933.
- [131] H. Peter, M. Brugger, J. Schreiber, A. Eschenmoser, *Helv. Chim. Acta* **1963**, *46*, 577–586.
- [132] A. I. D. Alanine, C. W. G. Fishwick, C. Szantay Jr, *Tetrahedron Lett.* **1989**, *30*, 6571–6572.
- [133] O. Pelkonen, K. Abass, J. Wiesner, *Regul. Toxicol. Pharmacol.* **2013**, *65*, 100–107.
- [134] D. W. Lachenmeier, J. Emmert, T. Kuballa, G. Sartor, *Forensic. Sci. Int.* **2006**, *158*, 1–8.
- [135] K. M. Hold, N. S. Sirisoma, T. Ikeda, T. Narahashi, J. E. Casida, *Proc. Natl. Acad. Sci. U. S. A.* **2000**, *97*, 3826–3831.
- [136] E. A. Crane, K. Gademann, *Angew. Chem. Int. Ed.* **2016**, *55*, 3882–3902; *Angew. Chem.* **2016**, *128*, 3948–3970.
- [137] J. Huang, R. Yokoyama, C. Yang, Y. Fukuyama, *Tetrahedron Lett.* **2000**, *41*, 6111–6114.

- [138] a) J. Iriondo-Alberdi, J. E. Perea-Buceta, M. F. Greaney, *Org. Lett.* **2005**, *7*, 3969–3971; b) G. Mehta, S. R. Singh, *Tetrahedron Lett.* **2005**, *46*, 2079–2082; c) L. Shi, K. Meyer, M. F. Greaney, *Angew. Chem. Int. Ed.* **2010**, *49*, 9250–9253; *Angew. Chem.* **2010**, *122*, 9436–9439; d) J. Xu, L. Trzoss, W. K. Chang, E. A. Theodorakis, *Angew. Chem. Int. Ed.* **2011**, *50*, 3672–3676; *Angew. Chem.* **2011**, *123*, 3756–3760; e) N. Nazef, R. D. Davies, M. F. Greaney, *Org. Lett.* **2012**, *14*, 3720–3723; f) L. Trzoss, J. Xu, M. H. Lacoske, E. A. Theodorakis, *Beilstein J. Org. Chem.* **2013**, *9*, 1135–1140; g) D. A. Siler, J. D. Mighion, E. J. Sorensen, *Angew. Chem. Int. Ed.* **2014**, *53*, 5332–5335; *Angew. Chem.* **2014**, *126*, 5436–5439; h) I. Paterson, M. Xuan, S. M. Dalby, *Angew. Chem. Int. Ed.* **2014**, *53*, 7286–7289; *Angew. Chem.* **2014**, *126*, 7414–7417; i) Y. Shen, L. Li, Z. Pan, Y. Wang, J. Li, K. Wang, X. Wang, Y. Zhang, T. Hu, Y. Zhang, *Org. Lett.* **2015**, *17*, 5480–5483; j) H. H. Lu, M. D. Martinez, R. A. Shenvi, *Nat. Chem.* **2015**, *7*, 604–607; k) J. Gomes, C. Daepfen, R. Liffert, J. Roesslein, E. Kaufmann, A. Heikinheimo, M. Neuburger, K. Gademann, *J. Org. Chem.* **2016**, *81*, 11017–11034.
- [139] a) D. A. Carcache, Y. S. Cho, Z. Hua, Y. Tian, Y. M. Li, S. J. Danishefsky, *J. Am. Chem. Soc.* **2006**, *128*, 1016–1022; b) L. Trzoss, J. Xu, M. H. Lacoske, W. C. Mobley, E. A. Theodorakis, *Chem. Eur. J.* **2013**, *19*, 6398–6408.
- [140] a) J. Xu, M. H. Lacoske, E. A. Theodorakis, *Angew. Chem. Int. Ed.* **2014**, *53*, 956–987; *Angew. Chem.* **2014**, *126*, 972–1004; b) R. A. Shenvi, *Nat. Prod. Rep.* **2016**, *33*, 535–539.
- [141] a) M. V. Sofroniew, C. L. Howe, W. C. Mobley, *Annu Rev Neurosci* **2001**, *24*, 1217–1281; b) E. J. Huang, L. F. Reichardt, *Annu. Rev. Neurosci.* **2001**, *24*, 677–736; c) M. V. Chao, *Nat. Rev. Neurosci.* **2003**, *4*, 299–309.
- [142] F. Longo, T. Yang, J. Knowles, Y. Xie, L. Moore, S. Massa, *Current Alzheimer Research* **2007**, *4*, 503–506.
- [143] S. R. Crabtree, W. L. A. Chu, L. N. Mander, *Synlett* **1990**, *1990*, 169–170.
- [144] G. Mehta, K. Pallavi, *Tetrahedron Lett.* **2006**, *47*, 8355–8360.
- [145] S. Pichlmair, M. de Lera Ruiz, K. Basu, L. A. Paquette, *Tetrahedron* **2006**, *62*, 5178–5194.
- [146] W. G. Salmond, M. A. Barta, J. L. Havens, *J. Org. Chem.* **1978**, *43*, 2057–2059.
- [147] E. D. Laganis, B. L. Chenard, *Tetrahedron Lett.* **1984**, *25*, 5831–5834.
- [148] L. Bouveault, G. Blanc, *Bull. Soc. Chim. France* **1904**, *31*, 666–672.
- [149] E. McNeill, J. Du Bois, *J. Am. Chem. Soc.* **2010**, *132*, 10202–10204.
- [150] The trifluoroethyl amide group was employed as a directing group for C–H functionalization J. Richers, M. Heilmann, M. Drees, K. Tiefenbacher, *Org. Lett.* **2016**, *18*, 6472–6475.
- [151] M. Shoji, M. Nishioka, H. Minato, K. Harada, M. Kubo, Y. Fukuyama, T. Kuzuhara, *Biochem Biophys Res Commun* **2016**, *470*, 798–803.
- [152] S. Gaali, A. Kirschner, S. Cuboni, J. Hartmann, C. Kozany, G. Balsevich, C. Namendorf, P. Fernandez-Vizarra, C. Sippel, A. S. Zannas, R. Draener, E. B. Binder, O. F. Almeida, G. Ruhter, M. Uhr, M. V. Schmidt, C. Touma, A. Bracher, F. Hausch, *Nat Chem Biol* **2015**, *11*, 33–37.
- [153] A sample of synthetic (–)-Jiadifenolide was kindly provided by Prof. Ryan Shenvi.
- [154] *Organic Syntheses* **2013**, *90*, 350–355.
- [155] Q. Michaudel, G. Journot, "TFDO Synthesis Procedure", Open Flask, **2014**, openflask.blogspot.de/2014/01/tfdo-synthesis-procedure.html (16.11.2015)
- [156] Y. Wang, C. Chen, J. Peng, M. Li, *Angew. Chem. Int. Ed.* **2013**, *52*, 5323–5327; *Angew. Chem.* **2013**, *125*, 5431–5435.
- [157] P. C. Chiang, Y. Kim, J. W. Bode, *Chem. Commun.* **2009**, 4566–4568.
- [158] J. J. Shie, J. M. Fang, *J. Org. Chem.* **2003**, *68*, 1158–1160.
- [159] G. V. Zyryanov, D. M. Rudkevich, *J. Am. Chem. Soc.* **2004**, *126*, 4264–4270.
- [160] D. A. Brown, W. K. Glass, R. Mageswaran, S. A. Mohammed, *Magn. Reson. Chem.* **1991**, *29*, 40–45.
- [161] P. Salehi, Z. Habibi, M. Zolfigol, M. Yousefi, *Synlett* **2007**, *2007*, 812–814.
- [162] R. J. Wakeham, J. E. Taylor, S. D. Bull, J. A. Morris, J. M. Williams, *Org. Lett.* **2013**, *15*, 702–705.
- [163] W. Zeinyeh, Z. Mahiout, S. Radix, T. Lomberger, A. Dumoulin, R. Barret, C. Grenot, L. Rocheblave, E.-L. Matera, C. Dumontet, N. Walchshofer, *Steroids* **2012**, *77*, 1177–1191.
- [164] R. Na, C. Jing, Q. Xu, H. Jiang, X. Wu, J. Shi, J. Zhong, M. Wang, D. Benitez, E. Tkatchouk, W. A. Goddard, H. Guo, O. Kwon, *J. Am. Chem. Soc.* **2011**, *133*, 13337–13348.

- [165] C. Fuganti, S. Serra, *J. Org. Chem.* **1999**, *64*, 8728–8730.
- [166] D. Brossard, M. Lechevel, L. El Kihel, C. Quesnelle, M. Khalid, S. Moslemi, J.-M. Reimund, *Eur. J. Med. Chem.* **2014**, *86*, 279–290.
- [167] R. M. Jacobson, G. P. Lahm, J. W. Clader, *J. Org. Chem.* **1980**, *45*, 395–405.
- [168] M. Sono, N. Doi, E. Yoshino, S. Onishi, D. Fujii, M. Tori, *Tetrahedron Lett.* **2013**, *54*, 1947–1950.
- [169] A. Gonzalez-de-Castro, C. M. Robertson, J. Xiao, *J. Am. Chem. Soc.* **2014**, *136*, 8350–8360.
- [170] B. Peng, D. Geerdink, N. Maulide, *J. Am. Chem. Soc.* **2013**, *135*, 14968–14971.
- [171] M. Pena-Lopez, H. Neumann, M. Beller, *Chem Commun* **2015**, *51*, 13082–13085.
- [172] I. Fleischer, K. M. Dyballa, R. Jennerjahn, R. Jackstell, R. Franke, A. Spannenberg, M. Beller, *Angew. Chem. Int. Ed.* **2013**, *52*, 2949–2953.
- [173] K. Nishimura, K. Tomioka, *J. Org. Chem.* **2002**, *67*, 431–434.
- [174] T. T. Upadhyaya, S. Gurunath, A. Sudalai, *Tetrahedron Asymmetry* **1999**, *10*, 2899–2904.
- [175] M. Harnik, Y. Aharonowitz, R. Lamed, *Tetrahedron* **1982**, *38*, 3173–3178.
- [176] B. B. Snider, B. Shi, C. A. Quickley, *Tetrahedron* **2000**, *56*, 10127–10132.
- [177] I. K. Stamos, G. A. Howie, P. E. Manni, W. J. Haws, S. R. Byrn, J. M. Cassady, *J. Org. Chem.* **1977**, *42*, 1703–1709.
- [178] C. A. Citron, P. Rabe, J. S. Dickschat, *J. Nat. Prod.* **2012**, *75*, 1765–1776.
- [179] K. C. Brannock, *J. Am. Chem. Soc.* **1959**, *81*, 3379–3383.
- [180] M. Noack, R. Göttlich, *Eur. J. Org. Chem.* **2002**, *2002*, 3171–3178.
- [181] J. Yang, Y. O. Long, L. A. Paquette, *J. Am. Chem. Soc.* **2003**, *125*, 1567–1574.
- [182] R. W. Holder, J. P. Daub, W. E. Baker, R. H. Gilbert, N. A. Graf, *J. Org. Chem.* **1982**, *47*, 1445–1451.
- [183] "Workup Tricks: Fieser Method", Not Voodoo ReduX, **2016**, chem.chem.rochester.edu/~nvd/pages/magic_formulas.php?page=aluminum_hydride_reduction (01.10.2016)
- [184] *Gaussian_09*, Revision C.2, M. J. Frisch, *et al.*, Gaussian, Inc., Wallingford CT, **2009**
- [185] a) S. H. Vosko, L. Wilk, M. Nusair, *Can. J. Phys.* **1980**, *58*, 1200–1211; b) Lee, W. Yang, R. G. Parr, *Phys. Rev. B* **1988**, *37*, 785; c) A. D. Becke, *J. Chem. Phys.* **1993**, 5648.
- [186] a) W. J. Hehre, R. Ditchfield, J. A. Pople, *J. Chem. Phys.* **1972**, 2257; b) M. M. Francl, W. J. Pietro, W. J. Hehre, J. S. Binkley, M. S. Gordon, D. J. DeFrees, J. A. Pople, *J. Chem. Phys.* **1982**, 3654.